A LABORATORY SIMULATION OF ADHESIVE WEAR OF HIGH SPEED RECIPROCATING COMPONENTS IN WATER POWERED MINING EQUIPMENT

by

Ulrich F. B. Kienle

A thesis submitted to the Faculty of Engineering,
University of Cape Town in fulfillment of the
degree of Master of Science in Engineering.

Department of Materials Engineering,
University of Cape Town,
November 1988

SYNOPSIS

A high speed reciprocating sliding wear test rig was used to examine the metal on metal surface interactions of materials under consideration for application in water powered stoping equipment.

The suitability of this test rig was investigated by implementing a test programme covering self-mated stainless steel and stainless steel-on-bronze couples. These couples were examined under water lubricated conditions in a broad test matrix, covering sinusoidal peak velocities of 1, 5 and 10 m/s; loads of 5, 10 and 20N and surface roughness values ranging from 0.2 to 0.4 μm, CLA.

Due to poor reproducibility and inconclusive wear behaviours, no inferences could be made as to the relative performance of the couples tested and no ranking tables could be compiled. In response to these findings, the emphasis changed to the design of a better test facility which could more accurately simulate the tribological interactions of interest.

A new laboratory test rig, capable of investigating the performance of material surfaces, rubbing against one another under conditions of high speed reciprocating sliding in specific environments, was designed, built and commissioned. Subsequent tests conducted on this new facility showed average reproducibility for a 122 stainless steel rubbing against a CZ114 manganese bronze to have improved by a factor of two to approximately $\pm$ 20%. Initial results confirmed that adhesive wear is the dominant wear mode for the materials under consideration. This is manifested by homogeneous transfer layers and subsequent grooving of these layers.

ACKNOWLEDGEMENTS

The work described in this thesis was performed under a collaborative agreement between the Chamber of Mines of South Africa and the University of Cape Town and formed part of the research programme of the Research Organization of the Chamber of Mines.

I would also like to thank all the people who assisted me in this research initiative and contributed to its final completion. In particular, I wish to thank the following:

- Prof A Ball, my supervisor, for his advice and encouragement throughout this research project.
- Prof C Allen, for the many hours of help he so readily rendered.
- Mr N Dreze and Mr G Newins for their assistance in things technical and in the preparation of test specimens.
- Mr D Dean for his expert help in all electrical matters.
- Mrs S Betz and Mrs H Böhm for their unfaltering help with technical drawings and experimental work.
- Mr B Greeves and Mr J Petersen for their photographic expertise.
- Mr M Batho and Mr L Watkins for the expert workmanship in machining the test rig.
- Ms D Chapman is thanked for her speed and efficiency in the typing of the manuscript, as well as her unfailing moral support.
- Mr G Harper and his colleagues at the Chamber of Mines for their help and guidance.

I would also like to express my thanks to the Chamber of Mines Research Organisation and the CSIR - FRD for their financial assistance.

Finally, I would like to thank my friends and colleagues in the department of Materials Engineering at UCT for their good humour and stimulating company.

TABLE OF CONTENTS

GLOSSARY

CLA	-	centre line average
COMRO	-	Chamber of Mines Research Organization
CPL	-	crankpin load
CVL	-	Cumulative Volume Loss
K	-	wear coefficient
m	-	change in mass
PSL	-	piston side load
R_c	-	Rockwell 'C' hardness
S	-	sliding distance
s/s	-	stainless steel
SWR	-	Specific Wear Rate
UCT	-	University of Cape Town
UHMWPE	-	ultra high molecular weight polyethylene
VHN	-	Vickers Hardness Number
WPL	-	wristpin load

1.0 INTRODUCTION

The South African gold mining industry has to work in exceptionally arduous conditions. Narrow and steeply inclined reefs at ever increasing depths need to be exploited. Recovery of gold bearing ore is further complicated by the hard and abrasive quartzitic rock surrounding the reefs. Highly stressed and consequently heavily fragmented, this rock causes extremely abrasive conditions underground.

Cooling of the stoping front, as well as the need for high pressure water to clear the workings after blasting, result in humid and therefore highly corrosive environments. Dissolution of minerals further aggravates this problem.

Only the simplest forms of stoping equipment have therefore been able to endure this synergistic effect of abrasion and corrosion. This coupled with the confined working spaces, has resulted in low levels of productivity. The ever increasing depths of exploration have made these levels unacceptable and the development of unique mechanized stoping methods and equipment has thus become necessary.

Work done in recent years by the Chamber of Mines Research Organisation has identified "hydro-power" as the most suitable means of providing the power requirements at the stoping front in the future generation of deep level mines.

This concept is unique in that it has the potential to replace all existing stope services of water, compressed air, hydraulic oil and electricity with a single high-pressure mine water supply (Gundersen [1]).

1.1 THE HYDRO-POWER CONCEPT

This concept makes use of the hydrostatic head gained when mine service water descends in pipes within the mine shafts. The unique feature of this concept is that the stored hydraulic energy in these water columns is used directly in the working areas where it is needed. The conventional route, in contrast, would first harness the hydrostatic head by converting it into mechanical energy using pelton wheel turbines which are placed in line with the vertical water pipes. This mechanical energy would then be reconverted into electrical or hydraulic energy for distribution to the workings.

The hydraulic energy in these pipes is exploited in two basic ways. Firstly, to clear the workings by using the impact force of water jets; and secondly, for powering the actuators in the various types of stoping equipment where the need for high forces in restricted spaces precludes the use of other forms of power. Such equipment includes rapid-yielding props, power packs, high performance rockdrills and rockbreaking impact hammers for non-explosive mining.

Hydro-power is also fully compatible with conventional mine cooling techniques. By chilling the water in surface refrigeration plants before it descends in pipes down the mine shafts, the cooling requirement of the entire mine can be met (Brown and Wymer [2]).

It is this combination of using one medium for ultimately all power and cooling requirements that holds such attraction in this concept. The biggest advantage, however, lies in its inherent simplicity and ease of maintenance. Some of the other noteworthy advantages of hydro-power are outlined below.

1.1.1 HEAT LOAD

Conventional stoping equipment adds a considerable amount of additional heat to the high geothermal heat loads in the stopes. Changing to hydro-power negates the need for heat rejection facilities as are required by conventional compressors, hydraulic oil power packs or electric motors.

1.1.2 FIRE HAZARD

No fire hazard is posed as water is inflammable. In addition, leakages from burst pipes or faulty connections will neither pollute the workings nor present significant financial losses for clean-up or replacement. Mineral oil on the other hand is costly, reduces yields by polluting the ore on leakage and presents a serious fire hazard.

Absence of high voltage or current power cables prevents electrocutions and fire hazards.

1.1.3 INFRASTRUCTURE

The number of support equipment and size of alternative stoping machinery is drastically reduced. Congestion in the stopes is thus significantly eased. This coupled with fewer mine services, greatly simplifies mine infrastructure and considerably increases safety in the mine.

Two major drawbacks are unfortunately linked to using pure water as the driving medium in stoping equipment: poor lubricicity and high corrosivity.

Of particular concern, with respect to these problems, are the reciprocating components in the rockdrills and impact hammers. Supply pressures to these components typically range from 15 to 20 MPa and oscillating frequencies of 5 to 50 Hertz are attained. These result in high surface loads and peak velocities of up to 10 m/s. Consequently the single biggest problem with these stoping machines are the high rates of surface degradation. The principal mechanisms responsible for these are:

- o cavitation and flow erosion
- o impact damage causing spalling and cracking
- o sliding wear - both adhesive and abrasive

The COMRO has tackled these problems from several angles: additive additions to confer corrosion protection and lubricicity to the service water (Lindsay-Scott and Wymer [19]); improved filtration and treatment plants; use of superior materials; and improved designs.

A good measure of success has consequently been achieved in overcoming most of the above problems. This has resulted in the implementation of a pilot plant, the operation of which has been very encouraging.

Problems do, however remain and finding solutions to minimize sliding wear damage and, more specifically, galling (adhesive wear) between metallic surfaces poses a big challenge. Adhesive wear is of particular interest as it is the only one of the four principal types of wear (adhesive, abrasive, corrosive and surface fracture) which can never be eliminated.

The obstacles that still need to be overcome for successful implementation of the hydro-power concept are thus identified as being of tribological nature. This thesis project will seek to make a contribution to help overcome these obstacles.

1.2 LONG TERM OBJECTIVES FOR THE HYDRO-POWER PROGRAMME

This research initiative is intended to make a short term contribution to the long term objectives of an ongoing research programme. These long term objectives, in turn, must be met in order to facilitate the eventual transition to hydro-power for all deep level gold mining.

The Chamber of Mines Research Organisation has identified three specific long term objectives, the realization of which are expected to contribute significantly to the successful implementation of hydro-power. These objectives are as follows:

- o produce ranking tables of material combinations suitable for use in stoping equipment operating on hydro-power,
- o extend the current boundaries of fundamental understanding of tribological interactions in general and the interactions at high speed reciprocating interfaces in particular, and
- o determine the threshold galling stresses for the ranked materials and development of empirical equations to describe the wear processes.

Motivation for the first objective comes about as a consequence to the proposed change of medium powering stoping equipment. A successful temporary transition was made from mineral oil and compressed air to water based emulsions. From there, a final transition is anticipated to pure mine service water. Because of this change in hydraulic medium, the

materials used in stoping equipment must now contend with poor lubricicity and high corrosivity.

Materials good enough for pre hydro-power machinery are thus no longer adequate for equipment operating on hydro-power. Only limited recourse can be made to the literature as tribological knowledge in respect of water lubrication is somewhat wanting, and design for wear as an engineering discipline is in its infancy stages.

Ranking tables will go a long way in determining to what extent existing stoping equipment designs can be upgraded to hydro-power through material upgrades, rather than complete redesigns. The former route is obviously favoured from an economic point of view and the fact that a move to hydro-power could be achieved much sooner and less reluctantly.

The second objective is of an academic interest, in that it seeks to clarify what bulk properties make for good "hydro-power materials". Ultimately, a better understanding of tribological systems will enable better materials to be developed in the future.

The third and last objective will help compare the performance of ranked materials with published information in the literature. In addition, empirical formulae could enable engineers to make definite predictions in respect of useful life for different materials under specific operating conditions.

With the field of tribology emerging only in recent years as an engineering discipline, the last two objectives are seen as somewhat ambitious and it is unlikely that this research initiative will make more than a modest contribution to these objectives.

1.3 OBJECTIVES FOR THIS RESEARCH INITIATIVE

To meet the long term objectives as set out in the previous section, a collaborative research agreement was initiated between the COMRO and the Department of Materials Engineering at UCT. The extent of the authors involvement in this ongoing research programme is outlined in fig. 1.1 below.

Because the programme hinges on stage 1 (the outcome of which was not certain at its inception), it was acknowledged that programme emphasis could change significantly. Consequently, the extent to which the short term objectives could be met was unknown.

In the first instance the authors brief was to investigate whether an existing high speed reciprocating sliding wear test rig could be used to meet the long term objectives outlined previously. This was to be done by way of testing various promising material combinations under different operating conditions on this test facility.

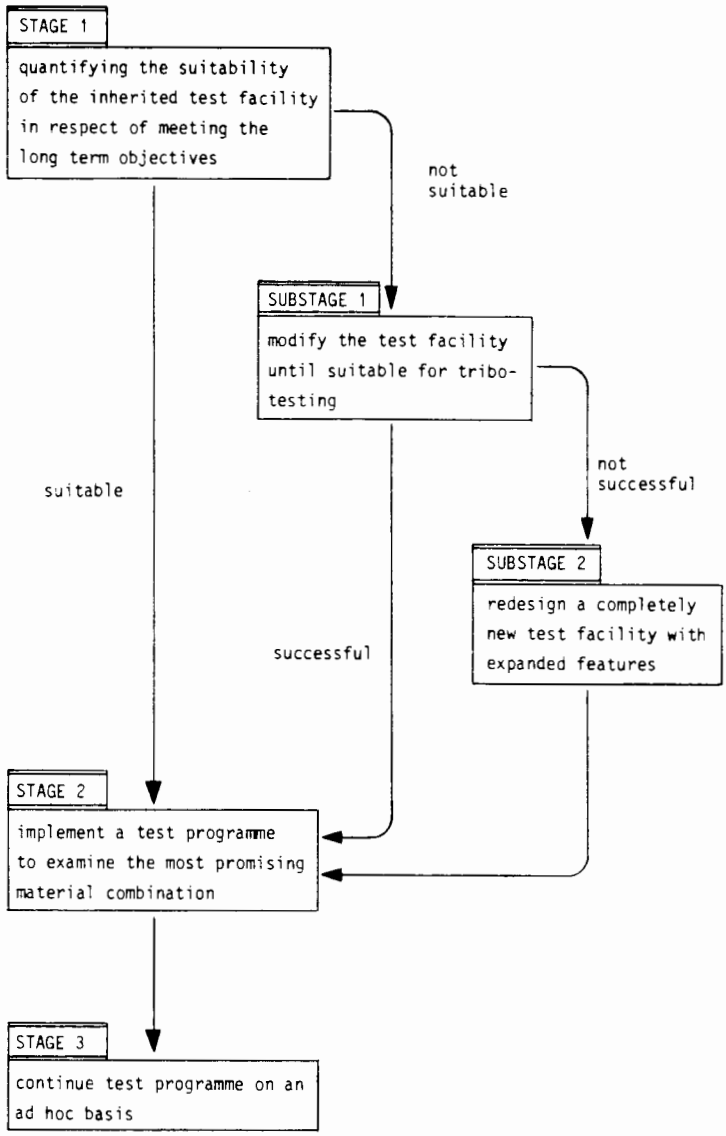

Fig. 1.1 STRUCTURE OF THE SHORT TERM CONTRIBUTIONS TO THE LONG TERM OBJECTIVES

If the test rig was to establish itself as yielding reproducible results on a consistent basis, then an extensive test programme was to be implemented as the second and final phase of the authors involvement. This test programme would look at the effects of surface finish, speed of reciprocation, loading, environments, temperature, pressure and lastly test duration to fully quantify the performance of a select group of different materials.

The purpose of this building up of experimental data is, on the one hand, to produce ranking tables and, on the other hand, to form a basis for compiling empirical equations and further basic understanding. Because the field of contender materials is vast, ranking tables for materials not covered in stage 2 would be tested under stage 3 on an ad hoc basis.

Should the outcome of stage 1 be unfavourable, however, stage 2 would be aimed for via substage 1. If modifications made under substage 1 were unsuccessful in respect of attaining reproducibility then all testing would be suspended. The author's attention would then focus on completely redesigning a new test facility.

Once substage 2 has been successfully completed the author would phase out of this project. Implementation of stages 2 and 3 would then be conducted by another researcher.

As it turns out, this research initiative was forced to follow the later route.

1.4 STOPING EQUIPMENT UNDER CONSIDERATION

Only the rockdrills and impact hammers are of interest in this thesis. Even more specifically, only those reciprocating components that are in metal to metal contact will be covered.

1.4.1 THE IMPACT HAMMER

The hydraulic impact rock breaking machine was developed for mechanized non-explosive mining using hydro-power as the powering medium. It consists of a chisel ended impact hammer mounted via hydraulic actuators to a machine frame. Housed in this frame are hydraulic generation systems and control mechanisms to manipulate the actuators. The frame in turn crawls along a guide rail which is linked to a rockhandling conveyor.

Based on the struck bit principle, the percussion mechanism in the hammer can deliver blows of 4 KJ at a frequency of 5 Hz. These blows fracture the rock, causing the collapse of the rock face. Fragmented rock is then scraped away from the workings and onto the conveyor for further handling.

To commence the firing stroke, the tool bit is driven hard up against the rock face. It is then struck by an impact head weighing 80 kg and moving through a stroke of 85 mm within the body of the machine. A maximum sliding velocity of 10 m/s is attained and fluid pressures rise to 18 MPa. Figure 1.2 shows one of these machines in operation underground.

During the return stroke, high pressure water forces the closure of the poppet valve mechanism. This causes the impact head to slide backwards, compressing hydraulic fluid in a cavity and gas behind an accumulator piston. The subsequent release of this pressure provides the thrust force during the firing stroke of the cycle.

Fig. 1.2 IMPACT ROCK BREAKING MACHINE IN OPERATION UNDERGROUND

Figure 1.3 gives a schematic representation of the internal components of an impact hammer. It also shows the approximate locations of bearings and seals. These were, until recently, made exclusively from polymeric materials. New moves are now afoot though to replace these bearings with metallic ones. This permits clearances to be tightened up and helps eliminate wobble of the impact head, which in turn causes localized contact and thus surface degradation.

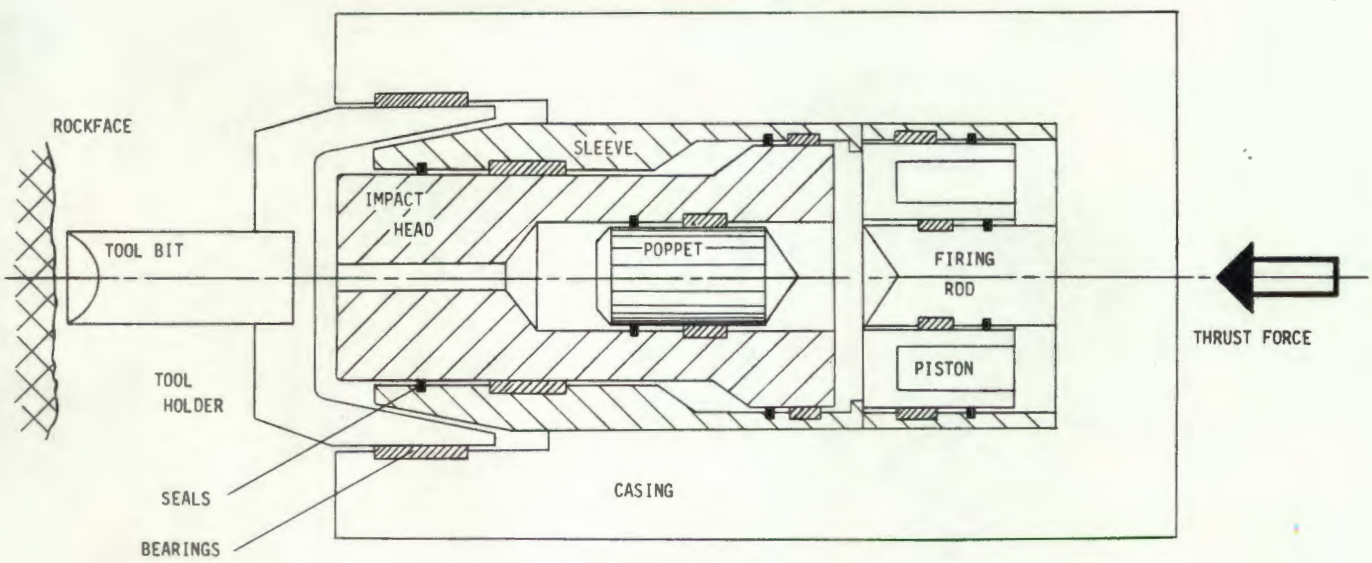

Fig. 1.3 SCHEMATIC LAYOUT OF ROCK HAMMER INNARDS

The authors prime interest is thus the reciprocating interaction of different metallic bearings.

1.4.2 THE ROCKDRILL

This too operates on the struck bit principle. Its operating mechanism consists of two separate actuators. One to produce rotary motion for the drill steel, the other to power the reciprocating impact piston. As in the case of the rock hammer, only the surface interactions of the reciprocating components are of interest.

Figure 1.4 shows a prototype rockdrill, operating on hydro-power, in operation underground.

Fig. 1.4 ROCKDRILL IN OPERATION UNDERGROUND

1.4.3 VELOCITY AND DISPLACEMENT PROFILES FOR THE STOPING EQUIPMENT

The velocity/time and displacement/time curves for the impact head in the impact hammer and piston in the rockdrill are presented in fig. 1.5 below for one complete operating cycle. In both cases similar trends are followed.

TABLE 1.1 OPERATING PARAMETERS FOR TYPICAL STOPING EQUIPMENT

		Frequ. (Hz)	Stroke (mm)	Max. Velocity (m/s)	P (MPa)	Blow Energy (J)
IMPACT HAMMER	Impact head	5	85	10	18	4000
	Poppet valve		32	20		280
	Piston		40	10		-
	Tool Holder		40	10		-
ROCK DRILL	Piston	50	28	10	35	70
	Spool Valve		9	20		-

ROCKDRILL

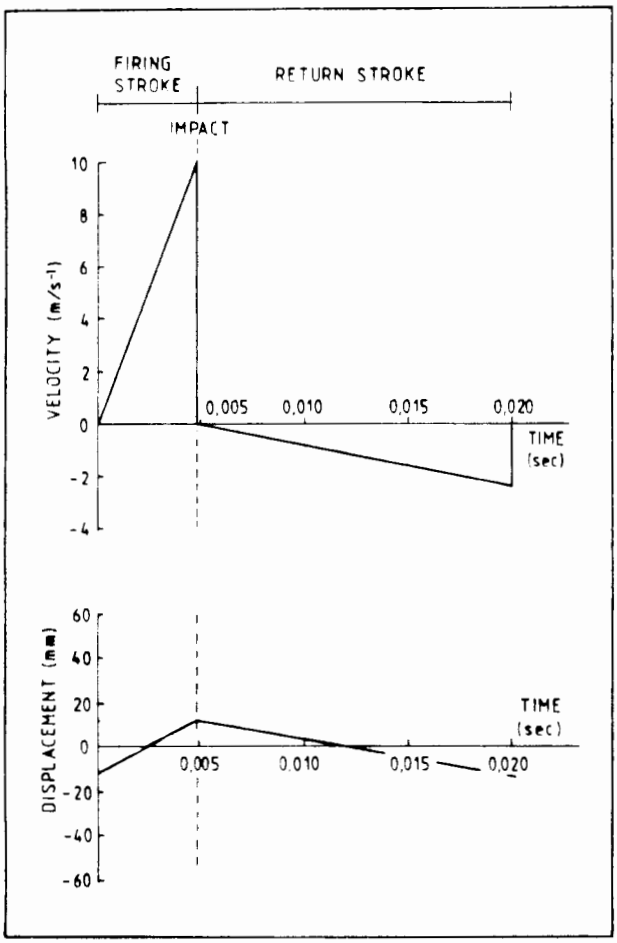

IMPACT HAMMER

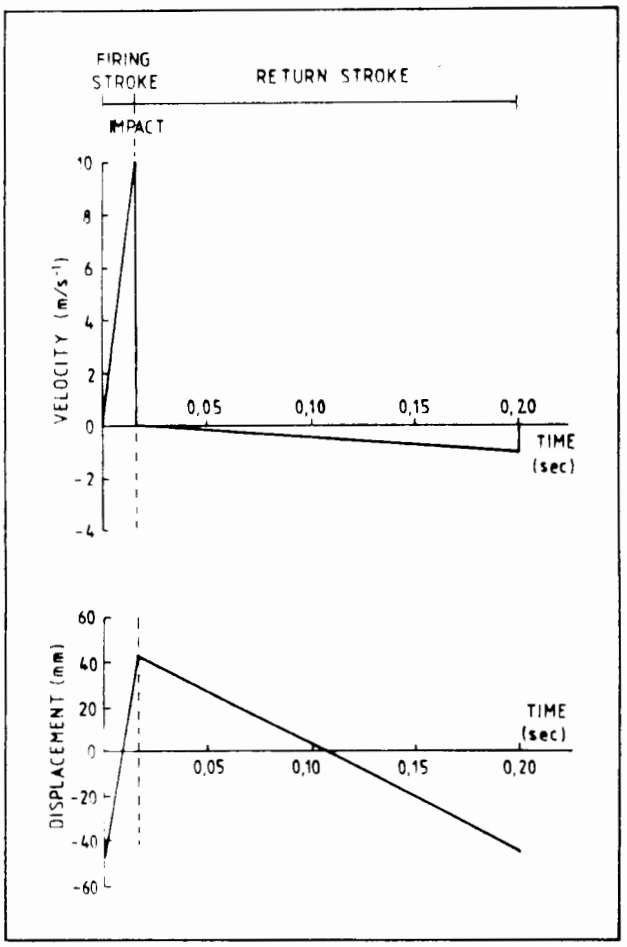

Fig.1.5 VELOCITY AND DISPLACEMENT PROFILES (Lloyd [3])

Table 1.1 summarises the salient features for both these components as well as the other reciprocating items in rockdrills and impact hammers.

1.5 THESIS LAYOUT

After presentation of a brief review of the literature relevant to this research initiative, the test programme which was implemented to meet the set objectives is discussed. This discussion will cover all aspects pertaining to test materials, specimen configurations, test facilities, test parameters and testing techniques used. The findings of the tests conducted on the various test facilities are presented and discussed next. A summary section follows in which all results obtained are summarized in terms of reproducibility levels attained and the dominating wear mechanisms observed.

Based on these findings, motivations are presented for the design of a new test facility. A formal problem statement and testing of the requirements, constraints and criteria for the new design are given thereafter. This is followed by chapter 5 which summarizes the specifications of the new test rig. Chapter 6 covers the concept formations stage for the new design which is then discussed in itS entirety in the succeeding chapter. An evaluation of the new test rig in respect of meeting its design requirements and the findings of a limited number of tests conducted on the rig are then presented. The conclusions that were arrived at and recommendations based on these conclusions make up the last two chapters respectively. All design calculations, general assembly drawings and component drawings are listed in appendices.

2.0 REVIEW OF THE RELEVANT LITERATURE

The discipline of "tribology" embraces all the work that was done in this research initiative and it therefore seems fitting to begin with an introduction into the topics which constitute this discipline. This is followed by a look at how wear progresses in sliding systems. Thereafter tribological testing and the modelling of both triboprocesses and of tribo-systems is reviewed. The chapter ends with a review of water as a lubricant and the work done by other researchers on bronze/brass-on-steel sliding systems.

2.1 DEFINITION AND SCOPE OF TRIBOLOGY

Tribology is a term that is derived from the Greek word "tribos", meaning rubbing. It was forwarded by a British committee on lubrication, chaired by Jost in 1966 and defined as "the science and technology of interacting surfaces in relative motion and of the practices related thereto" (as reported by Zum Gahr [4]). A more specific definition is offered by Czichos [5], who defines tribology as the study of the friction, lubrication, and wear of engineering surfaces that embraces all aspects of moving surfaces as well as the transmission and dissipation of energy and materials in mechanical systems."

Tribology, then, is a relatively new discipline which covers three specific topics : friction, wear and lubrication. Zum Gahr [4] suggests that each one of these topics can be interpreted as a dissipation process. Friction is a dissipation of energy, wear is a dissipation of surface structure and/or mass and lubrication is a dissipation of load between two solid bodies moving relatively to each other. Figure 2.1 presents a simplified "birds-eye view" of the subject of tribology as compiled by Archard [6].

Tribology is thus a truly interdisciplinary science and involves such traditional disciplines as fluid mechanics, solid mechanics, materials science, chemistry, physics, and mathematics. Research issues in tribology are therefore generally complex and require interdisciplinary team approaches. (Jahanmir [7]).

Being synonymous with reliability, long life and energy savings, tribology has emerged as one of the most important fields in science and engineering. Zum Gahr [4] cites several economic studies done in different industrialized countries in recent years, which peg economic losses due to friction, wear and corrosion to between 1% and 4.5% of the gross national product.

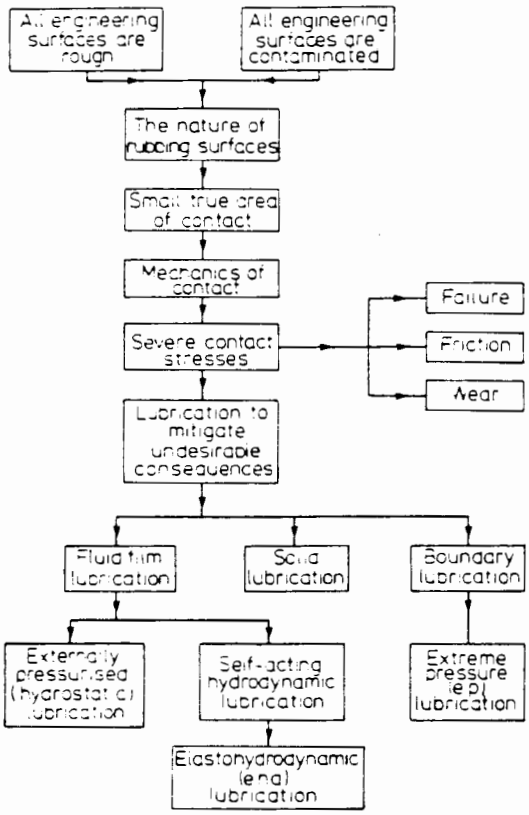

Fig. 2.1 BASIC TRIBOLOGY (ARCHARD [6])

The need for systematic research and improved transfer of theoretical knowledge in this field are today well recognized. Research activities in different countries (Czichos [8], Roberts [9]) emphasize the acceptance of and importance placed on this discipline.

2.2 SURFACE TOPOGRAPHY

In practice, all engineering surfaces are rough. In tribological terms this is their first important characteristic, as it implies that when two nominally flat surfaces are loaded together, they touch only over a very small part of their apparent area of contact. This difference between the apparent and real area of contact is clearly presented in fig. 2.2.

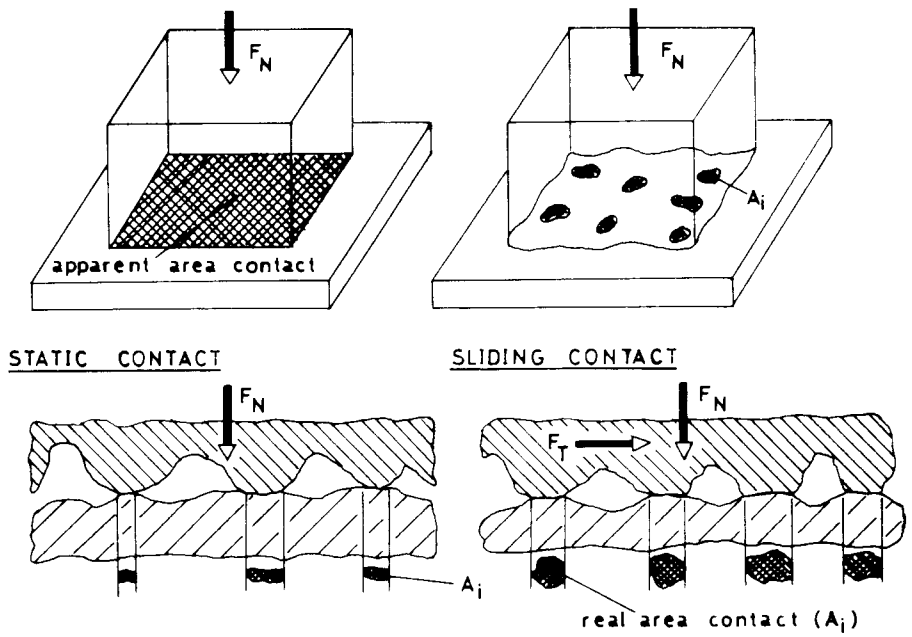

Fig. 2.2 APPARENT AND REAL AREA OF CONTACT (Zum Gahr [4])

The ratio of apparent to real area of contact can be several orders of magnitude and depends on essentially three factors:

- o distribution of surface irregularities
- o contact forces, F_n
- o yield strength of the softer material

The imperfections of a typical surface take the form of a series of peaks and valleys which vary both in height and spacing and result in a texture which, in feel and appearance, and in properties generally, is often characteristic of the process employed in its production (BS 1134 [10]). These surface irregularities are generally termed "asperities" (hills and valleys on a microscopic scale).

Figure 2.3 below shows a schematic of a typical 'rough' surface topography. The various geometric components that make up this solid surface are depicted in fig. 2.4.

A large number of instruments which measure surface roughness of engineering components have been developed. Of these, the stylus instruments are by far the most commonly used. In these devices, a fine diamond stylus traverses the surface and its vertical movements are amplified and recorded. The resultant profile represents only one pass in a linear direction across a three-dimensional surface. Despite several disadvantages, it has proved versatile and reliable in both the manufacturing and the research environment. It is also the instrument by which national standards are defined (Sherrington and Smith [11] and [12]). The disadvantages with this instrument are that:

- o it only provides information for a profile section of a surface i.e. two-dimensional (by recording several parallel profiles, each displaced laterally from the previous one by a short distance, an areal record can, however, be built up)
- o it relies on direct contact between stylus tip and surface of interest and therefore permanent damage can occur on the surface
- o it operates slowly, requires rigid supports and can not be used as an "in-process" measurement technique.

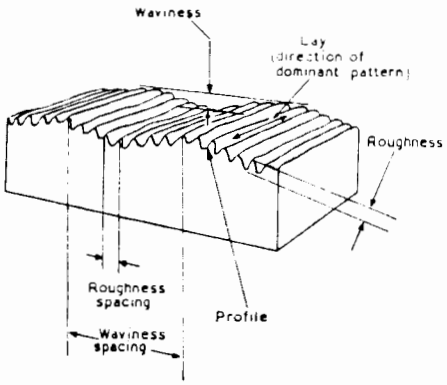

Fig. 2.3 SCHEMATIC REPRESENTATION OF SURFACE TOPOGRAPHY (BS 1134 [10])

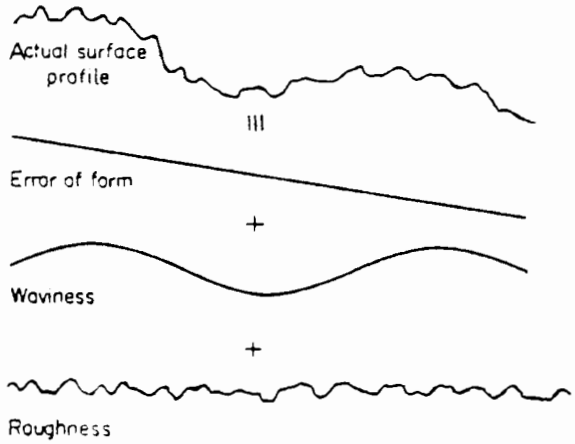

Fig. 2.4 CONSTITUENT GEOMETRIC COMPONENTS OF A SOLID (HALLING [13])

Today optical methods are beginning to replace stylus instruments as they suffer from none of the above limitations. Most of the current research programmes are, however, still based on two-dimensional surface roughness interpretations. It is for this reason and the lack of access to three-dimensional surface scanners that two-dimensional surface profilometry is used in this research initiative.

The internationally adopted parameter of surface roughness is the centre-line-average (CLA) height method of assessment, which is also known as the roughness average, R_a. This CLA value represents the arithmetic mean of the vertical deviations of the profile from the centre line, i.e. a line which is positioned such that the sum of the areas above and below it are equivalent. This is shown in fig. 2.5.

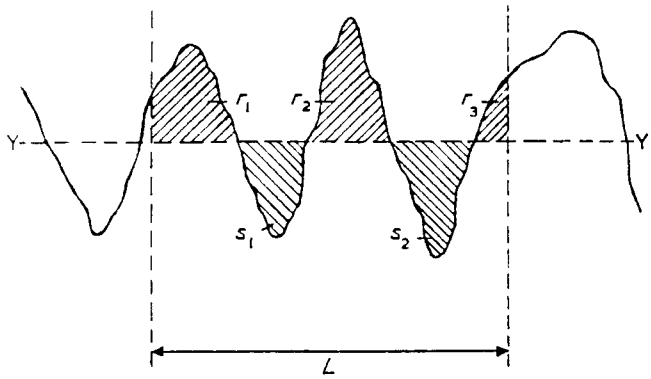

$$R_a = \frac{\Sigma \text{ areas } r + \Sigma \text{ areas } s}{\text{sample length, } L}$$

Fig. 2.5 THE CALCULATION OF R_a (BS 1134 [10])

Some caution is required in the use of this parameter, as it concerns itself only with the vertical deviations and provides no information about the slopes, shapes and sizes of the asperities or about the frequency and regularity of their occurrence. Identical CLA values can therefore be obtained for different profiles as depicted in fig. 2.6.

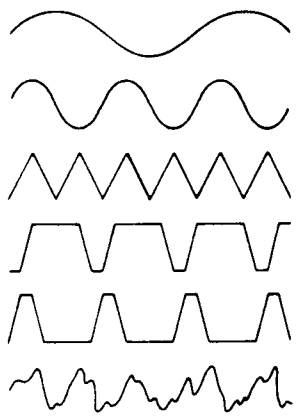

Fig. 2.6 PROFILES WITH IDENTICAL CLA VALUES (Halling [14])

2.3 LUBRICATION

Any material capable of reducing friction, wear or surface damage of sliding components is termed a lubricant. It functions by preventing or mitigating the formation of strong adhesive junctions between the high spots, or asperities, on opposing surfaces. Rowe [6] states that this may be accomplished by one or more of the following mechanisms:

- o the complete separation of the surface by a sufficiently thick hydrodynamic or elastohydrodynamic (EHL) film which prevents opposing asperities from contacting (regime IV in fig. 2.7).

- o formation of surface films by either physical or chemisorption of a gas (vapour), liquid, or compounds dissolved in a liquid (eg. oxide films)

- o formation of a tenacious surface film by chemical reaction of the lubricant with the metal surface

- o prior treatment of one or more of the surfaces with some material to form a tightly adhering solid film or coating.

Lubricants can thus be in a solid, liquid or gaseous phase. For the purpose of this research initiative, only liquid lubrication is of interest.

Over and above their primary function of controlling friction and wear by separating two surfaces in relative motion by way of an easily sheared fluid, liquid lubricants have two secondary functions. These are their ability to firstly remove wear debris, and secondly frictional heat from the interacting surfaces.

Depending on the thickness, (h) of the lubricant film, the materials, the interfacial height distribution of the film, the operating conditions and the degree of geometrical conformity, different lubrication modes can be distinguished (Czichos [5]). These are:

I. Boundary Lubrication (Also termed 'boundary friction zone' or 'thin (unstable) film')

II. Mixed film lubrication (also termed 'partial EHD lubrication' or 'quasi-hydrodynamic')

III. Transition Zone lubrication (usually incorporated under II)

IV. Hydrodynamic lubrication (also termed 'thick (stable) film' or'full fluid film'; also includes elastohydrodynamic, EHD, lubrication)

These zones are usually depicted in a 'Stribeck Curve' which plots the 'Hersey Number' as a function of the friction coefficient, μ. This Hersey Number is made up of the lubricant viscosity, Z, the relative sliding velocity, N and normal load, P. Figure 2.7 shows a typical Stribeck Curve.

In regime IV the surfaces are prevented from coming into direct contact, and wear - with the exception of surface fatigue wear, cavitation and flow effects - is essentially eliminated. Any resistance to motion is thus due only to the shear resistance or viscosity of the lubricant itself. If the Hersey Number decreases substantially, the number of asperity interactions increases as the film thickness becomes too thin to effectively prevent asperity contact through the film. This situation is termed boundary lubrication (I). In this regime the bulk rheological properties of the lubricant become less important and load is carried almost entirely

through the deformation of the asperities. Regimes II and III represent situations intermediate to boundary and hydrodynamic lubrication, where only a portion of the load is transmitted by the fluid pressure.

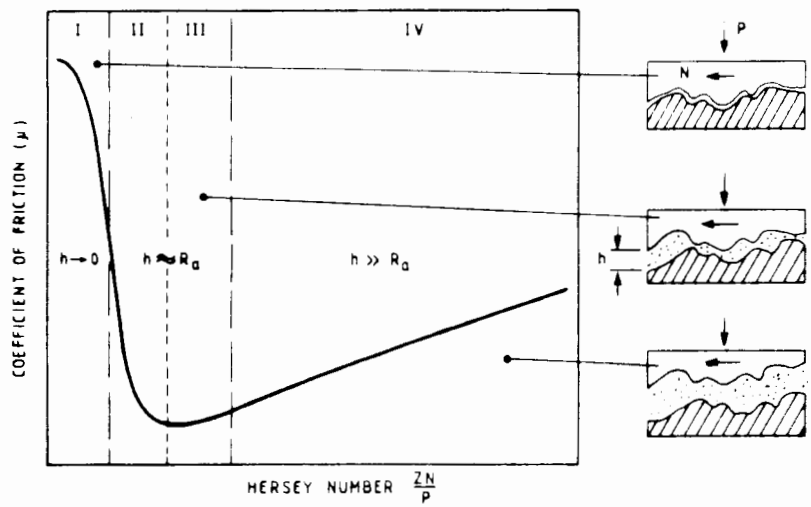

Fig. 2.7 STRIBECK CURVE (adapted from Smith [15] and Czichos [5])

Being dependent on speed, it is clear that irrespective of what regime constitutes normal operation for a given system, boundary lubrication will occur during starting or stoping. As the bulk of wear processes occur due to contact mechanics, wear will occur during the time spent under boundary lubrication.

2.4 FRICTION

Friction is a central issue in tribology. Halling [14] states that friction is due to some interaction between opposing surfaces and that this results in resistance to relative motion. As the surfaces move relative to each other, work is done by the forces causing this motion i.e. there is an energy loss at the contacting surfaces.

It was originally found experimentally that there are three basic 'laws of friction'. Amontons (1699) is credited with the first two, which are obeyed over a fairly wide range of conditions. The third law was introduced by Coulomb (1785) but the range of its applicability is much smaller.

- o 1st law : friction is independent of apparent area of contact between contacting bodies
- o 2nd law : friction force (F) is proportional to load (W) between bodies i.e. $F = \mu W$, where μ is a constant of proportionality termed the friction coefficient
- o 3rd law : kinetic friction is nearly independent of sliding speed.

These laws are in general use in the field of applied mechanics. But, because they do not hold for all cases, they are regarded as empirical laws of limited value only in the discipline of tribology.

Tabor [16] refers to three main factors which are today universally recognised as being involved in friction. These are : the true area of contact, the strength of the interfacial bond and thirdly the deformation process involved when these interfacial bonds are broken during sliding. The current state of knowledge in these fields is limited and many questions remain unanswered. Tabor [16] gives an excellent breakdown of what is known and which questions need still to be answered. Jahanmir [7] concurs with this, stating that much research still needs to be done. He also reiterates that there is no widely accepted theory for predicting friction. He ascribes this to the fact that friction depends on many complex processes that occur at the interface.

Nonetheless various theories have been advanced. Of these the adhesion theory has emerged as the most popular. The basis of this theory is the fact that when metal surfaces are loaded against each other they contact only at isolated high points. The real area of contact is thus only a fraction of the nominal area of contact (see fig. 2.2). Tabor [16] states that these surface asperities are themselves deformed elastically, plastically, viscoelastically or in a brittle manner and the area of contact is determined by deformation properties of the material and detailed topography of the surfaces. According to the adhesion theory, these contacting asperities deform until such time as they can support the given load. This intimate contact in turn allows strong adhesion to take place and the junctions 'cold-weld'. To satisfy the kinematic requirement when motion occurs, these junctions must then be sheared. Lim and Ashby [17] on the other hand believe that the average area of contact of an asperity remains constant and that it is their numbers and not size which increases with load. They cite several other investigators that concur and indirect experimental evidence appears to support this view.

The adhesion theory is, however, of limited use because it can not explain the discrepancy between experimentally measured and the theoretically predicted friction coefficient. Suh and Sin [18] have tried to explain the genesis of friction with a new theory which postulates that the frictional force (and therefore μ) are not inherent material properties but instead are affected by sliding distance and environment. The coefficient of friction, μ does not remain constant but instead moves about in friction space during sliding. They believe μ to be composed of three components : μ_d due to the deforming asperities, μ_p due to plowing by wear particles entrapped between the sliding surfaces and hard asperities; and μ_a due to the adhesion. With this theory Suh and Sin [18] have been able to narrow the gap between experimental and theoretical data for μ.

2.5 THE RELATIONSHIP BETWEEN FRICTION AND WEAR

Tabor [34] quotes from a conference in 1937 in which it was already recognized that "it is futile to predict wear reducing values from friction tests". Schuhmacher [20] observed that some metals sustain high friction and low wear whereas others exhibit low friction and high wear. High values of wear are therefore not necessarily associated with high values of friction. Ko [22] states that for common engineering materials under lubricated conditions, wear rates cover a range of approximately five orders of magnitude (i.e. 10^5) while values of coefficient of friction cover a range of only three.

De Gee [21] observed that wear in general is caused by overstressing of the surface zone of materials due to normal and tangential forces, with metal transfer from one mating component to the other possible but not necessary. This implies that friction (resulting from adhesive forces and ploughing) and the dynamic strength properties of other materials (subjected to friction) are equally important in determining wear resistance. He thus concludes that there can be no wear without friction. This does, however, not automatically imply that it would in general be possible to predict wear reasonably accurately from friction readings.

Kragelskii [23] reiterates the fact that neither friction nor wear are properties pertaining to the material, but are in fact characterized by an engineering system and therefore not interdependent.

2.6 WEAR CLASSIFICATIONS

Wear is generally defined as "the progressive loss of substance from the operating surface of a body occurring as a result of relative motion at the surface". This somewhat simple definition embraces many complex wear mechanisms involving a diversity of processes. Most of these are not fully understood and according to Ko [22] confusion exists to this day as to the classification of wear.

The attempts at systematic study of failure of surface layers during friction have resulted in a great number of classifications of wear types. According to Kragelskii [23] there is no universally accepted classification. He ascribes this to there being no clear-cut features on which to base such classifications. All classifications put forward thus far agree on adhesion and abrasion as being two distinguishable types of wear. There is, however, no agreement in describing other types of wear. In response to this Kragelskii [23] proposed that wear should, in the first instance, be catalogued according to whether molecular attraction (adhesion) or mechanical deformation (abrasion) are the dominating interaction. Secondly, the failure should be classified according to the following factors:

- o the nature of the main interaction
- o the type of deformation
- o the characteristic changes in the surface layer
- o the characteristic loading

In his excellent review paper on metallic wear, Ko [22] has summarized the various schemes according to which wear has been classified in the literature. These are:

- o by relative motion
- o by mechanisms of particle removal
- o by severity

Figure 2.8 is an attempt by Ko [22] to group together the various schemes (listed above) connecting the various motions with the possible basic mechanisms involved in the wear processes and the characteristic modes of damage that may result.

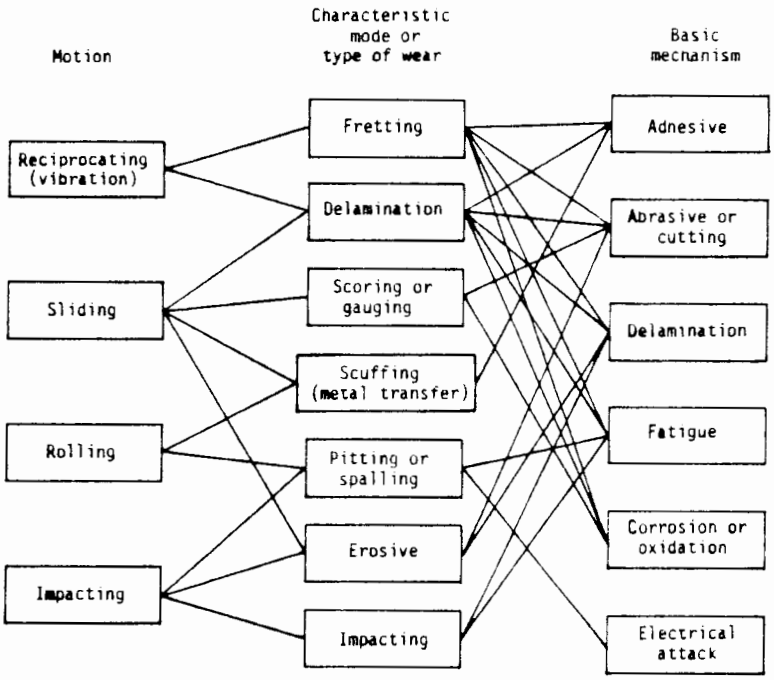

Fig. 2.8 CLASSIFICATION OF WEAR (Ko[22])

Zum Gahr [4] suggests that delamination and electrical attack represent merely a special case of what is a basic mechanism of surface fatigue and tribochemical reaction respectively. He therefore reasons that there are only four main wear mechanisms. These are schematically represented in fig. 2.9.

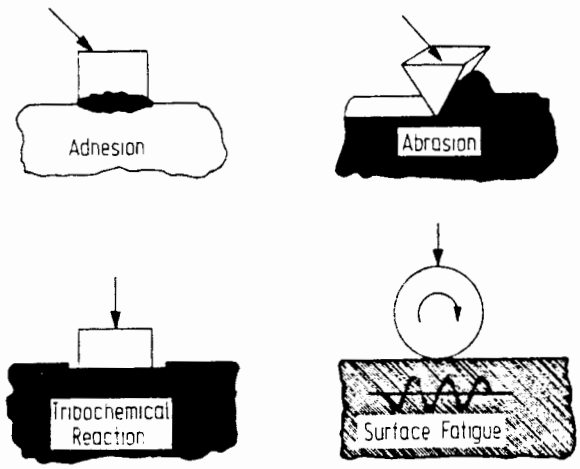

Fig. 2.9 THE FOUR MAIN WEAR MECHANISMS (Zum Gahr [4])

The West German Standard Din 50 320 [24] concurs with this classification as all other classifications presented in the literature can be grouped into one of these four mechanisms. DIN 50 320 defines each of these four basic mechanisms as follows:

- o ADHESION : formation and breaking of interfacial adhesive bonds (e.g. cold-welded junctions)
- o ABRASION : removal of material due to scratching
- o SURFACE FATIGUE : fatigue and formation of cracks in surface regions due to tribological stress cycles that result in the separation of material (e.g. pits).
- o TRIBOCHEMICAL REACTIONS : formation of chemical reaction products as a result of chemical interaction between the elements of a tribosystem initiated by tribological action.

2.7 ADHESIVE WEAR IN METAL-ON-METAL SLIDING SYSTEMS

This is the most fundamental of the four principal wear mechanisms because it is a basic phenomenon that takes place whenever two solid surfaces are in direct rubbing contact. Because the components of interest for this thesis undergo boundary contact during their oscillating motion and because this form of wear can not be 'engineered out', only this wear mechanism is relevant to this investigation.

Whenever two surfaces slide against each other they will contact over isolated asperities. These will deform plastically to support the applied load, and adhesive junctions are formed. On relative motion between the contacting surfaces, these junctions are ruptured and frequently transfer of material will occur from one surface to the other.

Figure 2.10 below shows different separations of surfaces welded together according to Zum Gahr [4]. In case (a) the contacting surfaces are disintegrated at the former interface if the shear strength of the junction is less than the strength of both materials.

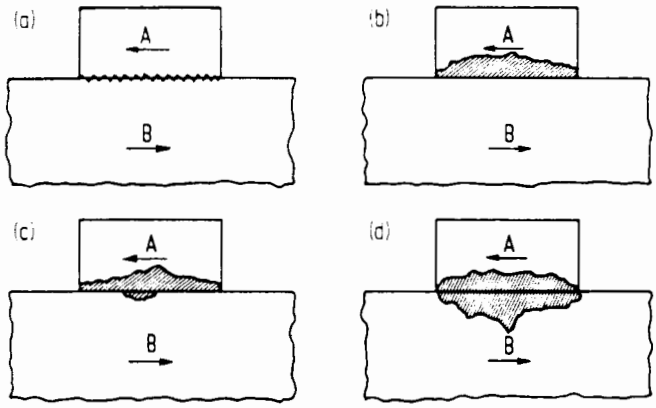

Fig. 2.10 DIFFERENT SEPARATIONS OF SURFACES WELDED TOGETHER (Zum Gahr [4])

This situation is typical of cases where oxide films reduced adhesion. Case (b) depicts characteristic rupture when one material is softer i.e. if strength of A is substantially less than either junction or B. For junctions of high strength, material A will rupture if its strength is lower than B (Case (c)). For similar metals of equal strength the junction exceeds both A and B in strength because of work hardening and when shear occurs a lump is torn out of both surfaces.

Ko [22] states that in general adhesive wear is more severe under unlubricated conditions. This is not unexpected because the absence of a lubricant/separating layer promotes greater asperity interaction and therefore adhesion.

Many theories of adhesion have been presented in the literature. The main groups of mechanisms of adhesion according to Zum Gahr [4] are:

- mechanical-interlocking theory
- diffusion theory
- electronic theory
- chemical theory
- adsorption theory

In sliding contact, wear can occur due to any of the four basic mechanisms previously listed. These are depicted in fig. 2.11 below, where (a) refers to formation of adhesive junctions, material transfer and grooving; (b) surface fatigue due to repeated plastic deformation on ductile solids; (c) surface fatigue resulting in cracking on brittle solids; (d) tribochemical reaction and cracking of reaction films.

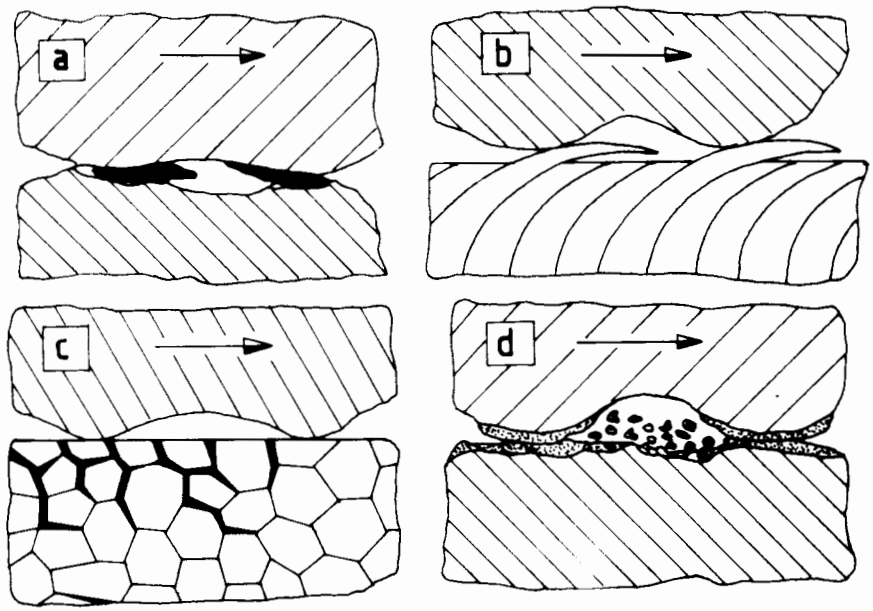

Fig. 2.11 WEAR MECHANISMS DURING SLIDING CONTACT (Zum Gahr [4])

Galling according to Schuhmacher [20], [25] is an insidious form of adhesive wear and almost always results in seizure of the mating surfaces. When two surfaces are loaded against one another, the contacting asperities form strong bonds due to the high localized pressure and heat generation by subsequent motion. If these bonds do not sever, fracture takes place in both surfaces and gross damage - galling results. The onset of this gross damage is termed the 'galling threshold stress'.

2.8 WEAR VARIABLES AND THE PROGRESSION OF WEAR IN SLIDING WEAR

According to Ko [22] the majority of variables affecting metallic wear fall into four categories:

- o OPERATIONAL - normal load (pressure), sliding distance, sliding time, number of cycles, relative sliding velocity, impact velocity, slide/sweep and slide/impact ratios, temperature rise

- o GEOMETRICAL - area, clearance, shape, size and finish

- o MATERIAL - mechanical and physical properties of contacting materials and lubricants

- o ENVIRONMENT - water chemistry, temperature, presence of medium (eg. air, gas, water, steam)

These variables are affected by other factors and are heavily interdependent. It is thus possible to find two opposing trends for one variable when it is subjected to two different set of test conditions or two different material combinations.

Peterson [6] summarized the general trends of selected operational variable for different lubrication conditions. Figure 2.12 below shows the effect of time, load, temperature, velocity and film thickness on wear rate for unlubricated (1), boundary lubricated (2) and fluid film lubricated (3) conditions; with the following fixed conditions: material, lubricant, viscosity, geometry, fluid and ambient temperature and pressure.

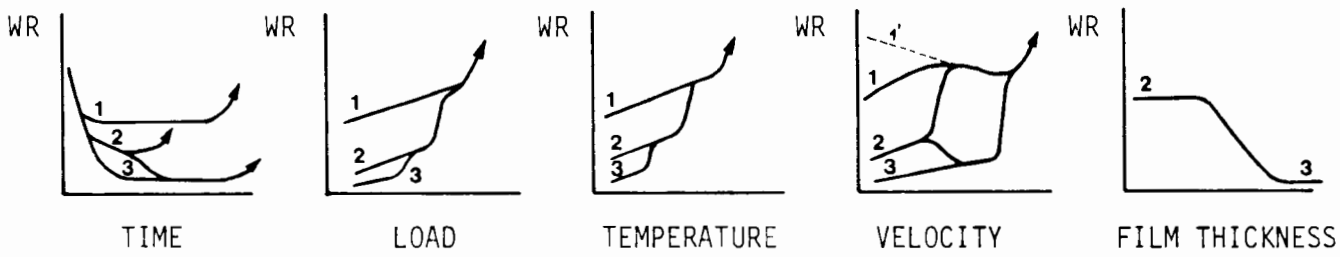

Fig. 2.12 WEAR RATE AS A FUNCTION OF DIFFERENT OPERATING VARIABLES (Peterson [6])

What is interesting to observe in all these trends is that a transition point or critical value occurs sooner or later with a rapid increase or decrease in wear rate.

Work done by Hirst and Lancaster [26] on dry sliding wear of brass on steel showed wear rate as a function of sliding velocity to decrease steadily to a minimum with increasing velocity and then rise sharply at a speed at which a critical temperature is attained (see also fig. 2.21 in section 2.13). This is depicted in the velocity graph of fig. 2.12 as 1'.

The progression of wear according to Sarkar [27] usually takes on a "curve linear" pattern with a rapid increase in volume loss during the so called running in stages and a constant rate of volume loss thereafter. Peterson [6] concurs with this but expands further on the stages of wear depending on the lubricating conditions as depicted in fig. 2.13 below.

Surface roughness affects the load carrying and lubricating capacity of the contacting surfaces. Generally the rougher the surface the greater the wear. Very smooth surfaces on the other hand (according to reference [28] below about 0.20 μm) lack the ability to store wear debris and/or lubricant due to the absence of valleys between asperities. In addition,

very smooth surfaces increase molecular interaction forces that promote cold welding. The force per unit area will however be smaller for smooth surfaces as more asperities per unit area are available to carry the applied load.

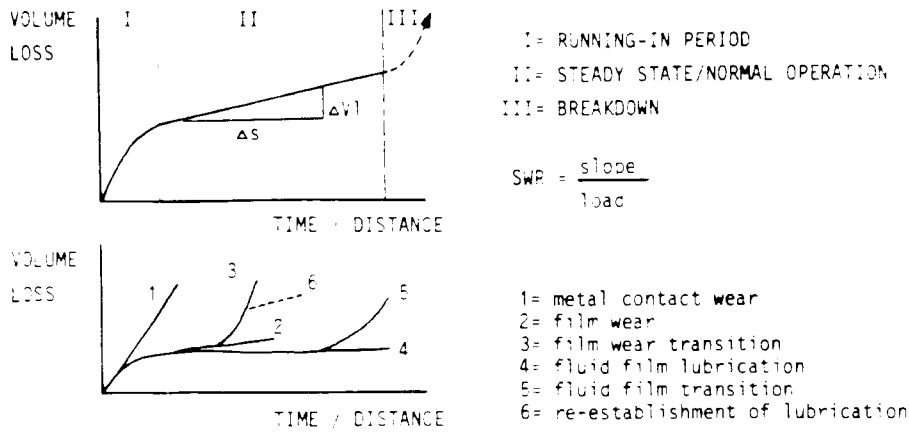

Fig. 2.13 EFFECT OF SLIDING TIME/DISTANCE ON WEAR VOLUME FOR METAL ON METAL SLIDING (after Peterson [6] and Zum Gahr [41]).

Krause and Senuma [29] state that surface temperature is the only factor which directly influences all tribological processes. In addition, many physical, chemical, thermal and metallographic properties are temperature dependent. Fig 2.14 below shows how the essential variables influencing wear are interrelated.

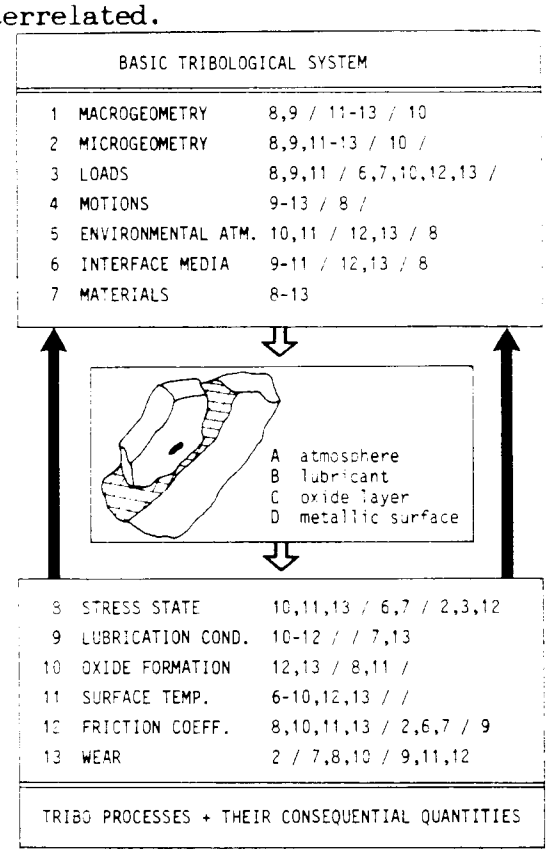

Fig. 2.14 THE RELATIONSHIP BETWEEN WEAR VARIABLES (after Senuma and Krause [26]).

2.9 WEAR THEORIES, WEAR COEFFICIENTS AND WEAR MAPS

It is generally difficult to formulate unequivocal laws of wear. Broadly speaking, wear increases with load and running time, but there are many exceptions to this and usually hard materials wear less than soft materials. Peterson [6] is therefore of the opinion that in discussing wear mechanisms, one can do so only in a qualitative rather than quantitative manner. Nonetheless the following three "laws of wear" are presented as they are correct more often than not:

- o Wear volume α load
- o Wear volume α sliding distance
- o Wear volume α {hardness}$^{-1}$
  (according to Lenel [31] this hardness is not the bulk hardness but rather that which is attained at the wear interface during relative motion)

Wallbridge and Dowson [30] state that it is usual for the quantitative analysis of wear rates in sliding wear to describe the rate of wear in one of two ways:

- o by the dimensionless Holm-Archard wear coefficient K, defined by

  $K = VH/(Lx)$ or

- o by the simpler, empirical wear factor, k or specific wear rate, SWR as proposed by Lancaster, given by

  $SWR[k] = V/(Lx)$ [mm³/Nm], where V = volume loss [mm³]
  H = hardness [N/mm²]
  L = applied load [N]
  x = sliding distance [m]

The later has proved more useful for the comparison of the wear behaviour of different materials, but K is frequently used as a basis for the comparison of wear data. Both of these have therefore been used in the presentation of results in chapter 3.0.

According to Ko [22], K is a proportionality number that may be interpreted as the probability of producing a wear particle at any given asperity encounter. K rarely takes on a constant value but will vary depending on the tribological conditions present. Thus, depending on the test conditions, design and contact geometry, different K values are possible for the same material combination. Caution therefore needs to be exercised when quoting values for K.

Rabinowicz [32] has compiled tables of typical wear coefficients that can be expected for sliding systems under different conditions of lubrication for each of the four basic wear mechanisms (see fig. 2.15) and for adhesive wear separately (fig. 2.16).

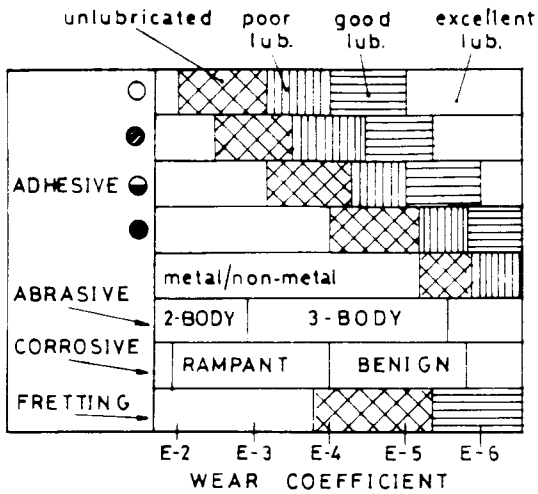

Fig.2.15 RANGE OF WEAR COEFFICIENTS FOR SLIDING WEAR (Rabinowicz [32])

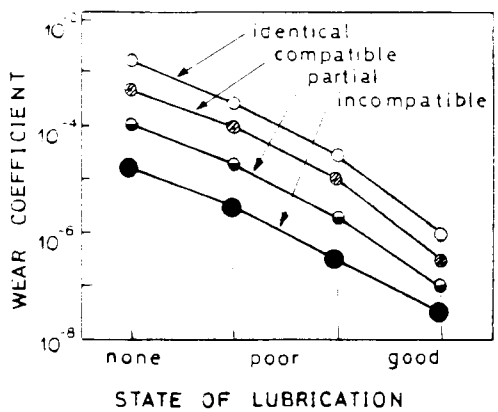

Fig.2.16 WEAR COEFFICIENTS FOR ADHESIVE WEAR AS A FUNCTION OF LUBRICATION (Rabinowicz [32]; Compatibility refers to the extent to which metals are alike)

More recently Rabinowicz [33] has condensed this information for metal on metal sliding systems on the chart shown in Fig. 2.17.

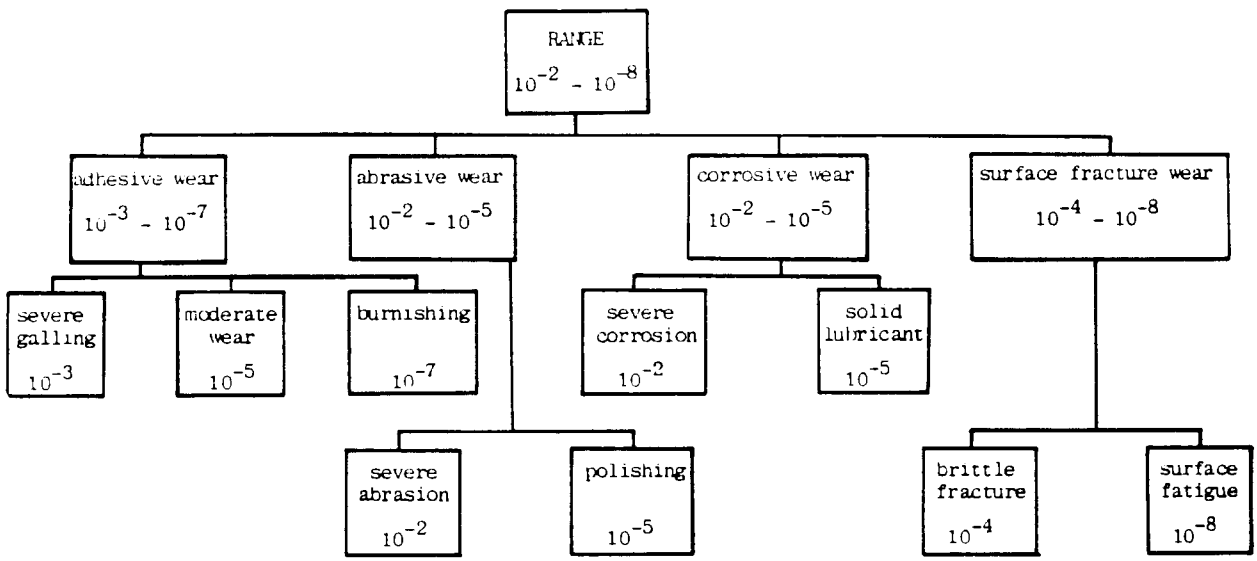

Fig. 2.17 TYPICAL RANGES OF WEAR COEFFICIENT K FOR METAL-ON-METAL SLIDING SYSTEMS (Rabinowicz [33])

The wear mechanism of principal interest in this investigation is adhesive wear. According to fig. 2.17 typical wear coefficients for this mechanism span over four orders of magnitude from 10^{-3} to 10^{-7}. As the other three wear mechanisms cover K values that overlap those of adhesive wear it becomes clear that dominant wear mechanisms cannot be established soley on the basis of a K value. Micro- and macrographical evidence is therefore needed to more fully quantify a wear mechanism.

Tabor [34] questions the use of conducting research into these specific wear mechanisms, because in practical wear situations it is not obvious that a single wear mechanism is dominant. Researchers concentrating on a particular wear mechanism should therefore make an effort to indicate the condition under which their mechanism ceases to be important.

Tabor [34] therefore suggests that in order to determine the relationship between mechanisms, "wear-mechanism-maps" should be constructed. These summarize data and models for wear, showing how the mechanisms interface, and allowing the dominant mechanisms, for any given set of conditions, to be identified. Jahanmir [7] feels that this is probably the best means of classification of wear mechanisms in an organized fashion. This concept was refined by Lim and Ashby [17] who followed two converging paths in constructing these maps: an empirical path (plotting normalized experimental data and identifying mechanisms at each point by observation) and secondly a physical modelling path (by model based equations describing wear rate caused by each mechanism and combining these into a total picture). Figure 2.18 below shows a typical wear map for a steel-on-steel sliding system.

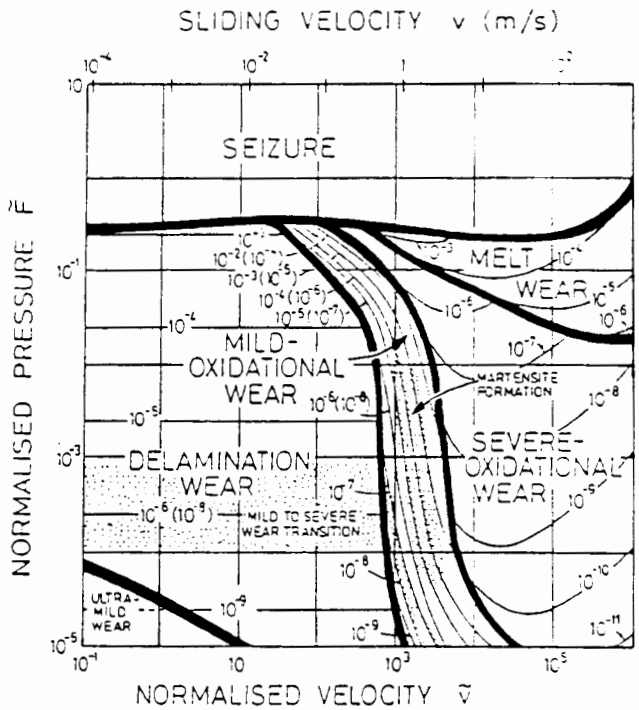

Fig. 2.18 WEAR-MECHANISM MAP FOR DRY STEEL-ON-STEEL SLIDING SYSTEM (Lim and Ashby [17])

The diagram uses normalized axes because this allows the important effects of surface hardness, thermal conductivity and sample geometry, as well as data from different test configurations and different materials to be plotted together. Thus a single diagram can describe, approximately, the wear behaviour of a wide range of steels as a function of load and velocity. Peterson [35] concludes that wear information can thus be reduced from theory to practice and in that manner become accessible to

design engineers. Again, caution must be exercised as these graphs are not precise but merely summarize the current, imperfect understanding of sliding wear.

2.10 SYSTEMS ANALYSIS

The foregoing sections have shown that wear of materials is not simply a material property but instead depends on the manner in which the materials and components involved in the wear process interact. Ko [22] stresses that wear must therefore be considered as a general characteristic of a given system.

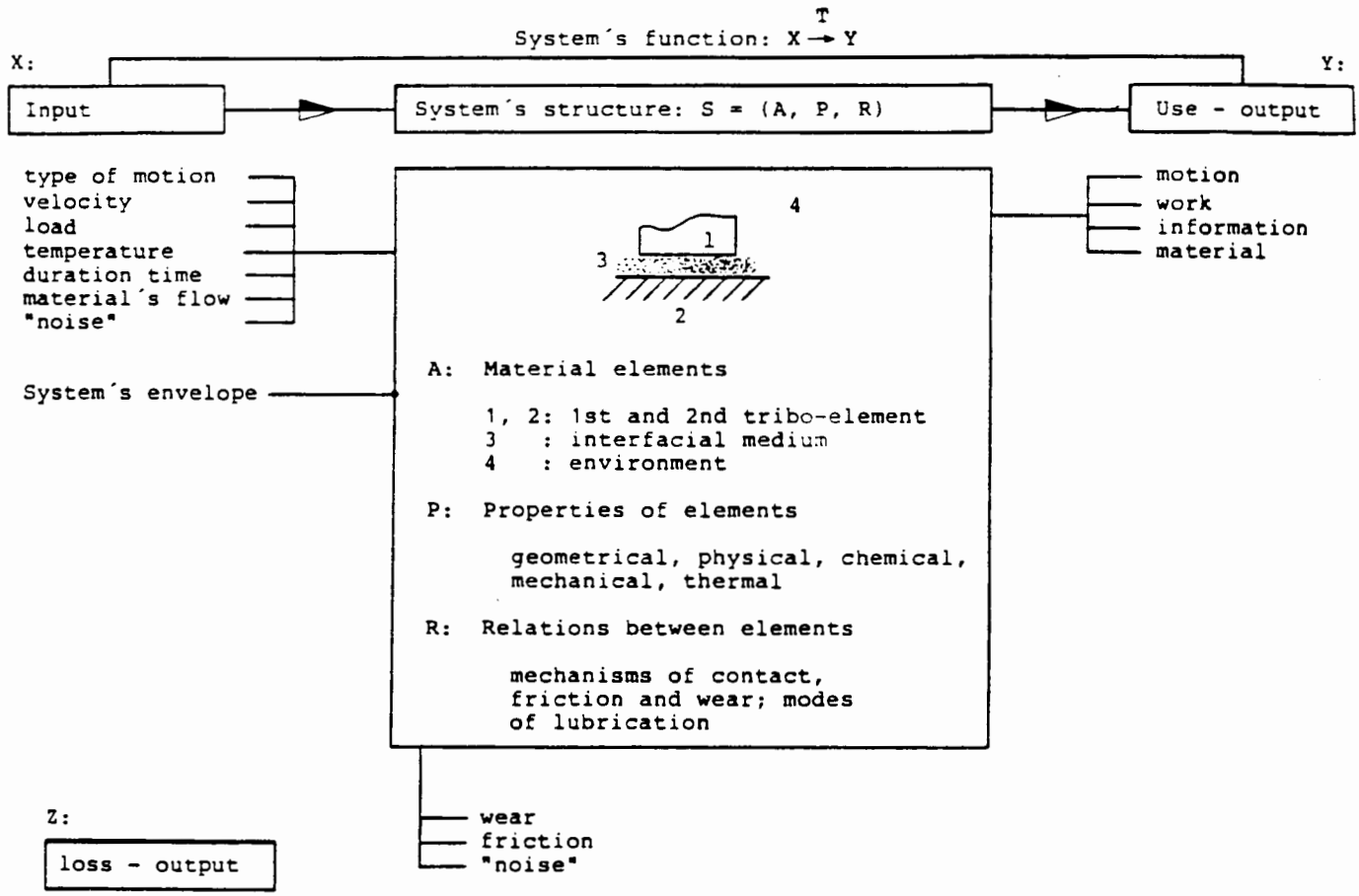

Fig. 2.19 GENERAL "INPUT-OUTPUT" DESCRIPTION OF A TRIBOSYSTEM (Frees [36])

Using systems thinking for tribological processes can be very useful in solving wear problems. Good summary descriptions of systems analysis techniques are given by Zum Gahr [4], Frees [36] and Kragelskii, Dobychin and Kombalov [48]. Essentially it comprises four fundamental steps:

- o characterization of the technical purpose of the system subjected to wear
- o compilation of operating variables
- o description of the structure of the system, consisting of:
  - the elements involved in wear
  - geometric and material properties of the elements
  - interaction between these elements
- o evaluation of wear characteristics and presentation of these as a function of operating variables and system structure.

Figure 2.19 above gives a diagram of a typical tribosystem according to Czichos (as reported by Frees [36]).

2.11 WEAR TESTING

Neal [37] and Peterson [35] recount that until approximately 50 years ago, laboratory tests were conducted only on full scale machine components, the reason being that it was considered "futile to attack problems of bearing materials by simplifying assumptions as simplified laboratory tests have no meaning". This attitude has stifled research in tribology more than any other factor. Fortunately, this attitude no longer prevails and it is considered reasonable to make simplifying assumptions when conducting model tests.

Using simplified models/components which simulate only certain aspects of real engineering systems has the merit, that being simple, they can be matched to basic theories without the complication of other variables. This technique has contributed vastly to basic understanding of generic technologies that lie behind the operation of real tribo-systems.

There are, to date, no ASTM or BSI standard test procedures for either adhesive wear testing or determining galling thresholds. Zum Gahr [4] states that a number of techniques have, however, received wide acceptance in laboratories around the world. Jahanmir [7] and Roberts [9] reiterate that the need for standard test procedures and methodologies, particularly for comparing results from different laboratories, nevertheless still needs to be met.

The only wear test rig commonly used by researchers in this field is the pin-on-disc apparatus. Other configurations that have been used by various researchers are depicted in fig. 2.20 below.

Czichos [8] concludes from a review into tribo research in West Germany that transferability of tribo data and studies of material compatibility in adhesive failure are the background of most of the studies currently undertaken. Amongst the other interesting factors to emerge are:

- o material combinations are the main interest in 71% of projects involved in metal-on-metal studies

- o sliding wear is cited in 55% of the projects
- o 27% of experimental work is conducted on so called model tests
- o the most often measured quantities are:
  - friction force (50%)
  - material loss (46%)
  - temperature (41%)
  - roughness (26%)

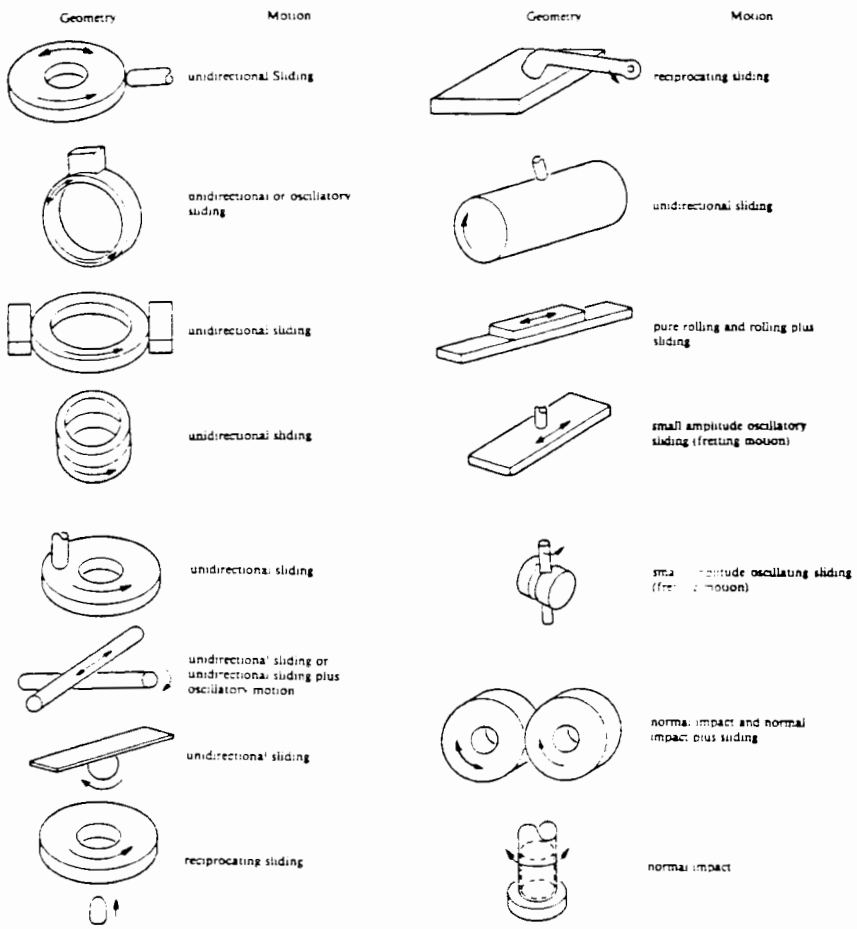

Fig. 2.20 TYPICAL WEAR TEST CONFIGURATIONS

According to Krause and Senuma [29] the influence of each of the wear variables must be known, as wear rate is system dependent. This is obviously very difficult to do as numerous factors interact in a complex manner. Fortunately, more often than not it is the qualitative statements which are important and not the absolute numerical data. It is emphasized that unless temperatures in the model are the same as those of the modelled system, it is virtually impossible to assess correctly the applicability of any test results. Ball and Ward [38] recognizing the above, suggest that in-situ tests should complement model testing.

Wear rate data generated from model testing shows considerable scatter, often over several orders of magnitude and all results to date are

presented as arithmetic means (Rabinowicz [32]). Wallbridge and Dowson [30] suggest that lognormality is a common feature of sliding wear and instead of additive combination of lognormal random variables, they should be multiplied out to give lognormal results.

2.12 WATER LUBRICATION IN TRIBOLOGY

Research on tribosystems operating under reciprocating sliding conditions in water lubricated environments is scarce. This, no doubt is due to the fact that water is not usually chosen as a lubricant because it possesses poor lubricicity and promotes corrosion in susceptible metals.

As outlined in section 2.3, a good lubricant must, among other things, possess high viscosity and be readily sheared if it is to function successfully. Having a viscosity of only one hundredth that of oil, water clearly is not a good lubricant. Black [39], Smith [15] and Stolarski [40] do, however, all concur that, depending on the particular conditions of sliding, the presence of water in any sliding system can result in fluid film lubrication, boundary lubrication or a mixture of the two.

Because of the low viscosity, water lubricated surfaces will, in general, have very thin lubricant films to support l ads and therefore spend a much greater proportion of their lives in the oundary or mixed film regions than would the same system under oil lubri ation. This is significant because in these two regimes material prop rties are significant in terms of affecting wear rate and friction and therefore service life.

Water is beneficial in sliding systems as it has a much higher heat capacity than oil and can therefore remove heat much more effectively from the interacting surfaces. Tolerance of thermal upsets associated with sudden speed or direction changes is thus much better. Smith [15] emphasizes the importance of this transient thermal behaviour when establishing minimum design clearances. If insufficient clearances are provided, the reciprocating components will close in until heat generation rises sharply, water viscosity decreases (as it is temperature sensitive), and seizure will ultimately occur.

Smith [15] also warns that wear and sliding data generated in dry tests can be very misleading if applied to water lubrication. Stolarski [40], who tested polymers and composites rubbing against stainless steel in water lubricated environments agrees. He found that the wear rates of the tested materials under lubricated conditions far exceeded those of the same materials when tested dry. This surprising difference in wear rates he ascribed to the formation of a uniform and coherent transfer film of polymer on the counterface under dry conditions. This film effectively masks the original topography. No explanation is offered for these observations.

Lloyd [3] also performed tests on polymers rubbing on stainless steels in water environments, but under reciprocating sliding conditions. His test specimens showed transfer film formation even in aqueous conditions, but not in uniform layers. Instead, the rupture of adhesively bonded interfacial junctions resulted in the deposition of discrete lumps of polymer on the counterface.

The difference in observation between Lloyd and Smith are presumed to be due to the difference in sliding conditions. In reciprocating sliding conditions the velocity profile is periodic and therefore moves through zero. Fluid film breakdown must thus occur and 'dry' conditions prevail at that instant. Reciprocating sliding motion in lubricated environments must therefore display wear rates of unidirectional sliding motion in lubricated and dry conditions.

Formation of these transfer films has also been reported for metal on metal sliding systems under reciprocating sliding conditions in aqueous environments (Black [39], Schuhmacher [41], Smith [42],[43],[44]).

2.13 BRONZE AND BRASS SLIDING AGAINST STEEL

Hirst and Lancaster [26] investigated the rate of wear of brass against hardened carbon steel under dry sliding conditions in the speed range 0.1 m/s to 10 m/s. They found that over this entire speed range the wear mechanism was of the 'severe' type in which metallic debris is produced and a film of transferred brass is built up on the steel counterface. No loose wear particles come directly from the brass. Instead, wear particles are detached from within the transferred film. Smith [42], working on self lubricated 316 stainless steel in reciprocating sliding suggests that this detaching of wear particles is through prow breakdown. He postulates that the stages leading to production of wear debris are: asperity adhesion, asperity interaction and transfer, formation of prows of transferred material and eventually prow breakdown due to fatigue. Transfer of metal is thus presumed to be the rate controlling step in wear. This is confirmed in fig. 2.21 below.

Sundberg et al [45] working on special brasses concluded that wear resistance is primarily determined by the properties of the transfer layer. Carro and Wert [46], researching bronze/steel couples in reciprocating sliding also observed transfer layers and concurred that transfer of the softer metal to the harder counterface controlled wear rates.

It was also found by Hirst and Lancaster [26] that the tendency of the dry wear rate to decrease with speed is limited by attainment of a critical temperature and not a critical speed. Thus if sufficient cooling is provided, wear rates will decrease with increasing speed. Results of their work are presented in fig. 2.21.

This critical temperature is approximately equal to that at which brass begins to soften. They also found that the rate of wear was equal to the rate of transfer over the whole speed range. This is somewhat surprising as transferred fragments may be repeatedly transferred back and forth between the interacting surfaces, the net wear rates will therefore depend on what Tabor [47] calls the 'transfer-back-transfer process'. It will also be influenced by the final mechanism which detaches the transferred fragments and converts these into wear particles.

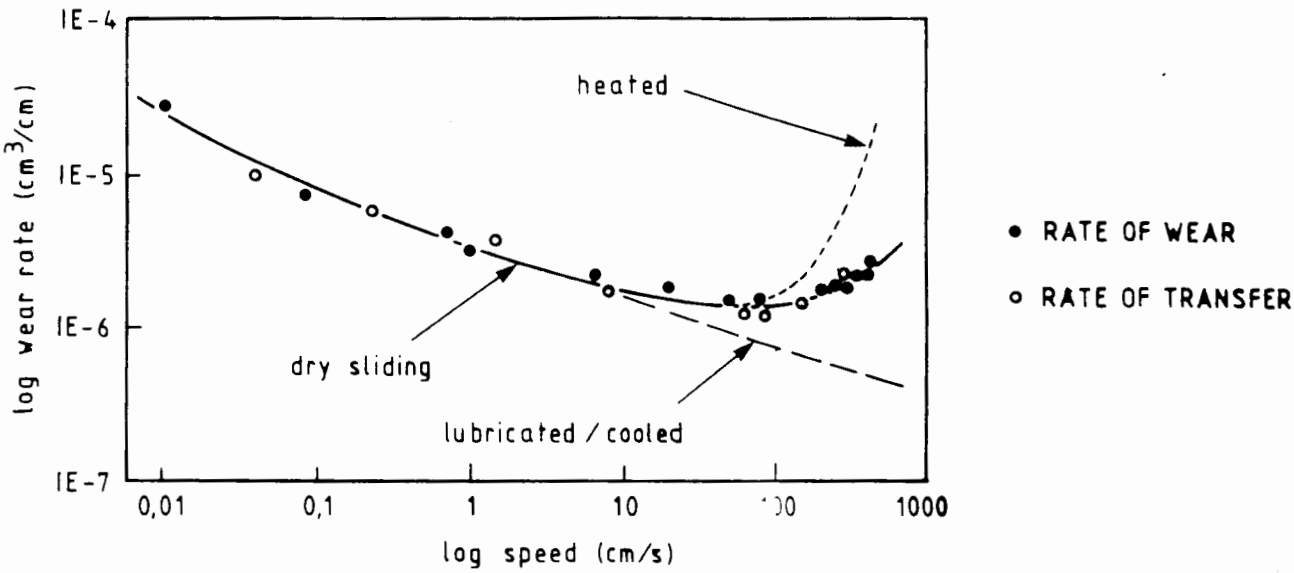

Fig. 2.21 VARIATION OF WEAR RATE WITH SPEED (Hirst & Lancaster [26])

Roberts [9] cites work done on friction and wear of bronze on steel under different conditions of lubrication. This research shows that wear in lubricated conditions is lower than in dry sliding. This is due to the fact that in lubricated conditions asperity interaction can not take place and therefore transfer layers, which generate wear debris, are not formed.

These observations no doubt hold true for conditions of constant velocity. In reciprocating sliding the velocity profile changes constantly and passes through zero twice every cycle. Thus if lubricants/coolants are present, they are ineffective at the zero positions and metal to metal contact occurs. Transfer layers will therefore be built up even if sliding couples are lubricated.

Hirst and Lancaster [26] found that the wear rates of brass/steel couples were exceptionally reproducible and proportional to load. Sarkar [27] who performed tests on dry sliding of brass on steel confirmed this to be true for the steady state or normal operation regime. During run-in, a large scatter in wear rates was, however, observed. This is ascribed to the fact that the sliding faces are not properly matched initially and require a certain time period before they have 'bedded-in' against each other.

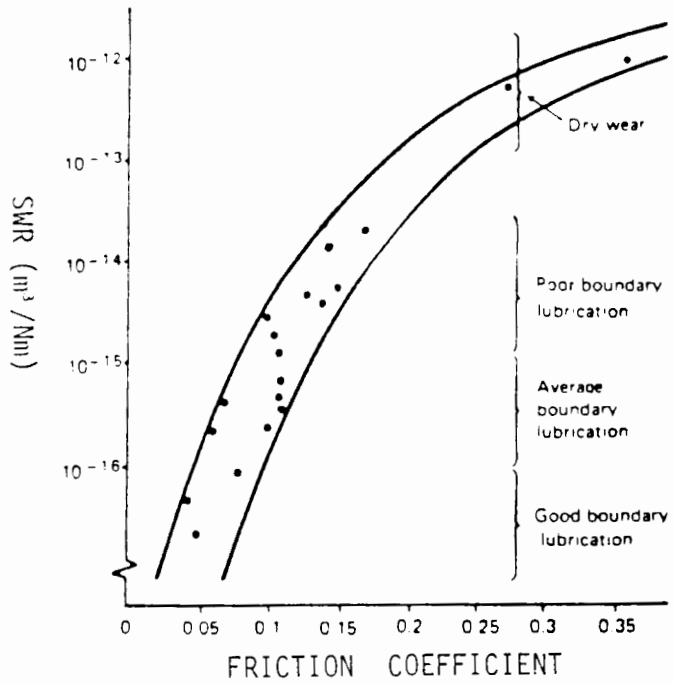

Fig. 2.22 EXPERIMENTAL FRICTION AND WEAR RESULTS FOR BRONZE SLIDING ON STEEL UNDER VARIOUS LUBRICATING CONDITIONS (R. [illegible] [9])

3.0 THE IMPLEMENTED TEST PROGRAMME

This chapter will cover all aspects of the test programme which was initiated to meet the short term objectives (refer to fig. 1.1). It begins by introducing the materials under consideration. From there, the original test equipment, test specimen, selected test parameters and experimental techniques are covered. Modifications made to the test facility are then discussed. Results for each of the couples tested are presented thereafter and the important features are brought together and compared in the summary of results section. The chapter concludes by motivating for a new test rig design.

3.1 TEST MATERIALS

A large number of material combinations were recognized as possible contenders for the hydro-power concept. To initiate this programme, the following couples were selected:

- o self-mated couples : AISI 630 precipitation hardened stainless steel
  : AISI 431 stainless steel
- o dissimilar couples : development alloy 122/aluminium bronze AB2
  : development alloy 122/manganese bronze CZ114

Table 3.1 COMPOSITION AND MECHANICAL PROPERTIES OF MATERIALS UNDER INVESTIGATION

	STAINLESS STEELS			BRONZES	
Element	174 PH	431	122	AB2	CZ114
C	0.07 max	0.12-0.2	0.21		
Ni	3-5	2-3	0.11	5	
Cr	15-17.5	15-18	12.00		
Mn	1.00 max	1.00 max	0.92		1.5
Cu	3-5		0.016	80.5	58
Zn					38
Al			0.013	9.5	
Fe				5	0.75
Pb					1.0
Sn					0.75
Si	1.00 max		0.330		
P	0.04 max		0.017		
S	0.03 max				
Co+Ta	0.15-0.45				
Tested Condition	H1025	As Specified	1050.QQ.TT200	AR	AR
UTS (MPa)	1070	850-1000	1650	650-700	460-490
0.2% YS (MPa)	1000	680	1330	250-310	210-270
% elongation	12	11	12.5	13-20	15-20
Density (Kg/m³)	7760	7760	7760	7400	8200
Hardness VHN(30kg)	350-420	408-430	490	234	164
Charpy impact energy (J)	20	—	—	—	—
E (GPa)	206	206	206	100-120	—

The reproducibility of tests done with each of these materials was too poor to facilitate correlation of material performance to particular bulk properties or microstructural features. Consequently no detailed examination is justified for these materials and only a brief resumé will be given for each metal. Compositions and mechanical properties are summarised in Table 3.1 above. Details on heat treatments are listed under Appendix A.

3.1.1 AISI 630

This is a precipitation hardened stainless steel (also known as 17-4 PH) with a two phase structure consisting of ferrite stringers in a martensitic matrix. It exhibits a good combination of high strength, hardness, excellent corrosion resistance and easy heat treatment. Additional features of this alloy are its high resistance to crack propagation, good transverse properties, and resistance to stress corrosion cracking in marine atmospheres.

3.1.2 AISI 431

This is a hardenable martensitic stainless steel. Corrosion resistance is fair and it exhibits high wear resistance. Its toughness is however inferior to the other stainless steel groups (ferritic, austenitic and precipitation hardened). This material is tested in a heat treated condition that involves several different stages as detailed in Appendix A.

3.1.3 ALLOY 122

This is a newly developed stainless steel [53] (similar to AISI420) which is tested in the tempered condition. Chromium content is about 12% and a relatively high 0.21 % carbon ensures good hardenability. Additions of nickel are also significantly lower than for the previous two steels. This steel has an exceptionally high strength - yield strength = 1330 MPa.

Figure 3.1 below shows the microstructure obtained for this steel in the as received, quenched and tempered conditions respectively.

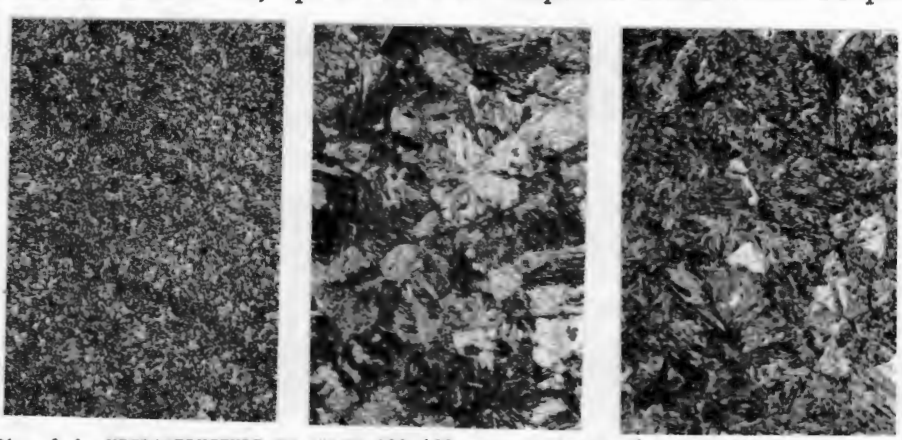

Fig. 3.1 MICROSTRUCTURE OF ALLOY 122 (40 x magnification)

3.1.4 AB2

This alloy belongs to the family of the aluminium bronzes. These are alloys of copper and aluminium, but other elements such as iron, nickel, manganese and lead are added to improve properties. These alloys have outstanding mechanical properties and because of a thin continuous oxide film exhibit excellent resistance to corrosion. They are widely used in applications as bearings and are especially suited for marine applications and for use in other aggressive media.

AB2 is a duplex $\alpha - \beta$ aluminium alloy in which the α phase (white) is distributed in a matrix of transformed eutectoid β (dark). Figure 3.2 shows an optical micrograph of an etched microstructure.

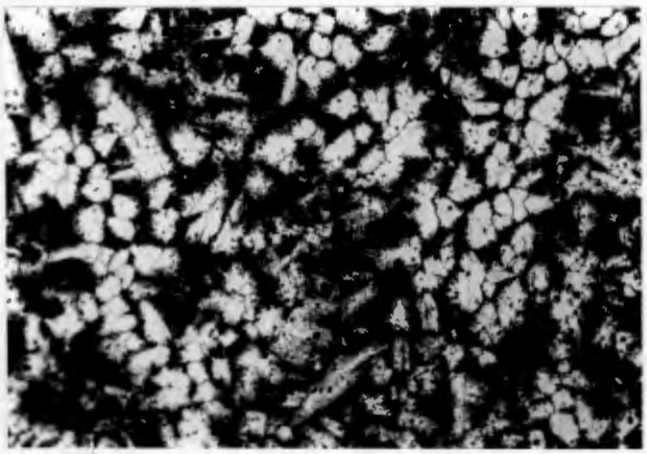

Fig. 3.2 MICROSTRUCTURE OF AB2

3.1.5 CZ114

This is an alloy of copper and zinc with additions of manganese, iron, aluminium, tin and nickel which collectively bring about increased strength and resistance to corrosion. This family of alloys is often referred to as "Manganese Bronzes", but this is somewhat of a misnomer as these alloys are actually high tensile $\alpha - \beta$ brasses.

More specifically, CZ114 is a 60/40 $\alpha - \beta$ brass which is used specifically in marine environments. Figure 3.3 below shows the microstructural features of this alloy. The white needles correspond to α phase which are distributed in the β matrix. Due to different planes, the grains show up in different shades of grey.

Fig. 3.3 MICROSTRUCTURE OF CZ114 (40×magnification)

3.2 THE ORIGINAL TEST EQUIPMENT - TEST FACILITY A

The test facility that was inherited by the author for this research initiative is presented in this section. Test specimens used, test parameters selected and experimental technique employed are described.

3.2.1 BASIC LAYOUT OF TEST FACILITY

Figure 3.4 shows a general assembly drawing of the test cell and reciprocating drive for the inherited test rig. A belt driven crank slider produces the reciprocating motion. It consists of a connecting rod, turning eccentrically about a rotating drive shaft and terminating in a piston running in a bore. The drive shaft pulley to motor pulley ratio is such that 6300 rpm can be obtained when the 1.5 kW dc motor is running at its maximum rating of 3000 rpm. This translates into a peak velocity of 10 m/s.

A pushrod, positioned in line with the reciprocating axis is rigidly screwed to the piston. It reciprocates centrally in the test cell in a vertical orientation. Two removable assemblies, functioning as both bearing and sealing units, guide this pushrod at the lower and upper ends of the test cell.

The pushrod in turn is made up of two parts which screw into each other. The rod diameter is stepped down from 12 mm to 8 mm over a length of 50 mm downwards of the screwed joint. This step down permits the reciprocating specimen, which has a hole drilled down its long axis, to be placed over the pushrod and in line with the reciprocating axis, once the upper end of the pushrod has been unscrewed from its lower end.

Fig. 3.4 GENERAL ASSEMBLY OF ORIGINAL TEST CELL

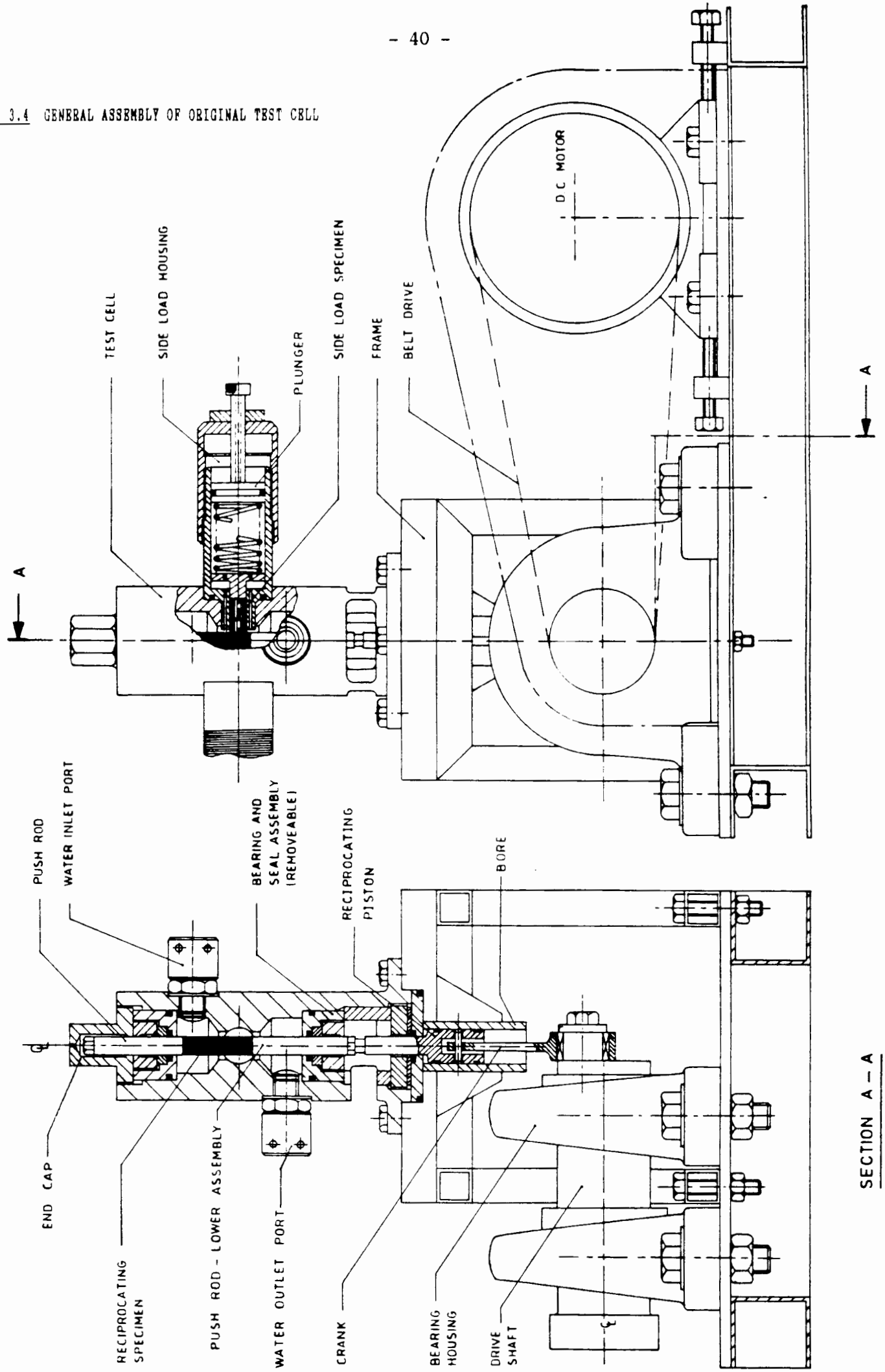

Two side load housings, which contain the two side specimens are screwed into the test cell at right angles to the reciprocating axis and exactly opposite to each other along a shared diametrical axis that bisects the axis of reciprocation. The two side specimens can thus be loaded against the two parallel faces of the reciprocating specimen by compressing the load spring with the threaded plunger at the back of these housings.

An inlet port for the lubricating and coolant fluid is provided at the top side of the test cell. The outlet port is situated below the side specimen housing. Both ports are located such that they share a diametrical axis that is at right angles to both the reciprocating and loading axes.

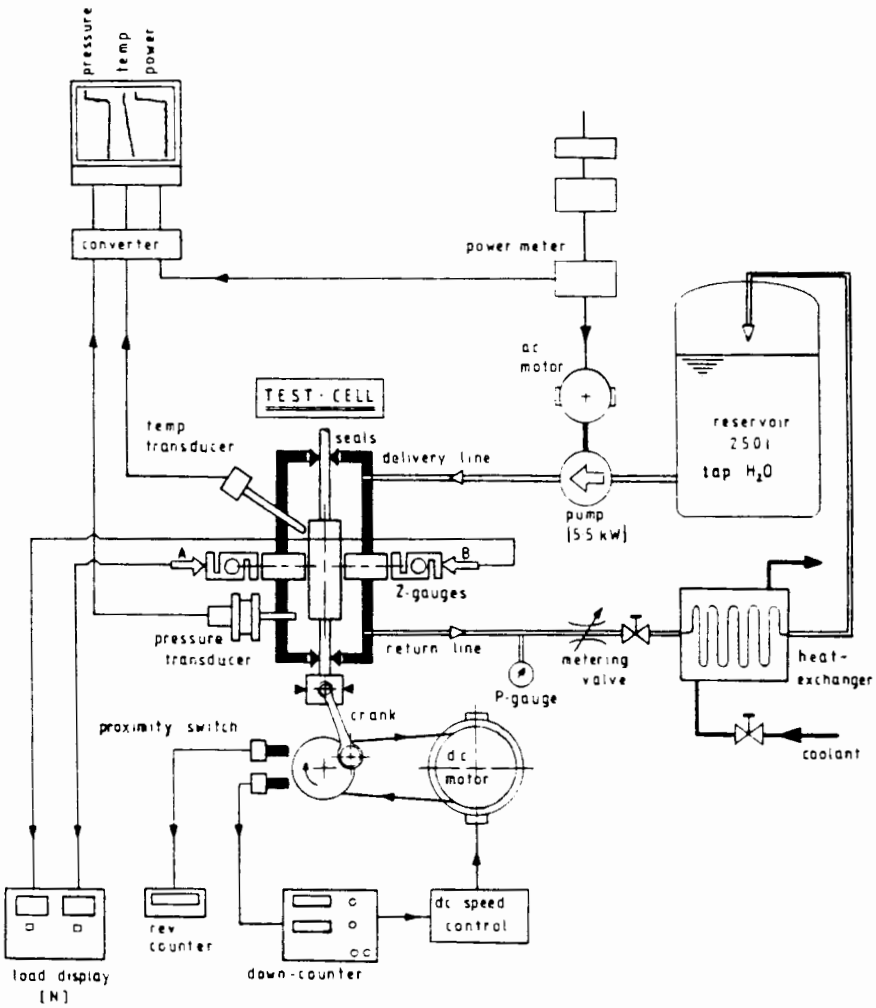

Fig. 3.5 LAYOUT OF ORIGINAL TEST FACILITY (TEST FACILITY A)

Relief holes are drilled into the side specimen housings to permit fluid pressures in the test cell and housing to be equilibrated. This ensures that the only load acting on the rubbing interface originates from the spring force. The fluid pressure in the test cell can be raised to a maximum of 5 MPa by adjusting a metering valve downstream of the test cell.

Figure 3.5 above gives a complete schematic layout of the test facility with the auxiliary equipment fitted. The test cell is fed from a closed loop fluid circuit. This comprises of a reservoir from which the medium is pumped to the test cell. After exiting from the outlet port and backpressure valves, the medium rejects frictional heat in a heat exchanger, before closing the loop by refilling the reservoir.

The desired number of testing cycles are set on the down counter. Once these have elapsed, the drive is switched off automatically. All other auxiliary equipment performs a regulating or monitoring function.

3.2.2 TEST SPECIMENS

Figure 3.6 below depicts the geometry of the test specimens used. The reciprocating specimen is of a rectangular format with a square cross section. A hole, drilled down the centre of its long axis enables the specimen to be fitted in line with the centre line of the reciprocating drive assembly of the test apparatus. To economise on material, all four faces are intended to be utilized, with two parallel faces being tested simultaneously at any give time.

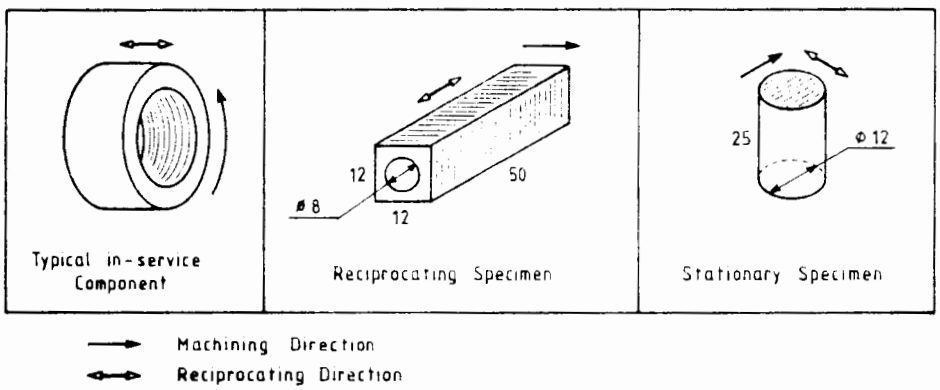

Fig. 3.6 TEST SPECIMENS USED

The side specimens are of a round bar design and are loaded against the desired two parallel faces of the reciprocating specimen. One reciprocating and two stationary specimen thus make up one wear couple.

Specimen dimensions are governed by the design of the test rig and there is no leeway for using different sizes or geometries. Appendix C gives details of the exact test specimen dimensions.

Machining considerations cause the directionality of the ground surfaces for in-service components to be at right angles to the direction of reciprocation. In order to duplicate this for the test specimen, they too were ground at right angles to the axis of oscillation.

As ground surfaces of surface roughness values ranging from 0.1 μm to 0.8 μm CLA are used for the components of interest, different test specimens were machined up to cover this range. In addition, to economise on machining time and cost, specimens were intended to be reground and reused, once a test series had been completed.

3.2.3 TEST PARAMETERS SELECTED

The following test parameters were selected for stage 1 of this programme.

- **Reciprocating speed = 6300 rpm**
  This was selected as it equates to a peak velocity of 10 m/s which coincides with the highest velocity obtained by the reciprocating components under consideration (refer back to Table 1.1) Furthermore it represents the maximum attainable speed for the test rig and thus helps to quantify its performance limit.

- **Specimen surface finish = 0.2 μm CLA**
  Specimens could not be ground consistently to finishes better than 0.2 μm $\pm$ 10%. The decision was therefore made to commence the test programme with this finish and progress to coarser finishes later.

- **Backpressure of cooling/lubricating medium = 5 MPa**
  This corresponds to the highest setting possible for the test facility. Again this was selected for reasons similar to those of testing at maximum velocity.

- Side load = 5 N
  Theoretically, loads between reciprocating components and the housings confining them can vary between zero and infinity-depending over which area the side load is carried. So as not to commence with excessive loads which would destroy specimens and given that load is one of the parameters under investigation, a low load was initially selected. As 5 N increments can readily be set on the load housing it was decided to start testing with a load of 5 N and thereafter increase loads in steps of 5 N up to the maximum possible setting of 30 N

for later tests. Given a specimen diameter of 12 mm, these loads relate into 44 kPa and 264 kPa respectively.

- **Test duration = 24 km**
  Table 3.2 below summarizes distances covered by typical components and the test rig at different speeds over a given running interval.

Table 3.2 SLIDING DISTANCE AS A FUNCTION OF SPEED

Component	Cycles/ 0.25s	Frequ. (Hz)	Distance/ Cycle (mm)	Distance/ Hour (km)	Distance/ 400 000 Cycles (Km)
Impact Hammer Head	1	5	120-170	3	48-68
Rockdrill piston	10	50	56	10	22.4
Testing @ 1 m/s peak velocity	2.1	10.7	60	2.3	24
2 m/s peak velocity	4.3	21.3		4.6	
5 m/s peak velocity	10.6	53.1		11.5	
7.5 m/s peak velocity	15.9	79.6		17.2	
10 m/s peak velocity	21.1	106.0		22.9	

A distance of 24 km was selected as an adequate test length as work done by Lloyd [3] suggests that the wear rate lies well within the 'normal operation' regime after 5 to 15 km. Should it be found however that this distance is insufficient for recognizable trends to have established themselves, then the distance would be extended.

3.2.4 EXPERIMENTAL TECHNIQUE

The following step by step procedure was adopted for testing:

- immerse specimens in alcohol and place into an ultrasonic bath; blow dry and air cool to room temperature
- take surface roughness readings at five positions against and three with the grinding direction for the reciprocating specimen, and three with, three against for each of the stationary specimens. Record average CLA (centre line average) values in either direction for each specimen
- determine the VHN (Vickers Hardness Number) at five positions for each specimen
- repeat step one, thereafter record mass in mg
- place reciprocating specimen over stepped down bottom end of pushrod and screw on upper pushrod end
- replace top bearing and seal assembly and secure with end cap
- set desired spring load in side specimen housing by screwing the outer plunger in against the spring
- insert the two side specimens marked A and B into their

respective housings and screw housings tightly into test cell
- select desired number of cycles on down counter and set speed to required rpm on speed controller
- start the pump and let the flow stabilize in the circuit (i.e. test cell properly vented and no trapped air bubbles)
- open coolant inflow valve at heat exchanger
- close down metering valve slowly until desired back pressure is registered in the test cell
- zero inputs to chart recorder and start recording
- begin test by starting up dc motor
- once selected number of cycles have elapsed, down counter trips dc motor
- switch off pump, pause chart recorder and open metering valve fully
- close heat exchanger coolant inflow valve
- unscrew side specimen housings and extract the two side specimens
- remove end cap and upper bearing and seal assembly
- bring piston to top dead centre and take reciprocating specimen out of test cell
- wash all three specimens as detailed in step one; then reweigh and record mass loss/gain and sliding distance for the interval
- reload specimens and repeat procedure for successive test intervals

While testing proceeds, graphs of mass loss, volume loss, specific wear rate and wear coefficient, all as a function of sliding distance are plotted for the interval. At the conclusion of a particular test repeat surface roughness measurements at the original positions.

All optical and SEM microscopy was be completed prior to reusing the specimens. Some specimens were sectioned to study the side elevation of the interacting surface. Micro hardness traces were taken on each of these sectioned specimens to establish the extent of work hardening or softening.

3.3 MODIFICATIONS TO THE TEST SET UP

The performance of the inherited test facility under the conditions selected in section 3.2.3 did not meet the short term objectives as listed for stage 1. Consequently, the programme had to be diverted to substage 1 (refer to fig. 1.1)

This section will outline what modifications were made in respect of the hardware used but for the sake of brevity, no reasons will be given. The following section will present the results of all the tests and exemplify the reasons for the modifications.

In addition to testing on the original test facility (which will hence forth be termed test facility A), testing was conducted on three other layouts. Each of these represents a modification of the original.

3.3.1 TEST FACILITY B

Figure 3.7 below gives a schematic layout of this facility. It differs from A in three significant respects :

- o the entire closed loop high pressure circuit for the cooling/lubricating medium has been replaced with an open circuit which feeds tap water under water mains pressure into the test cell, from where it exhausts into a drain. This negates the need for a heat exchanger as the tap water remains approximately constant in temperature
- o all monitoring equipment other than revolution and cycle counter have been removed as no meaningful data could be obtained from any of these
- o the second side specimen is not used and the side specimen housing is replaced with a brass plug

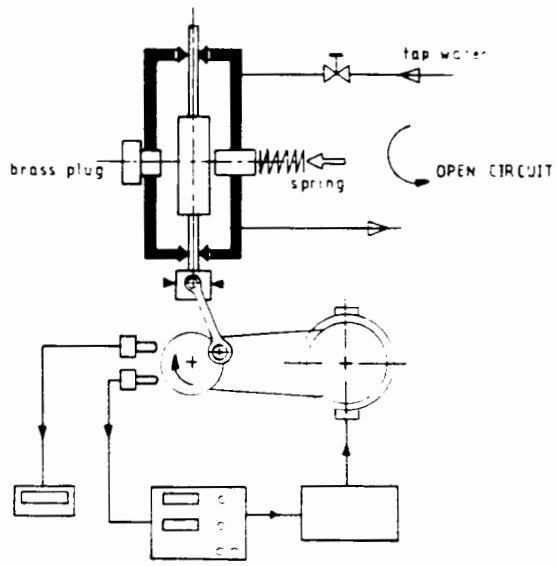

Fig. 3.7 LAYOUT OF TEST FACILITY B

3.3.2 TEST FACILITY C

Apart from the complete absence of a medium circuit, this facility is identical to that described as facility B. This layout was used for conducting dry tests.

3.3.3 TEST FACILITY D

Again this test facility is, with the exception of the medium circuit, identical in all respects to facility B. Figure 3.8 depicts the difference in the medium circuit. A mono pump feeds distilled water from the reservoir via a sintered glass filter into the test cell. The exhaust port returns the medium to the reservoir.

No heat exchanger was required as the reservoir was sufficiently large to dissipate any temperature rise in the medium due to the frictional heating at the rubbing interface. Pipe friction heating was insignificant due to the low flow rates.

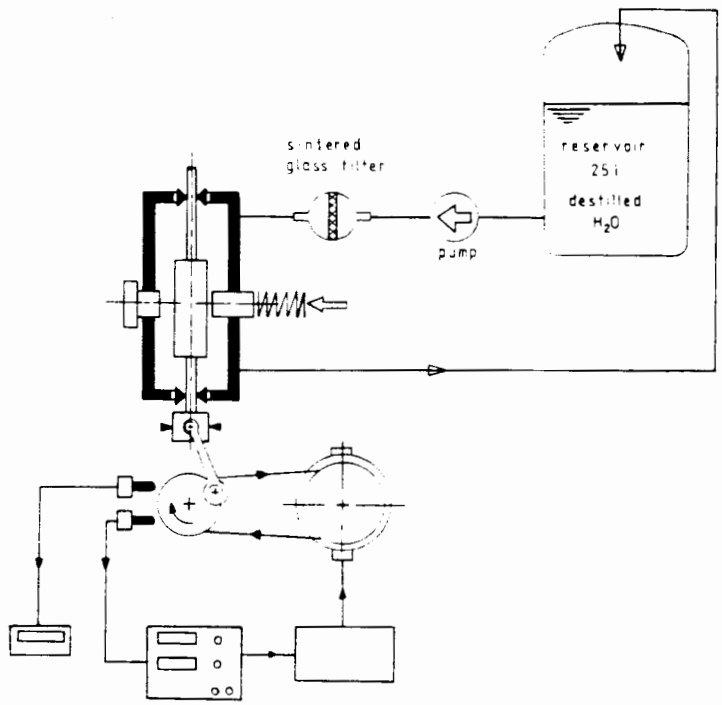

Fig. 3.8 LAYOUT OF TEST FACILITY D

3.4 RESULTS FROM THE IMPLEMENTED TEST PROGRAMME

This section will present and discuss separately the results obtained from each of the four different test facilities used. The results will be conveyed in both graphical form and by way of micro- and macro-graphs.

The graphical information will be presented in sets of two graphs : Graph one showing cumulative mass - and volume-loss, both as a function of sliding distance; and the second graph plots the wear coefficient and specific wear rate for the same results, also as a function of distance covered.

In all cases only the changes for the side specimens are plotted. This was done because the counterfaces were the harder of the interacting surfaces and, although showing degradation, their mass remained essentially constant.

Appendix B defines each of the above terms and gives a sample calculation to clarify how these graphs are interrelated. To facilitate ready comparison between the different results, the same distance scales and exponents for the ordinate scales are used for all graphs.

3.4.1 RESULTS FOR TEST FACILITY A

Figure 3.9 shows results obtained for three consecutive tests using the original test facility with two side specimens per test (refer also to fig. 3.5).

All six self-matched AISI 630 side specimens show extraordinary amounts of material loss after only a few hundred metres of sliding. Mass losses fluctuate between approximately 60 and 180 mg after 5 km. This correlates into a reproducibility of only around $\pm$ 50%, which compares very unfavourably indeed with the worst repoducibility of $\pm$ 21.5% reported by Lloyd [3].

Mass loss on it own is, however, not a good indication as to how good or bad a material is performing. SWR and wear coefficient, K are a much better basis for comparison. Thus, dividing the slope of the CVL versus sliding distance graph by the applied load is an indication of the rate at which wear progresses. A linear graph would yield a constant value of SWR and we are interested in this value for the normal operating regime (refer to fig. 2.13). Although the band within which SWR fall has narrowed somewhat after 5 km, no general trend is recognizable.

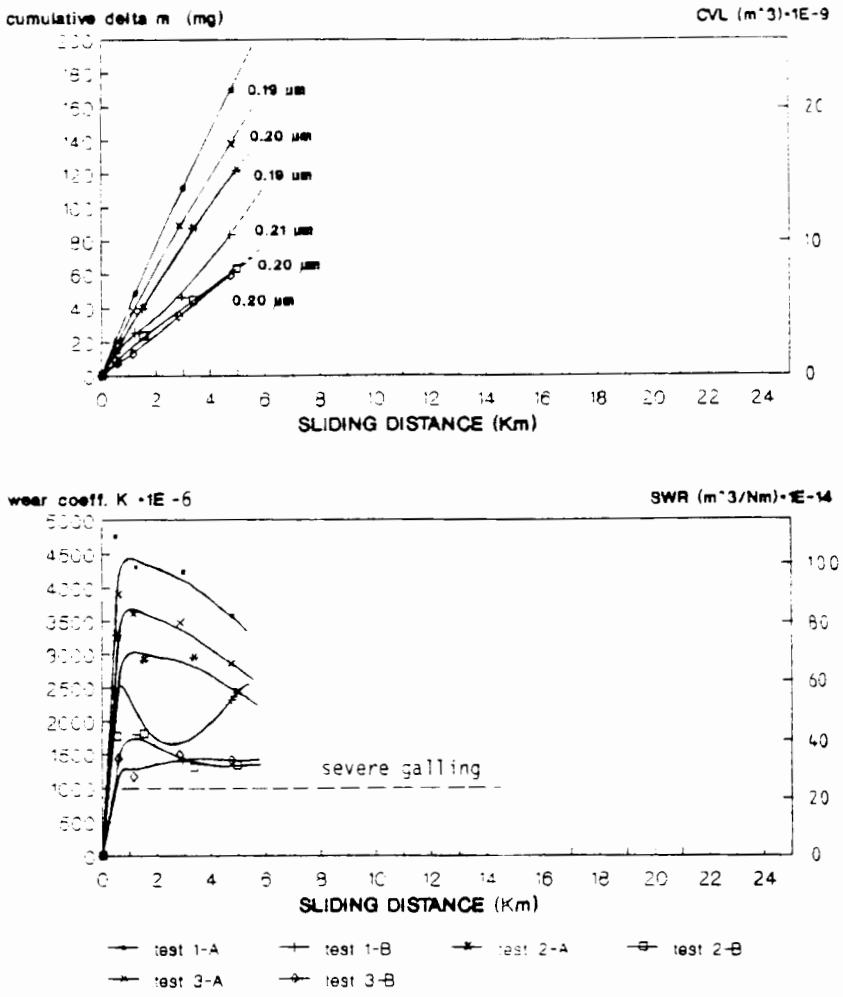

Fig. 3.9 RESULTS OF SELF-MATED AISI 630 COUPLE
5N load, 10 m/s peak velocity, pressurized tap water lubricated/cooled at 5 MPa
VHN (30 KG) : counterface = 440 ± 5
: side specimen = 380 ± 5

Multiplying the SWR by the Vickers Hardness Number (VHN) gives the dimensionless wear coefficient, K. Work done by Rabinowicz [22] suggests that for metal on metal sliding systems, typical values for K fall into a range between 10^{-5} to 10^{-2} for abrasive wear and 10^{-7} to 10^{-3} for adhesive wear. Superimposing these ranges onto the lower graph of fig. 3.9 shows that the K values for each of the six tests done exceed the upper limit of the adhesive wear zone and the largest values are approaching severe abrasion which is the upper limit of the abrasion zone.

Although these figures by no means specify absolute ranges, they nevertheless suggest that we are not testing adhesive wear under the set conditions. This coupled with the poor reproducibility quoted above was sufficient motivation for abandoning testing and not proceeding to the desired test length of 24 km.

Figure 3.10 shows a series of micrographs which clarify the extent of surface degradation of the counterfaces and side specimens. What is apparent from these pictures is that an abrasive wear mechanism does indeed rapidly become the principal wear process. In fact, this process is observed to have manifested itself within 60 m of sliding distance (fig. 3.10 b).

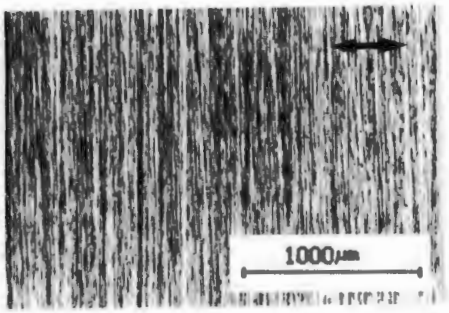

a.) counterface A before test

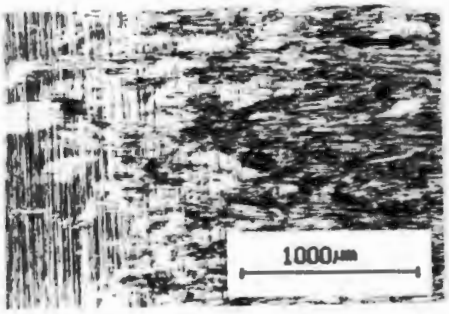

b.) wear damage on counterface A after 2 x 5s test intervals (= 60m of sliding)

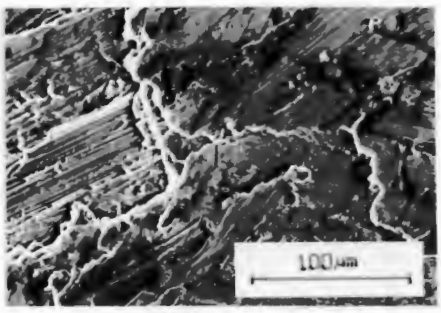

c.) side specimen A after 300m of reciprocating sliding

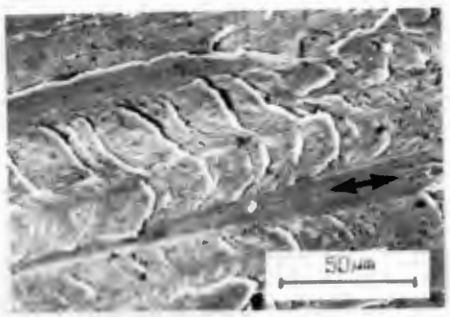

d.) adhesive marks ("stick slip") produced by momentary friction welding on counterface A after 2500m of sliding

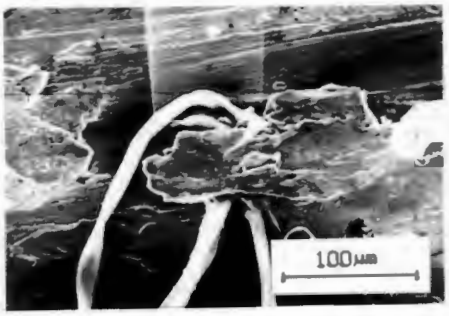

e.) counterface A after end of test, showing transferred material peeling off

f.) sectioned counterface A showing transferred platelet about to be peeled off and become a third body abrasive

Fig. 3.10 MICROGRAPHS FOR SELF-MATED AISI 630 COUPLE

Third body abrasion makes the largest contribution to total wear and originates from two sources. Firstly through asperity shearing (high points left by grinding process) and secondly through peeling off of transferred platelets (figs. 3.10 e and f). Both plough, scratch and gouge out the surfaces. Although present, adhesive wear (fig. 3.10 d) is found in only very few locations and is thus not thought to significantly contribute to total wear.

For the counterfaces the majority of abrasion marks run along the specimen length, consistent with the reciprocating axis. The interacting surfaces of the stationary specimen in contrast show no directionality. Instead, abrasive grooves criss-cross the surface at random. This is ascribed to the fact that these specimens are free to rotate in their housings. The interacting surfaces can therefore not bed in against each other and progressively 'rougher' surfaces result with consequently higher wear.

Over and above the problem outlined above, several other deficiencies needed to be contended with. These are briefly summarized below:

- o testing two side specimens against two opposite counterfaces of a single reciprocating specimen was found undesirable as it is impossible to proportion what percentage of total system wear is due to which specimen.
- o the hardware for the coolant/lubricant circuit was underrated to the extent that it would trip every 20 seconds at 5 MPa. This would require no less than 192 test intervals to cover 24 km at 10 m/s. Clearly this is not feasible. Fully opening all backpressure valves, reduced the test cell pressure to its lowest possible setting of 2 MPa. The trip interval was thus reduced to 70 seconds and 54 test intervals would have been required.
- o ingress of rust and scale from the pipe work contaminated the test cell, thereby contributing to unrealistically high wear rates.
- o Because the reciprocating specimen is mounted to the pushrod with a clearance fit, it has three degrees of freedom i.e. it can rotate, pitch and move axially. The force of the incoming medium jet thus helps misalign the specimens and full area contact was therefore not established on all interfaces.
- o As the diameter of the side specimen is equal to the width of the reciprocating specimen, the edges become fouled and hence the faces at right angles can not be used for other tests.

To confirm that all preceding observations were not unique to the 17-4/17-4 couple, three tests using just one side specimen but otherwise identical test conditions were conducted with couples of 431/431. As in the case of the results obtained for the previous couple, severe abrasive wear resulted, the average K value being 10^{-2}. This is equivalent to severe abrasion. Figure 3.11 shows a micrograph of the damage to the 431 counterface after only 1000 m of sliding.

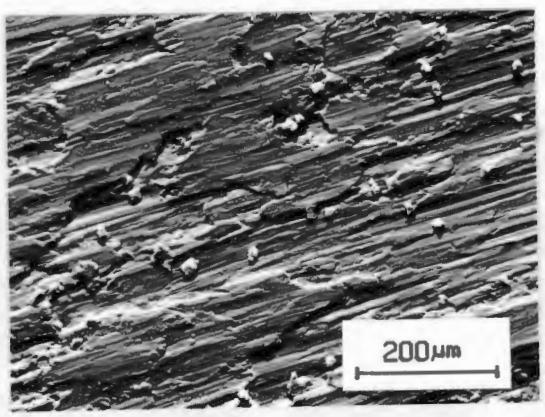

Fig. 3.11 MICROGRAPH OF 431/431 COUPLE

Before abandoning this test facility completely, a decision was made to do a limited number of tests using metal counterfaces (17-4 and 431) rubbing against polymer side specimens (UHMPE, filled UHMWPE and Polyacetal). The motivation for these tests was twofold. Firstly to see if this test facility was in fact capable of yielding any form of reproducible results at all and secondly if it could be used for testing polymers on metal instead of metals on metals.

In all cases, fragments formed during initial counterface grinding, became loosened at random during testing and embedded themselves in the soft polymer. There they acted as aperities, scratching and cutting their parent material. Figure 3.12 shows micrographs of typical surface degradation on each specimen.

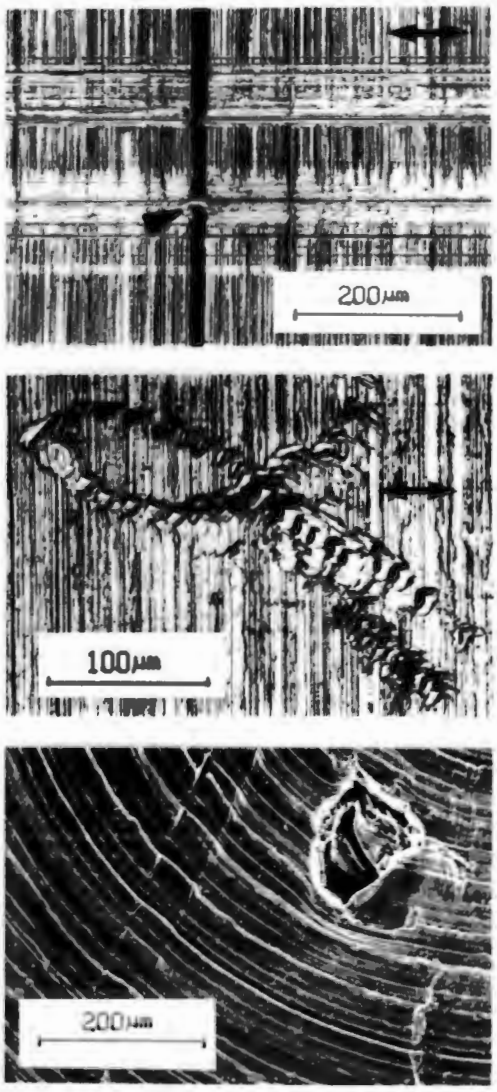

a.) counterface showing flattening of machining marks and formation of wear fragments in machining valleys (◀)

b.) counterface showing skipping wear fragments loosely embedded in polymer causing smears on the 174 surface

c.) polymer side specimen showing pit formed by initially embedded 174 fragment

Fig. 3.12 MICROGRAPHS OF TYPICAL METAL/POLYMER COUPLE

Based on the foregoing observations, the poor reproducibility is thus ascribed to both the specimen preparation (grinding fragments) and the test rig inadequacies previously outlined. The rig is thus not suited to either couple combination.

Given all the above the decision was made to scale down the severity of test parameters and use a simpler test facility. A move was thus made into substage 1 (refer fig. 1.1). This is outlined in the next section.

3.4.2 RESULTS FOR TEST FACILITY B

This test facility was described in section 3.3.1. Testing speed was dropped to 1 m/s and the loading increased to 10 N for two of the tests done and 20 N for 5 further tests. As the self-mated metal couples in the previous section fared very poorly indeed, the first of the dissimilar couples introduced in section 3.1 were used for tests on this facility. Figure 3.13 plots results obtained for the bronze side specimens of each of the seven tests done.

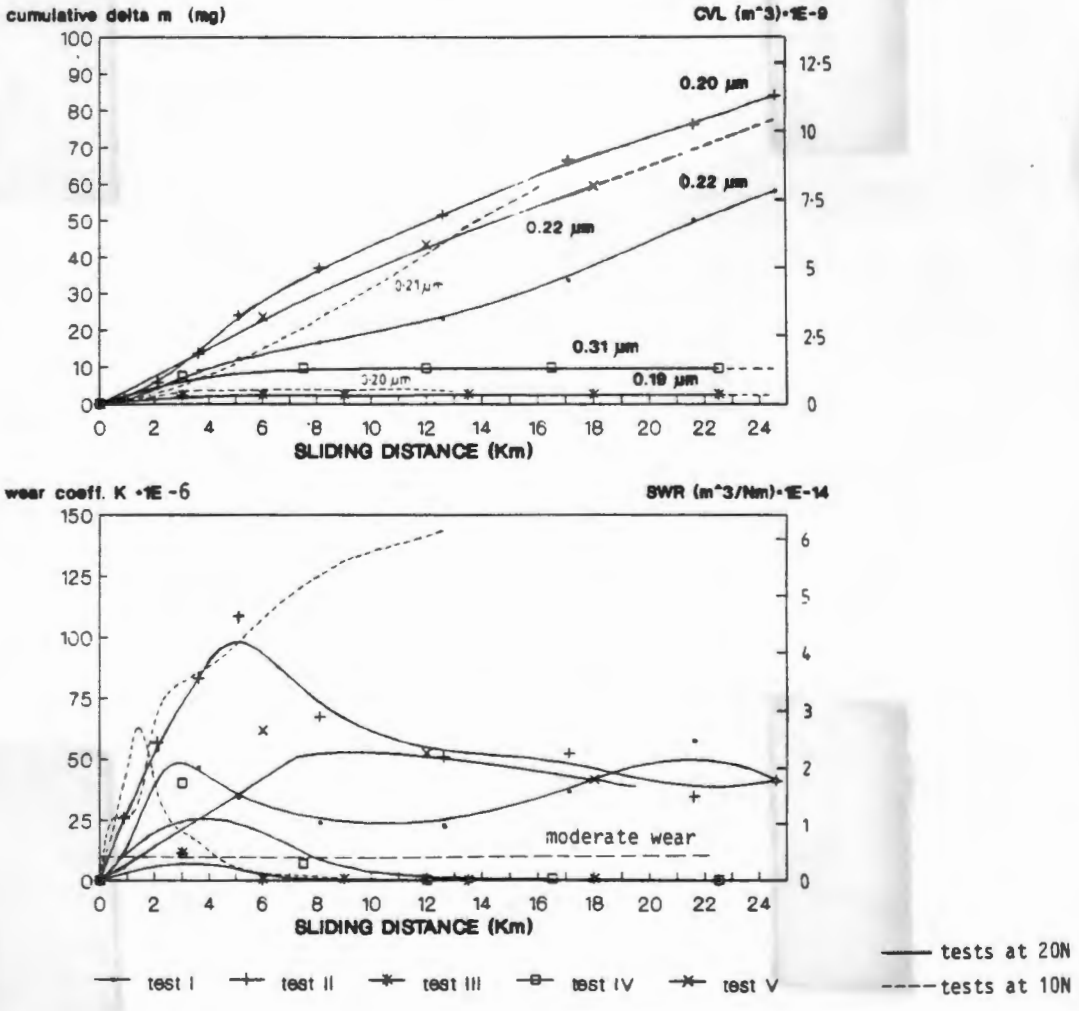

Fig. 3.13 RESULTS FOR 122/AB2 COUPLE
10 N and 20 N loads, 1 m/s peak velocity, tap water lubricated/cooled (water mains pressure)
VHN (30 kg) : counterface = 490 ± 5
: side specimen = 230 ± 5

Specific wear rates have dropped by two orders of magnitude compared with the 17-4/17-4 couple and the wear coefficients for the seven tests fall into a zone stretching from above moderate wear right down to zero wear. Reproducibility for the five tests at 20 N load is an appalling ± 87%. If test III and IV are however discounted (as they behave very differently, showing no mass loss after 5 & 7 km respectively) a credible reproducibility of ± 17% is attained.

Increasing the load from 10 to 20 N resulted in more closely spaced values. The most encouraging feature of these tests is the fact that for tests I, II and V the slopes of the CVL versus distance graphs are very similar from around 12 km onwards, suggesting that a steady wear rate has been attained and the couples are now performing in the 'normal operating regime'.

Figure 3.14 shows typical microscopic and macroscopic features for the five test of 122 and AB2 at 20 N load. All five 122 counterfaces show evidence of having been in full area contact at one time or other during the duration of the test. As the test progresses and surface degradation increases a distinct line at right angles to the reciprocating axis appears at each stroke extremity. These lines match up with a distinct band along the diametrical axis of the stationary specimen.

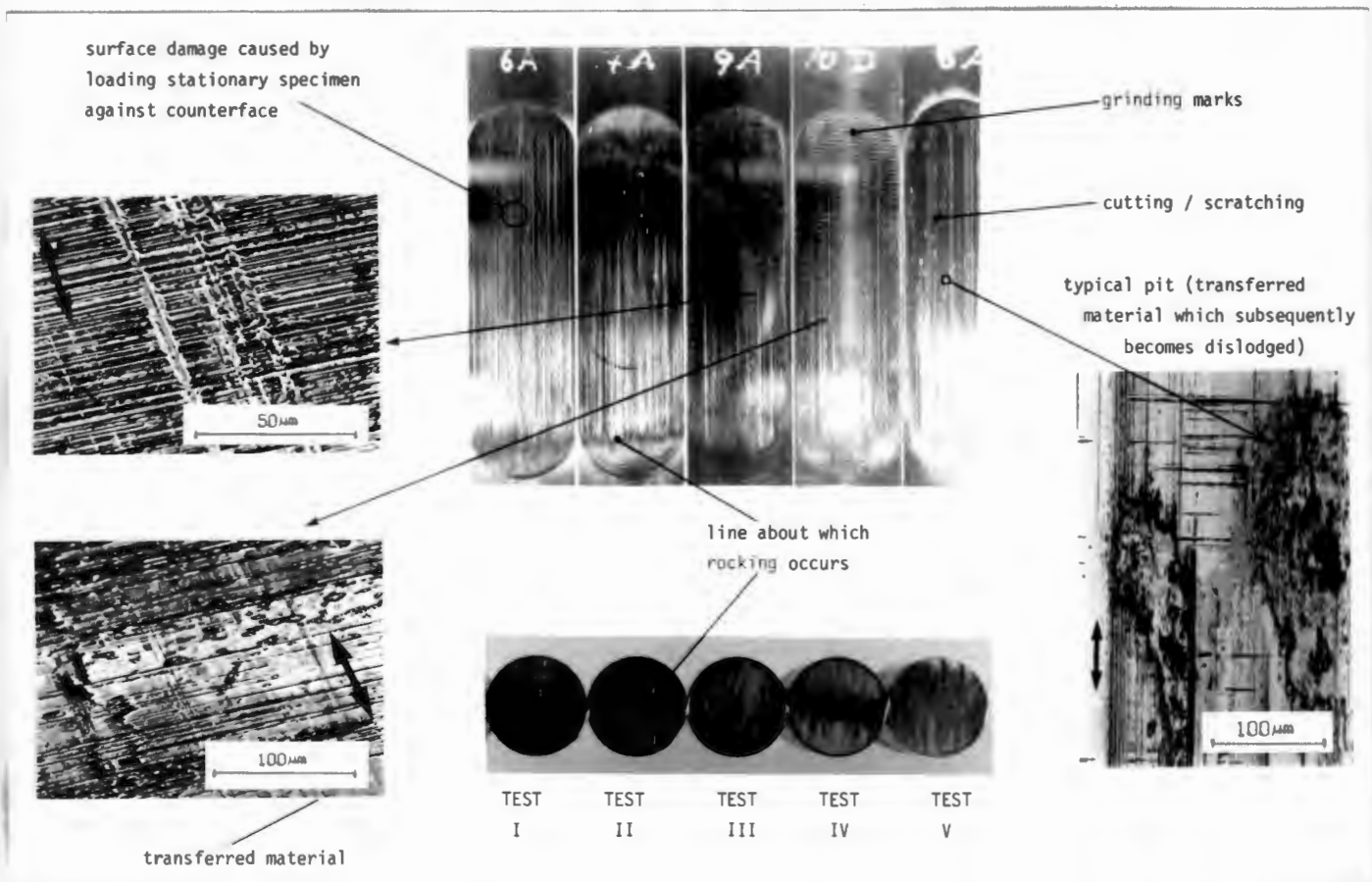

Fig. 3.14 MICRO/MACROGRAPHS FOR 122/AB2 COUPLE

This phenomenon is ascribed to the fact that the stationary specimen rocks back and forth each time a direction reversal occurs. Figure 3.15 illustrates this effect.

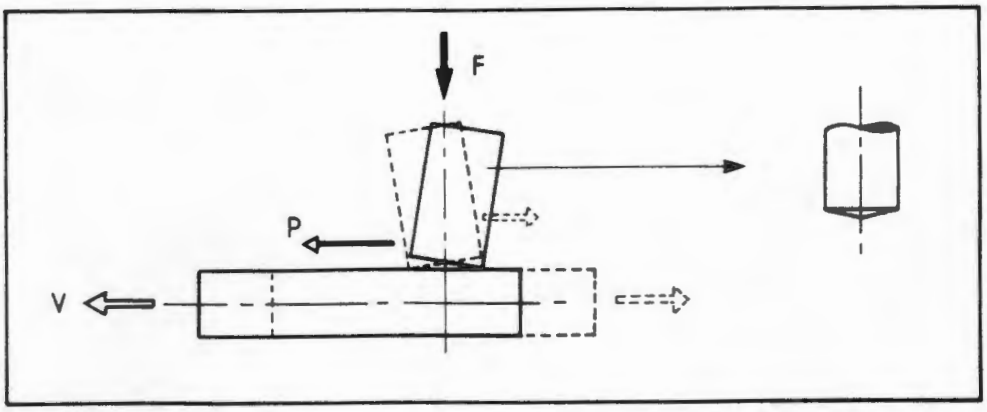

Fig. 3.15 ROCKING ACTION OF SIDE SPECIMEN

The rocking action is possible because the specimen sits in the housing with a clearance fit. Combined with the ability of the specimen to rotate to some degree, all side specimens ended up with a more or less conical wear face.

The problems associated with side specimens rotating in their housing was largely eliminated in test facilities B through D. This was done by inserting a grub screw into the threaded section of the side specimen housing. The grub screw in turn is secured against a flat, ground onto the side of the long axis of each side specimen. This flat stops 5 mm short of each face, thus permitting limited axial but almost no rotational movement.

Unlike the 17-4/17-4 couple, directionality of the wear grooves on the interacting surfaces of the couples is thus maintained. Specimens can therefore bed in against each other and, as expected, lower wear rates were thus recorded.

Another feature which was not observed with the 17-4/17-4 couple was the damage caused to the rubbing interface by loading the side specimen against the counterface. Because the side load housings are screwed into the test cell, side specimens are rotated against the reciprocating specimens under load. A circular mark bears evidence of this on specimen 6A and 7A (test I & II in fig. 3.14). The formation of this circular groove results in wear fragments that contribute to the cutting and scratching action.

A general trend observed on all counterfaces is that the high points of the grinding marks are flattened and the valleys filled in with the soft AB2. The transferred platelets are however ripped out on a random basis leaving smeared pits behind.

Figure 3.16 shows the progressive flattening off of grinding marks and filling in of valleys on a 122 counterface. Successive pictures were taken on a single specimen at approximately the same position at the start of the test and then after 3, 10 and 24 Km.

This transfer of material from the softer to the harder surface covers almost the entire interacting surface. It is however interspersed with pits and scratches.

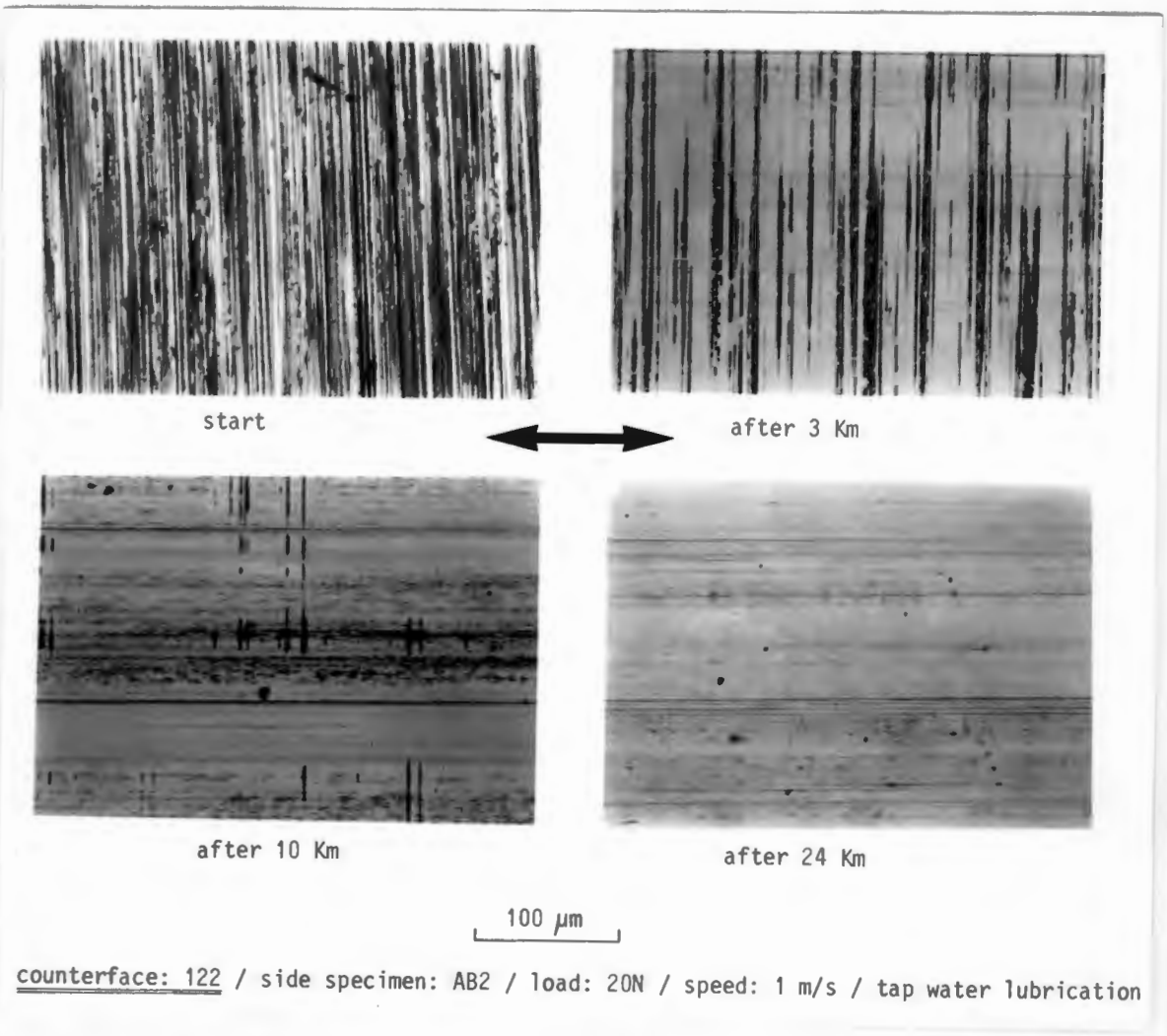

Fig. 3.16 TYPICAL SURFACE MODIFICATION OF A 122 COUNTERFACE

As the counterface becomes more and more covered in transferred material, so it becomes smoother. Friction effects thus decrease, fluid films are more readily supported and the rate of wear should consequently be expected to drop. Indeed this is supported by the graphical evidence of fig. 3.13.

The absence of mass loss for test III and IV coincides with significantly less evidence of scratching on their respective 122 counterfaces. The flattening off of machining marks is also very clearly shown by these two specimens. Thus, the micrographs and graph plots substantiate each other.

Because the reproducibility for the five test done at 20 N are still so poor, a decision was made to do a series of tests under dry conditions. This was instigated so as to eliminate effects due to tap water composition or ingress of water borne debris. These results are presented in section 3.4.3.

3.4.3 RESULTS FOR TEST FACILITY C

For these tests counterface material was 122 as previously but the manganese bronze (CZ114) was used for the side specimens. Tests were conducted at 1 m/s and 5 m/s and the results obtained are plotted in fig. 3.17 below. CLA surface roughness values for the specimens were relaxed to 0.4 μm $\pm$ 10 %.

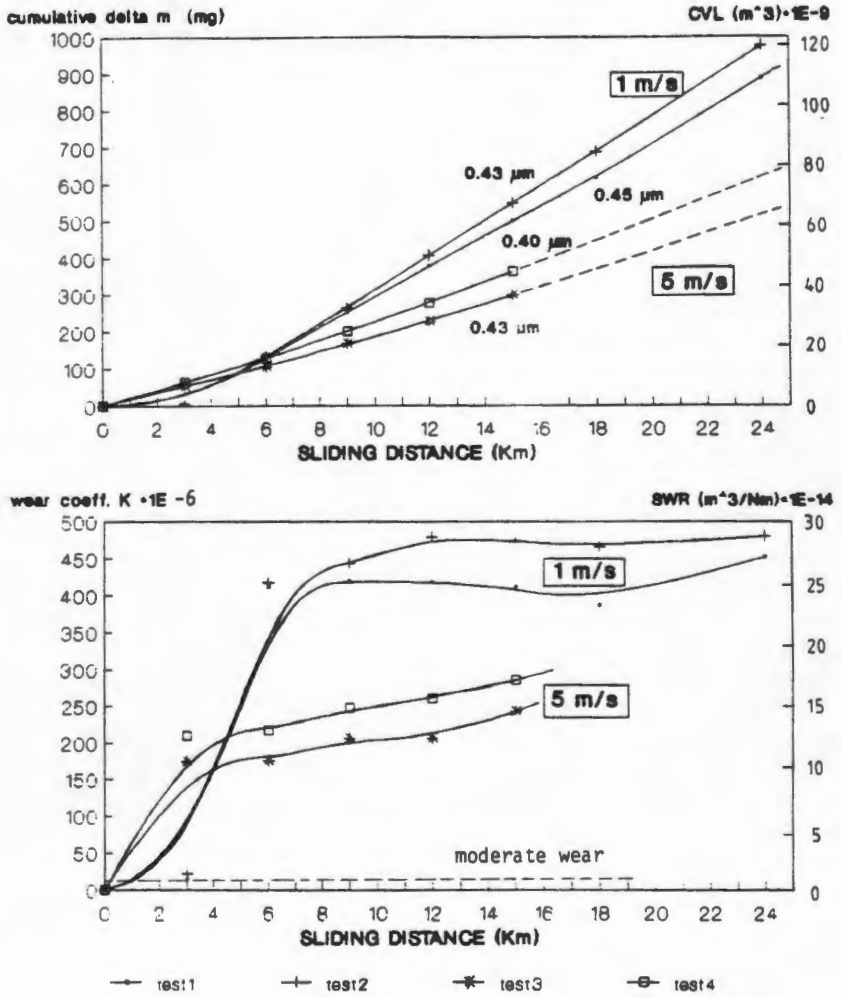

Fig. 3.17 RESULTS FOR 122/CZ114 COUPLE
20 N load, 1 m/s and 5 m/s peak velocity, dry conditions
VHN (30 kg) : counterface = 440 $\pm$ 5
: side specimen = 160 $\pm$ 5

As expected, wear coefficient K approaches severe galling ($K = 10^{-3}$), but the highest value of K for these tests is still more than half a magnitude smaller than the lowest K value for the 17-4/17-4 system.

For both the 1 m/s and 5 m/s cases, reproducibility has improved to a very good ± 6% and ± 11% respectively. These graphs are also the best ones obtained thus far that follow the pattern of service life in three distinct stages although only two of the stages are shown for the interval tested - a short run-in period, followed by an approximately constant SWR, indicating that steady state conditions have been attained.

The graphs for the two speeds are well separated, clearly indicating that higher speeds result in less wear. This effect for dry sliding has been reported by other researchers [26]. The reason for this is ascribed to the bigger frictional heating at higher speeds. As flash temperatures can attain several hundred degrees centigrade the melting point for CZ114 is readily exceeded. A semi molten interfacial layer of CZ114 thus separates the side specimen from the counterface and a constant wear rate results. The largest contribution to wear occurs during starting and stoping cycles as the interfacial layer becomes more viscous as it solidifies and shearing occurs over large areas. Mass loss remains small as material is transferred back and forth between the two interfaces. This transfer and back transfer is consistent with observations by Smith [45] and Zum Gahr [4].

This shearing over big areas causes a very coarse topography on the counterface as big lumps of transferred material stick to it at random. Figure 3.18 illustrates this clearly.

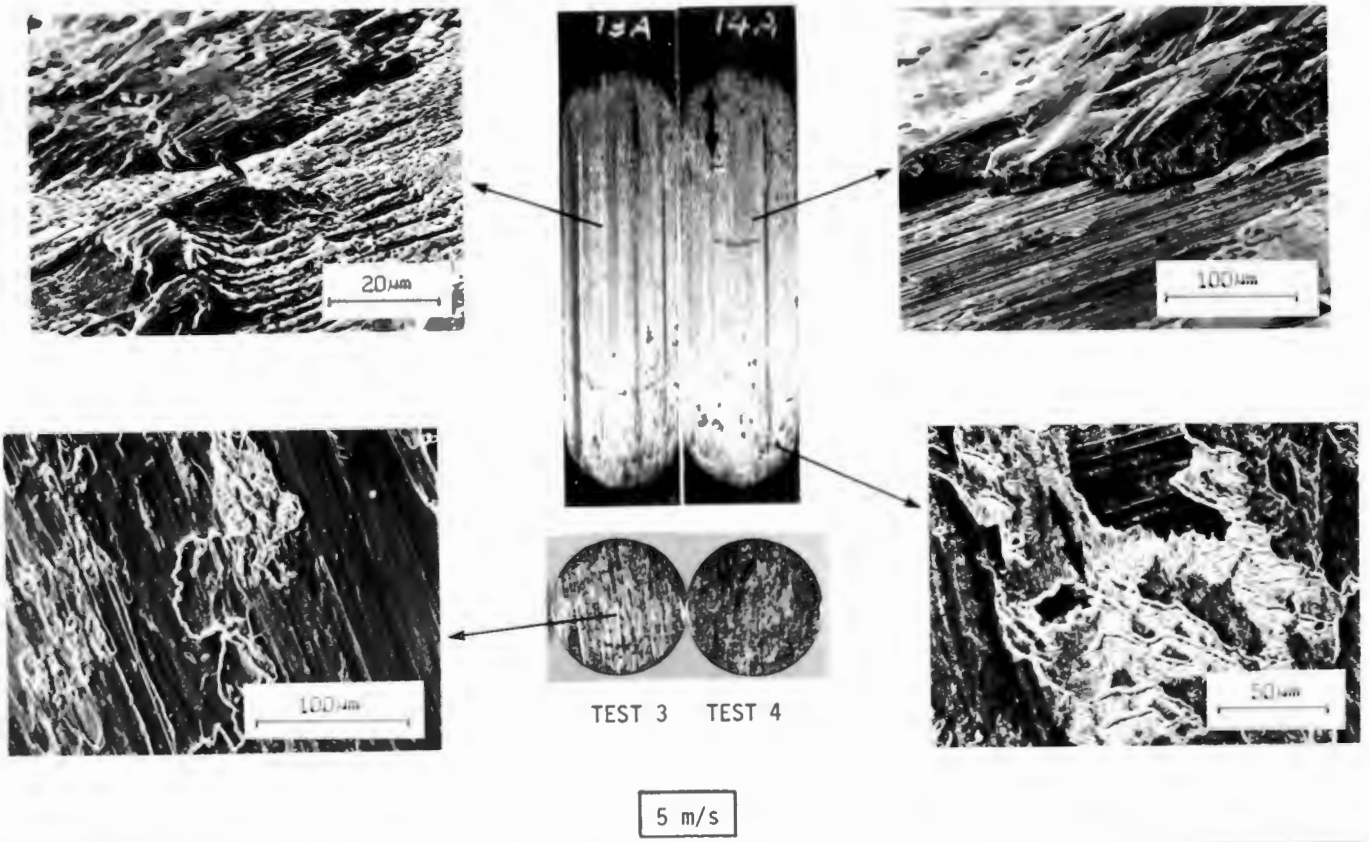

Fig. 3.18 MICRO/MACROGRAPHS FOR 122/CZ114 COUPLES AT 5 M/S

The temperature effect is also demonstrated by the side specimens. The softening of the interacting face cause an increase in diameter of over 25% and the edges show a pronounced lip.

The thickness and sizes of the transferred platelets is clearly shown in fig. 3.18.

Figure 3.19 shows a series of slides for the same test specimen but at the lower speed of 1 m/s. The amount of transferred material is much less pronounced and the relatively 'cooler' conditions cause a more abrasive wear mechanism which grates off layer by layer of the side specimen face.

Thus although the counterface is much less damaged, the material mass loss is about double at the lower speed. The circular marks resulting from the damage caused by the loading mechanism are clearly shown for 11A and 12A in fig. 3.19.

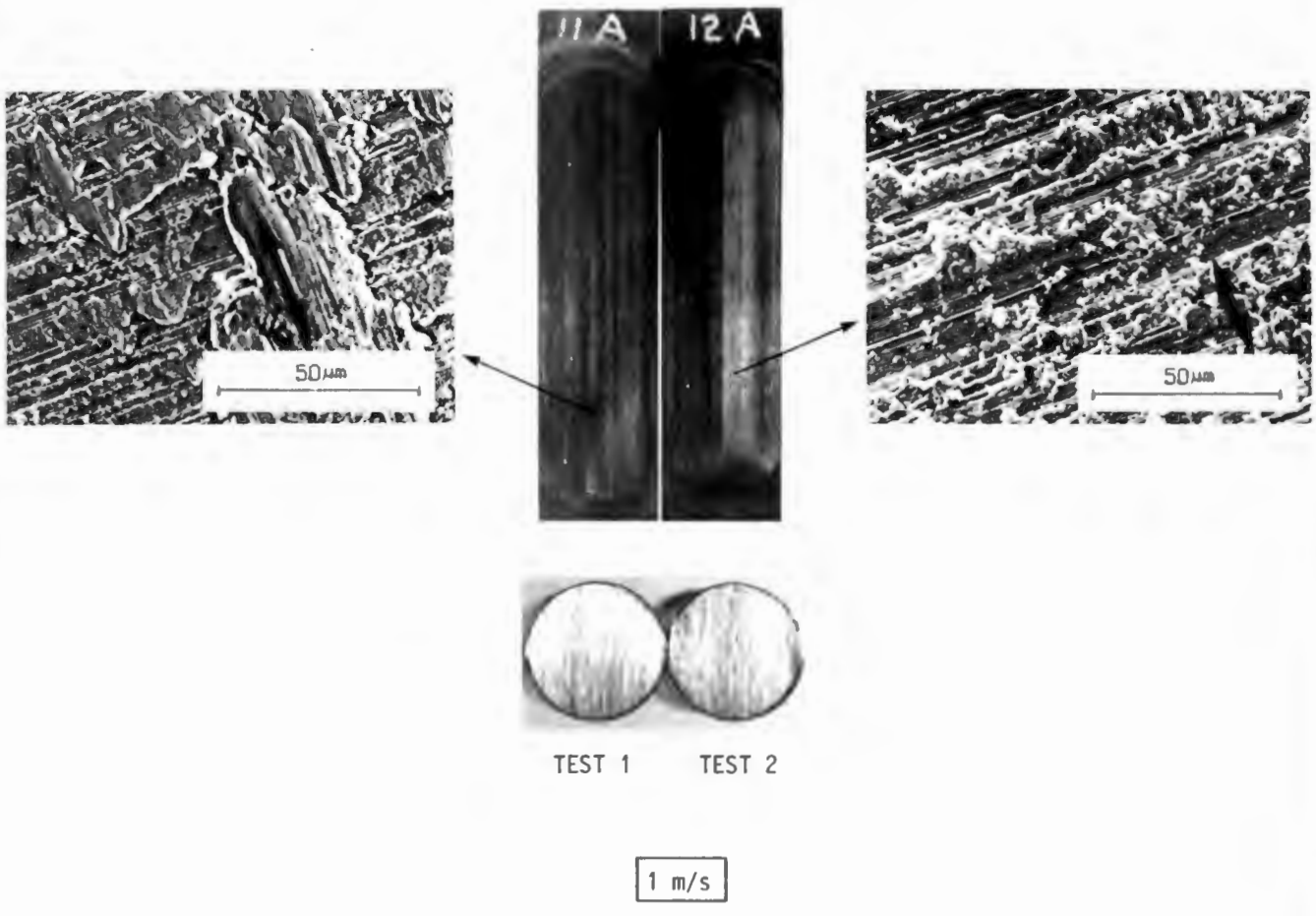

Fig. 3.19 MICRO/MACROGRAPH FOR 122/CZ114 AT 1 M/S

Encouraged by the improved reproducibility and the fact that the effect of speed was clearly distinguishable it was decided to continue testing under these conditions and with the same couple but under lubricated/cooled conditions.

Distilled water was chosen to eliminate uncertainty in tap water quality and a filter was included in the medium circuit to prevent ingress of potential third body abrasives into the test cell. The results of this last modification are outlined in the next section.

3.4.4 RESULTS FOR TEST FACILITY D

The layout of this test facility was described in section 3.3.3. Figure 3.20 below shows the results obtained for four tests done at 1 m/s and 5 m/s.

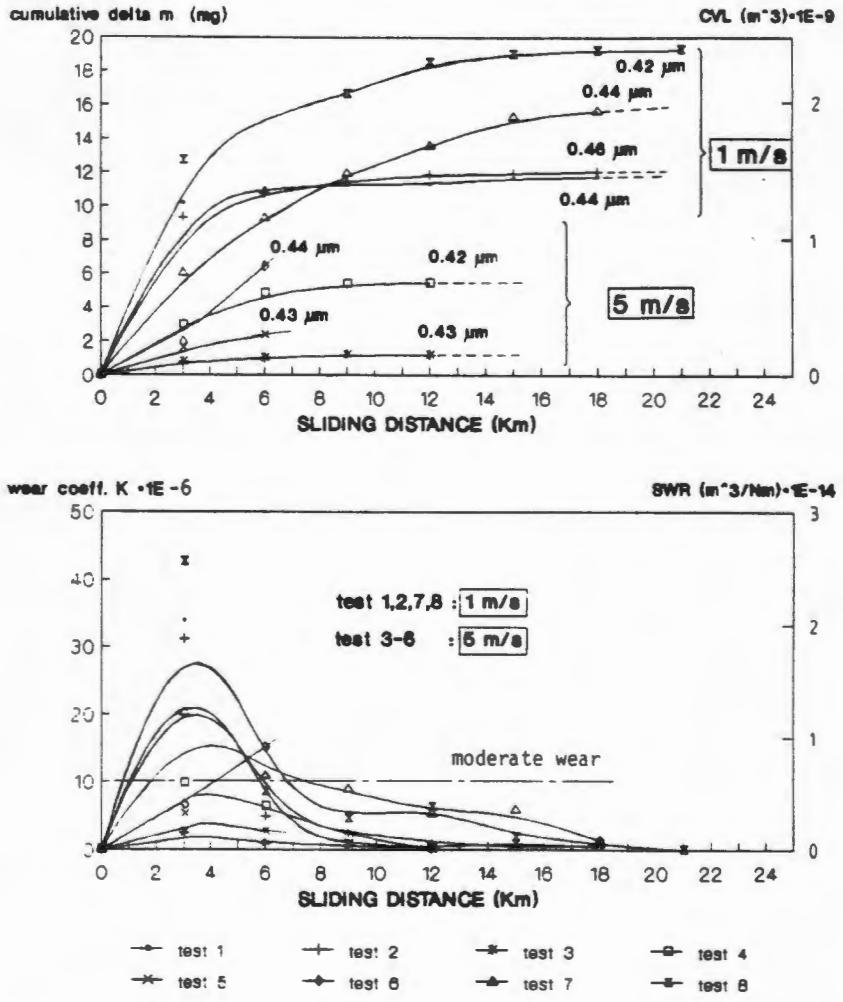

Fig. 3.20 RESULTS FOR 122/CZ114 COUPLE
20 N load, 1 m/s and 5 m/s peak velocity, distilled tap water lubricated/cooled conditions
VHN (30 kg) : counterface = 440 ± 5
: side specimen = 160 ± 5

The results for the 1 m/s test are particularly encouraging as reproducibility of ± 27% is attained - the best so far recorded for lubricated/cooled conditions. For the 5 m/s test reproducibility is, however, a low ± 50%.

After approximately 7 km, the wear coefficient, K for 7 of the 8 tests done is well within the adhesive wear regime. Based on these graphs it would then appear that a test facility has at last been found which yields adhesive wear data. Most of the plots show both a run-in period and then a reduced wear rate during what would be the normal operating or steady state regime.

Figure 3.21 shows micro- and macrographs for test 7 and 8 at 1 m/s.

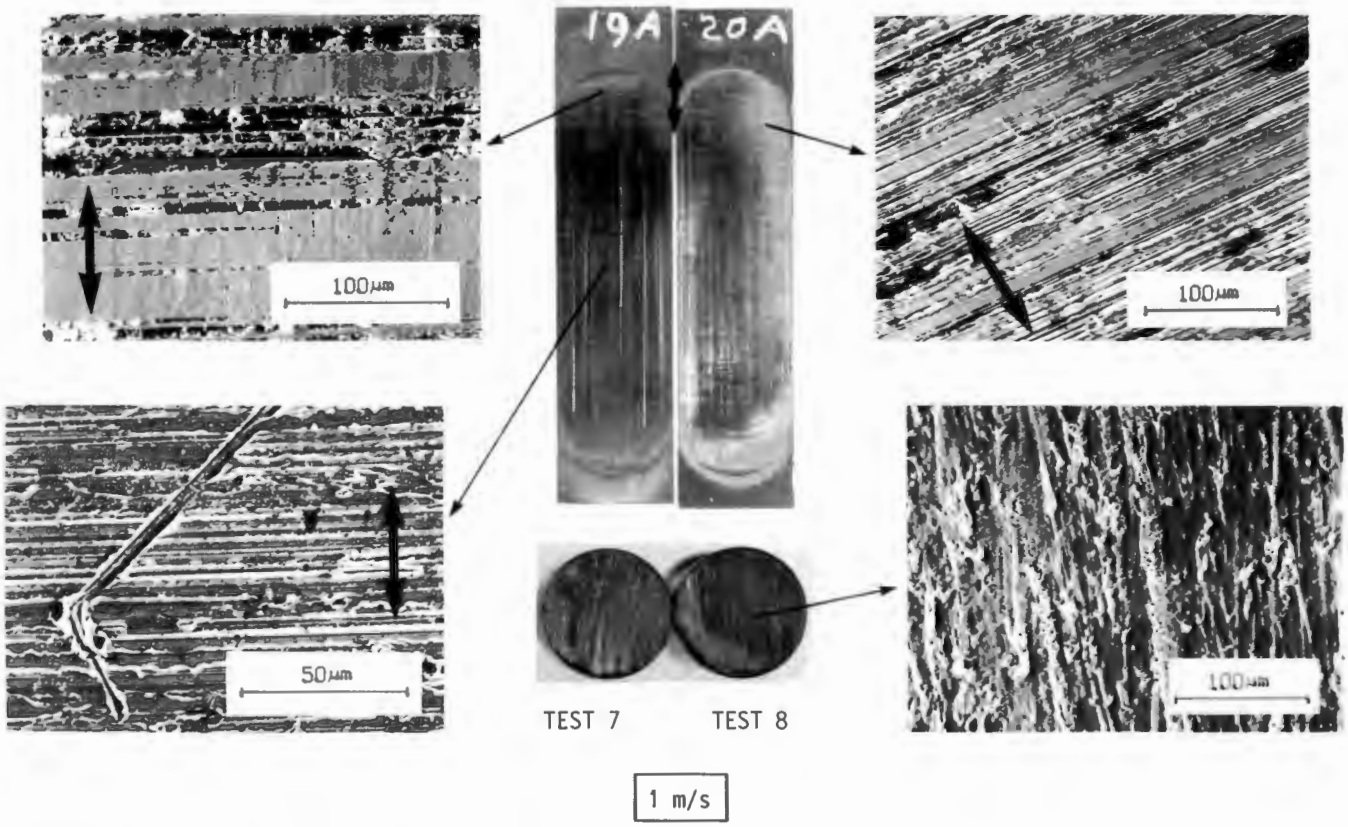

Fig. 3.21 MICRO-/MACROGRAPHS FOR 122/CZ114 COUPLES AT 1 M/S

Both the 1 m/s and 5 m/s tests showed the now familiar flattening off of ridges on the counterface and subsequent filling in of the valleys between ridges with transferred bronze. The consequences of this smoothing of the counterface results in a more refined counterface. But because this process also generates third body abrasives - dislodged transfer material and grinding fragments - it is inconceivable that wear could be prevented altogether, even once the entire counterface is covered.

In fact, scratches begin to form within the transferred layer at an accelerated rate the more covered the specimen becomes. (refer also to fig. 3.21). Thus despite graphical indication that suggest that wear is due to adhesive mechanisms, it is in fact due to transfer and formation of abrasive particles which then proceed to groove the surfaces.

Figure 3.22 shows a series of photographs for the tests done at 5 m/s. The same general trends are observed as previously but the counterfaces appear more polished and less bronze has been transferred. The lower wear rate in this case is ascribed to poor matching of the interacting surfaces. In fact, only 50% of the area of the side specimen is in contact for tests 5 and 6.

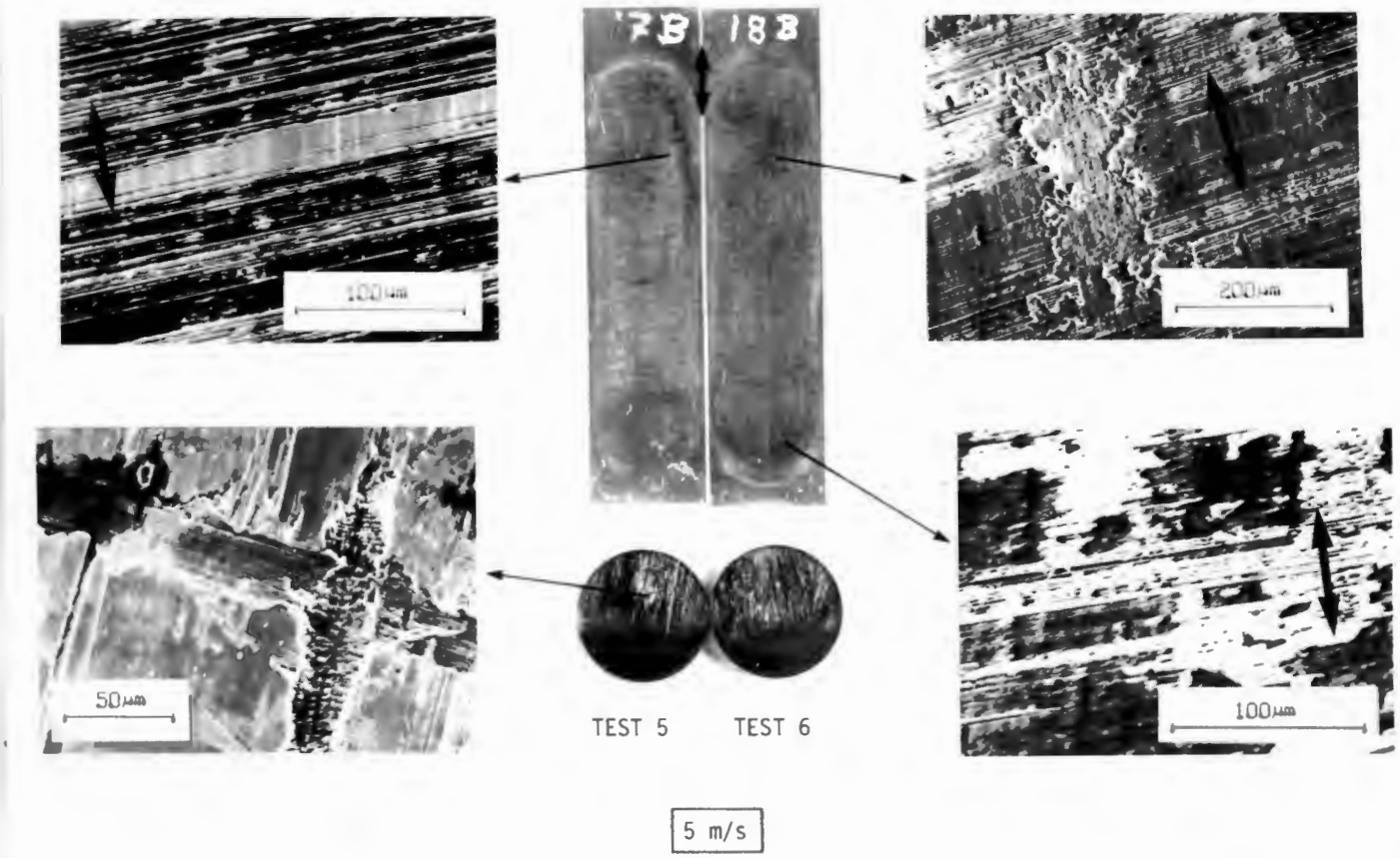

Fig. 3.22 MICRO-/MACROGRAPH FOR 122/CZ114 COUPLE AT 5 M/S

Doubts are cast as to the validity of all the results obtained on this test facility, as nearly no wear is recorded after fairly short sliding distances, in spite of macrographical evidence to the contrary. No explanation could be found for this other than that the induced wedges (due to the rocking action explained in (fig. 3.15) assist in separating the interacting surfaces.

3.5 SUMMARY OF ALL RESULTS OBTAINED TO DATE

This section will attempt to summarize the results of all the tests done to date in a manner that will facilitate comparison between the different couples, and assist in the interpretation of the graphs. Three specific areas will be covered. Firstly, the reproducibility of the generated data will be scrutinized; secondly the results will be explained in terms of what wear mechanisms dominate; and lastly the results will be interpreted in respect of their meeting the set objectives.

It should also be noted at the outset of this section that interpretation and comparisons are not straight forward because:

- three different couples have been tested
- testing parameters of speed, load and surface roughness are not consistent throughout the test programme
- the lubrication/cooling medium differed four times
- sliding distances did not remain constant

Nevertheless, certain qualitative trends can be identified and specific statements made about the implemented test programme.

3.5.1 REPRODUCIBILITY

Figure 3.23 summarizes the cumulative mass losses as a function of sliding distance for all six test done. The top graph is plotted on a 1000 mg scale and the lower one is a repeat plot for the same distance, but scaled only to 100 mg.

The results can be broken up into two distinct groups. Group I includes the tests done on the 17-4/17-4 couple and the two dry test on 122/CZ114. In all three cases mass losses are far in excess of 100 mg after 15 km of sliding.

Group II covers the remaining tests which were all conducted in water lubricated/cooled environments under much scaled down test conditions. The mass losses for this group are substantially less than 100 mg after the same sliding distance.

Ignoring the dry tests and looking only at the three different water lubricated tests, show that a good measure of success has been attained in improving reproducibility from the original test set up to the final test facility D. Reproducibility, as expressed by the $\pm$ deviation in mass loss, shows an improvement from a worst case of $\pm$ 87% with facility B, to a best value of $\pm$ 27% with the last setup used. This "best" value does however still compare unfavourably with the $\pm$ 21.5% quoted by Lloyd [3].

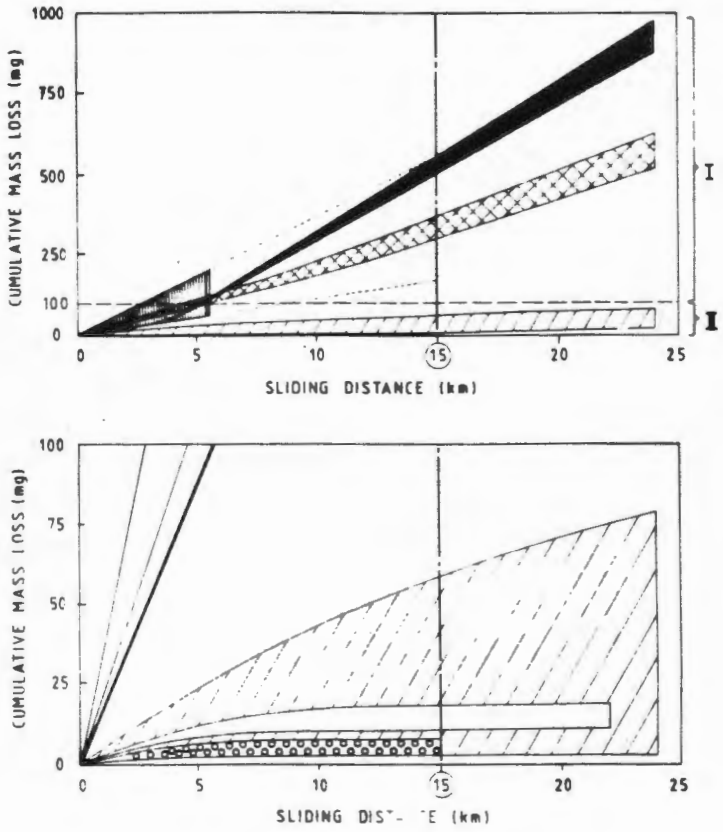

TEST FACILITY	GROUP	COUPLE	LUBRICATION/COOLING	SPEED	LOAD	*	$	CLA ± 10%
A	I	174/174	pressurized tap H_2O	10m/s	5N	360 ± 195	±54%	0.2
B	II	122/AB2	tap H_2O	1m/s	20N	32 ± 28	±87%	0.2
C	I	122/CZ114	dry	1m/s	20N	530 ± 30	± 6%	0.4
C	I	122/CZ114	dry	5m/s	20N	340 ± 37	±11%	0.4
D	II	122/CZ114	distilled H_2O	1m/s	20N	15 ± 4	±27%	0.4
D	II	122/CZ114	distilled H_2O	5m/s	20N	6 ± 3	±50%	0.4

* cumulative mass loss after 15Km in mg ±△mg

$ △mg expressed as a % of mg

Fig. 3.23 SUMMARY OF CUMULATIVE MASS LOSSES FOR THE INITIATED PROGRAMME

The reasons for the generally poor reproducibility in these results are the inadequacies of the basic test rig hardware, the poor design of test specimens, inconsistent surface finishes of test specimens and poor surface matching.

It is a well recognised feature of tribotesting that results fall into a wide scatter band [44]. The simpler the tribosystem, the narrower this band. Figure 3.24 below shows a typical CVL versus sliding distance curve for a given tribosystem and the 'inherent' scatter band is indicted by "A". Due to the inadequacies listed in the results section, the actual scatter band for the results obtained to date, is in fact much greater and is denoted by "B" in fig. 3.24.

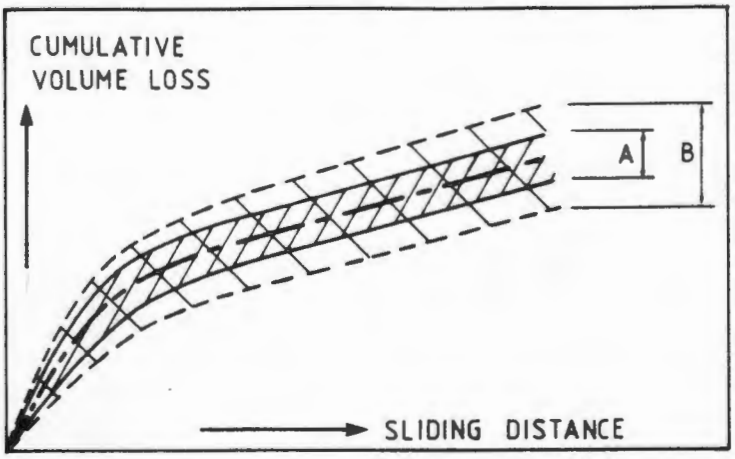

Fig.3.24 DATA SCATTER BAND FOR TRIBOTESTING

It is thus reasoned that by improving the test rig hardware and using a simpler design for the specimens, the scatter band can be narrowed down from the current B width to the inherent minimum A.

Based on the above, the recommendation is thus made to design both a new test facility and simpler test specimens. Particularly because the viable modifications to the original layout have been exhausted and the results to date have illustrated that it is entirely feasible to progress from a scatter band width of B to one approaching A.

3.5.2 DOMINANT WEAR MECHANISMS

The dimensionless wear coefficient, K is probably the most realistic parameter by which the six different tests can be compared, as it takes load, sliding distance, hardness, density and mass loss into account. It conveys essentially the same information as SWR, i.e. the slope of the graph listed in fig.3.24.

Figure 3.25 below summarizes the wear coefficients for the six types of tests done on the four test facilities. The excessive mass loss of group I tests is confirmed - all three of the tests show ranges for K that approach the upper limit of the zone within which abrasive wear is typically encountered. The remaining three tests fall under group II and results for these tests spread across both the abrasive and adhesive wear zones identified by Rabinowicz [33].

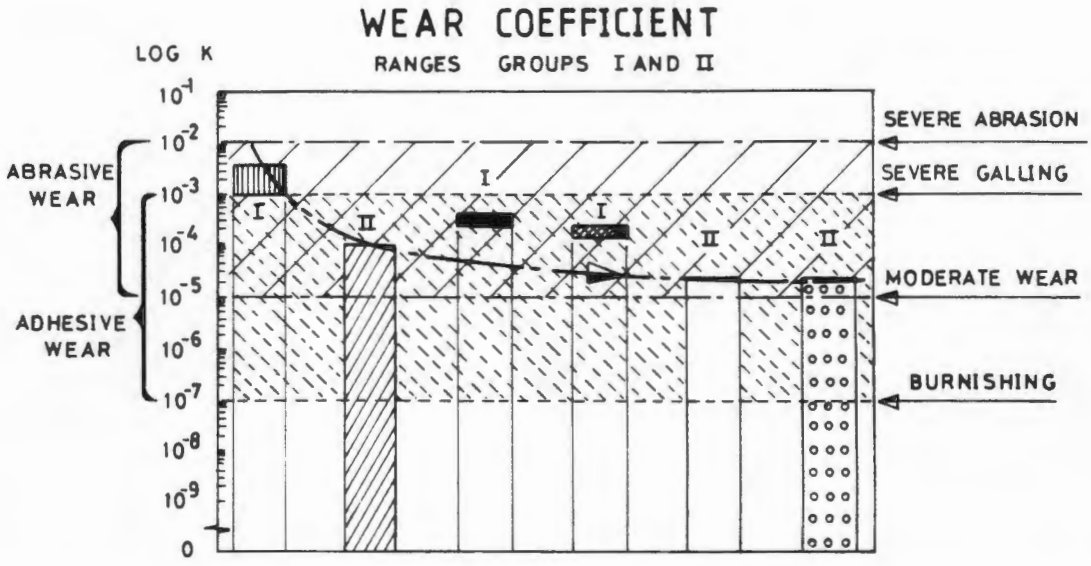

TESTFACILITY	GROUP	COUPLE	LUBRICATION/COOLING	SPEED	LOAD	*	$	CLA ± 10%
A	I	174/174	pressurized tap H_2O	10m/s	5N	360 ± 195	±54%	0.2
B	II	122/AB2	tap H_2O	1m/s	20N	32 ± 28	±87%	0.2
C	I	122/CZ114	dry	1m/s	20N	530 ± 30	± 6%	0.4
C	I	122/CZ114	dry	5m/s	20N	340 ± 37	±11%	0.4
D	II	122/CZ114	distilled H_2O	1m/s	20N	15 ± 4	±27%	0.4
D	II	122/CZ114	distilled H_2O	5m/s	20N	6 ± 3	±50%	0.4

* cumulative mass loss after 15Km in mg ±Δmg

$ Δmg expressed as a % of mg

Fig. 3.25 SUMMARY OF WEAR COEFFICIENTS, K
(ranges for typical values of K for metal on metal sliding systems as compiled by Rabinowicz [33] have been superimposed onto this graph)

Considering only the water lubricated tests, a curve can be drawn which joins the maximum K values for each of the couples. This curve shows that an improvement of more than two orders of magnitude has been achieved by improving/simplifying the original test facility. But as no further improvement on these figures could be attained, the recommendation is made once again to design an improved facility.

Wear coefficients alone do not clarify what wear mechanisms predominate as the adhesive and abrasive zones overlap and the definition of their boundaries is not absolute. Recourse must therefore be made to the micro - and macroscopic features of the interacting surfaces.

These show quite convincingly that abrasive wear does in fact become the predominant wear mechanism in all tests. Third body abrasives, generated from three different sources cause scratching, ploughing and cutting on the counterfaces. This is not at all surprising as in reciprocating sliding, wear debris is not removed from the rubbing area [43]. The three sources are as follows: from asperity shearing, breaking off of machining fragments and thirdly dislodging of transferred material, either from the side specimen to the counterface or vice versa. Being the softer material, the rubbing face of the side specimens show clear evidence of grooving (abrasion) damage in all cases.

Some evidence of adhesive wear and plastic smearing of generally only the side specimens or the transferred side specimen material on the counterfaces, is noted on isolated portions of the counterfaces. Its contribution to the overall wear process is however considered negligible.

In all cases substantial changes in topography have occurred and monitoring of these using two dimensional CLA traces proved futile. A non intrusive method of building up a three dimensional picture for the surface (e.g. optical or laser methods) would have helped in quantifying the changes.

3.5.3 INTERPRETATION OF DATA

The results thus far generated under both stage 1 and substage 1 (refer fig. 1.1) indicate that neither stage was successful in terms of meeting the set objectives and that the programme therefore needed to be diverted to substage 2 i.e. the design of a new test facility.

Reproducibility has significantly improved and the wear coefficients have taken on more realistic values in response to the modifications made. Nonetheless two principal deficiencies remain. Firstly neither the "run-in period" or the slope of the "normal operation period" (if distinguishable in the first place) are the same between tests. Run-in can be ignored as different surfaces will take different lengths of time to bed in. But the slopes are the important information which is required. They give an indication of the rate at which wear proceeds during normal operation and hence define the service life of the components of interest.

Secondly, the wear regime spans over too wide a range of wear coefficients and can not be positively identified as being adhesive wear. Perhaps it is unreasonable to expect this type of testing to fall into an adhesive wear band. To confirm whether or not high speed reciprocating sliding systems should yield adhesive wear, recourse should be made to information about the surface damage encountered by the in-service components under consideration. This detailed information would also be essential in terms of relating the model test results to rockdrill and impact hammer performance. More tests should have been conducted for each of the couples to improve statistical interpretation. Because of the foregoing and the fact that specimens were costly and difficult to machine and grind, this could not be justified.

A database on the performance of contender materials under conditions of reciprocating sliding in water cooled/lubricated environments requires that a test facility exists, which produces reproducible data on a consistent basis. All the foregoing has demonstrated that the original test facility is incapable of doing this.

The results thus far generated - although interesting by themselves - are of no use in terms of advancing the understanding of fundamentals of tribology or building up of ranking tables. It is also not possible to make conclusive statements as to the performance of individual materials.

It was therefore decided to abandon the original test facility completely and instead concentrate all effort on the design of a new test rig as motivated by substage 2 of fig. 1.1.

3.6 MOTIVATION FOR A NEW TEST RIG

Efforts had been made to modify and improve the existing facility in a quest to meet the set objectives of this research initiative. But because the concept on which the inherited test facility was based is flawed, it became essential to redesign a test rig if a successful transition is to be made to stage 2 of the short term objectives (refer also to fig. 1.1).

The reasons for why the generated test results are of limited use are summarized below:

- o reproducibility poor
- o results cover too large a wear regime
- o no testing could be done at maximum settings
- o rig wears itself out as quickly as the test specimens are worn out
- o limited control over test parameters

These points in turn stem from several deficiencies in respect of the test specimens and test rig hardware. The more relevant of these points are listed below as they help consolidate the motivation for a new test rig.

3.6.1 TEST SPECIMEN DEFICIENCIES

- o roundbar design for stationary specimens is poor as rotation can not be prevented in bore and no reference face available for reinserting specimens in identical position after each and every interval during interrupted testing.

- o machining a hole down the long axis of the reciprocating specimen (refer fig. 3.6) is unwise as deposits collect which can not be monitored or properly cleaned.

- o using all four faces on the reciprocating specimen is impractical. Those faces not in current use will invariably become damaged and those already used could pick up deposits, loose wear debris or contribute third body abrasives.

- o edge effects are significant as the diameter of the side specimen equals the width of the counterface. Edges of the faces at right angles are therefore spoilt. Counterfaces should instead be wider than the widest dimension of the surface of the side specimen.

- o philosophy of reusing specimens is shortsighted. No reference can subsequently be made and valuable information could be lost.

- o concept of testing two side specimens at once is unwise as it becomes impossible to proportion what percentage of total wear is due to which face

- o specimen design is tedious and expensive to machine as far too fine tolerances are required. It would be much better to incorporate necessary accuracy in the test rig and use simpler specimens.

3.6.2 HARDWARE DEFICIENCIES

- o components rapidly deteriorated and frequent replacement was necessary because the reciprocating drive was under-designed, no lubrication was provided and inadequate provision had been made for proper alignment

- o material selection for components (other than test cell itself) was incompatible with water environment and substantial corrosion damage resulted

- o seals and bushes required replacement after one or two tests, depending on speed at which tested

- o original lubricant/coolant circuit underrated and electrical system therefore tripped too frequently

- o dc motor underrated and trips at high side loads

- o specimen mounting arrangements inadequate:
  - reciprocating specimen has too many degrees of freedom
  - side specimen can rotate and rock in housing. Machining flats onto specimen and inserting a grub screw limited only the rotation

- o loading of stationary specimen against reciprocating counterface is inadequate as stationary specimen is rotated against the counterface under load and wear damage therefore results before a test has even started

- o specimens are not readily accessible and alignment disrupted every time reciprocating specimen is extracted. Sloppy fits and poor alignment thus resulted

- o general maintenance on rig is awkward as wearing items not readily accessible

- o ingress of scale and rust from pipework of original medium circuit

- o specimens can not be relocated in identical positions during interrupted testing

It was decided to redesign the test facility such that additional features (over and above those which will address current inadequacies) are incorporated. The actual requirements set for the new design are listed in section 4.0.

4.0 DESIGN OF A NEW TEST RIG - DEFINITION OF THE PROBLEM

4.1 PROBLEM STATEMENT

Design a test rig, capable of investigating the performance of material surfaces, rubbing against one another under conditions of high speed reciprocating sliding in specific environments.

4.2 REQUIREMENTS OF THE DESIGN

The design must:

- permit speed of reciprocation to be adjustable from 0 to a maximum peak velocity of 10 m/s;
- give a sinusoidal velocity profile over the entire speed range catered for;
- provide for a consistent maximum load of 100 N to be applied onto the reciprocating plane of the test specimens;
- enable the stroke length to be adjustable between 0 and 30 mm;
- have a service life of 1000 hours under maximum test conditions;
- facilitate that both test specimens are readily accessible and that locating and then securing in position are simple to achieve;
- feature a specimen loading device which will allow no relative movement between the test specimens (before or after surface contact is established), other than along the axis of the applied load;
- guarantee the test specimens to be repositioned in an identical fashion after each and every test run in order to ensure that the reciprocating surfaces remain perfectly matched;
- enable the friction force at the rubbing interface to be constantly monitored over the entire speed and load range;
- monitor the number of cycles done so that sliding distance can be kept constant from test to test;
- permit tests to be conducted under dry conditions and in various synthetic mine water environments (containing for example Cl^- and SO_4^{2-} ions), both under flowing or stagnant conditions and with or without temperature control;
- make provision for an environmental chamber to be positioned around the reciprocating interface so as to control ambient temperature, pressure and humidity level;
- make it possible to cater for the following three specimen configurations:
  a) flat on flat
  b) piston in a longitudinally sectioned bore
  c) sphere on flat
- permit specimens of a simple design to be used so as to attain required surface finish along the simplest and quickest manufacturing route;
- enable the smallest possible specimens to be used so that cost and weight are minimised, but not at the expense of introducing surface effects or making fabrication and handling awkward.

4.3 CONSTRAINTS IMPOSED ON THE DESIGN

The design must:

- incorporate materials which are compatible with synthetic mine water environments, as well as temperatures not exceeding 100 C;
- the design must not become a single purpose device that will subsequently become obsolete. It must therefore be built in a modular fashion such that existing features can readily be expanded upon or existing components be exchanged without requiring major modifications;
- allow for all wearing components (seals, bushes, bearings) to be readily accessible for routine inspection and/or replacement;
- make provision for attaching other drive mechanisms that will permit saw-tooth, square wave, random or periodic velocity profiles to be obtained, if so desired;
- incorporate the D.C. motor and speed controller from the original test facility as the primary drive for the reciprocating drive mechanism;
- incorporate within itself the required precision for reproducible testing such that machining tolerances on test specimens can be relaxed. This means that testing is less affected by deviations in dimensional consistency from specimen to specimen;
- not exceed the budgeted total cost of South African Rands 15 000,-;
- not require any special workshop facilities;
- not exceed a fabrication period of two months;
- make it possible to accommodate the specimens that were machined for the previous test rig, as a large number of them were made up and represent a large investment in machining time and cost.

4.4 CRITERIA SOUGHT FOR IN THE DESIGN

The design should:

- be as simple and functional as possible;
- use standard material dimensions wherever possible;
- utilize as many standard components as possible, particularly for the wearing components;
- permit wear fragments to be trapped and/or collected;
- minimise noise generation;
- be simple to operate;
- be of a compact design so as to minimise required laboratory space.

5.0 SOLUTION SPECIFICATION FOR THE NEW TEST RIG

DESCRIPTION

A prototype laboratory test rig intended for investigating the performance of material surfaces rubbing against one another under conditions of high speed reciprocating sliding in specialist environments.

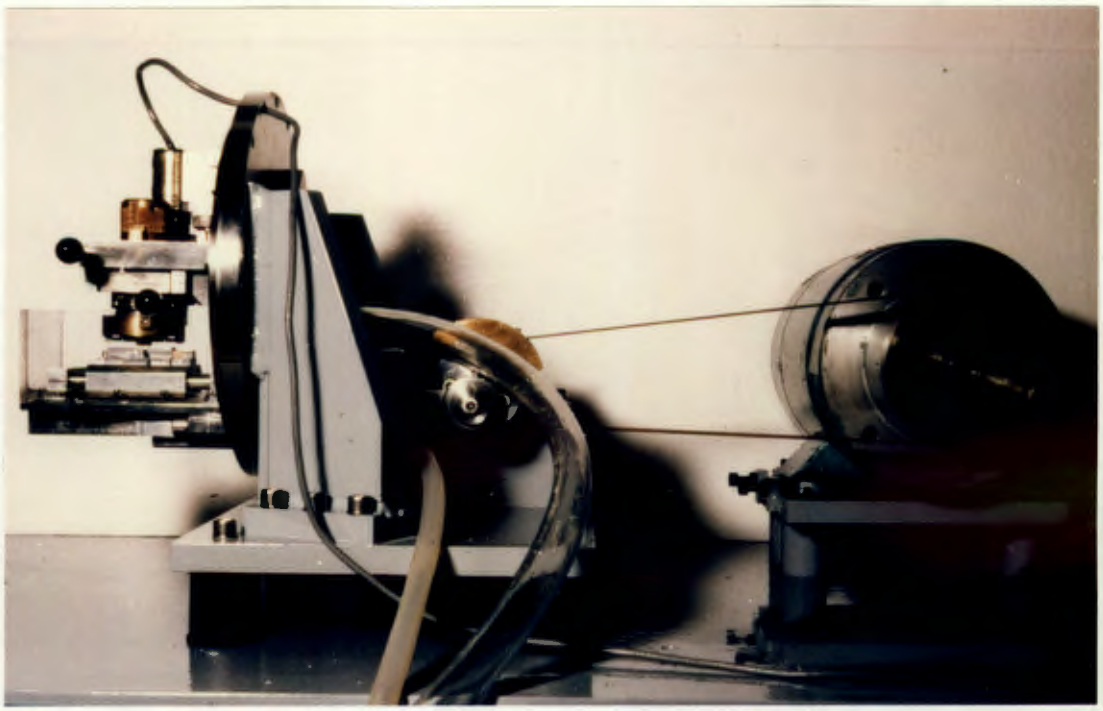

Fig. 5.1 THE NEW TEST RIG

HARDWARE

- overall dimensions (mm)	:	length = 690 - 1090 width = 615 height = 410
- primary drive	:	GEC 1.5 kW/220 V DC motor
- speed regulation	:	GEC variable speed controller
- reciprocating drive	:	belt driven crank slider (balanced in primary forces)
- stroke length	:	30 mm *
- velocity profile	:	sinusoidal *

TEST SPECIMENS

- maximum dimensions possible for basic test rig layout *

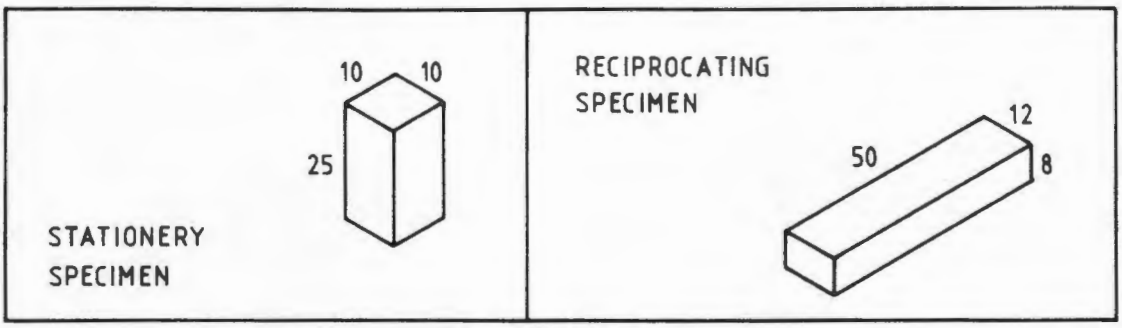

Fig. 5.2 TEST SPECIMENS RECOMMENDED

OPERATING PARAMETERS

- reciprocating speed : 0 - 106 Hz (= 0 - 6365 RPM @ crank driven end)
  (= 0 - 10 m/s peak velocity)
  (= 0 - 6.36 m/s average velocity)
- loading of specimens: spring force adjustable 0 - 100 N in 5 N increments
  (0 - 1 MPa; to increase this load, decrease specimen area)
  : dead weight 0 - 2 kg

TESTING ENVIRONMENTS

- dry testing *
- testing in a bath filled with desired medium under stagnant or flowing conditions. *

FEATURES

- continuous read out of friction force over entire speed and load range
- repositioning in an identical position is guaranteed for both test specimens after each and every test run. Reciprocating surfaces will therefore remain matched even during interrupted testing.

OPTIONS

Provision has been made in the design to allow for exchanging components or adding to the basic test rig in order to expand on specifications marked *, as follows:

Hardware

- stroke length adjustable 0 - 30 mm if crank pin holding plate (item 78) is interchanged

- velocity profile can be modified for low speed investigations (< 1 m/s) using a pneumatic piston drive in place of the crank pin slider of the basic design. This would permit modelling any of the following velocity profiles : saw-tooth, square, random or periodic
- an environmental chamber can be fitted to the existing rig if tests are to be conducted in specialist environments.

Test Specimens

- the test rig can cater for several specimen designs if the specimen mounting plate (item 28) is modified:

  o type I : simple geometry, intended for rapidly building up material ranking tables.
  o type II : best approximation of a piston/shaft reciprocating in a bore/housing.
  o type III: for theoretical work where actual areas of contact are of interest.
  o any other geometry within the dimensional limits specified.

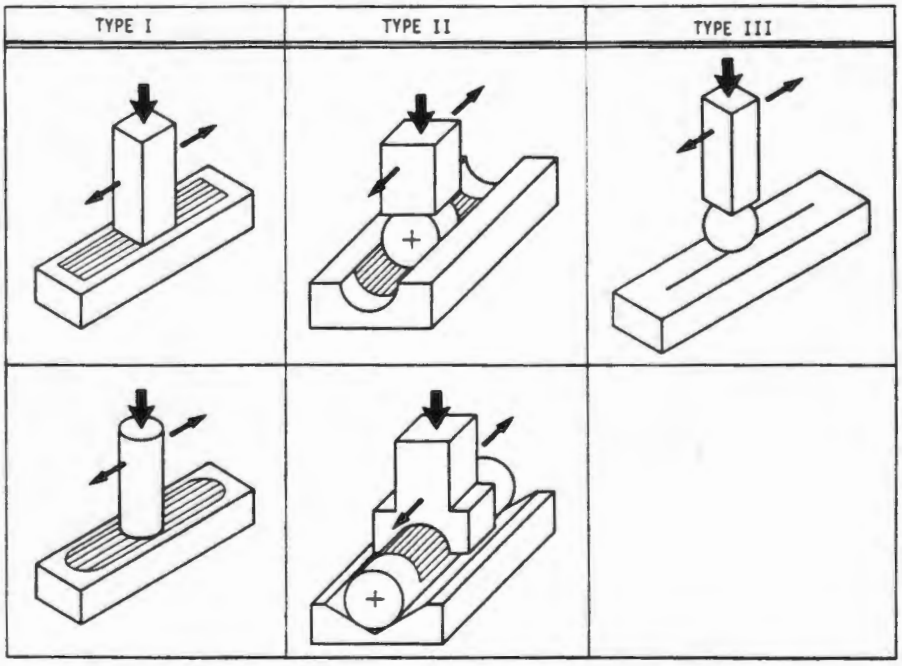

Fig. 5.3 POSSIBLE TEST SPECIMENS

Features

- provision has been made for monitoring temperature of the bath by way of thermocouples
- if the environmental chamber is utilized, provision has been made for the continuous monitoring of pressure and temperature.

Testing Environments

- flow rate and/or temperature can be controlled within the bath;
- if the environmental chamber is mounted over the basic test cell, the following specialist environments can be achieved:
  - o testing in controlled environments in respect of temperatures, pressure and humidity levels
  - o testing at depressed or elevated temperatures
  - o testing under conditions of partial vacuum or at pressures above atmospheric pressure
  - o flooding the entire test cell for testing under fully hydrostatic conditions.

MATERIALS USED

- internal workings of test cell :316 stainless steel, P-bronze, 440C stainless steel, Aluminium - 7017, Perspex, Solidur Ds
- external features of test rig : 431 stainless steel , En24 mild steel, En3 mild steel, Brass

COST (IN SOUTH AFRICAN RANDS)

- total cost of materials and standard components	R 3 358	
- manufacturing cost		
o consumables	R 699	
o labour	R 8 835	
o sub contracted jobs	R 483	
- total final cost of rig	R 13 375	(This corresponds to 5650 US Dollars or English Pounds 3180 at November 1988 exchange rates)

6.0 CONCEPT FORMATION FOR THE NEW TEST RIG

6.1 GENERAL POINTS

The extent to which tribological data can be extrapolated into service performance predictions decreases from field test to model test. Transferability of this data from the model test to service can only be expected to be successful if the same loading conditions, the same structure of the tribosystem and the same wear mechanisms predominate. The various levels of simplification in going from field testing to simple model tests are depicted in fig. 6.1 below.

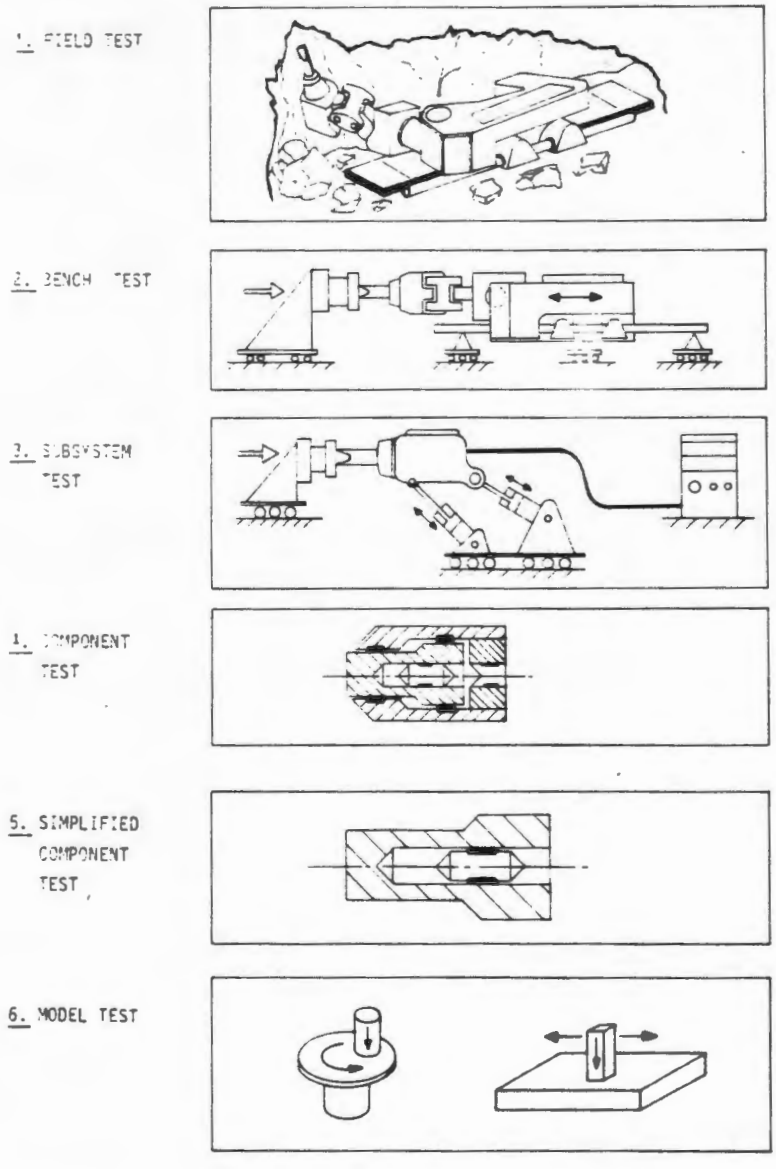

Fig. 6.1 CLASSIFICATION OF DIFFERENT TRIBO TESTS
(adapted from Zum Gahr [4])

The best test rig is obviously the field test itself. It is, however, discounted as an option for this research initiative for the following reasons:

- high cost is tying up prototype rock drills and impact hammers;
- prohibitive cost and lead time in machining up the individual components under investigation;
- long test periods and logistics problems in setting up test facilities underground;
- difficulty in controlling operating conditions and changing test parameters;
- every material and component change requires the unit to be returned to a specialist workshop;
- as several wear mechanisms compete during the surface degradation, only a tribosystem approach can be used for the analysis;
- fundamental knowledge in respect of how different parameters affect degradation is impossible to build up, as too many variables compete.

Model testing in contrast is advantageous for scientific investigations because they afford greater reproducibility of test parameters and hence test results. In addition experimental conditions are readily altered, testing expenses are relatively small, simple specimens can be used and the time taken to obtain useable data is drastically reduced.

Taking cognizance of the above and realizing that the important requirement for the hydropower programme is one of screening contender materials, model tests are at present sufficient. Once suitable material couples have been identified, the necessary justification will be there to ascend the levels of tribo testing from model tests to eventually field tests.

The testing facility that is sought models a tribological process. It therefore seems fitting to represent the problem as defined in chapter 4.0 with the very simple tribosystem depicted in fig. 6.2.

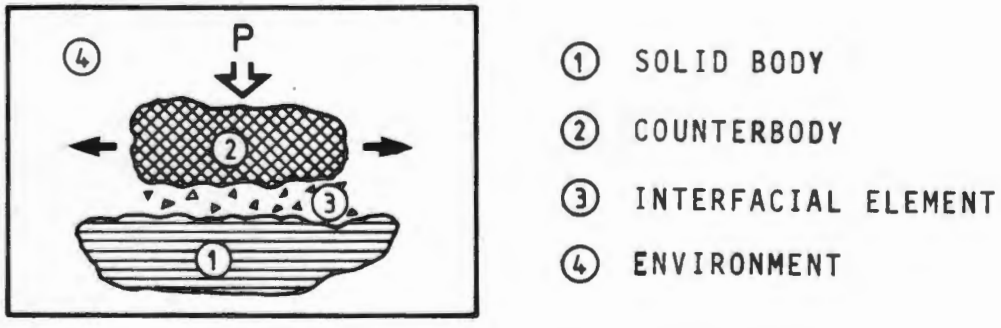

Fig. 6.2 THE TRIBOSYSTEM OF INTEREST
(no distinction is made between (3) and (4), as in this case both are the working fluid which is treated mine water)

In both macro- and microscopic terms, this model is a fair representation of what happens at the interfaces of oscillating components inside the rockdrills and impact hammers. As an extension of the above argument, a simple specimen, rubbing back and forth on a matching surface is also represented by this model.

Using a reciprocating pin on plate model test thus seems a reasonable starting point. No suitable commercial or custom built test rigs of this nature could be found in the literature scrutinized. The designs reviewed either fell short of the desired specifications, were not versatile enough, or too costly and not readily available.

This partly stems from the fact that this type of test set up is rarely used in researching interacting surfaces. The vast majority of work in this field is conducted on pin on disc type test rigs. Researchers have a preference for these because they show good reproducibility thanks to their simplicity and are perfectly adequate for work of a fundamental nature.

In pin on disc tests (unidirectional motion) the velocities remain constant and as there are no cyclical reversals through zero, the lubrication characteristics and contact mechanics are very different to those encountered by reciprocating components. Transferability of data generated on pin on disc apparatus to reciprocating stoping equipment is thus poor and these test rigs are thus deemed not suitable.

In the realization then that a simple model test is quite removed from the actual tribosystem, it makes sense to conceive a multiple purpose reciprocating pin on plate test rig. Concepts therefore need to be generated for a hybrid design that simulates the stoping equipment in simple reciprocating pin on plate terms. The design called for must be flexible in terms of usable specimen configurations and controllable parameters.

6.2 DECISIONS MADE PRIOR TO DEVELOPING VIABLE SOLUTIONS

Two fundamental decisions regarding velocity profile and drive mechanism needed to be made. The saw tooth velocity profile of the stoping equipment cannot be duplicated by mechanical means unless peak velocities are significantly dropped. By using a sinusoidal velocity profile, the same peak velocities are attainable but the number of transitions from boundary to hydrodynamic lubrication are significantly increased.
Figure 6.3 contrasts the two velocity profiles.

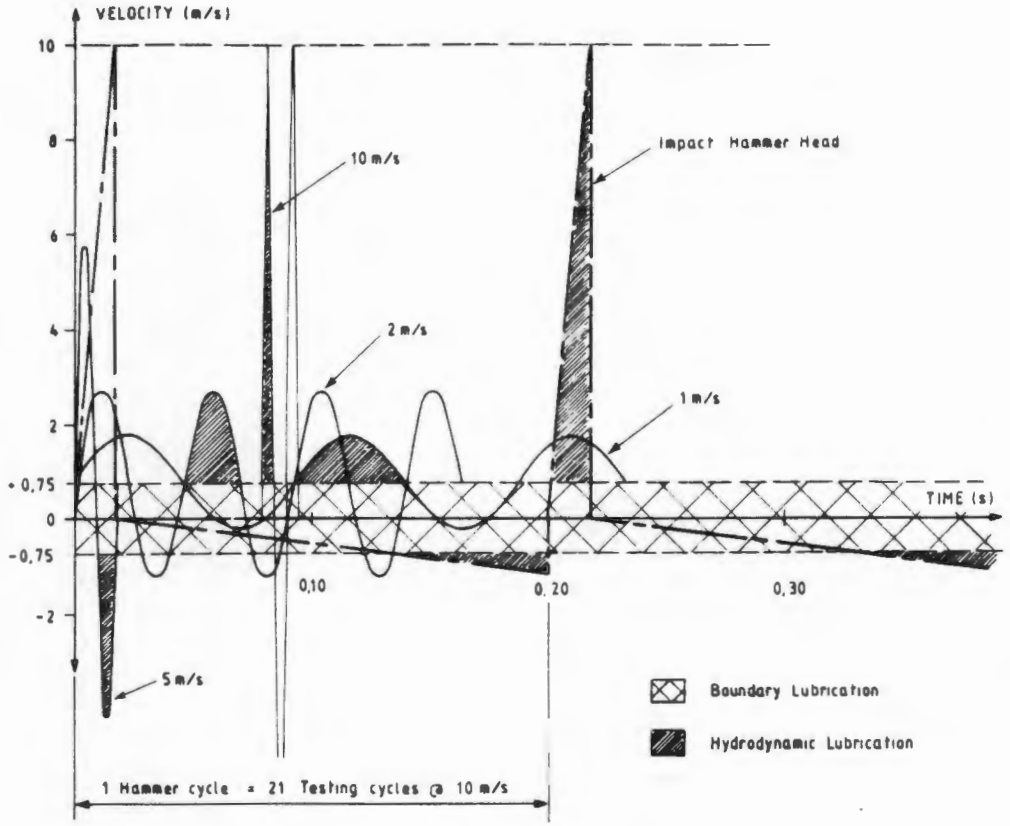

Fig. 6.3 CONTRASTING VELOCITY PROFILES FOR IMPACT HAMMER HEAD AND TEST RIG AT 10, 5, 2 AND 1 m/s (limits of boundary lubrication zone according to Lloyd [3])

This sinusoidal velocity profile is however deemed adequate as the two most important aspects causing wear are retained - the rapid rise to a high velocity and the instantaneous reversal once a peak is reached.

By testing at speeds between 0 and 10 m/s, different regions of interest for the impact and return strokes can be modelled fairly easily. Time spent under boundary - or hydrodynamic lubrication, as well as maximum or average velocities can thus be approximated for each portion of a full operating cycle in the rockdrill or impact hammer. In this manner, a complete picture of what happens in each cycle can gradually be built up.

The choice of a drive mechanism for this profile could only be made from a crank slider or scotch yoke arrangement. Although others were considered, they all had to be rejected. More specifically : pneumatics are incapable of performing reliably above 1 m/s; hydraulics and electromagnetic drives are capable of either the required stroke or frequency but not both together.

A crank slider was forwarded as the preferred choice due to its simplicity over the scotch yoke (which among other things requires an oil bath), particularly because it was felt that the inherent unbalance in a crank slider could be adequately contained (see section 7.2).

Before possible solutions could be generated, several decisions, inspired by the lessons learnt from the old test rig, had to be made:

- o only two test specimens will be tested against each other at any given time;
- o specimens will not be reused;
- o only one face will be tested on each specimen;
- o interacting plane to be horizontal.

Lastly, a number of decisions had to be made regarding which of the two specimens should be loaded, which specimen is coupled to the friction measuring transducer which should reciprocate, which should provide for vertical adjustment and lastly which is swung away from the interacting surface to facilitate access to the specimens. The decision matrix shown in Table 6.1 was thus drawn up to help decide which combination represents the best compromise.

Table 6.1

OPTION	reciprocating mass minimized	can recip assembly run unlubricated	is wear debris collection possible	spring load and dead load possible	bath left full after each test interval	only actual area of contact loaded	ease of replacing recipro. specimen	ease of replacing stationary specimen		RATING points	RATING posnt.
1	N	Y	Y	Y	N	Y	N	Y		5	2
1*	N	N	N	N	Y	Y	Y	Y		4	3
2	Y	N	Y	Y	Y	Y	Y	Y		7	1
2*	Y	Y	N	N	N	Y	N	Y		4	3
3	N	N	Y	N	Y	N	Y	Y		4	3
3*	N	Y	N	Y	N	N	N	Y		3	4
4	Y	Y	Y	N	N	N	N	Y		4	3
4*	Y	N	N	Y	Y	N	Y	Y		5	2

Option 2 established itself as the most viable configuration. Designs could therefore be generated that would fit very specific requirements and constraints as summarized in fig. 6.4.

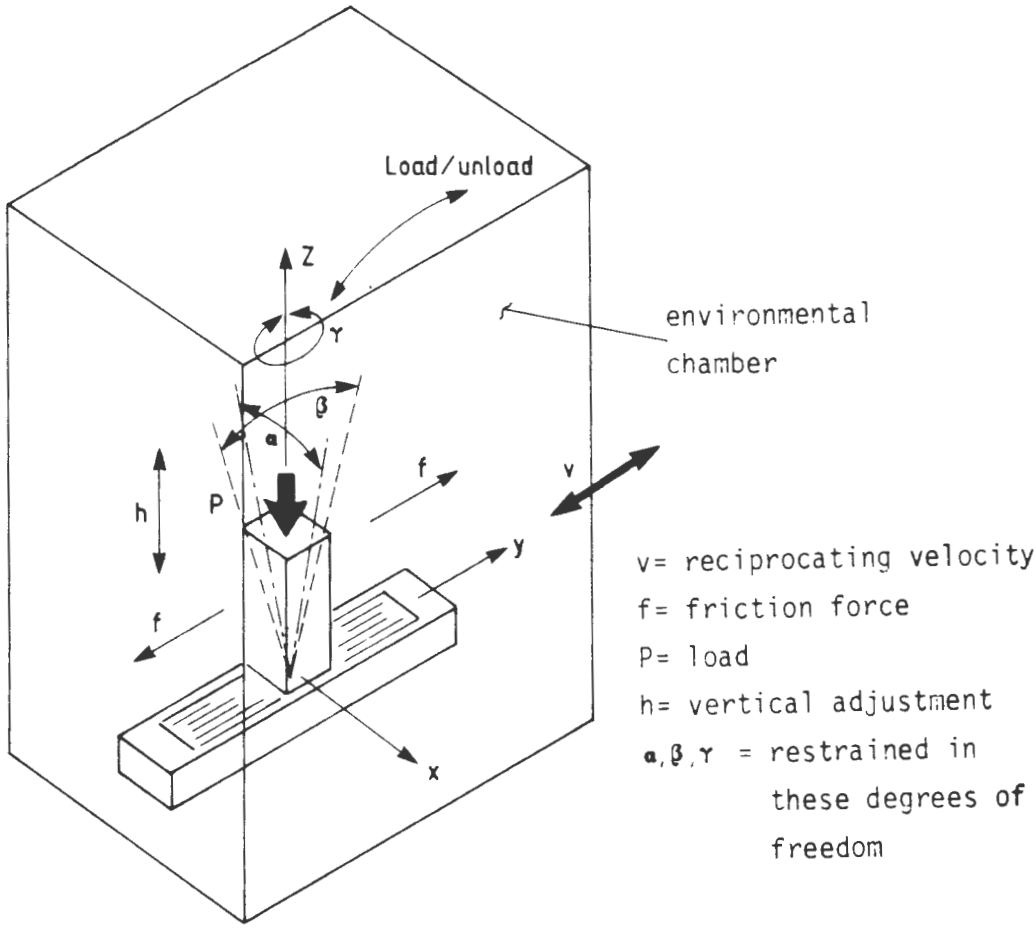

Fig. 6.4 PICTORIAL REPRESENTATION OF WHAT THE NEW TEST RIG MUST BE CAPABLE OF DOING

Several concepts were initially generated. In order not to restrict the free flow of ideas, these designs were evaluated only very broadly during this stage. Those designs which showed potential, were however analyzed further- in accordance with the design requirements, constraints and criteria drawn up in section 4.0. In particular three such designs were forwarded as viable solutions. These are briefly discussed in the pages to follow and only the major advantages and disadvantages are listed.

6.3 SOLUTION A

The reciprocating specimen is mounted to a shuttle which is free to oscillate back and forth on two guide shafts as shown in fig. 6.5 below. Reciprocating motion is by pneumatic cylinder for speeds up to 1 m/s and by a crank slider mechanism for higher speeds.

A housing which can be secured in any position along the length of the load arm retains the stationary specimen. The load arm is pinned at its one end by a universal joint which permits two degrees of freedom. Neutral balance for the load arm assembly is provided for with a counterweight at the short end.

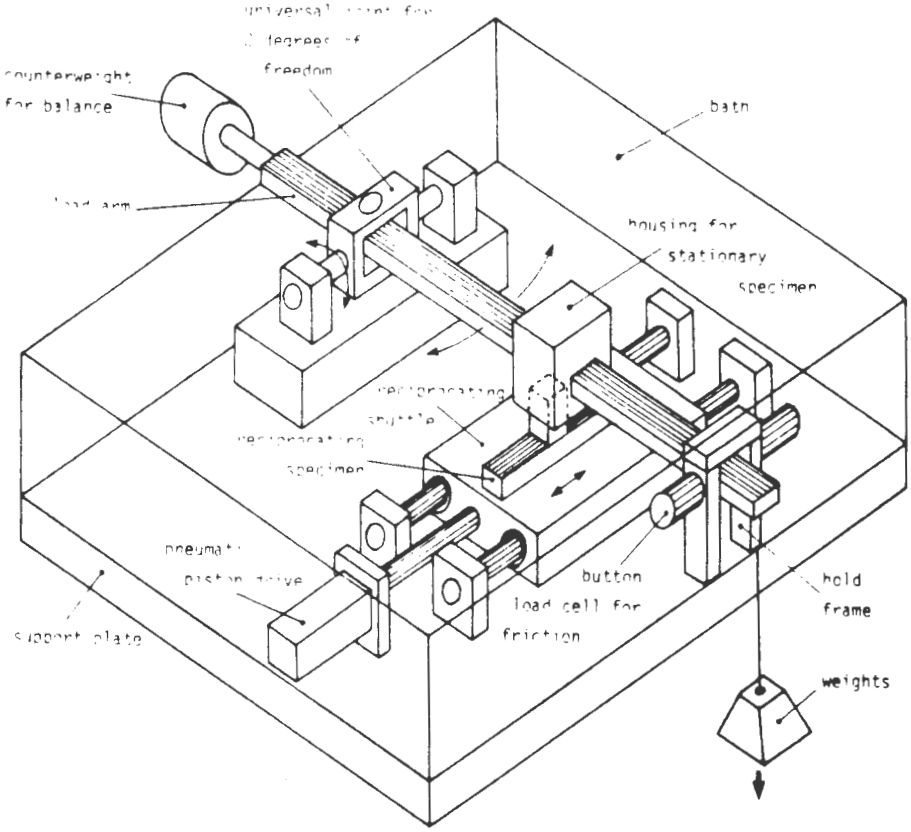

Fig. 6.5 SOLUTION A

The interacting surfaces are loaded by hanging weights to the long end of the load arm. At the long end the two side faces of the load arm bear up against two button load cells which record the friction force. Specimen mounting and replacing is readily achieved by removing weights and releasing a catch at the top of the hold frame. The load arm can then be swung into a vertical position and access is gained to both specimens. All components are mounted to a support plate and surrounded by a bath which contains the desired medium.

6.3.1 ADVANTAGES

- o simple fabrication;
- o vast range of loads possible;
- o easy to operate.

6.3.2 DISADVANTAGES

- o load arm needs to be as long as possible to make rig sensitive to friction force - bulky design thus results;
- o friction transducer not directly fixed to load arm and brought into contact and removed periodically. This lack of positive location results in shoddy contacts and possible frequent recalibration;
- o friction force not measured in line but in an arc due to pivoted load arm;

- o load not applied in vertical axis but in an arc about pivot point. This is likely to be problematic with materials that wear rapidly;
- o sealing the test rig for studies in controlled environments is difficult due to the hanging mass and no tests are feasible in hydrostatic conditions.

6.4 SOLUTION B

This design is depicted in fig. 6.6 below. The reciprocating specimen is mounted to a base which oscillates on a single guide shaft. It is prevented from rotating by the piston rod of the reciprocating drive.

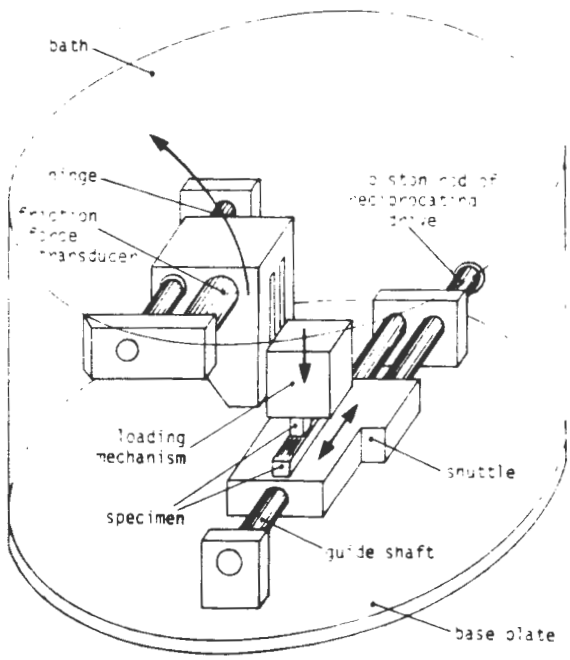

Fig. 6.6 SOLUTION B

The stationary specimen is positioned in a housing which is free to slide vertically up and down the face of the hinge plate. Load is applied by a spring or dead weight.

The hinge plate can slide axially on the hinge shaft, thereby facilitating friction force to be picked up by the transducer. Releasing a locking mechanism enables the hinge plate and stationary specimen to be rotated into a horizontal attitude and access is gained to the two specimens.

6.4.1 ADVANTAGES

- o compact design;
- o chamber easily sealed.

6.4.2 DISADVANTAGES

- o components not readily accessible for maintenance;
- o friction force measurement is not in line with reciprocating motion
- o involved/costly machining.

6.5 SOLUTION C

A support plate is fixed midway to a vertical backing plate. Mounted to it are two parallel shafts on which the shuttle securing the reciprocating specimen oscillates. Mounted on the other face of the backing disc and at the same level as the support plate is a crank slider arrangement.

The stationary specimen is secured inside a holder which is fixed to a hinge plate via a Z-gauge load cell for friction force measurement. Loading is by spring or dead weight. Mounted on rollers running on two rails, an environmental chamber can be slid over the assembly in the horizontal plane and sealed tight against the backing disc. To separate specimens, the upper assembly is rotated about the pinned hinge plate. Figure 6.7 below shows the essential features of this design.

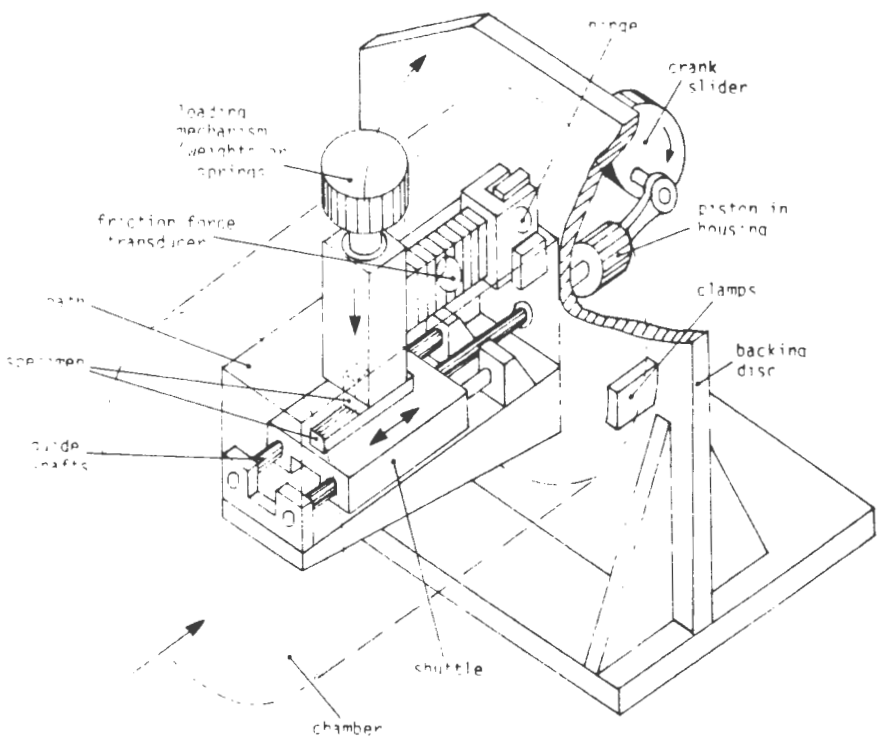

Fig. 6.7 SOLUTION C

6.5.1 ADVANTAGES

- o very compact design;
- o all components readily accessible;
- o friction force measured in line with reciprocating axis;
- o environmental chamber easily fitted;
- o specimens remain axially loaded irrespective of volume loss.

6.5.2 DISADVANTAGES

- o involved/costly machining

Solution C fares relatively more positive and was thus forwarded for refinement and development into a workable test rig. The final design submitted is discussed in the next chapter.

7.0 DISCUSSION OF THE NEW TEST RIG DESIGN

The submitted prototype design is capable of meeting all the requirements, constraints and criteria that were set in Chapter 4.0. Due to its complexity, the design will be discussed under several sub headings in this section. Extensive reference is made to the sub-assembly drawings and this chapter is therefore to be read in conjunction with drawings 1 to 5. If greater detail is required, make reference to the full size drawings in Appendix G and the detail component drawings in Appendix F. Relevant calculations are contained in Appendix E. For a summary listing of prototype specification, refer to Chapter 5.0. Reference can also be made to a series of photographs depicting the finished prototype. These are appended to Chapter 8.0.

7.1 A SUMMARY OF THE BASIC LAYOUT

Refer to drawing 3. The backing disc (42) is the central component of the test rig. To its one face are mounted all test cell components that facilitate specimen mounting, testing and monitoring of relevant parameters. Only materials with excellent anti-corrosion properties are specified for the components used on this face. If desired, the optional environmental chamber (59) can also be clamped to this face.

The other face is bolted to gusset stands (47), which hold the disc vertically aloft such that its central axis is horizontal. Both of the gusset stands are splayed out at 25 degrees to the disc centre, so that access is eased to the reciprocating drive.

The bearing housings (81), that retain the driveshaft (79), and the gusset stands are bolted to platform (82), which acts as an independently sprung base for the whole test rig. Rubber mountings (87) isolate the platform from the table (93). Rig vibrations are thus minimised as the platform can move in the xy plane and the transfer of rig borne vibrations to the table are eliminated.

A 1.5 kW/220V dc motor (85) is rigidly mounted on a fixed plate (84). Driven and driving pulleys are connected by fabric belt and ratioed 1:2.1 such that the maximum motor rating of 3000 rpm is stepped up to 6300 rpm at the drive shaft.

It is also emphasized that a philosophy of optimising between weight, strength and compactness without compromising functionality, underlines the entire test rig. Also note that to retain precision all bolted components are first pinned together.

7.2 THE RECIPROCATING DRIVE MECHANISM

Refer to drawing 2 for details on the reciprocating drive. As discussed in Chapter 6.0, a crank slider arrangement was chosen to produce the desired sinusoidal velocity profile.

The larger diameter end of the driveshaft (79) is driven by a fabric belt. Bolted to its end is the crank pin holding plate (78). A spigoted and tapped hole for crankpin (77) is located 15 mm off centre in this plate. A stroke length of 30 mm is thus achieved at the piston end. If stroke lengths less than 30 mm are desired (resulting in decreased peak and average velocities), item (78) would be swopped for a similar one, but with the crank pin hole located closer to its centre.

Both stroke length and rpm ratings are identical for the old and new rigs. This was done to ensure that a basis of comparison is retained by which previously generated results can be compared to those that will be initially accumulated on the new test rig.

In order to balance primary forces, a brass counterweight (74) is bolted to disc (78). Being replaceable, fine tuning the vibrations should be readily achieved by adding or removing mass. No secondary force balance is provided as this would significantly complicate the design. The rational behind this lies in the acknowledgement that if resonant frequencies are encountered at a given testing rpm, raising or lowering the speed by a few rpm will negate this vibration problem (e.g. $\pm$ 25 rpm = $\pm$ 0.04 m/s).

The connecting rod (73) forms the link between crankpin and reciprocating piston (68). It is crank end guided and float is provided with the crankpin end cap (76). Due to the severity and fluctuation in loading encountered at the crank and wrist end with every revolution, a high strength martensitic stainless steel (AISI431) was specified for conrod and wristpin (72).

Both crankpin and wristpin ends of the conrod are mounted in needle roller bearings. To simplify machining, the wristend needle roller is specified with an inner and outer race. On the crankpin end however only an outer race is required as the crankpin (77) is hardened and ground, thereby providing a suitable surface for the needle rollers and thus negating the need for an inner race. Journal bearings were deemed inadequate for the same reasons that they are not used in high reving single piston engines. No reliance can be made on oil mist to lubricate these bearings for fear of contaminating the test cell. The needle roller bearings are therefore packed with a water repellent grease.

Wristpin (72) joins the conrod to the piston. A 7000 series Aluminium alloy, 7017, was specified for this piston in an attempt to reduce reciprocating mass and therefore loading. The piston shaft (67) completes the reciprocating assembly. At its one end it is tightly screwed into a female thread in the piston top. Its other end is tightened by socket cap screw against a blind recess in the reciprocating shuttle (23). This shuttle in turn carries the reciprocating specimen (27).

Split polymer seals (70) provide a bearing surface and hence guidance to the piston in the housing (69). An O-ring energized seal (66) rubs against shaft (67), thereby ensuring that the test cell innards are sealed to the outside. It is positioned in the piston shaft sealing assembly consisting of items (61) - (66). The two sets of polymeric seals are therefore recognized as performing very different functions : the one provides only alignment, the other only sealing.

Both the bore of (69) and shaft (67) are hard chromed to reduce friction between the reciprocating surfaces as well as to help tighten up tolerances. Vent holes are drilled into the piston housing at its lower end. Material choice for the reciprocating components is such that water cooling can readily be added to the piston housing if the frictional heat generated at the reciprocating interfaces exceeds the thermal stability of the polymers used.

It was decided to specify a double sintered UHMWPE with Teflon filler (SOLIDUR DS) for the polymeric seal. This was done because this material combines the excellent wear resistance characteristics of UHMWPE with the very low friction properties of PTFE (Teflon).

The test rig simulates a tribosystem and is itself a tribosystem. It is therefore unavoidable that it too will wear out. It is anticipated that the polymeric seals will have to be replaced every 10 or so tests (corresponding to some 250 km of sliding distance), before slackness in the seals becomes intolerable.

As a by-product to the actual test programme (which looks at metal on metal interactions), seal wear could also be monitored and inferences made accordingly. Over and above this, the seals could be machined from different polymers to test the effectiveness of different seal materials. Given the above, ease of seal replacement is recognized as being crucial to the success of the test rig.

To replace the piston seals (70), the following procedure needs to be adopted. Firstly, remove item (76), then unscrew crankpin from holding plate (77). On releasing the socket cap screw, which holds piston shaft to shuttle, the entire reciprocating mechanism is freed and can be extracted in one piece. Piston seals can now be replaced and the assembly reinserted.

Because of its small size and its awkward location within the backing disc, it was decided to incorporate the piston shaft seal (66) within a removable housing. If it should become necessary to replace this seal, the reciprocating assembly will first have to be removed as outlined previously. Once this has been done, the piston housing (69) needs to be unbolted from its spigoted recess in the backing disc. This piston shaft sealing assembly is now readily accessible and is removed by screwing out the outer housing (62). With the unit now removed, it can be split by unscrewing inner housing (63) from outer housing (62). This frees the seal and O-ring which can now be replaced. To reassemble, simply follow the dismantling procedure in reverse.

Separating sealing and bearing features in the manner outlined above was done because the old test rig showed that combining the two did not seem to work. It was also decided to position both features on what is the outside of the test cell, so as not to intrude on the test cell innards. Placing one or both of them on the inside would have made the layout less compact, necessitating stiffer supports and therefore greater cross sections to withstand the increased loading.

7.3 THE INTERNAL WORKINGS OF THE TEST CELL

This chapter makes reference to drawing 1. The discussion of the internal workings of the test cell is divided into two sections. One dealing with the lower base plate (32) assembly and the other dealing with the upper base plate (7) assembly.

7.3.1 THE LOWER BASE PLATE ASSEMBLY

This consists of a rectangular plate (32), mounted low down to the backing disc (42), such that its long axis is horizontal and at right angles to item (42). A thick through section was selected for this plate so that the second moment of area is high and deflections are < 0.01 mm under maximum load conditions. Also note that the choice of materials for this plate and all those components that are mounted to it, has been made so as to be compatible with the corrosive media that will be used.

Bolted to the lower base plate are two support brackets (30) which hold the two parallel shafts (29) on which the shuttle (23) reciprocates in a horizontal plane. Both shuttle and support blocks are machined from a high strength aluminium alloy with excellent anti corrosion properties (7017). This was done in a bid to reduce the reciprocating mass and therefore loading, as well as to reduce the bending moment on the base plate.

A stainless steel specimen mounting plate (28) is screwed to the top face of the shuttle. The reciprocating specimen (27) is located and secured on top of this plate. Accommodating different specimens is therefore readily achieved by simply exchanging item (28).

Two parallel holes are drilled down the long axis of the shuttle. Into each are inserted two stainless steel linear ball bushings. The bushings, in turn, run back and forth on high strength stainless steel shafts (440C) that have been case hardened to 58 R_c and ground to a 0.1 μm finish.

The ball bushings are sized such that a minimum life of 50 hours will be achieved under maximum test conditions (max. stroke, rpm and load) and in the absence of any lubrication other than that of the test medium. This would correspond to $\approx$ 1000 km of sliding distance or 40 tests of 25 kms each (refer to Appendix E).

Due to the requirement of wishing to test in various media in general and simulated mine waters in particular, oil lubrication could not be considered. Oil seal integrity can not be guaranteed and even minute traces would contaminate the medium and significantly affect results. Rubber bellows were considered as an alternative but rejected due to their demands on space, venting problems and resultant increases in power demand.

The ball bushings in the prototype will nevertheless initially be packed with a water repellant grease and have seals at each of the four exposed ends. This is done in an attempt to extend the service life, reduce noise/vibrations and to have a barrier against wear fragments from being introduced into the bushings. Should this however result in increased frictional drag, or worse, if it is found that the grease becomes suspended in the medium, then the grease will be flushed out of the bushings and they will be used without lubrication and/or seals.

Ball bushings were selected in preference to simple sliding bushings as they pose less frictional drag, require lower break-away forces, carry greater loads per unit weight and lastly because they can be bought as standard 'off the shelf' items.

7.3.2 THE UPPER BASE PLATE ASSEMBLY

As in the case of the lower base plate assembly, materials were selected for the upper base plate assembly which are entirely compatible with the corrosive nature of the media of interest.

The upper base plate (7) is held in a horizontal position above the lower base plate (32), such that both plates are perfectly parallel to each other. Two support brackets (24) are bolted to the bottom face of the upper base plate. They retain two parallel hard chromed shafts (14), which run in polymer bearings (13) that are housed in the friction plate (12). The load assembly housing (15) which secures and loads the stationary specimen, is rigidly fixed to this friction plate.

To the upper face of plate (7) is bolted the upright plate (45). Inserted into this plate are bushings (39) which permit it to be hinged about pin (36). This pin in turn is clamped at either end by two mounting blocks (37) which are bolted to the inner face of the backing disc.

It is thus possible to swing the entire upper base plate assembly through 90 degrees about the hinge pivot. The upper and lower base plate assemblies can therefore be separated and access can now be gained to the two test specimens.

When in the horizontal or testing position, the bottom face of the upper base plate rests on the support block (46). It can be screwed against this block by tightening down knurled thumbscrew (44) by hand or by means of a pin inserted into the holes provided. A milled slot in the back face enables item (7) to fit over the thumbscrew as it is swung up or down. The actual area of contact between the two is forward of the vertical axis through the centre of the hinge point. The base plate is thus flush with the support only when it is actually horizontal and therefore cannot overshoot. To prevent damage if the plate is brought down too quickly, a stop or damper can be provided. Diligent use should however preclude this.

Mounted between a cut out in the back of the hinge plate and a milled slot in the backing disc is the latching hook (40). Drawing 5 shows the position that the base plate takes up in the horizontal/testing or vertical/hold positions and how the latching hook holds it there.

In the hold position the spring loaded head of the latch hook jumps into the recess machined into the top of item (45). To release the assembly from this position, the latch release lever (35) is simply pulled forward and the upper assembly is swung down using the upper base plate lever (8).

7.4 SPECIMEN LOCATION AND SECURING IN POSITION

The provisions made for firstly locating and secondly securing the specimens in their located positions, is discussed separately for the two specimens. In both instances, location mechanisms are such that they guarantee the specimens to be repositioned in an identical fashion after each and every test run. This means that specimens once matched after a running-in period, will remain in full area contact for the remainder of their test life.

7.4.1 THE RECIPROCATING SPECIMEN

The reciprocating specimen (27) is placed onto the flat surface of specimen mounting plate (28). Its long axis is positioned in line with the reciprocating axis by means of three locating pins (18). Screwing down the wedge blocks (52) forces the specimen tightly against the pins. Two such clamping arrangements are provided. The one pushes the specimen against a pin in line with its long axis, the other pushes the near side against two pins on the far side.

7.4.2 THE STATIONARY SPECIMEN

Refer to drawings 1 and 4. The stationary specimen is held in a vertical orientation by means of a specimen chuck consisting of two Phosphor-bronze jaws - one fixed (91), the other adjustable (90). Both jaws are mounted inside a square recess milled into the stainless steel specimen holder (20).

The fixed jaw is screwed against one of the inner faces. The adjustable jaw is positioned opposite the fixed jaw, the separation between the two being adjusted by turning the grubscrew (89). Both the grubscrew and the screw retaining the fixed jaw are recessed into the circular outer face of the holder. By exchanging the jaws, specimen geometries can be used that can not presently be accommodated.

Specimen holder (20) fits into the load assembly housing (15). Two diametrically opposed slots are machined along the outer face of the holder. These enable it to fit over the two hold fingers (17) covering the housing entrance, as it is being inserted. An easy running fit has been provided between housing and holder. Because the holder is removed after every test and then reinserted, its outer diameter has been hard chromed over the full area to minimise galling and friction. The holder and therefore specimen is thus able to move axially and rotate in the housing.

To prevent this rotation and ensure that the holder can only be inserted in one position, two different diameter holes have been drilled into its top face. These holes couple up with two matching pins protruding from the connecting plunger (10). The plunger is free to move axially in the housing (15) but is prevented from rotating in it. This is facilitated by three spring loaded balls (19) which, protruding from threaded holes in the housing, sit in three grooves machined axially into the plunger side at 120 degrees separation.

The stationary specimen thus relies on two different connections for axial guidance and rotation prevention. These are : holder (20) in housing (15) and holder (20) coupling to plunger (10) respectively.

7.5 THE LOADING MECHANISM

In chapter 6.0, the decision was made to load the stationary specimen in a vertical axis from the top down against the horizontal reciprocating specimen. To facilitate specimen accessibility, a further decision was made to swing the stationary specimen from its vertical test position into a horizontal attitude for loading/unloading (refer also to drawing 5).

This would, however mean that irrespective of whether under load or not, the stationery specimen would scrape along the reciprocating specimen as it rotates upwards. Similarly, the two surfaces would be damaged prior to testing if the assembly was swung down in this manner. To prevent this damage from happening, a mechanism was required which would separate the two specimens before either the up or down swing .
In the design submitted, the required separation (≈ 2 mm) is achieved by pushing the specimen holder (20) into its housing (refer drawing 4). This is done by letting the hold fingers (17) ride up against the lip machined onto the outer diameter of the holder mouth. As the resetting ring (26) is turned up its coarse thread, the hold fingers push the holder up. Rotating the resetting ring lever (34) through 170 degrees will push the holder approximately 2 mm into the housing.

A bracket (25) is screwed to the top of the resetting ring at the end opposite to the lever (34). It houses a spring loaded stainless steel ball which can sit in one of ten dimples machined into the housing at 36 degree intervals. The purpose of this ratchet is to ensure that the resetting ring is held securely in any of ten circumferential positions desired as it is wound up or down its thread.

The actual loading of the specimen is achieved by a compression load spring (5) which is designed to give a linear response of 0 - 100 N over 20 mm of deflection. Adjustment of the spring force is done by turning screw cap (1). This has linear graduations marked off in 1 mm increments (corresponding to 5 N each) on its outer face. To prevent

cross threading and seizure on the housing thread, the screw cap is made from a dissimilar metal, P-bronze. To help keep the spring from rotating as it is compressed, a needle roller bearing (2) has been fitted to the load plunger (3).

One of the big advantages derived from this specimen separation mechanism is the fact that the spring must not be slackened off after each test interval. It is set at the start of a test series and readjusted only if a different load setting is required. As an option, the cap screw and spring can be replaced by a dead weight. Given the fact that nominal amounts of material will be removed from the interacting surfaces, the axial relaxation in the spring and therefore slackening off in load is negligible. The use of a dead weight is not convenient, particularly because it would have to be removed before the assembly could be swung up.

7.6 FRICTION FORCE MEASUREMENT

Mounted to the hinge plate (45) is a beam load cell transducer (38). At its lower end the transducer is bolted to the friction plate (12), which running on guide shafts (14) is free to oscillate along the reciprocating axis. Bolted to the friction plate is the load assembly housing (15) in which is inserted the specimen holder (17) that retains the stationary specimen (21).

The friction force resulting from the interaction between stationary and reciprocating specimens causes the load assembly housing and therefore friction plate to move in sympathy. In so doing, it deflects the beam load cell and a signal is generated from strain gauges glued to the upper transducer shank. This signal is boosted and the friction force is displayed on an oscilloscope or plotted on a chart recorder.

Under maximum test conditions the shuttle (23) will be reciprocating at a frequency of 106 Hertz. This lies well within the kilohertz frequency rating for the beam load cell transducer. The maximum load capacity for the transducer is 200 N in either direction with a total deflection not exceeding 0.2 mm. Given that a maximum load of 100 N can be applied to the reciprocating interface, the coefficient of friction would have to be greater than two, before the specifications of the transducer are exceeded.

Placing the transducer parallel to the loading axis, as opposed to in line with it, was done to retain a compact design.

7.7 THE LUBRICANT/COOLANT BATH

A perspex enclosure (60) has been fitted to the lower base plate (32). It consists of three sides with reinforcing strips at the bottom and open end. Into these strips is cut a groove for an O-ring that seals the

enclosure when it is screwed down onto the base plate. The enclosure is readily fitted or removed by fastening or loosening eleven screws.

Perspex was chosen in preference to any other material as it affords a side view onto the interacting surfaces.

The medium is introduced into the bath by a pipe which feeds through a fitting (53) screwed into the outer face of the backing disc. From there the medium proceeds through a horizontal and then vertical hole, drilled into the lower base plate, to fill the bath from the bottom up. The entry hole into the bath has been chosen such that it will always be covered by the shuttle, irrespective of shuttle position or piston stroke. This was done so that the force of the incoming jet can not interfere with either the shuttle oscillation or the interacting surfaces.

Positioning the inflow at the bottom, permits the bath to be completely drained and helps retain a compact design. An O-ring (97) seals the base plate against the inner face of the backing disc.

A second larger diameter fitting is provided for the outflow. It is positioned vertically above the inflow fitting, high enough to afford complete medium immersion for the interacting surfaces, and low enough to prevent overflowing from the bath. To empty out the bath, the drain valve fitted at the inflow side is opened.

7.8 SPECIMEN DESIGNS

In keeping with the requirements set in chapter 4.0, the design is capable of accommodating several different specimen designs as shown in fig. 7.1.

Type I specimens are intended for rapidly building up material ranking tables. Their geometries are simple and they are therefore easily machined. Square or circular through sections not exceeding dimensions (in mm) of 12 x 12 or ø12 respectively can be used for the stationary specimen. Appendix D gives the actual dimensions of the type I specimens that have been selected as optimum for the test rig. They represent the best compromise between several conflicting criteria. On the one hand specimens must be large so that:

- a large area of interaction is available for macroscopic examinations
- edge effects are insignificant
- they can be readily handled and easily machined and ground.

On the other hand, they need to be small so that:

- reciprocating masses and therefore loading is small
- material cost for test specimens remains small

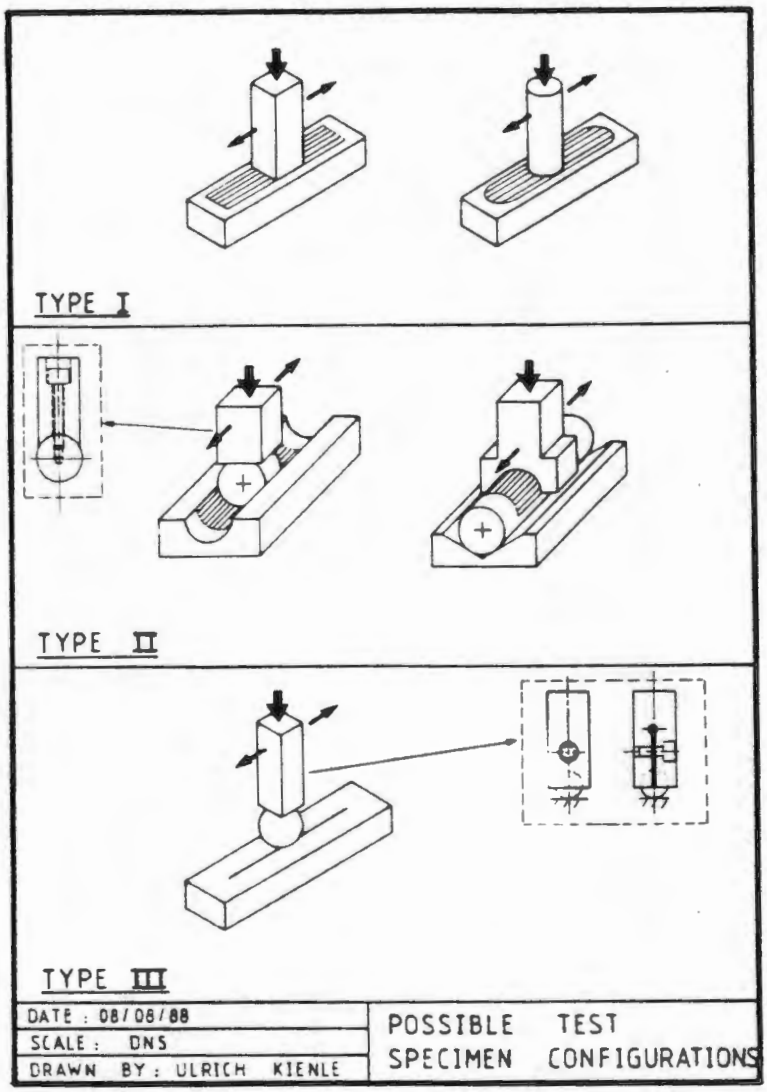

Fig. 7.1 POSSIBLE TEST SPECIMEN CONFIGURATION

Type II specimens represent the best approximation of what happens at the reciprocating interfaces in the stoping equipment of interest, short of testing an actual piston/shaft in a bore/housing. Testing with specimens of this nature is only anticipated once a programme based on type I specimens has been successfully completed.

Type III specimens are intended for conducting reciprocating studies in which actual - as opposed to nominal - areas of contact are of interest.

Any specimen geometry can be accommodated by the test rig, provided the dimensional limits specified are not exceeded. Minor modifications {exchanging chuck jaws (90) and (91), and mounting plate (28)} need to be made if specimens other than the type I specimens detailed in Appendix D are used.

7.9 TEST RIG OPERATING PROCEDURE

This section will be presented as a step by step guide to beginning and ending a test. Starting from the assumption that the upper assembly is in the testing position (refer to drawing no 5 and with reference to drawings 1 and 4) :

- loosen retaining thumbscrew (44);
- use upper base plate lever (8) to swing assembly into hold position, ensuring that latching hook (40) has properly engaged;
- rotate resetting ring lever (34) until hold finger (17) are positioned over axial slots in specimen holder (20);
- extract holder from load assembly housing (15) and open up gap between jaws by turning grubscrew (89);
- insert specimen in holder (20) and clamp tightly by fastening grubscrew;
- reinsert holder in housing ensuring that it couples up correctly with load plunger (10) pins;
- turn resetting ring lever until hold fingers ride on holder lip and push holder fully into housing against the spring force;
- adjust to required load setting by turning down screw cap (1) (1 mm = 5 N);
- release wedge block (22) screws;
- place reciprocating specimen on mounting plate (28) and tighten down wedge blocks against stop blocks (52);
- release latching hook by pulling latch release lever (35) and using upper base plate lever swing the assembly down gently;
- tighten down thumbscrew;
- load the stationary specimen against the reciprocating specimen by gently lowering the holder by turning resetting ring lever (34) until it no longer rides on the holder (20) lip;
- switch on coolant flow (if desired) and wait till stabilised;
- select number of cycles to be done on down counter;
- set desired speed and switch on chart recorder;
- start motor.

To end a test:

- down-counter will have automatically stopped motor after set cycles have elapsed;
- turn off the coolant (if present);
- turn resetting lever (34) until holder (20) pushed into housing and the two specimens are well separated;

- release thumbscrew (44);
- holding on to upper base plate lever (8) swing upper assembly into hold position, ensuring latching hook engages;
- turn resetting ring lever (34) until hold fingers (17) are positioned over axial slots in specimen holder (20);
- spring tension will assist in extracting holder;
- remove specimen from holder by releasing grubscrew;
- slacken off wedge block screws (22) and remove the reciprocating specimen;
- wash both specimens in alcohol in an ultrasonic bath, then blow dry and air cool to room temperature;
- weigh specimens and record mass change;
- reposition specimens in their respective locations, ensuring that they are orientated as before and properly secured;
- continue procedure as outlined previously.

7.10 OPTIONS CATERED FOR

Provision has been made in the design to firstly allow an environmental chamber to be placed over the entire internal workings of the test cell and secondly to replace the crank slider mechanism with a pneumatic cylinder.

7.10.1 ENVIRONMENTAL CHAMBER

This chamber (59) is mounted on rollers (59b) which are guided along two parallel shafts (59c) extending out from the platform (82) and terminating at the far end in an antivibration mounting. A seal, sitting in a groove machined into the inner face of the backing disc (42) ensures that the chamber completely seals the internal workings when the toggle latch (59a) is fastened against item (42). For testing in more arduous conditions requiring better sealing, the chamber can be bolted to the backing disc. The environmental chamber makes the test facility more flexible in respect of environments in which tests can be conducted. The following options are possible:

- testing in controlled environments in respect of temperature, pressure and humidity levels;
- testing at depressed or elevated temperatures;
- testing under conditions of partial vacuum or at pressures above atmospheric pressure;
- flooding the entire test cell for testing under fully hydrostatic conditions.

Perspex and stainless steel have been identified as suitable materials for the chamber.

7.10.2 PNEUMATIC DRIVE

The crank slider mechanism was selected as the most suitable means of providing reciprocating motion with peak velocities of up to 10 m/s. If velocity profiles other than sinusoidal are sought, then a pneumatic piston drive would replace the crank slider, subject to peak velocities not exceeding 1 m/s. The pneumatic cylinder would be bolted to the backing disc in place of the present piston housing and the piston rod end would be screwed against the recess in the shuttle.

7.11 SCHEMATIC LAYOUT OF THE TEST FACILITY

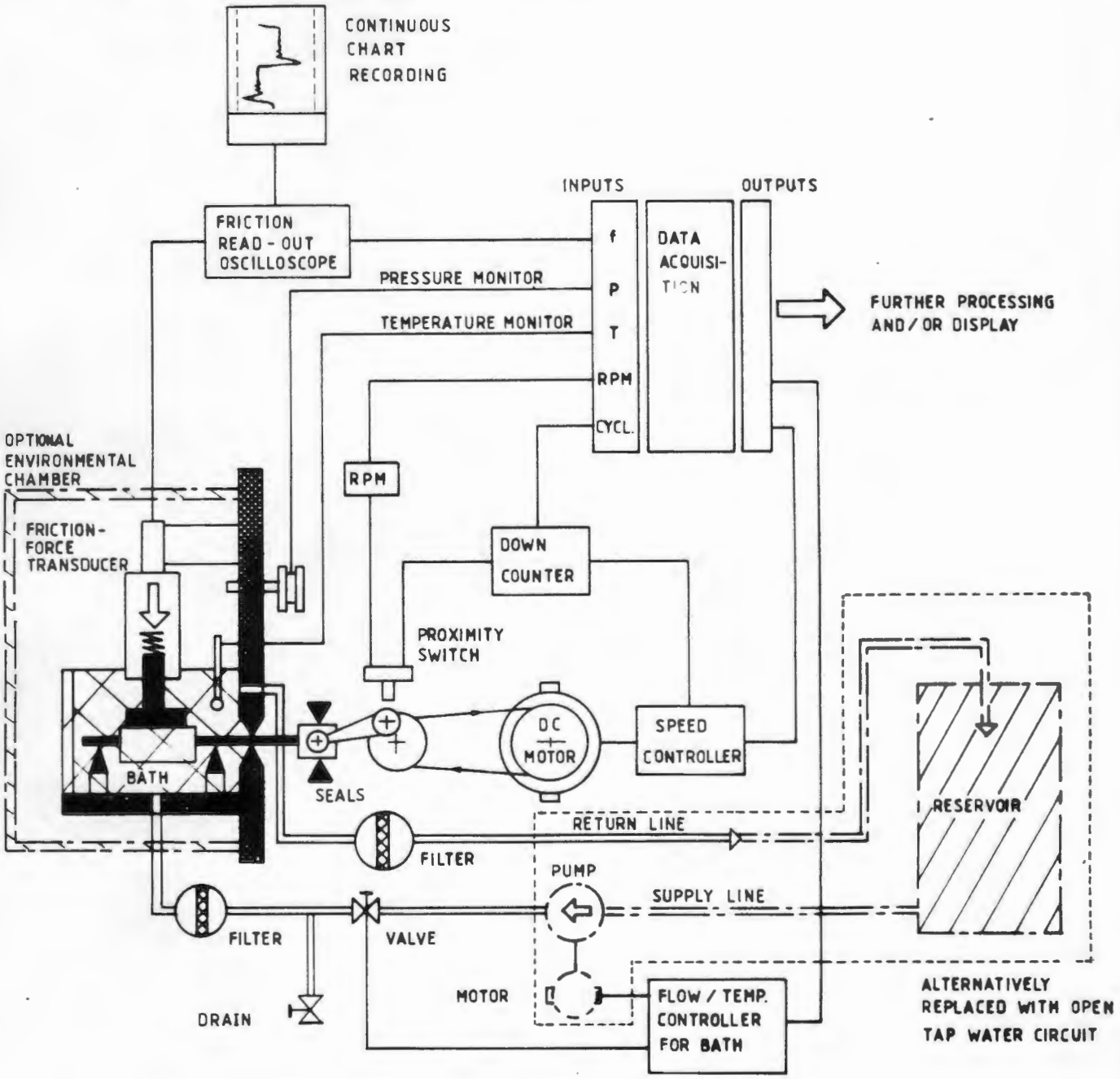

Fig. 7.2 SCHEMATIC LAYOUT OF THE COMPLETE TEST FACILITY

Figure 7.2 gives a schematic layout of the test cell, the reciprocating drive, fluid circuit and monitoring equipment. Interfacing a computer for data capture and presentation of data in tabular or graphical form is seen as an extension to the present system.

					57	CHAMBER O-RING SEAL	nitrile rubber	1	GACO RM 2493-57	46	UPPER BASE PLATE SUPPORT BLOCK	316 S/S	1	
					56	TUBING (9mm ⌀ bore)	PLASTIC	-	cut to suit	45	HINGE PLATE	316 S/S	1	
					55	HOSECLAMP	S/S	1		44	RETAINING THUMBSCREW	316 S/S	1	
					54	FEMALE HOSE CONNECTOR	BRASS	1		43	LATCHING LEVER HINGE MOUNTING	316 S/S	2	
97	O-RING		1		53	DOUBLE NIPPLE (type E) 1/4"	BRASS	1		42	BACKING DISC	316 S/S	1	
96	BATH SEALING O-RING	nitrile rubber	1	GACO RM 1795-30	52	STOP BLOCK	316 S/S	2		41	LATCH SPRING	316 S/S	1	
95	LOCATING PIN (⌀10mm)	316 S/S	2		51	TUBING (13mm ⌀ bore)	PLASTIC	-	cut to suit	40	LATCHING HOOK	316 S/S	1	
82	PLATFORM	070M20 (En3)	1		50	HOSECLAMP	S/S	1		39	HINGE BUSHING	P-BRONZE 034	2	
60	PERSPEX BATH	PERSPEX	1		49	FEMALE HOSE CONNECTOR	BRASS	1		38	BEAM LOAD CELL TRANSDUCER	S/S	1	LCS HBL/G/20
59	ENVIRONMENTAL CHAMBER	as required	1	OPTIONAL	48	DOUBLE NIPPLE (type E) 1/2"	BRASS	1		37	HINGE MOUNTING BLOCKS	316 S/S	2	
58	LATCH PIN	316 S/S	1		47	GUSSET STAND (LHS and RHS)	070M20 (En3)	◐1		36	HINGE PIN	316 S/S	1	

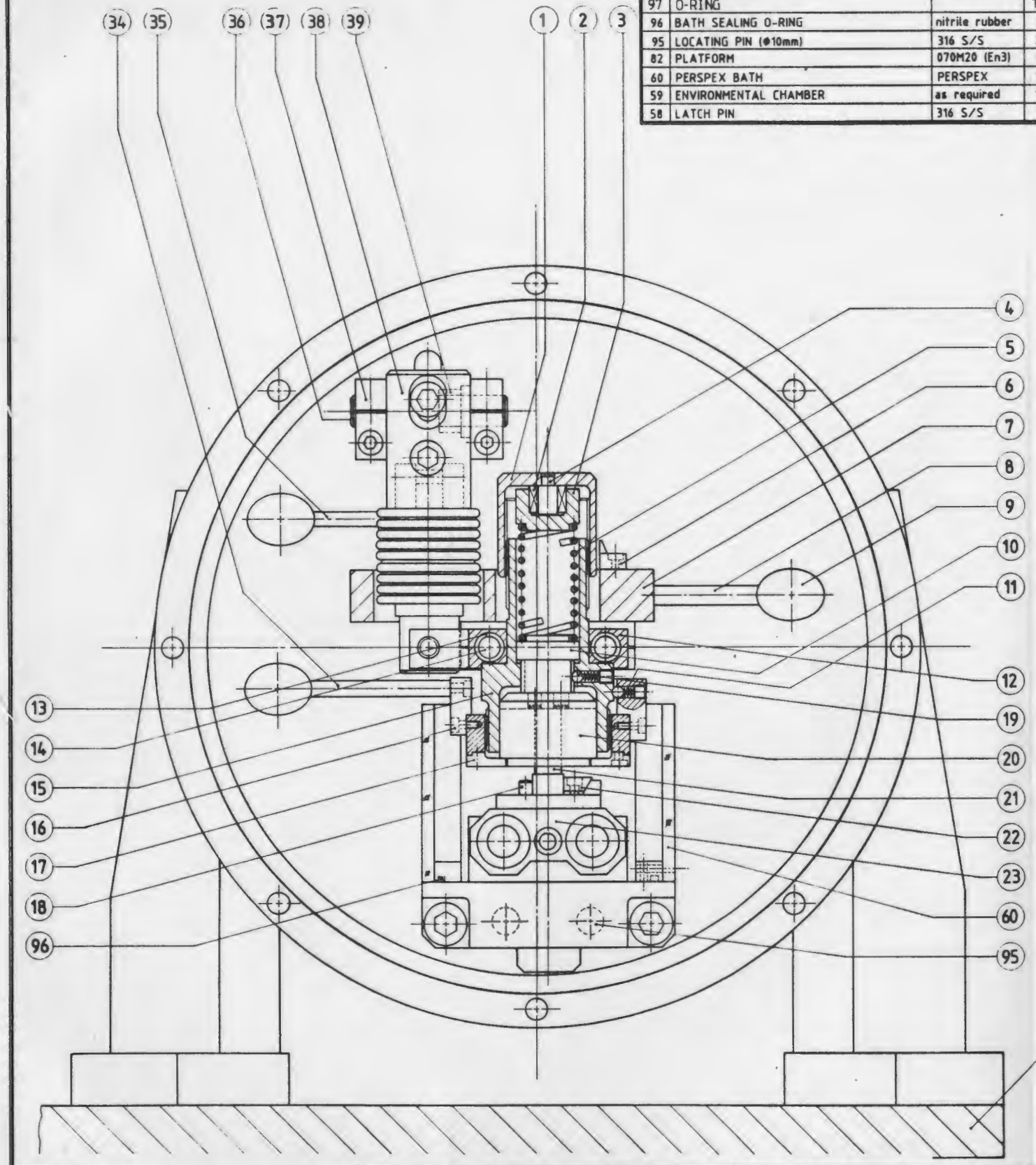

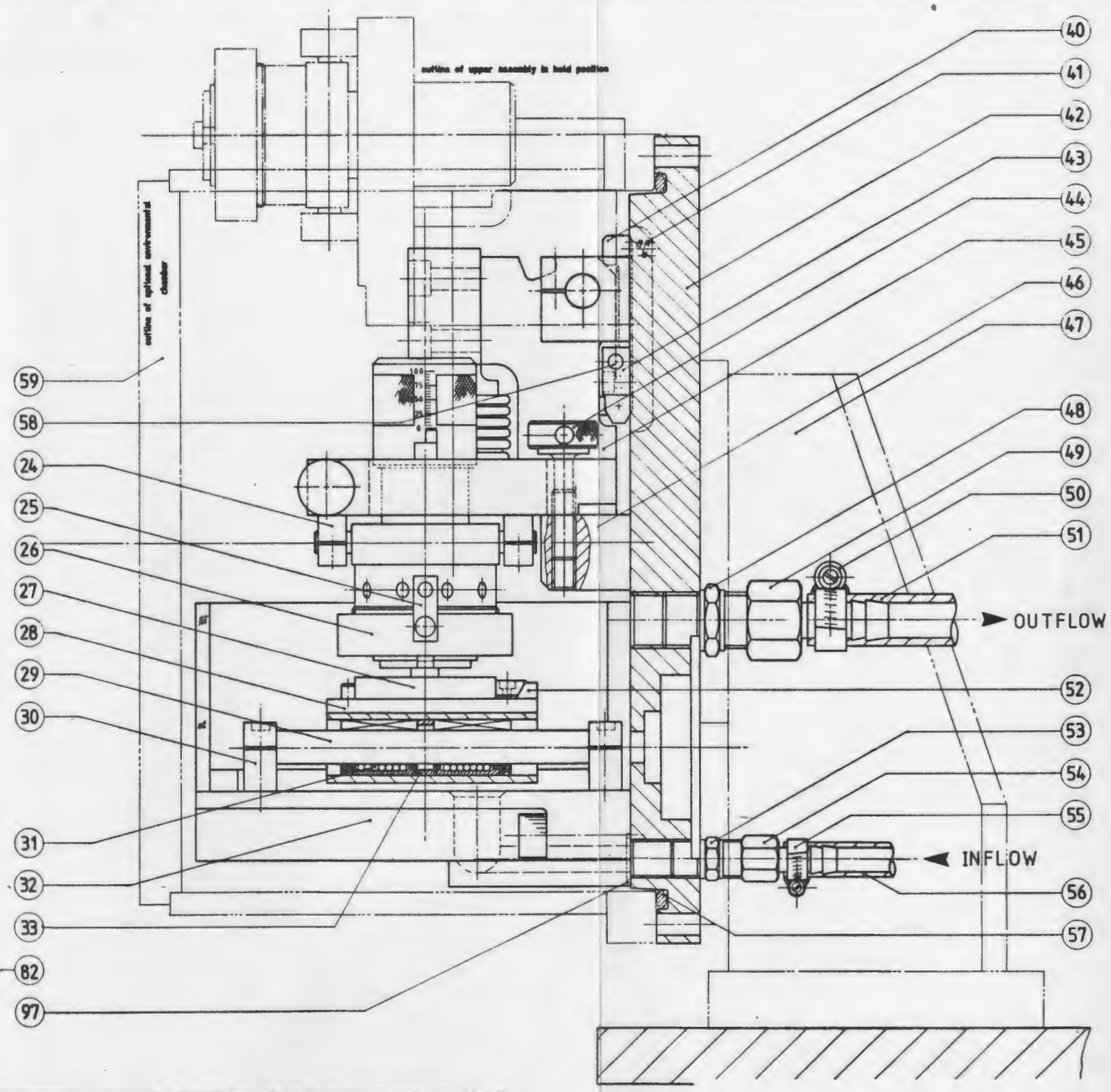

11	BALL SPRING	316 S/S	2		23	RECIPROCATING SHUTTLE	aluminium 7017	1		35	LATCH RELEASE LEVER	316 S/S	1	
10	CONNECTING PLUNGER	316 S/S	1		22	WEDGE BLOCK	P-BRONZE 034	2		34	RESETTING RING LEVER	316 S/S	1	
9	BALL KNOB	PLASTIC	3		21	STATIONARY SPECIMEN	test material	1		33	SPACER RING	P-BRONZE 034	1	
8	UPPER BASE PLATE LEVER	316 S/S	1		20	SPECIMEN HOLDER	316 S/S	1	HARD CHROME	32	LOWER BASE PLATE	316 S/S	1	
7	UPPER BASE PLATE	316 S/S	1		19	BALLS (⌀4 mm)	S/S	4		31	LINEAR BALL BUSHINGS (and SEALS)	-	4	RADE-BRZ-30 and 1331-SIR-30
6	POINTER	P-BRONZE 034	1		18	LOCATING PINS (⌀5 mm)	316 S/S	10		30	SUPPORT BRACKET - SHUTTLE ASSEMBLY	aluminium 7017	2	
5	LOAD SPRING	316 s/s	1		17	HOLD FINGERS	316 S/S	2		29	SHUTTLE GUIDE SHAFT	440C	2	hardened and ground
4	PIN	316 S/S	1		16	LEVER BRACKET	P-BRONZE 034	1		28	SPECIMEN MOUNTING PLATE	316 S/S	1	
3	LOAD PLUNGER	316 S/S	1		15	LOAD ASSEMBLY HOUSING	316 S/S	1		27	RECIPROCATING SPECIMEN	test material	1	
2	NEEDLE ROLLER BEARING - LOAD PLUNGER	-	1	FAG DNK7/19TN	14	FRICTION PLATE GUIDE SHAFT	431 S/S	2	HARD CHROME	26	RESETTING RING	P-BRONZE 034	1	
1	SCREW CAP	P-BRONZE 034	1		13	FRICTION PLATE SHAFT BEARINGS	filled UHMWPE	4	SOLIDUR DS	25	RATCHET BRACKET	P-BRONZE 034	1	
ITEM NO	DESCRIPTION	MATERIAL	NO OFF	REMARKS	12	FRICTION PLATE	316 S/S	1		24	SUPPORT BRACKET - UPPER ASSEMBLY	aluminium 7017	2	

UNIVERSITY OF CAPE TOWN
DEPARTMENT OF MATERIALS ENGINEERING

SUBASSEMBLY DWG OF INTERNAL WORKINGS OF TEST CELL

SCALE : 1 : 2	SHEET 1 OF 42 SHEETS
DATE : 08/08/88 - -	DWG NO ①
DRAWN BY : ULRICH F.B. KIENLE	

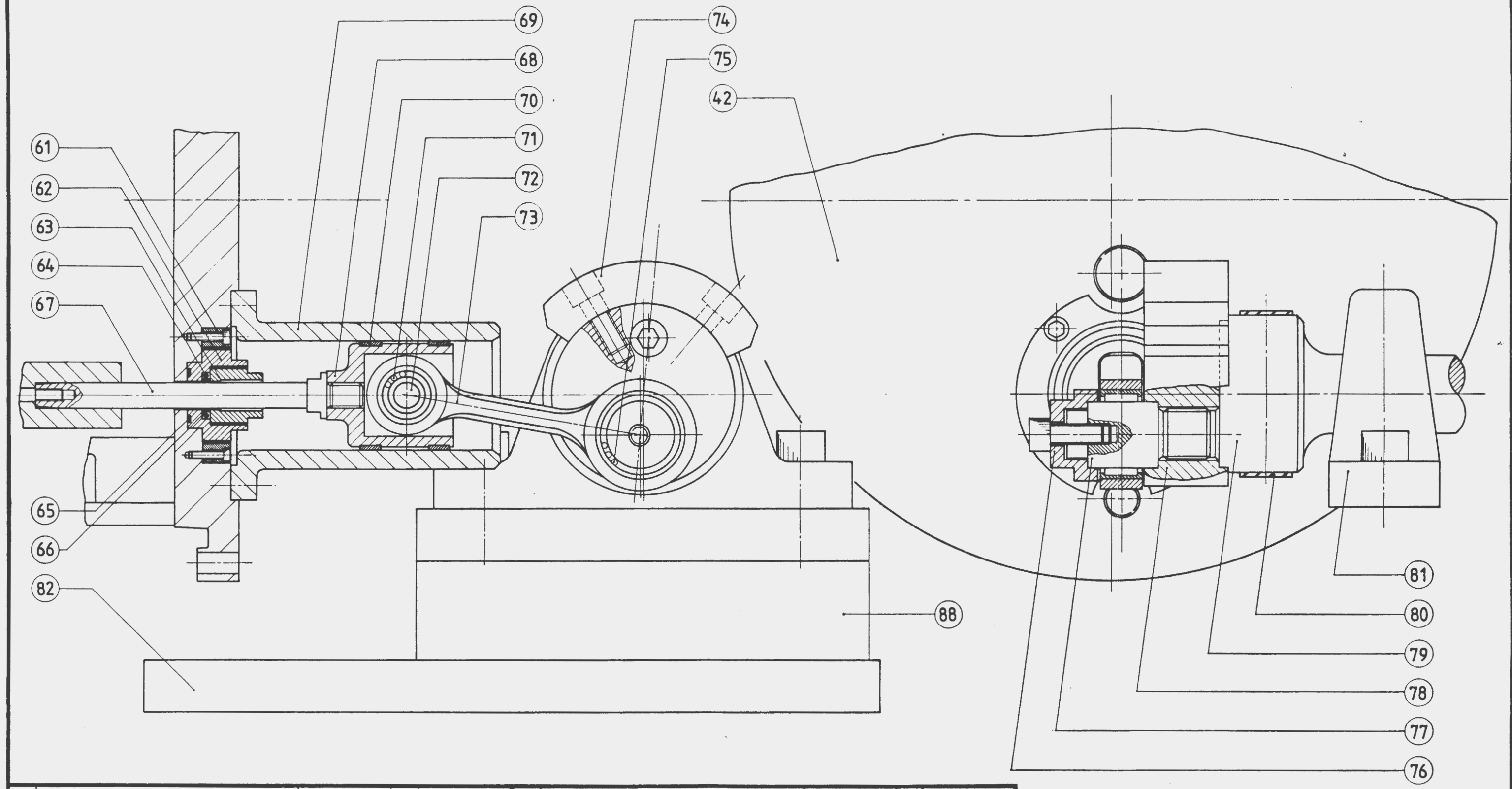

ITEM NO	DESCRIPTION	MATERIAL	NO OFF	REMARKS
71	NEEDLE ROLLER BEARING - WRIST END	-	1	FAG DNKJ10/16A
70	PISTON SEALS	filled UHMWPE	2	SOLIDUR DS
69	PISTON HOUSING	431 S/S	1	
68	RECIPROCATING PISTON	aluminium 7017	1	
67	RECIPROCATING PISTON SHAFT	431 S/S	1	
66	PISTON SHAFT SEAL	filled UHMWPE	1	
65	O-RING - PISTON SHAFT SEALING ASS.	nitrile rubber	1	GACO RM 0161-16
64	O-RING - PISTON SHAFT BACKING SEAL	nitrile rubber	1	GACO RM 0126-24
63	PISTON SHAFT SEAL. ASS. - INNER HOUSING	316 S/S	1	
62	PISTON SHAFT SEAL. ASS. - OUTER HOUSING	P-BRONZE	1	
61	PISTON SHAFT SEAL. ASS. - OUTER RING	431 S/S	1	
42	BACKING DISC	316 S/S	1	
88	BRACKET FOR PLUMMERBLOCKS	070M20 (En 3)	2	PAINTED
82	PLATFORM	070M20 (En 3)	1	PAINTED
81	PLUMMERBLOCK	-	2	RHP NP30
80	DRIVE BELT	FABRIC MIX	1	
79	DRIVESHAFT	817M40 (En 24)	1	
78	CRANK PIN HOLDING PLATE	431 S/S	1	
77	CRANK PIN	431 S/S	1	
76	CRANK PIN END CAP	431 S/S	1	
75	NEEDLE ROLLER BEARING - CRANK END	-	1	FAG DNK26/16A
74	COUNTERWEIGHT	BRASS	1	
73	CONNECTING ROD	431 S/S	1	
72	WRISTPIN	431 S/S	1	

UNIVERSITY OF CAPE TOWN
DEPARTMENT OF MATERIALS ENGINEERING

SUB ASSEMBLY DWG OF THE RECIPROCATING DRIVE

SCALE : DNS
DATE : 08/08/88
DRAWN BY : ULRICH F.B. KIENLE

SHEET 2 OF 42 SHEETS

DWG NO ②

UNIVERSITY OF CAPE TOWN
DEPARTMENT OF MATERIALS ENGINEERING

SUBASSEMBLY DWG OF PLATFORM LAYOUT

SCALE : 1 : 4
DATE : 08/08/88
DRAWN BY : ULRICH F.B. KIENLE

SHEET 3 OF 42 SHEETS
DWG NO ③

ITEM NO	DESCRIPTION	MATERIAL	NO OFF	REMARKS
42	BACKING DISC	316 S/S	1	
59	ENVIRONMENTAL CHAMBER	as may be requd.	1	OPTIONAL
59a	QUICK RELEASE TOGGLE LATCH	Zn plated steel	4-8	OPTIONAL
59b	GUIDE ROLLERS	431 S/S	4	OPTIONAL
59c	GUIDE SHAFTS	431 S/S	2	OPTIONAL
47	GUSSET STAND (LHS and RHS)	070M20 (En 3)	1	
69	PISTON HOUSING	431 S/S	1	
73	CONNECTING ROD	431 S/S	1	
74	COUNTERWEIGHT	BRASS	1	
76	CRANK PIN END CAP	431 S/S	1	
79	DRIVESHAFT	817M40 (En 24)	1	
80	DRIVEBELT	FABRIC MIX	1	
81	PLUMMERBLOCKS	-	2	RHP NP30
82	PLATFORM	070M20 (En 3)	1	PAINTED
83	DRIVE PULLEY	070M20 (En 3)	1	trim down existing
84	MOTOR MOUNTING BASE	070M20 (En 3)	1	PAINTED
85	DC MOTOR (and CONTROLLER)	-	1	GEC (existing)
86	SPACERS	070M20 (En 3)	4	PAINTED
87	ANTI VIBRATION MOUNTINGS type D	RUBBER MIX	4	REMAG 5218-112
92	BELT DRIVE COVER	070M20 (En 3)	1	
93	TABLE	070M20 (En 3)	1	

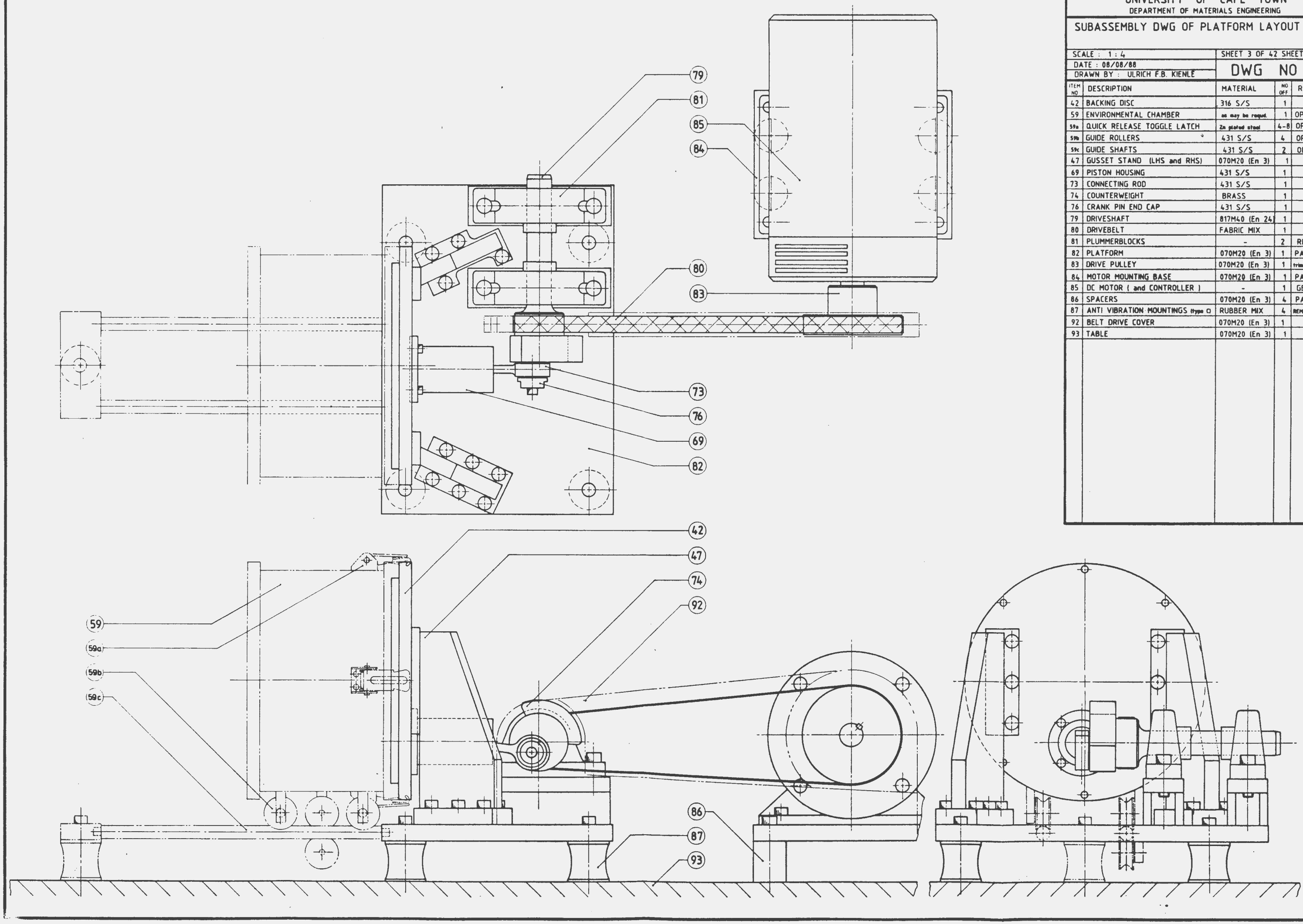

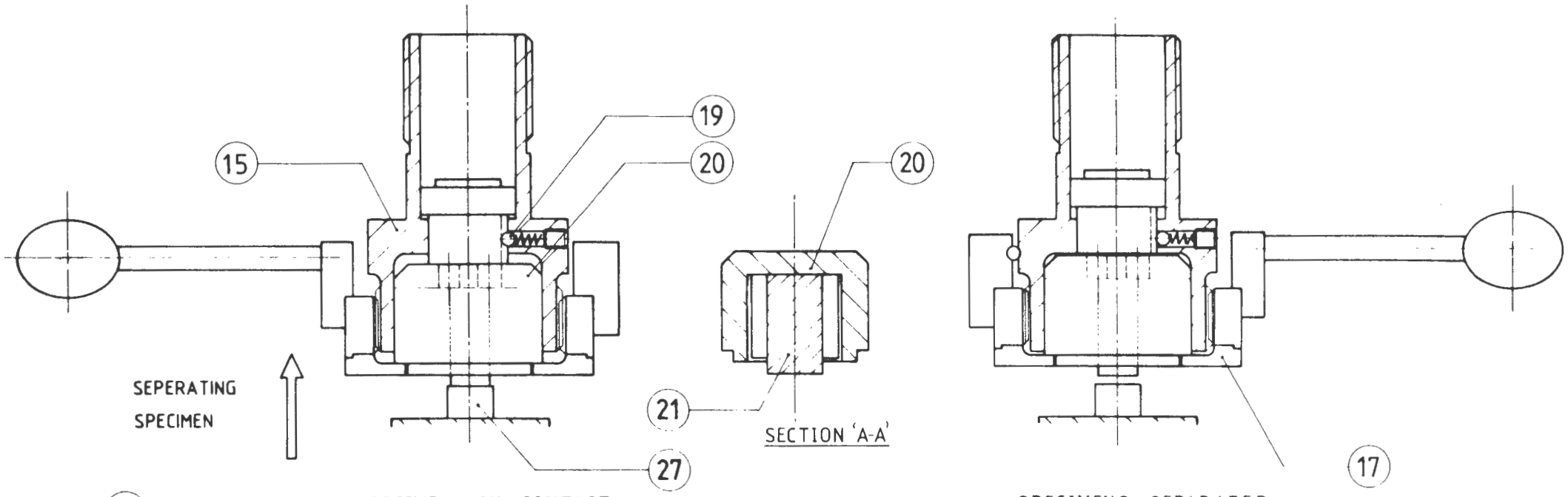

SPECIMENS IN CONTACT

SPECIMENS SEPARATED

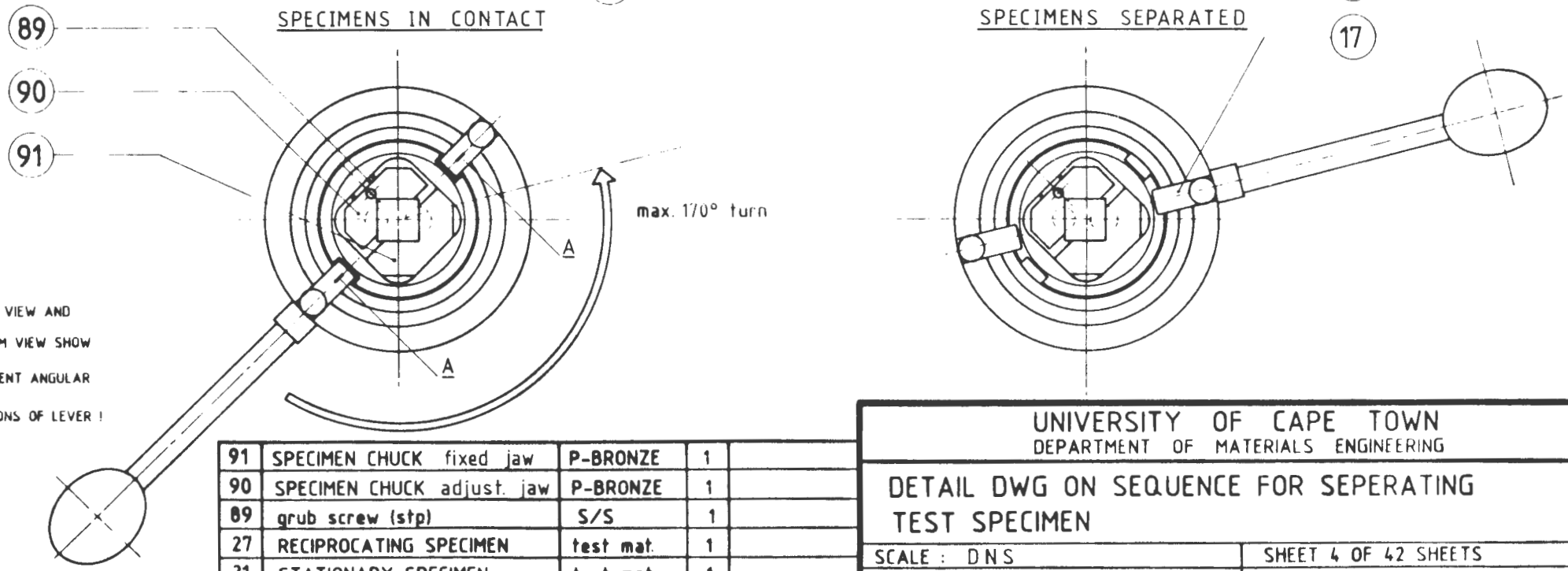

NB

FRONT VIEW AND BOTTOM VIEW SHOW DIFFERENT ANGULAR POSITIONS OF LEVER !

ITEM NO	DESCRIPTION	MATERIAL	NO OFF	REMARKS
91	SPECIMEN CHUCK fixed jaw	P-BRONZE	1	
90	SPECIMEN CHUCK adjust. jaw	P-BRONZE	1	
89	grub screw (stp)	S/S	1	
27	RECIPROCATING SPECIMEN	test mat.	1	
21	STATIONARY SPECIMEN	test mat.	1	

UNIVERSITY OF CAPE TOWN
DEPARTMENT OF MATERIALS ENGINEERING

DETAIL DWG ON SEQUENCE FOR SEPERATING TEST SPECIMEN

SCALE : DNS

DATE : 08/08/08

DRAWN BY : ULRICH F B KIENLE

SHEET 4 OF 42 SHEETS

DWG NO (4)

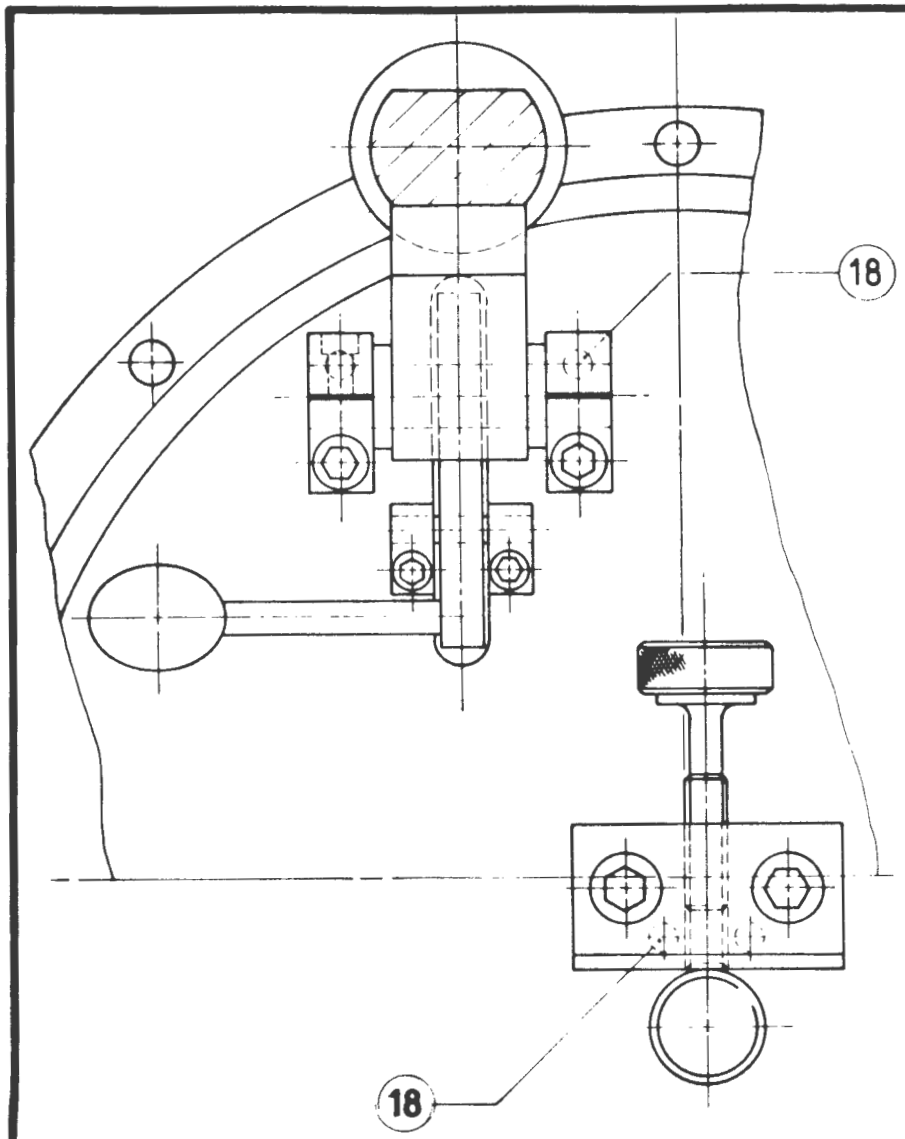

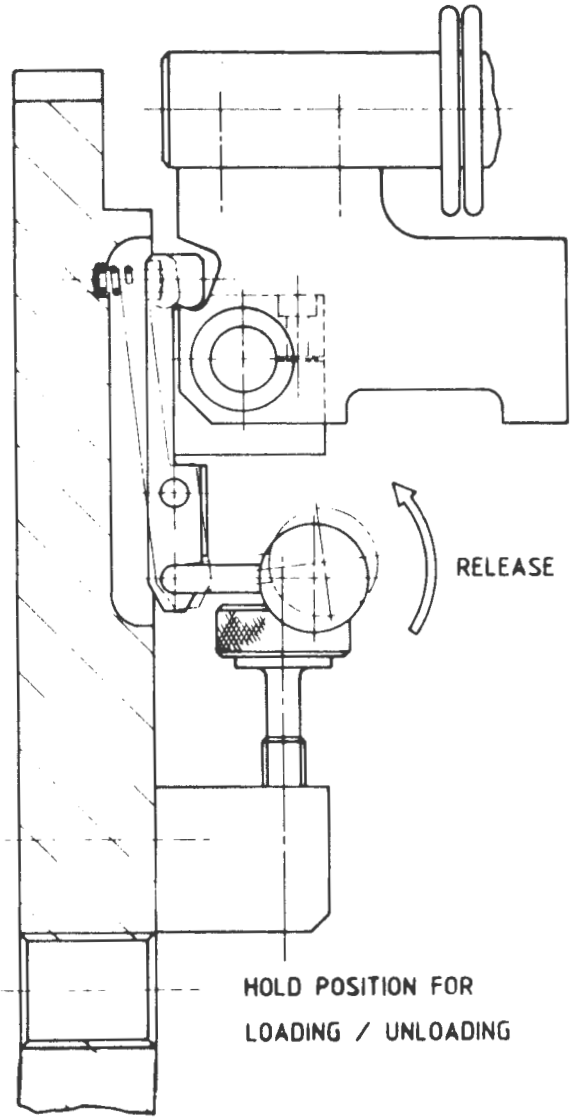

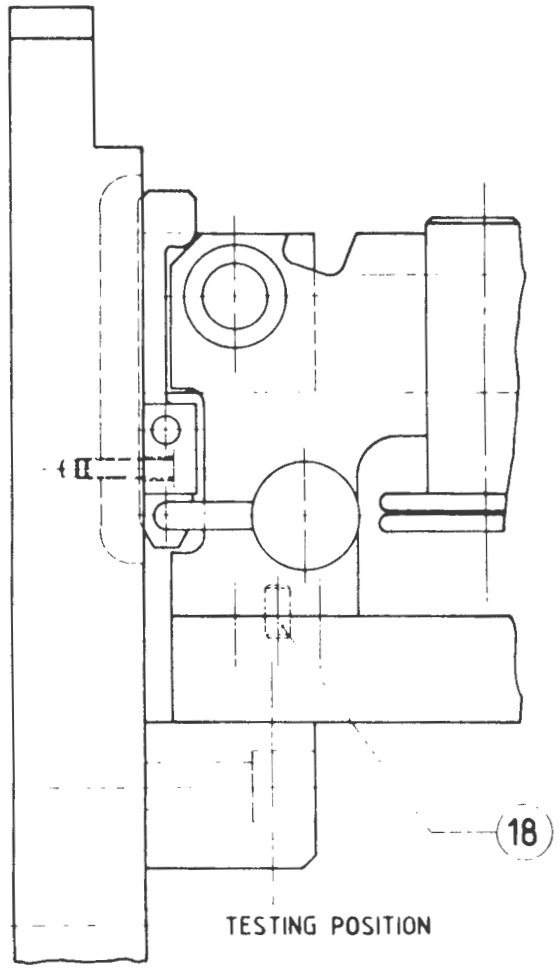

ITEM NO	DESCRIPTION	MATERIAL	NO OFF	REMARKS
18	LOCATING PIN	316 S/S	18	

UNIVERSITY OF CAPE TOWN
DEPARTMENT OF MATERIALS ENGINEERING

DETAIL DWG ON SEQUENCE FOR LATCHING SPECIMEN IN HOLD AND TEST POSITIONS

SCALE : DNS

DATE : 08/08/88

DRAWN BY : ULRICH F B KIENLE

SHEET 5 OF 42 SHEETS

DWG NO (5)

8.0 EVALUATION OF THE NEW TEST RIG

Construction of the test rig was completed within two months and inside the allocated budget. As part of the commissioning stage, three tests were conducted under identical test conditions and on the same material couple as the last series of tests which were done on the old test facility (D). The intention here was to firstly ensure that all the features of the rig work properly and secondly that the reproducibility has improved from the best previous of ± 27% (refer to fig. 3.23).

8.1 TEST RESULTS

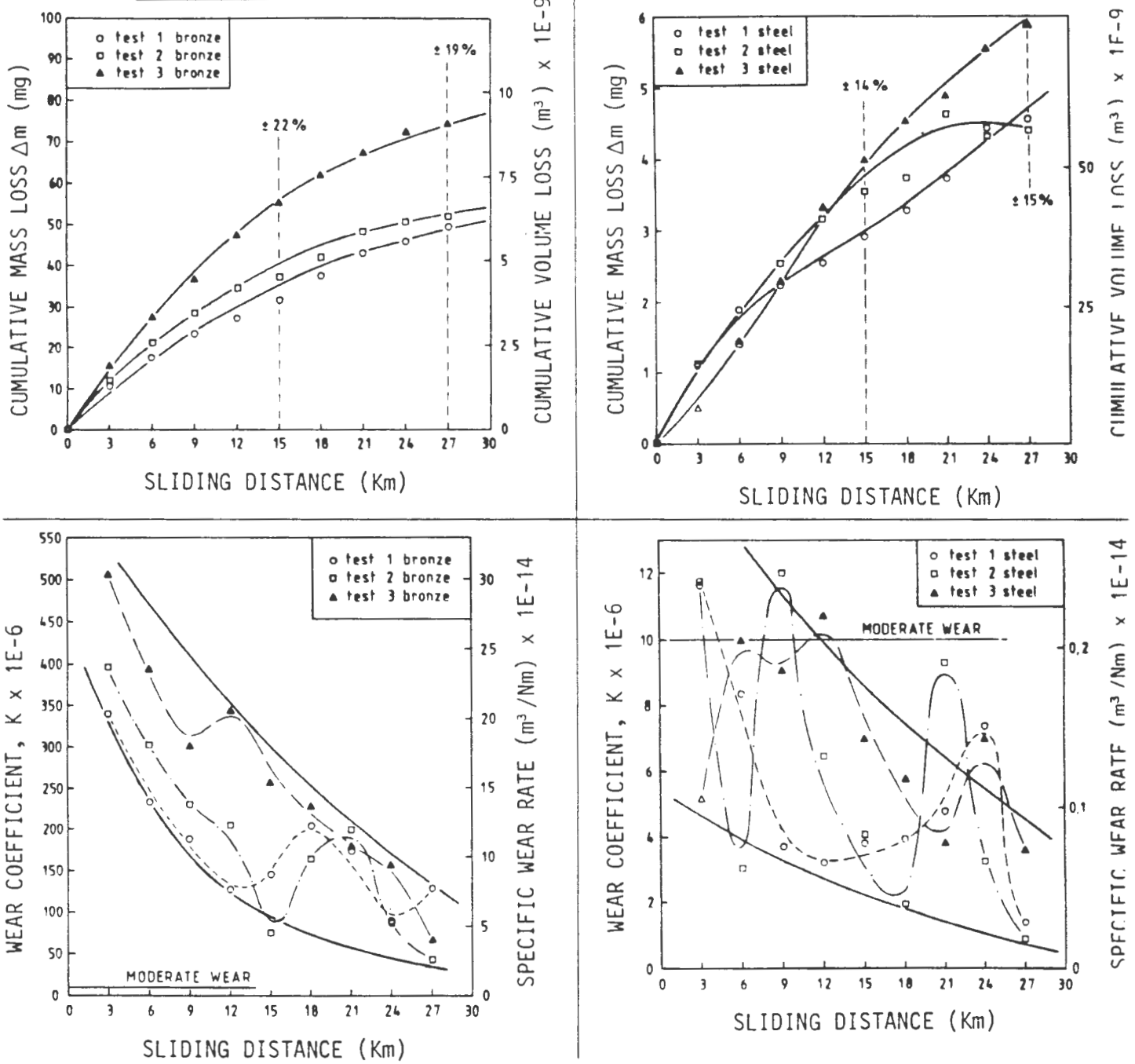

Fig. 8.1 RESULTS OF REPRODUCIBILITY TESTS DONE ON THREE SETS OF 122/CZ114 COUPLES USING THE NEW TEST RIG IN DISTILLED WATER (STATIONARY SPECIMEN IS BRONZE, RECIPROCATING SPECIMEN IS STAINLESS STEEL)

Material couple :	122 stainless steel/CZ114 manganese bronze		
Test parameters :	reciprocating speed	=	peaking @ 1 m/s
	surface roughness	=	0.40 μm CLA $\pm$ 10%
	load	=	20 N
	test intervals	=	every 3 km
	total test distance	=	27 km
	lubricant/coolant	=	distilled water

Figure 8.1 above shows the results obtained for the reproducibility test. To afford comparison with chapter 3.0, results were plotted on the same axes as previously. Reproducibility as expressed by the $\pm$ deviation in mass loss after 15 km is a creditable $\pm$ 22% and $\pm$ 14% for CZ114 and 122 respectively. After 27 km, fluctuation in mass loss improves to $\pm$ 19% and $\pm$ 15 % respectively. These values must not be seen in isolation though, as depending on the initial surface match between the specimens, bedding-in rates will differ and different amounts of mass loss are therefore likely. As stated previously (section 3.4.1) the rate of increase of mass loss is a much more important criteria for comparison. In all three cases the graphs show this rate to be decreasing with sliding distance and after approximately 21 km the slopes (and therefore wear rates) of the three bronze specimens approach very similar values - unlike the widely fluctuating slopes of previous results.

The wear coefficients for the bronze specimens fall into a region stretching from 5 x 10^{-4} at the start of the test to 5 x 10^{-5} at test conclusion. This lies well within the upper adhesive wear zone bounded by severe galling (10^{-3}) at its top end and moderate wear (10^{-5}) at the lower limit (Rabinowicz [32]). Figure 8.2 shows a comparison between the K ranges obtained for these results and those under water lubricated/cooled test conditions generated previously. This diagram clearly shows how a much narrower, and therefore more reproducible wear coefficient band was obtained with the new test facility.

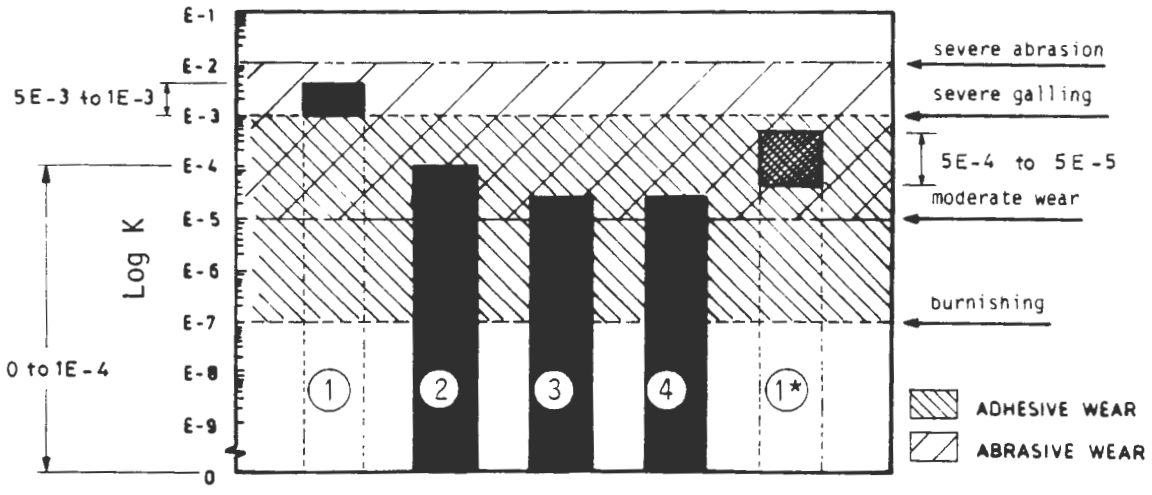

Fig. 8.2 COMPARISON OF WEAR COEFFICIENTS, K FOR ALL WATER LUBRICATED RESULTS TO DATE
(1 - 4 : results on previous test facilities A - D;
1* : results for new test rig)

Heeding the cautionary notes on validity of the K-value, as discussed in chapter 2.0, these results appear to indicate that these tests were in fact conducted in the correct wear regime. Further evidence of this is borne out in fig. 8.3, which shows a macrograph of the worn surfaces for all three tests. It shows transfer of bronze to the counterface to be uniform over the entire area of interaction. It also shows that 100% surface match was attained.

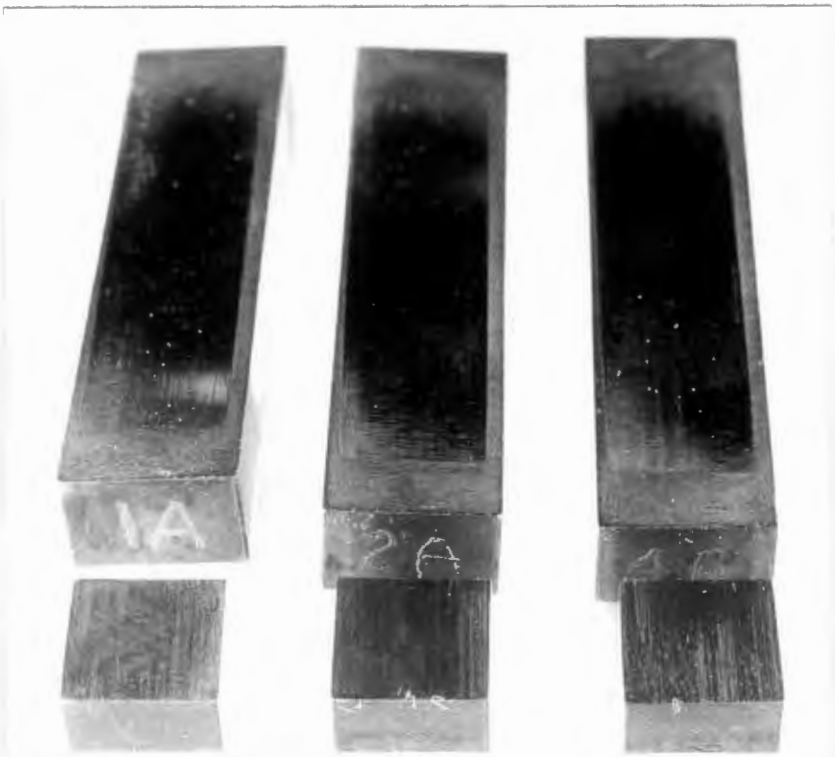

Fig. 8.3 MACROGRAPH OF THE THREE BRONZE/STEEL INTERFACES AFTER TEST COMPLETION

It is also interesting to note that, whilst the general trend is a decreasing wear rate with sliding distance, the values of K oscillate from test interval to test interval. The jumps up in wear rate are thought to be due to transferred platelets peeling off and the decreases in wear rate due to the lag period in which transfer layers are being reconditioned. More work obviously needs to be done to confirm this.

8.2 TEST RIG

The chosen concept has proved successful. All requirements, constraints and criteria were met and in some instances exceeded. Specimen changes can be done in under two minutes and the seals for guiding the reciprocating assembly and sealing the piston shaft from the bath can be replaced within ten minutes.

In total, the rig completed 1.35 million reciprocating testing cycles or 81 km of sliding distance (3 tests @ 27 km and 50 000 cycles = 3 km).

In addition, two lots of three test runs (without specimens) of 50 000 cycles (= 3 km) each were conducted at peak velocities of 5 m/s and 10 m/s respectively, adding a further 0.3 million cycles. Noise levels, although higher than at 1 m/s are still minimal and present no noise pollution hazard to other laboratory users. The vibrations appear to be adequately contained by the counterweight and residual vibrations are almost completely absorbed by the rubber mountings.

No appreciable temperature rise was recorded for the reciprocating piston and after stripping down the test rig, no signs of thermal damage, wear or slackness could be detected in any of the seals, bushes or bearings.

It is also important to note that the test rig is a prototype. If further units are to be built at any future stage, certain minor design changes will have to be made to simplify manufacture; the basic concept will, however, remain unchanged.

Figure 8.4 below gives a sample recording of the variation in friction force for one test interval. No attempts have been made to calibrate the friction transducer as yet and the intention was merely to confirm that a fluctuation could indeed be picked up in either direction.

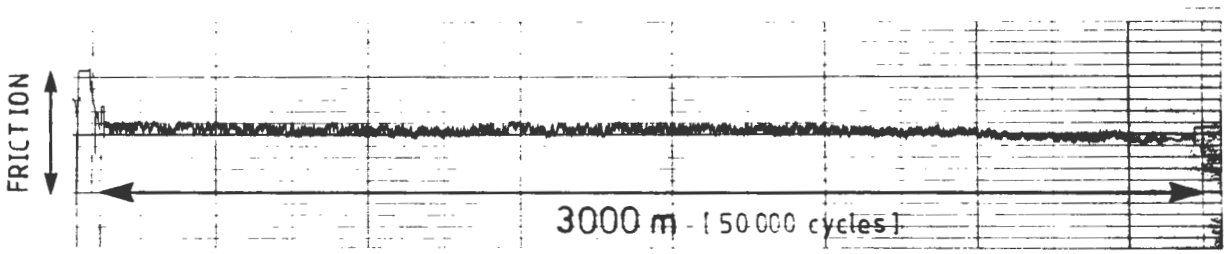

Fig. 8.4 VARIATION IN FRICTION FORCE WITH SLIDING DISTANCE

A series of photographs are given over the page (fig.'s 8.5 - 8.7), showing the test rig in the testing and holding positions. Also shown are details of the reciprocating drive with its bearing and sealing arrangement; the reciprocating shuttle; loading mechanism and friction transducer and lastly the two specimens about to be brought into full contact under load.

HOLDING POSITION

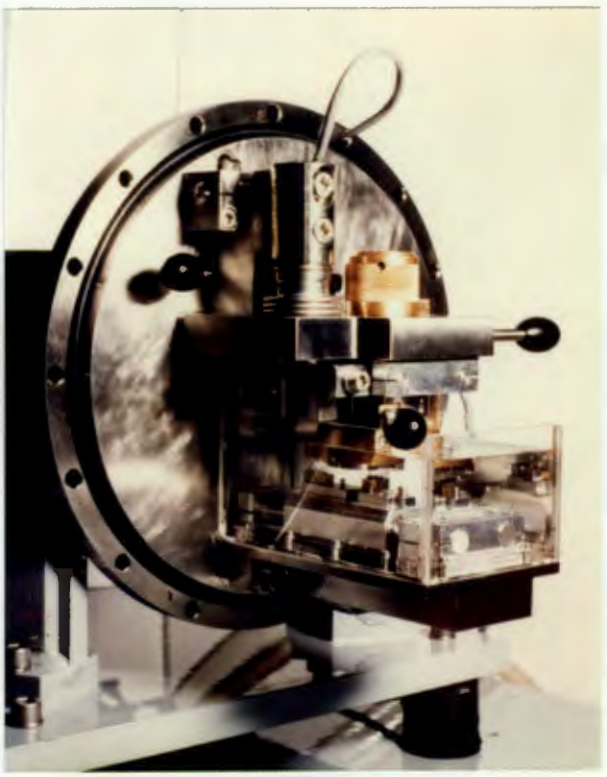

TESTING POSITION

INTERMEDIATE POSITION

Fig. 8.5

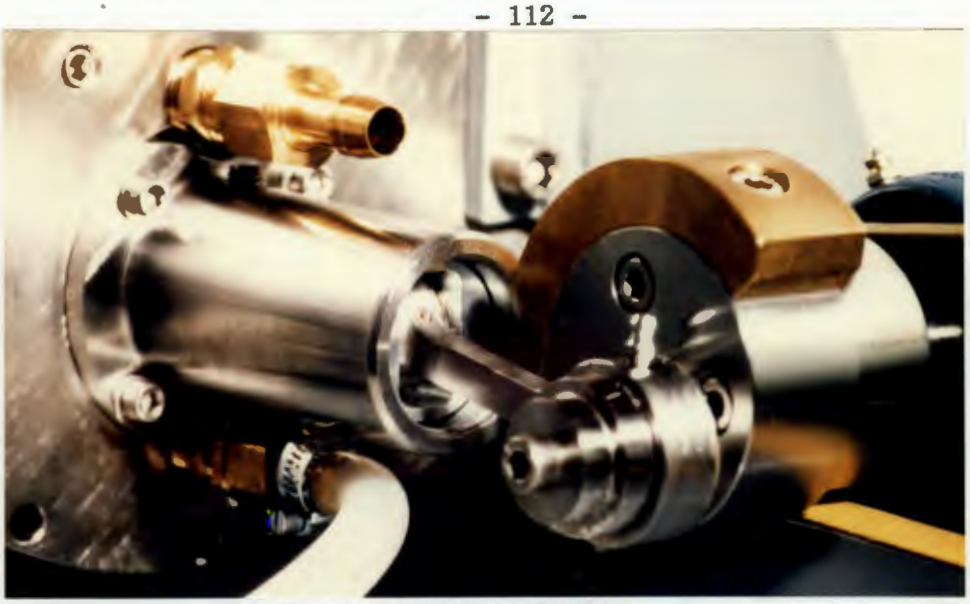

RECIPROCATING ASSEMBLY

CRANKPIN EXTRACTED

SEALING ASSEMBLY

RECIPROCATING ASSEMBLY WITH PISTON HOUSING REMOVED

Fig. 8.6

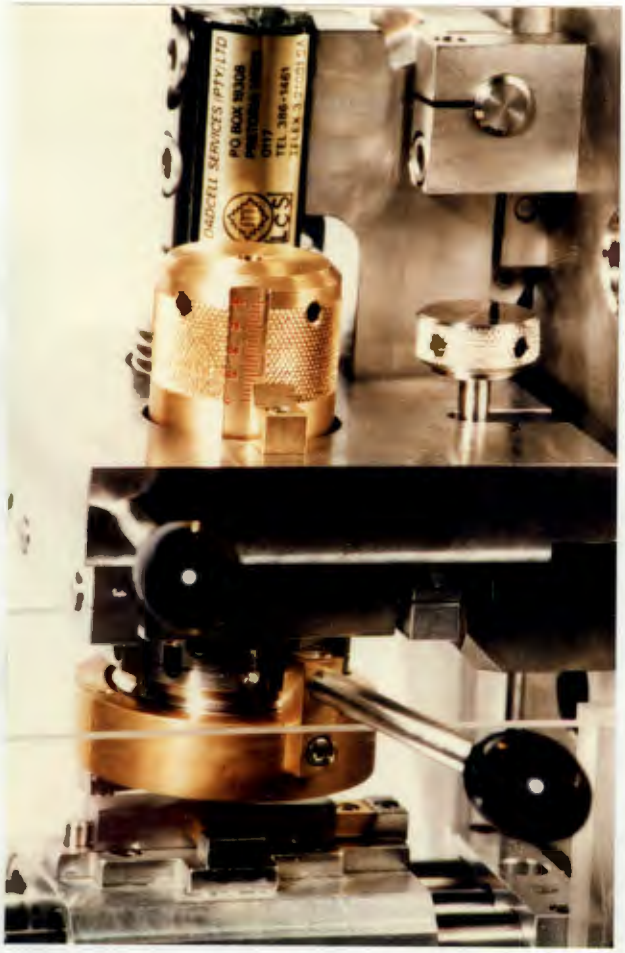

DETAIL LOADING ARRANGEMENT

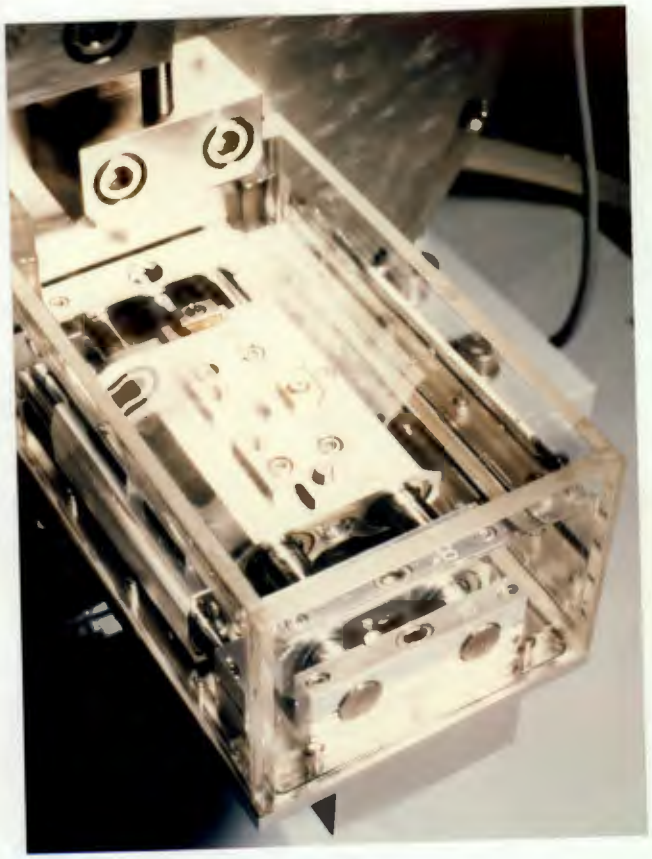

RECIPROCATING SHUTTLE IN BATH

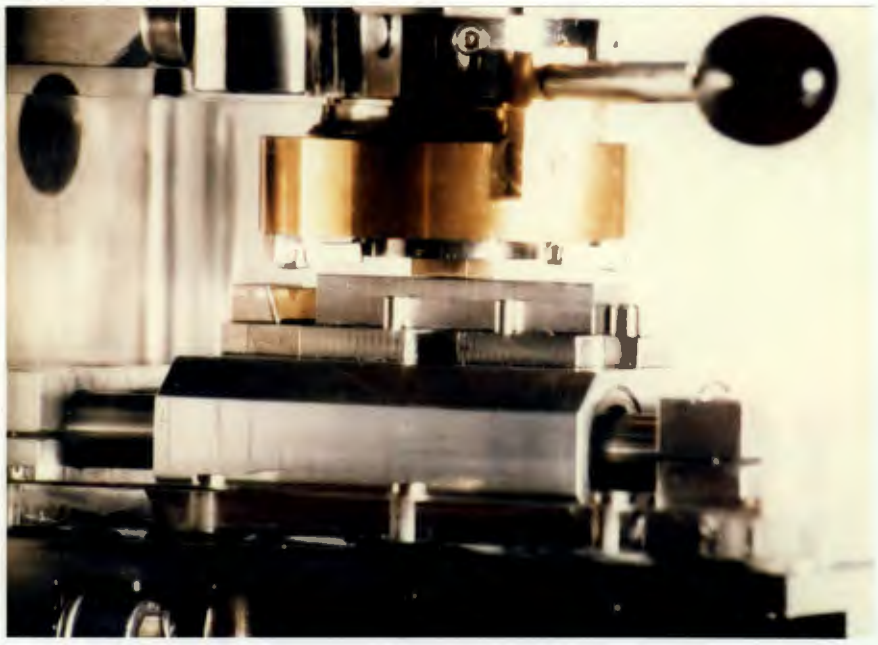

SPECIMENS BEING LOADED AGAINST EACH OTHER

Figure 8.7

9.0 CONCLUSIONS

This section will deal separately with each of the conclusions in respect of: the attainment of the set objectives, inferences drawn from the implemented test programme and thirdly, the performance of the new test rig.

9.1 ATTAINMENT OF SET OBJECTIVES

1. The short term objectives have been met to the extent that commencing with stage 2 - which calls for the implementation of a test programme to examine the most promising material combinations for reciprocating components operating on hydro-power - is now possible.

2. No ranking tables, galling threshold stresses or empirical wear equations have yet been compiled or formulated.

3. Substage 2 of the objectives was completed with the successful commissioning of a new test facility.

9.2 INFERENCES DRAWN FROM INITIAL TEST PROGRAMME

1. Reproducibility, as expressed by the $\pm$ deviation in mass loss after 15 km of sliding distance, was reduced from a worst initial value of $\pm$ 87% to a best of $\pm$ 27%, after extensive modifications to the inherited test facility.

2. Wear coefficients, which give an indication of the rate of wear, were shown to cover a range of several orders of magnitude, stretching across both adhesive and abrasive wear regimes.

3. No single wear mechanism was responsible for surface degradation in the tests done. Instead, evidence of adhesive -, abrasive - and surface fatigue wear could be seen on different specimens.

4. It was confirmed that wear coefficient value K alone will not specify the predominant wear mechanism. Recourse must therefore be taken to micro- and macrographs as well as profile sections.

5. Transfer of nearly homogeneous layers of material from the softer bronze specimens (CZ114 and AB2) onto their respective stainless steel counterfaces was observed for all bronze/steel couples.

6. Wear rates for the self-mated stainless steels approached the upper limit of the abrasive wear domain.

7. An insufficient number of tests were conducted (due to low reproducibility and inadequacies of test facility and test specimens) to quantify which of the tested couples performs best in terms of low wear rates.

8. Quoting two dimensional surface roughness data for three dimensional surfaces is inadequate as topography changes can not be adequately interpreted.

9. The effect of water quality on the results obtained has not been quantified.

10. No trends can be quoted as error bands for different test-runs overlap each other, thereby masking trends.

9.3 PERFORMANCE OF THE NEW TEST RIG

1. The lessons learnt from the performance of the inherited test facility, as well as the modifications made thereto, were instrumental in the design of the new test rig.

2. All requirements, constraints and criteria initially set for the design were fully met.

3. A test facility, capable of investigating the performance of material surfaces rubbing against one another under conditions of high speed reciprocating sliding in specialist environments, is now available.

4. A series of three tests performed on the new test facility yielded reproducibility figures of $\pm$ 22% after 15 km of sliding and $\pm$ 19% after 27 km.

5. The range within which wear coefficients fall for the three tests done, has been substantially reduced by several orders of magnitude. The range now spans from 5×10^{-4} to 5×10^{-5}.

6. Macrographical evidence showed formation of homogeneous bronze surface layers on steel counterfaces for all three tests. As testing progressed, mild grooving of the transfer layer occurred. These observations are consistent with adhesive wear mechanisms and are further supported by the K values obtained.

7. All specimens show that they have been in full area contact from after the running-in period (which varied from 0 - 6 km) to test completion on attainment of 27 km.

8. The test rig completed a total of 1.65 million reciprocating cycles and after a complete strip down no indication of degradation to any of the wearing components (bushes, seals, bearings) could be detected.

10.0 RECOMMENDATIONS

The following recommendations are made in response to the conclusion drawn in chapter 9.0 :

1. Stage 2 of the short term objectives should be undertaken using the new test rig.

2. The implemented test programme should commence with a test matrix that starts with low speeds and light loads and progresses upwards once an adequate data base has been built up.

3. At a later stage, testing should be conducted with type II and III test specimens.

4. Parallel to testing different material couples, the performance of the polymeric seals and bushes should be monitored.

5. Data capture of friction force, temperature, pressure and velocity should be linked to a computer. This should be coupled to a program which plots mass loss and wear coefficient after each test interval.

6. COMRO should make available information on exactly how in-service components, operating on hydro-power, deteriorate. This should be backed up by detail topography scans, micro/macro-photography and micro hardness traces.

7. The implemented test programme should, if at all possible, make use of non-intrusive surface roughness measurements.

8. The question of whether components should be used with a ground or polished finish needs to be reviewed (ground finishes contribute wear fragments).

9. Because the only effective way of eliminating adhesive wear is by separating the contacting surfaces by a film of lubricant, self lubricating bearings and coatings should be re-examined.

10. Thoughts should be given to whether or not it is reasonable to think of water lubricated systems as "oil lubricated systems with poorer lubricicity". A programme looking at water as a lubricant in its own right should therefore by considered.

11. To meet testing demands of the vast numbers of contender hydro-power materials, batch production of several more units of the submitted test rig should be considered.

11.0 REFERENCES

1. GUNDERSEN, R. (1987): "High-pressure Water as an energy source in deep-level mines", The S.A. Mech. Eng. Journ., vol. 37, pp. 69-80.

2. BROWN, C. & WYMER, D.G. (1987): "Engineering of water-powered equipment for mine hydro-power systems", The S.A. Mech. Eng. Journ., vol. 37, pp. 55-67.

3. LLOYD, A.I.G. (1986): "The sliding wear of UHMWPE against steel", Msc Thesis, University of Cape Town.

4. ZUM GAHR, K.H. (1987): "Microstructure and Wear of Materials", Elsevier Science Publishers B.V., Tribology series 10, Amsterdam.

5. CZICHOS, H. (1978): "Tribology. A systems approach to the Science and Technology of Friction, Lubrication and Wear", Elsevier, Amsterdam.

6. ASME (1980): "Wear Control Handbook", editors Peterson, M.B. & Winer, W.O., N.Y.

7. JAHANMIR, S. (1987): "Future directions in Tribology Research", trans. of ASME, Journal of Tribology, vol. 109, pp. 207-221.

8. CZICHOS, H. (1984): "Review on wear research - activites in the F.R.G.", WEAR, 100, pp. 579-589.

9. ROBERTS, W.H. (1986): "Some current trends in tribology in the UK and Europe", TRIBOLOGY International, vol. 19, nr. 6.

10. BSI (1976): "BS 1134 Part 1 and 2 - Method for the assessment of surface texture", London.

11. SHERRINGTON, I. & SMITH, E.H. (1988): "Modern measurement techniques in surface metrology: part I; stylus instruments, electron microscopy and non-optical comparators", WEAR, 125, pp. 271-288.

12. SHERRINGTON, I. & SMITH, E.H. (1988): "Modern measurement techniques in surface metrology: part II; optical instruments", WEAR, 125, pp. 289-308.

13. HALLING, J. (1976): "Introduction to Tribology", Wykenham Publications, London.

14. HALLING, J. (1978): "Principles of Tribology", MacMillan Press, London.

15. SMITH, W.V. (1973): "Material Selection Criteria for water lubrication", WEAR, 25, pp. 139-153.

16. TABOR, D. (1981): "Friction - the present state of our understanding", Journ. of Lub. Techn., vol. 103, April edition.

17. LIM, S.C. & ASHBY, M.F. (1987): "Wear-Mechanism Maps", Acta metall., vol. 35, no. 1, pp. 1-24.

18. SUH, N.P. & SIN, H.C. (1981): "The Genesis of Friction", WEAR, 69, pp. 91-114.

19. LINDSAY-SCOTT, H. & WYMER, D.G. (1984): "The investigation of high water-based hydraulic fluids for mining machines in South African gold mines", Inst. of Mech. Eng., C350/84, pp. 105-111.

20. SCHUHMACHER, W.J. (1977): "Wear and galling can knock out equipment", CHEMICAL ENGINEERING, May issue, McGraw-Hill.

21. DE GEE, A.W.J. (1981): "A note on the relation between friction and wear", WEAR, 65, pp. 397-398.

22. KO, P.L. (1987): "Metallic Wear - a review with special reference to vibration induced wear in power plant components", TRIBOLOGY International, vol. 20, nr. 2.

23. KRAGELSKII, I.V. & MARCHNKO, E.A. (1982): "Wear of Machine Components", trans. of ASME, Journ. of Lub. Techn., vol. 104, pp. 1-7.

24. DIN 50 320 (1979): "parts I, II and III", Beuth Verlag, Berlin.

25. SCHUHMACHER, W.J. (1981): "A stainless steel alternative to cobalt wear alloys", CHEMICAL ENGINEERING, September issue.

26. HIRST, W. & LANCASTER, J.K. (1960): "The influence of speed on metallic wear", Proc. Roy. Soc. A, vol. 259, pp. 228-241.

27. SARKAR, A.D. (1976): "Wear of Metals", Pergamon Press, Oxford.

28. Committee of Stainless Steel Producers (1978): "Review of the Wear and Galling characteristics of stainless steel", AISI, Washington D.C.

29. KRAUSE, H. & SENUMA, T. (1982): "A contribution towards improving the applicability of laboratory wear tests to practice", WEAR, 74, pp. 67-83.

30. WALLBRIDGE, N.C. & DOWSON, D. (1987): "Distribution of wear theory", Int. conf. on Wear of Materials, ASME, Houston.

31. LENEL, U.R. (1987): "Tribology goes below ground", Indust. Lub. and Tribo Journ., Jan/Feb edition.

32. RABINOWICZ, E. (1981): "The Wear Coefficient - Magnitude Scatter, Uses", trans. of ASME, Journ. of Lub. Techn., vol. 103.

33. TABOR, D. (1987): "Friction and Wear-developments over the last fifty years", Inst. of Mechn. Eng., C245/87, pp. 157-172.

35. PETERSON, M.B. (1987): "Advancements in tribological materials 1937-1987-2002", Inst. of Mechn. Eng., C249/87, pp. 583-593.

36. FREES, N. (1987): "Characterizing and solving of Industrial wear problems", WEAR, 115 pp. 193-202.

37. NEAL, M.J. (1987): "The application of tribology to design", Inst. of Mechn. Eng., C247/87, pp. 697-699.

38. BALL, A. & WARD J.J. (1986): "An approach to material selection for corrosive-abrasive wear by systematic in-situ and Laboratory testing procedures", TRIBOLOGY International, vol. 18, no. 6.

39. BLACK, S.A. (1982): "Seawater Hydraulics: Development of an experimental vane motor for powering diver-held tools", Naval Civil Engineering laboratories, California.

40. STOLARSKI, T.A. (1980): "Wear of Water-lubricated Composite materials", WEAR, 58, pp. 103-108.

41. SCHUHMACHER, W.J. (1978): "Adhesive Wear Resistance of Engineering Alloys", METAL PROGRESS, vol. 114, no. 6.

42. SMITH, A.F. (1984): "The friction and sliding wear of unlubricated 316 stainless steel at room temperature in air", WEAR, 96, pp. 301-318.

43. SMITH, A.F. (1986): "The friction and sliding wear of unlubricated 316 stailess steel in air at room temperature in the load range 0.5-9.0 N", WEAR, 110, pp. 151-168.

44. SMITH, A.F. (1988): "The unlubricated reciprocating sliding wear of a martensitic stainless steel in air and CO_2 between 20 and 300°C", WEAR, 123, pp. 313-331.

45. SUNDBERG, M. et al (1987): "Metallographic aspects on wear of special brass", WEAR, 115, pp. 151-165.

46. CARRO, G. & WERT, J. (1987): "An X-ray diffraction study of the triaxial normal residual stresses in worn aluminium bronze surfaces", WEAR, 115, pp. 285-299.

47. TABOR, D. (1977): "Wear - A critical synoptic view", trans. of ASME, Journ. of Lub. Techn., October issue, pp. 387-395.

48. KRAGELSKII, I.V.; DOBYCHIN, M.N. & KOMBALOV, V.S.(1982): "Friction and Wear - Calculation Methods", Pergamon Press, Oxford.

49. HANNAH, J. & STEPHENS, R.C. (1984): "Mechanics of Machines", Edward Arnold Publishers, London.

50. SHIGLEY, J.E. (1977): "Mechanical Engineering Design", 3rd edition, McGraw-Hill.

51. FRANCIS, T.M. & WILSON, R.L. (1978): "Mechanical Considerations for the design of needle roller big end bearings for two cycle engines", Conf. Inst. Mechn. Eng., Isle of Man.

52. STAR (1985): "Linear Motion Product Catelogue", Deutsche Star Kugelhalter GmbH.

53. METCALFE, B.; WHITAKER, W.M. & LENEL, U.R. (1987): "Development of corrosion - abrasion resistant steels for South African gold mining industry", Int. Conf. Stainless Steels '87, Inst. of Metals, York, UK.

* 34. TABOR, D. (1987): "Friction and wear - developments over the last fifty years", Inst. of Mechn. Eng., CZ245/87, pp. 157-172.

APPENDICES

APPENDIX A - HEAT TREATMENTS FOR STAINLESS STEELS TESTED

AISI 630 (17-4 PH)

- solution treat @ 1088 ± 14°C for ½ hour/25 mm section
- oil cool to below 32°C
- age harden @ 552°C for 4 hours
- air cool

AISI 431

- preheat @ 540°C ± 10°C for ½ hour/25 mm section
- preheat @ 775°C ± 10°C for ½ hour/25 mm section
- soak @ 1040°C ± 10°C for ½ hour/25 mm section
- marquench @ 175°C for 5 minutes/10 mm section
- air cool
- hot alkaline wash
- sub-zero heat treatment @ -75°C for 30 minutes
- within 2 hours:
  - o double temper @ 260°C for 2 hours per temper
  - o air cool to room temperature in between tempers
- passivate in 20% nitric acid + sodium dichromate 20gms/l for 30 min @ 50-60°C.

ALLOY 122

- soak @ 1050°C for ½ hour/25mm section
- oil quench
- temper @ 200°C for 2 hours
- air cool

APPENDIX B - SAMPLE CALCULATIONS

Definition of symbols:

Δm	=	incremental mass loss [mg]
ΔVL	=	incremental volume loss [m^3]
CVL	=	cumulative volume loss [m^3]
Δs	=	incremental sliding distance [m]
P	=	applied normal load [N]
VHN	=	Vickers Hardness Number [N/m^2]
SWR	=	specific wear rate [m^3/Nm]
K	=	wear coefficient
ρ	=	density [kg/m^3]

Definition of equations:

$$CVL = \frac{\Delta m}{\rho} \quad \left[\frac{mg * 1E6}{kg/m^3} \right] = [\, m^3 * 1E6 \,]$$

$$SWR = \frac{\Delta VL}{P * \Delta S} \quad \left[\frac{m^3}{N * m} \right] = [\, m^3/Nm \,]$$

$$K = SWR * \text{hardness} \quad [m^3/Nm * N/m^2 = \text{dimensionless}]$$

Taking 122/CZ114 test 2 (graph 3.17, Page 57) as an example:

Consider test interval 12 to 15 km:

- o s = 3000 m
- o m = 141.78 mg
- o ρ = 8180 kg/m^3
- o P = 20 N
- o VHN = 164 kg/mm therefore hardness in SI units is 164 * 1E6 x 9.81 = 1.609 E9 N/m^2

Thus $\Delta VL = \frac{141.78 * 1E6}{8180} = 1733.3$ E-11 [m^3]

$SWR = \frac{1733.3 \text{ E-}11}{20 * 3000} = 28.9$ E-14 [m^3/Nm]

K = 28.9 E-14 * 1.609 E9 = 4.65 E-4

APPENDIX C - ORIGINAL TEST SPECIMENS

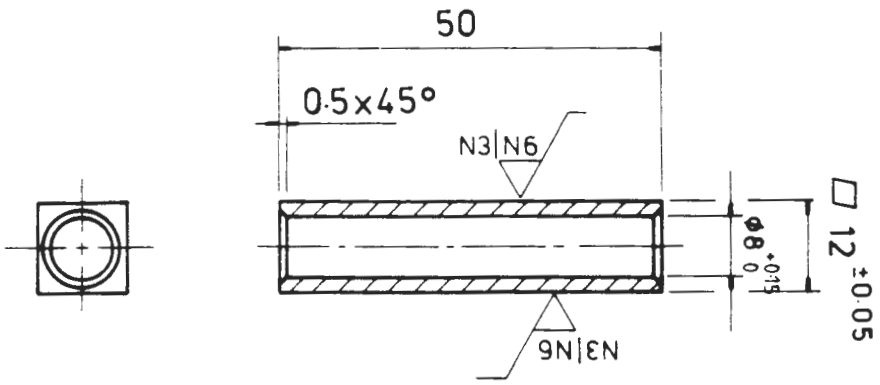

RECIPROCATING SPECIMEN, 1 OFF

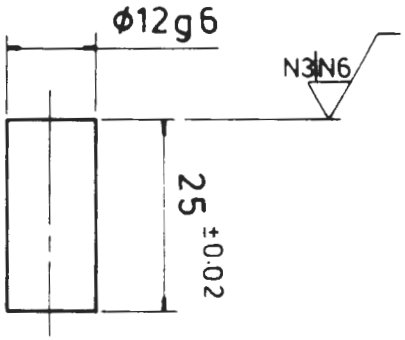

STATIONARY SPECIMEN, 2 OFF

DATE : 14/10/88	TEST SPECIMEN
SCALE : 1:1	FOR ORIGINAL TEST FACILITY
DRAWN BY : U F B KIENLE	

APPENDIX D - TEST SPECIMENS FOR NEW DESIGN

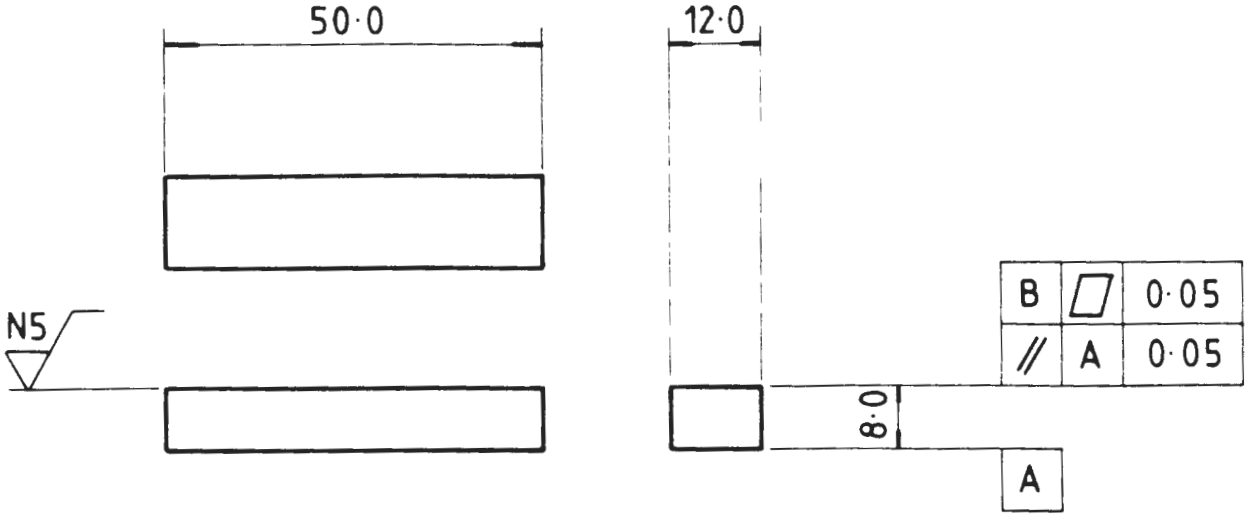

ITEM No (27) RECIPROCATING SPECIMEN , 1off , test material

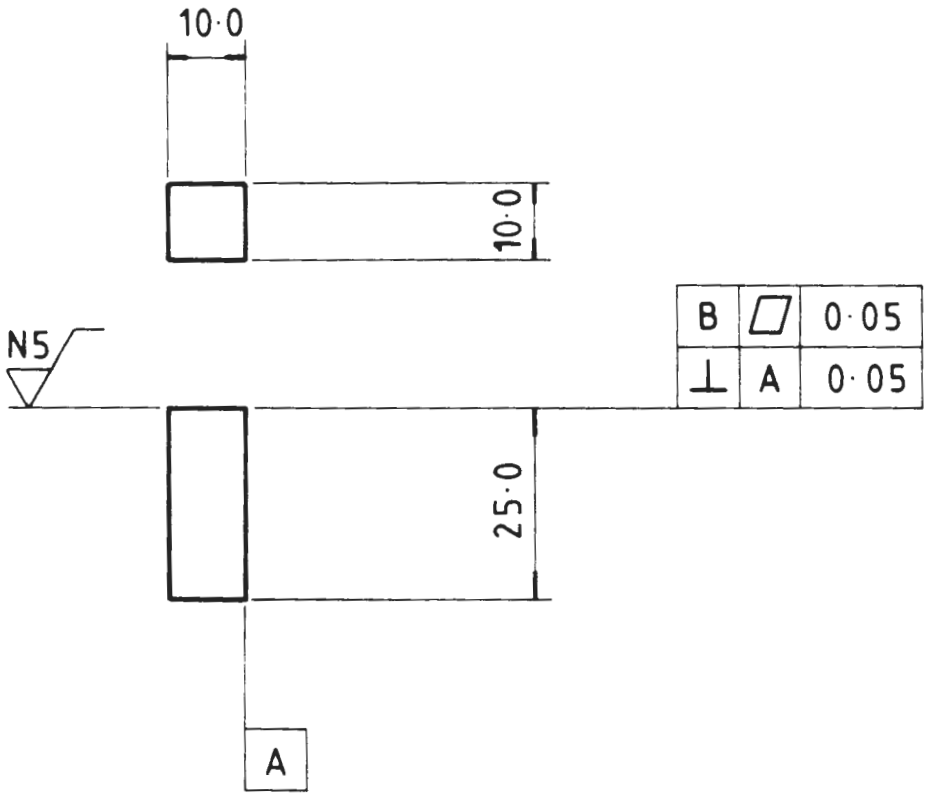

ITEM No (21) STATIONARY SPECIMEN , 1off , test material

DATE : 08/08/88	TEST SPECIMEN
SCALE : 1:1	TYPE I
DRAWN BY : ULRICH KIENLE	

APPENDIX E - DESIGN CALCULATIONS

A lengthy, iterative design process underlines the sizing of all the components that make up the final test rig design, as compromises had to be made between many competing demands. More specifically, efforts were made to maximize mechanical properties, minimize weight, size and cost, optimize fabrication routes and ensure accessibility to and compatibility between all components.

Due to the large number of components which make up the test rig, abridged calculations will be presented for only some of the more critical items. For the sake of brevity, these calculations will not reflect the iterations which were done to arrive at the final dimensions. Instead, an analysis pertaining only to the actual components used, will be given.

A. THE CONNECTING ROD (Item 73)

Figure E1 below gives a schematic representation of the forces acting on the conrod.

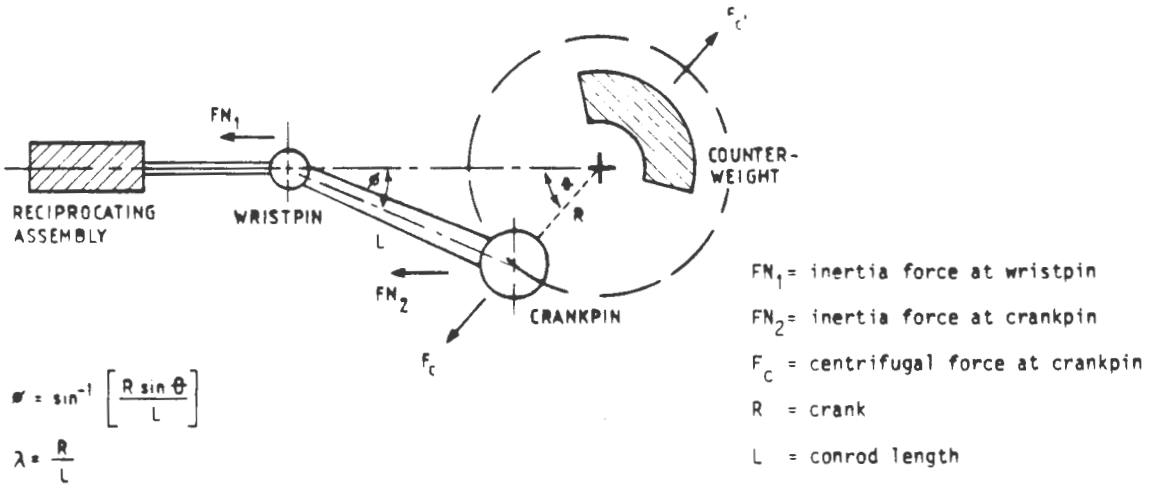

Fig. B1 FORCES ON CONROD

Only two forces are of interest for this assembly:

(1) those due to the reciprocating masses, given by
$F = Mw^2R (\cos\theta + \Gamma \cos 2\theta)$ and
(2) those due to centrifugal effects of the rotating mass, given by: $F = Mw^2R$

where F = resultant force
M = mass
w = angular velocity (rad/s)

Each of these forces varies in magnitude and direction during one revolution and reaches maxima and minima at different positions. A program was written to compute the wristpin load (WPL), crankpin load (CPL) and piston side load (PSL) as a function of crank angle position for the maximum speed of 6366 rpm (corresponding to a peak velocity of 10 m/s). Figure E2 below shows the resultant plot for one revolution. Superimposed onto this graph are equivalent loads for the WPL and CPL. These are defined as uniform loads which would have the same effect in terms of life on the bearings as the fluctuating load which actually exists. The equivalent loads are calculated as follows:

$P_{equivalent} = [\Sigma P^{10/3} / X]^{3/10}$ where X are the number of increments used.

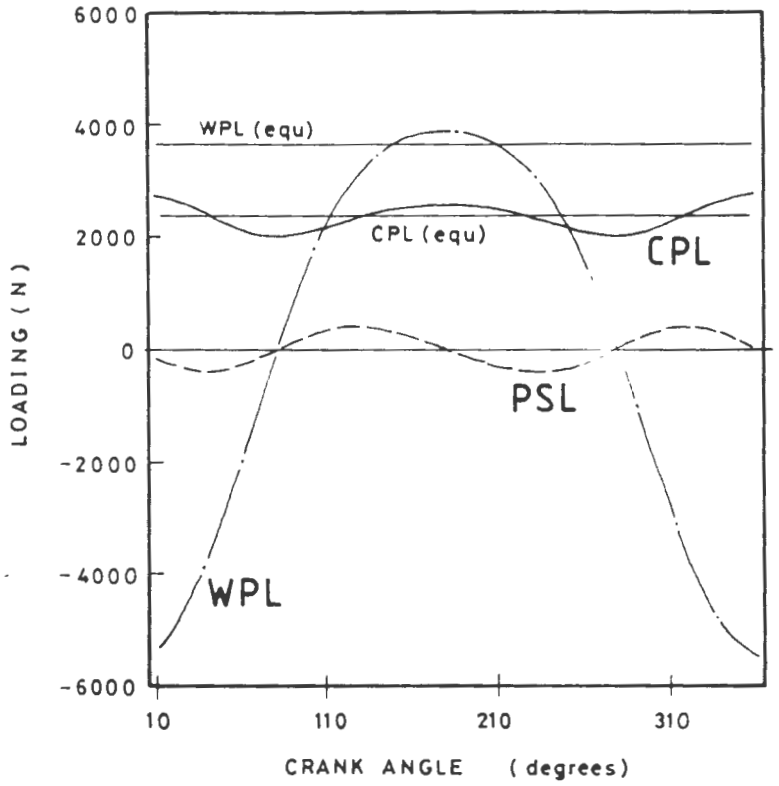

Fig. E2 CRANK SLIDER FORCE ANALYSIS
(6366 rpm or 10 m/s peak velocity)

The literature [49] recommends $1/6 < \Gamma < 1/4$. To retain a shallow angle ϕ so that the PSL is small yet minimize shank weight, a ratio of 1/6 was selected for Γ. Given that a stroke length of 30 mm is required, R and L are therefore equal to 15 mm and 90 mm respectively.

It is also usual to consider the connecting rod to be a reciprocating mass, connected to a rotating mass by a shank of zero mass. The actual mass of the shank is proportioned such that a third contributes to the small end and two thirds adds to the rotating mass at the crankpin [51].

The net reciprocating and rotating masses are 627 gms and 352 gms respectively. For the force analysis, these figures were inflated by approximately 10% and the mass acting at the crankpin was split into two components, thus:

- reciprocating mass at wristpin = 0.7 kg
- reciprocating mass at crankpin = 0.1 kg
- rotating mass at crankpin = 0.3 kg

Referring back to fig. E2 shows that the WPL fluctuates between +3.9 kN and -5.4 kN with every revolution and the CPL oscillates between 2 kN and 2.8 kN. To balance the primary forces, a counterweight of mass equal to that of the rotating mass is bolted to the driveshaft opposite the crankpin on a shared diametrical axis (item 74). 431 stainless steel was specified for the conrod, as it represents the best compromise between corrosion resistance and high strength. Figure E3 below indicates potential failure across areas A_1 and A_2 and shear failure across area A_3. As the later represents the limiting case, calculations are presented for the safety factor (SF) for failure in shear across area A_3.

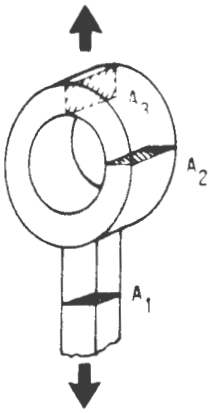

Area A_3 $[16 * 4 - \frac{1}{2}(\pi/4 \times 6^2)]E\text{-}6 = 50E\text{-}6\ m^2$

Mean and alternating loads :

$F_{mean} = \frac{1}{2}(+3.9+(-5.4)) = -0.75$ kN

$F_{alternating} = \pm 4.65$ kN

Converting these into shear stresses :

$\Upsilon_{mean} = 15$ MPa

$\Upsilon_{alternating} = 93$ MPa

Fig. E3 LOADING OF CONROD

for 431, ultimate tensile strength, $S_u = 900$ MPa
The following calculations are all based on ref. [50], which by the distortion energy theory, gives the endurance limit in shear as:

$$S^*_{SE} = 0.577 * 0.5 * S_u = 260 \text{ MPa}$$

This S^*_{SE} is multiplied by two correction factors:

k_a = correction for surface finish = 0.75 for machined components

k_b = reliability factor = 0.72 for 99.999% reliability

The actual endurance limit in shear is thus:

$$S_{sE} = k_a\ k_b\ S^*_{sE} = 0.75 * 0.72 * 260 = 140 \text{ MPa}$$

The fatigue failure line in shear can now be calculated from

$$\Upsilon_a/S_{sE} + \Upsilon_m/S_{su} = 1/FS$$

$$FS = (93/140 + 15/(0.577*900))^{-1} = 1.44$$

This safety factor is relatively low, but because the wristend bearing (comprising of an inner and outer race) is press fitted into the wristend eye of the conrod, the actual area across which shear must occur is in fact greater by 60% (considering only the outer race of the bearing). Recalculating the safety factor for this larger area, yields an acceptable SF = 2.5.

Considering failure to occur by tension, safety factors for areas A_1 and A_2 are 4.0 and 2.5 (respectively excluding the outer race!).

B. BEARINGS

Instantaneous speeds of the bearings at crankpin and wristpin change from minimum to maximum and back with each revolution. As it is impossible to keep rapidly accelerating rollers under load, slippage and therefore heat generation results. Thus smaller diameter rollers with lower inertia are preferred, but a compromise must be made with the lower load carrying capacity of these smaller rollers.

Actual speed variations for the chosen conrod fluctuate between 5305 rpm and 7427 rpm. Taking cognizance of this and using equivalent loads for WPL and CPL of 3.6 kN and 2.4 kN respectively (refer back to fig. E2) the following bearings were selected:

Table B1

BEARING	WRISTEND	CRANKEND
Type	FAG DNKJ 10/16A	FAG DNK26/16A
Max Speed	16 000 rpm	9 500 rpm
Dynamic Load Rating	10 kN	13.5 kN

Using a 1% fracture probability, these bearings guarantee a minimum life of 150 hours, corresponding to 4355 km of sliding distance of the reciprocating assembly. This is equivalent to 180 tests over 24 km each at 6366 rpm.

The size of bearings selected for the driveshaft was influenced by the minimum diameter required for the crankpin holding plate. The smallest feasible diameter for the driveshaft bearings was therefore determined to be 30 mm. This guarantees a minimum service life of 500 hours for these bearings.

C. CRANKPIN AND WRISTPIN

Both pins are manufactured from 431 stainless steel with safety factors exceeding SF = 3 for the diameters choosen.

D. SHUTTLE ASSEMBLY BALL BUSHINGS

The maximum load which can be applied to the shuttle top is 100 N. Each of the four linear ball bushings therefore carries a radial load of 25N.

The smallest available stainless steel ball bushings were selected. They are rated for a dynamic radial load not exceeding 250 N. Several correction factors needed to be applied to this rating, however, as the proposed operating conditions are exceptionally severe:

- short stroke correction factor, f_w = 0.83 for a 30 mm stroke
- lubrication loss factor, f_o = 0.6 for dry conditions/water lubrication
- velocity factor, f_r = 0.6 for velocities > 5 m/s
- hardness factor, f_H = 0.7 for a guide shaft of R_c 58
- temperature factor, f_t = 1.0 for temperatures < 150°C

The actually usable dynamic rating is thus only

$$C_{actual} = C_{rated} \times f_w \times f_o \times f_r = 250 \times 0.83 \times 0.6 \times 0.6 = 75 \text{ N}$$

A life factor, f_L can be calculated next.

$$f_L = F/(f_H \times f_t \times C_{actual}) = 25/(0.7 \times 1 \times 75) = 0.476$$

This life factor yields a minimum travel distance of 960 km or 40 tests at maximum load, speed and test distance, before ball bushings deteriorate noticeably. These calculations are based on information supplied by the manufacturers of the ball bushings used [52].

E. LOAD SPRING

BS 2056 (1983) - stainless steel wire for mechanical springs suggests three suitable materials:

- o precipitation hardened S/S - very expensive
- o martensitic S/S - hardenable by heat treatment but poor corrosion resistance
- o austensitic S/S - non-hardenable but excellent toughness and corrosion resistance

A 316 S/S with an ultimate tensile strength, S_u of 800 MPa and torsional shear modulus, G of 80 GPa was therefore selected.

desired parameters : deflection, y = 20 mm
spring index, C = 8
free length, L_f = as small as possible
diameter, D = as small as possible
maximum load, F = 100 N

Final parameters : coil diameter, d = 2.5 mm
diameter, D = 20 mm
windings, N = 10 turns
free length, L_f = 45 mm
solid length, L_s = 25 mm

Figure E4 below shows the calibration curve for the spring manufactured according to the above specifications. Hysteresis is minimal and a linear graph giving a maximum of 100 N for 17 mm of compression is obtained.

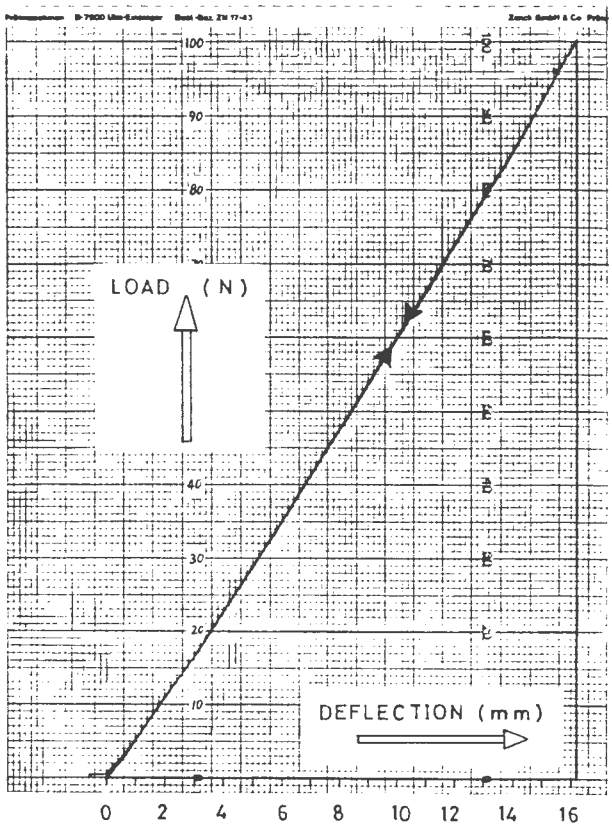

Fig. E4 LOAD/DEFLECTION GRAPH FOR SPRING

F. PISTON SHAFT (Item 67)

A shaft diameter of 10 mm was choosen for this item as this permits an M5 threaded hole to be tapped into the end securing this shaft to the shuttle (refer to sub assembly drawing no. 1 and 2). Provided that this thread is engaged to a depth, h of 12 mm a safety factor of 2.5 guards against fatigue failure by thread shearing.

for 431 stainless steel S_u = 900 MPa
from distortion energy theory (ref. [50]), endurance limit in shear is corrected as follows:

$$S_{sE} = k_a\ k_b\ k_c\ k_d\ k_e\ k_f \times 0.5 \times 0.577 \times S_u$$

where
k_a = 0.75 for machined components
k_b = 0.85 for diameters < 50 mm
k_c = 0.62 for 99.9999% reliability
k_d = 1.0 for temperature < 150°C
k_e = 0.8 for threads
k_f = 0.8 for corrosive environments

thus S_{sE} = 65 MPa

from section A : $F_a = \pm 4.65$ kN and $F_m = -0.75$ kN

therefore $\Upsilon_a = F_a/(\pi dh) = 4.65E3/(\pi * 5E\text{-}3 * 12E\text{-}3) = \pm 25$ MPa
and $\Upsilon_m = 4$ MPa

thus factor of safety guarding against fatigue by shear is

$$FS = (\Upsilon_a/S_{sE} + \Upsilon_m/S_{su})^{-1} = (25/65 + 4/520)^{-1} = 2.5$$

G. <u>RECIPROCATING PISTON</u> (item 68)

The dimensions of this piston were influenced by both the wristend of the conrod and minimum shaft diameter of the piston shaft. The most susceptible area for fatigue failure is the threaded hole into which the piston shaft is screwed.

Aluminium alloy 7017 was choosen for this piston in an effort to minimize the reciprocating mass. A penalty is however paid for this in that the strength of 7017 is inferior to the stainless steel previously used and the tolerable fatigue stress is much lower.

The allowable fatigue stress in shear for this alloy is approximately 100 MPa. This figure is based on a fatigue life of 50 x 10^6 cycles, which would correspond to some 3000 km of sliding distance for the reciprocating assembly under maximum operating conditions.

The screwed hole is threaded to M10 and the depth of thread engagement, h = 12 mm. Thus

$\Upsilon_a = 4.65E3/(\pi * 10E\text{-}3 * 12E\text{-}3) = 12$ MPa and $\Upsilon_m = 2$ MPa

The allowable fatigue stress is corrected by six factors as outlined in Section F.

i.e. $k_a = 0.75$, $k_b = 0.85$, $k_c = 0.62$, $k_d = 1.0$, $k_e = 0.8$, $k_f = 1.0$

thus usable fatigue stress = 0.75 * 0.85 * 0.62 * 1.0 * 0.8 * 1.0 * 100 MPa

= 31 MPa

and $FS = (\Upsilon_a / (\text{usable fatigue stress}) + \Upsilon_m / S_{su})^{-1}$
$= (12/31 + 2/240)^{-1} = 2.5$

H. GUIDE SHAFTS (item 29)

Assuming that each of these two shafts carries half of the applied load (i.e. 50 N) and that this force is a point load, maximum deflection will occur at mid span.

$\delta_{max} = Fl^3/(48EI)$ and $I = \pi d^4/64$ for a circular shaft

thus δ_{max} = 64 * 50 x (110E-3)^3/(48 x 210E9 x (12E-3)^4) = 6.5 μm

where E = Youngs Modulus = 210 GPa
l = span length = 110 mm
d = shaft diameter = 12 mm
F = applied load = 50 N

It is emphasized that these are highly simplified assumptions and that the resultant deflection is probably too conservative. In spite of this, the deflection quoted is extremely small.

I. GUIDE SHAFT (Item 14)

Using the same approach as for the previous section, a maximum deflection of 4.1 μm is calculated for these shafts at midspan under maximum load conditions.

Because most of the remaining components are not dynamically loaded, the consequences if they should fail are not critical. No further calculations are therefore presented.

It is also noted that in all cases generous safety factors have been applied and most components are designed with rigidity in mind. Quoting safety factors is thus relatively meaningless.

APPENDIX F - PARTS DRAWINGS

PARTS LIST

ITEM NO	DESCRIPTION	MATERIAL	NO. OFF	DWG REF	REMARKS	CONTRACTED TO/SUPPLIER	PART NO.
1	SCREW CAP	P-BRONZE (SERIES 0.04-hard)	1	16		MICHELONIE	
2	NEEDLE ROLLER BEARING-LOAD PLUNGER		1	-		WOOD (FAG)	(DNK7/10TN
3	LOAD PLUNGER	316 S/S	1	17			
4	PIN	316 S/S	1	42			
5	LOAD SPRING	316 S/S	1	18		HESPER ENG	
6	POINTER	P-BRONZE 0.04	1	17			
7	UPPER BASE PLATE	316 S/S	1	7			
8	UPPER BASE PLATE LEVER	316 S/S	1	29			
9	BALL KNOB	PLASTIC	3	-		WOOD	
10	CONNECTING PLUNGER	316 S/S	1	19			
11	BALL SPRING	316 S/S	2	18		HESPER ENG	
12	FRICTION PLATE	316 S/S	1	20			
13	FRICTION PLATE SHAFT BEARING	FILLED UHMPE	4	33			SOLIDUR DS
14	FRICTION PLATE GUIDE SHAFT	431 S/S	2	25	HARD CHROME AND GRIND		
15	LOAD ASSEMBLY HOUSING	316 S/S	1	8			
16	LEVER BRACKET	P-BRONZE 0.04	1	40			
17	MOULD FINGERS	316 S/S	2	27			
18	LOCATING PINS (3mm)	316 S/S	18	42			
19	BALLS (4mm)	S/S	4	-		WOOD	
20	SPECIMEN HOLDER	316 S/S	1	21	HARD CHROME AND GRIND		
21	STATIONARY SPECIMEN	TEST MATERIAL	1	-			
22	NEEDLE BLOCK	P-BRONZE 0.04	2	39			
23	RECIPROCATING SHUTTLE	ALUMINIUM - 7017	1	22			
24	SUPPORT BRACKET-UPPER ASSEMBLY	ALUMINIUM - 7017	2	23			
25	RATCHET BRACKET	P-BRONZE 0.04	1	23			
26	RESETTING RING	P-BRONZE 0.04	1	40			
27	RECIPROCATING SPECIMEN	TEST MATERIAL	1	-			
28	SPECIMEN MOUNTING PLATE	316 S/S	1	34			
29	SHUTTLE GUIDE SHAFT	440C	2	-	HARDENED & GROUND	WOOD	
30	SUPPORT BRACKET-SHUTTLE ASSEMBLY	ALUMINIUM - 7017	2	24			
31	LINEAR BALL BUSHINGS (& SEALS)	S/S	4	-	WATER REPELLANT GREASE PACKED	WOOD (STAR)	8668-012-30
32	LOWER BASE PLATE	316 S/S	1	9			
33	SPACER RING	P-BRONZE 0.04	1	25			
34	RESETTING RING LEVER	316 S/S	1	29			
35	LATCH RELEASE LEVER	316 S/S	1	29			
36	HINGE PIN	316 S/S	1	25			
37	HINGE MOUNTING BLOCKS	316 S/S	2	26			
38	BEAM LOAD CELL TRANSDUCER	S/S	1	-		L C S	10L/G/20
39	HINGE BUSHING	P-BRONZE 0.04	2	25			
40	LATCHING HOOK	316 S/S	1	27			
41	LATCH SPRING	316 S/S	1	18		HESPER ENG	
42	BACKING DISC	316 S/S	1	6			
43	LATCHING LEVER HINGE MOUNTING	316 S/S	2	24			
44	RETAINING THUMBSCREW	316 S/S	1	27			
45	HINGE PLATE	316 S/S	1	26			
46	UPPER BASE PLATE SUPPORT BLOCK	316 S/S	1	26			
47	GUSSET STAND (LHS & RHS)	U7UM2U (En3 M/S)	#1	10	PAINT		
48	DOUBLE NIPPLE (¼" type E)	BRASS	1	-		IMPOREX (Festo)	3580
49	FEMALE HOSE CONNECTOR (¼")	BRASS	1	-		IMPOREX	2026
50	HOSECLAMP	S/S	1	-		IMPOREX	
51	TUBING (13mm bore)	PLASTIC	-	-	CUT TO SUIT	IMPOREX	
52	STOP BLOCK	316 S/S	2	39			
53	DOUBLE NIPPLE (¼" type E)	BRASS	1	-			3575
54	FEMALE HOSE CONNECTOR (¼")	BRASS	1	-			2023
56	HOSECLAMP	S/S	1	-			
56	TUBING (9mm bore)	PLASTIC	-	-	CUT TO SUIT		
57	CHAMBER O - RING SEAL	NITRILE RUBBER	1	-	OPTIONAL		(RM 2493-5/
58	LATCH PIN	316 S/S	1	29			
59	ENVIRONMENTAL CHAMBER	as may be reqd.	1	-	OPTIONAL		
59a	QUICK RELEASE TOGGLE LATCH	Zn PLATED STEEL	4-8	-		IMPOREX (Festo)	TL1UU A)
59b	GUIDE ROLLERS	431 S/S	4	-			
59c	GUIDE SHAFTS	431 S/S	2	-			
60	PERSPEX BATH	PERSPEX	1	14			
61	PISTON SHAFT SEALING ASSEMBLY-OUTER RING	431 S/S	1	30			
62	PISTON SHAFT SEALING ASSEMBLY-OUTER HOUSING	P-BRONZE 0.04	1	30			
63	PISTON SHAFT SEALING ASSEMBLY-INNER HOUSING	316 S/S	1	30			
64	PISTON SHAFT BACKING O-RING SEAL	NITRILE RUBBER	1	-		GACO	(RMU126-24)
65	PISTON SHAFT SEALING ASSEMBLY O-RING	NITRILE RUBBER	1	-		GACO	(RMU161-16)
66	PISTON SHAFT SEAL	FILLED UHMPE	1	33			SOLIDUR DS
67	RECIPROCATING PISTON SHAFT	431 S/S	1	31	HARD CHROME AND GRIND		
68	RECIPROCATING PISTON	ALUMINIUM - 7017	1	32			
69	PISTON HOUSING	431 S/S	1	11	HARD CHROME AND GRIND		
70	PISTON SEAL	FILLED UHMPE	2	33			SOLIDUR DS
71	NEEDLE ROLLER BEARING - WRIST END	-	1	-		WOOD (FAG)	NKJ10/10A
72	WRIST PIN	431 S/S	1	34			
73	CONNECTING ROD	431 S/S	1	35			
74	COUNTERWEIGHT	BRASS	1	17			
75	NEEDLE ROLLER BEARING - CRANK END	-	1	-		WOOD (FAG)	NK26/10A
76	CRANK PIN END CAP	431 S/S	1	36			
77	CRANK PIN	431 S/S	1	36			
78	CRANK PIN HOLDING PLATE	431 S/S	1	37			
79	DRIVESHAFT	817M4U (En24 M/S)	1	11			
80	DRIVE BELT	FABRIC MIX	1	-			
81	PLUMMERBLOCK	-	2	-		WOOD	HHP NP30
82	PLATFORM	U7UM2U (En3 M/S)	1	12	PAINT		
83	DRIVE PULLEY	U7UM2U (En3 M/S)	1	13	trim down existing pulley		
84	MOTOR MOUNTING BASE	U7UM2U (En3 M/S)	1	41	PAINT		
85	DC MOTOR (& CONTROLLER)	-	1	-	use existing unit	LEC	
86	SPACER	U7UM2U (En3 M/S)	4	41	PAINT		
87	ANTI VIBRATION MOUNTINGS (type C)	RUBBER MIX	4	-		HEMAG	S218 112
88	BRACKET FOR PLUMMER BLOCKS	U7UM2U (En3 M/S)	2	38	PAINT		
89	GRUB SCREW	S/S	1	39			
90	SPECIMEN CHUCK - ADJUSTING JAW	P-BRONZE 0.04	1	39			
91	SPECIMEN CHUCK - FIXED JAW	P-BRONZE 0.04	1	40			
92	BELT DRIVE COVER	U7UM2U (En3 M/S)	1	15	PAINT		
93	TABLE	U7UM2U (En3 M/S)	1	-	use existing unit		
94	LOCATING PIN (6mm)	316 S/S	1	42			
95	LOCATING PIN (10mm)	316 S/S	2	42			
96	BATH SEALING O-RING	NITRILE RUBBER	1	-	CUT TO SUIT	GACO	1796-30
97	LOWER BASE PLATE O-RING SEAL	NITRILE RUBBER	1	-		GACO	1051-16

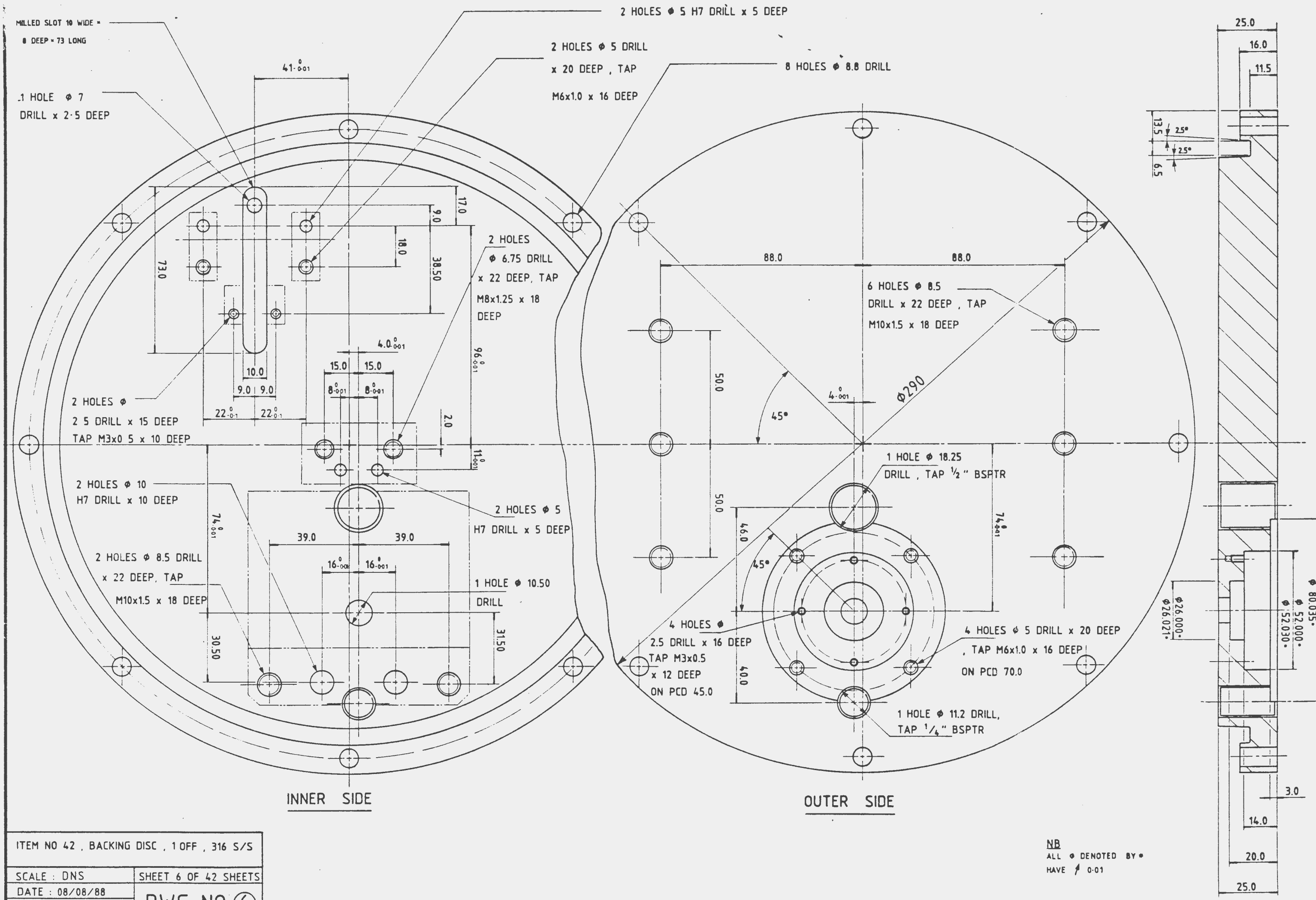

ITEM NO 42 , BACKING DISC , 1 OFF , 316 S/S

SCALE : DNS	SHEET 6 OF 42 SHEETS
DATE : 08/08/88	DWG NO ⑥
DRAWN BY : U KIENLE	

NB
ALL ⌀ DENOTED BY ⌀ HAVE ∮ 0·01

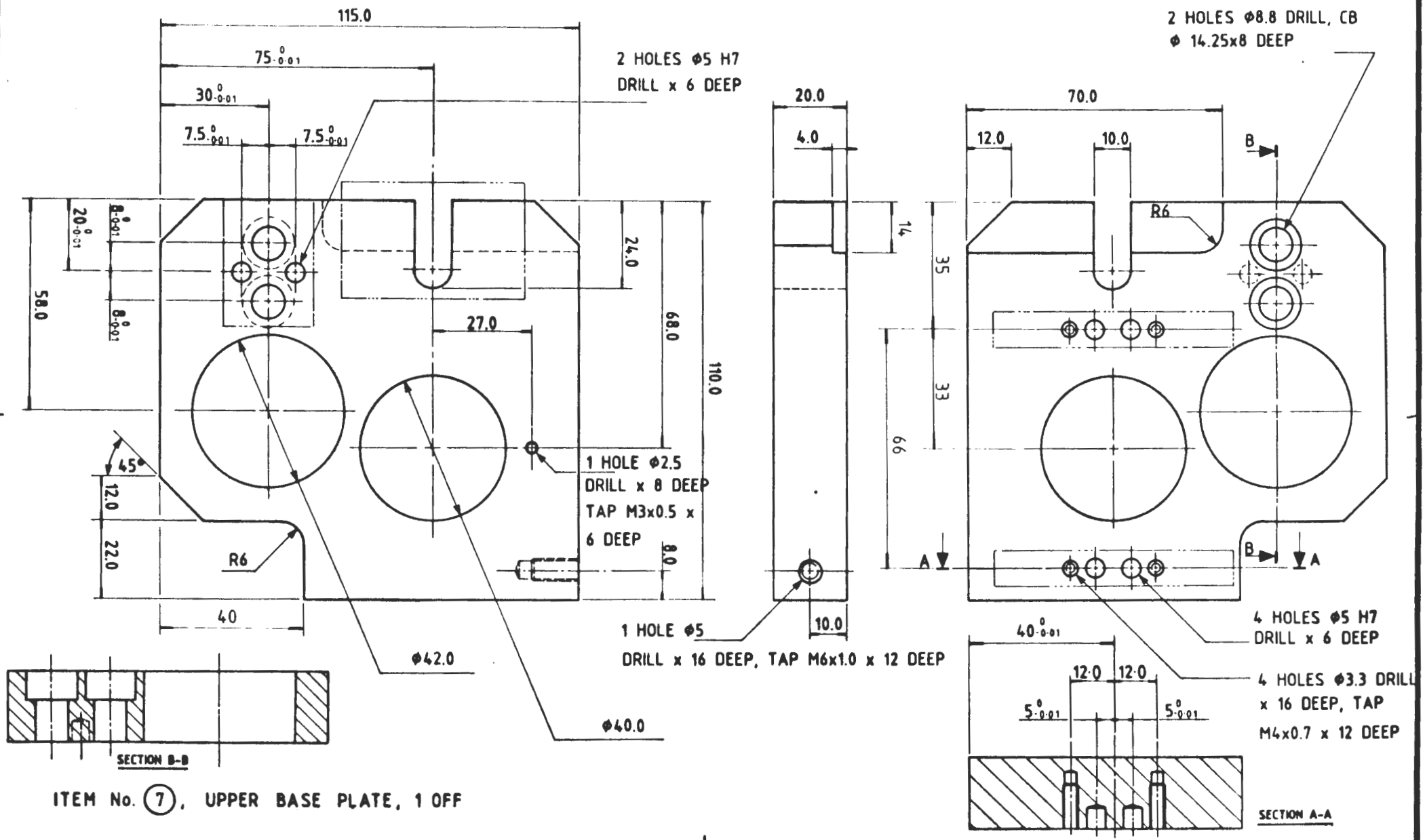

ITEM No. (7), UPPER BASE PLATE, 1 OFF

DEPARTMENT OF MATERIALS ENGINEERING – WORKSHOP					UNIVERSITY OF CAPE TOWN	
TECHNICAL ASSISTANCE REQUESTED BY –	GENERAL ASSEMBLY	DETAIL			WORK CATEGORY M.Sc. THESIS	DATE ACCEPTED
STAFF MEMBER –	SHEET 7 OF 42	SCALE	D.N.S.		WORK ASSIGNED TO	DATE REQUESTED
STUDENT ULRICH F.B. KIENLE	DRAWN BY	ULRICH F.B KIENLE			WORK SUPERVISED BY N. DREEZE	DATE PROMISED
SUPERVISOR PROF A. BALL	MATERIAL SCHEDULE SUPPLIED	YES	NO			DATE COMMENCED

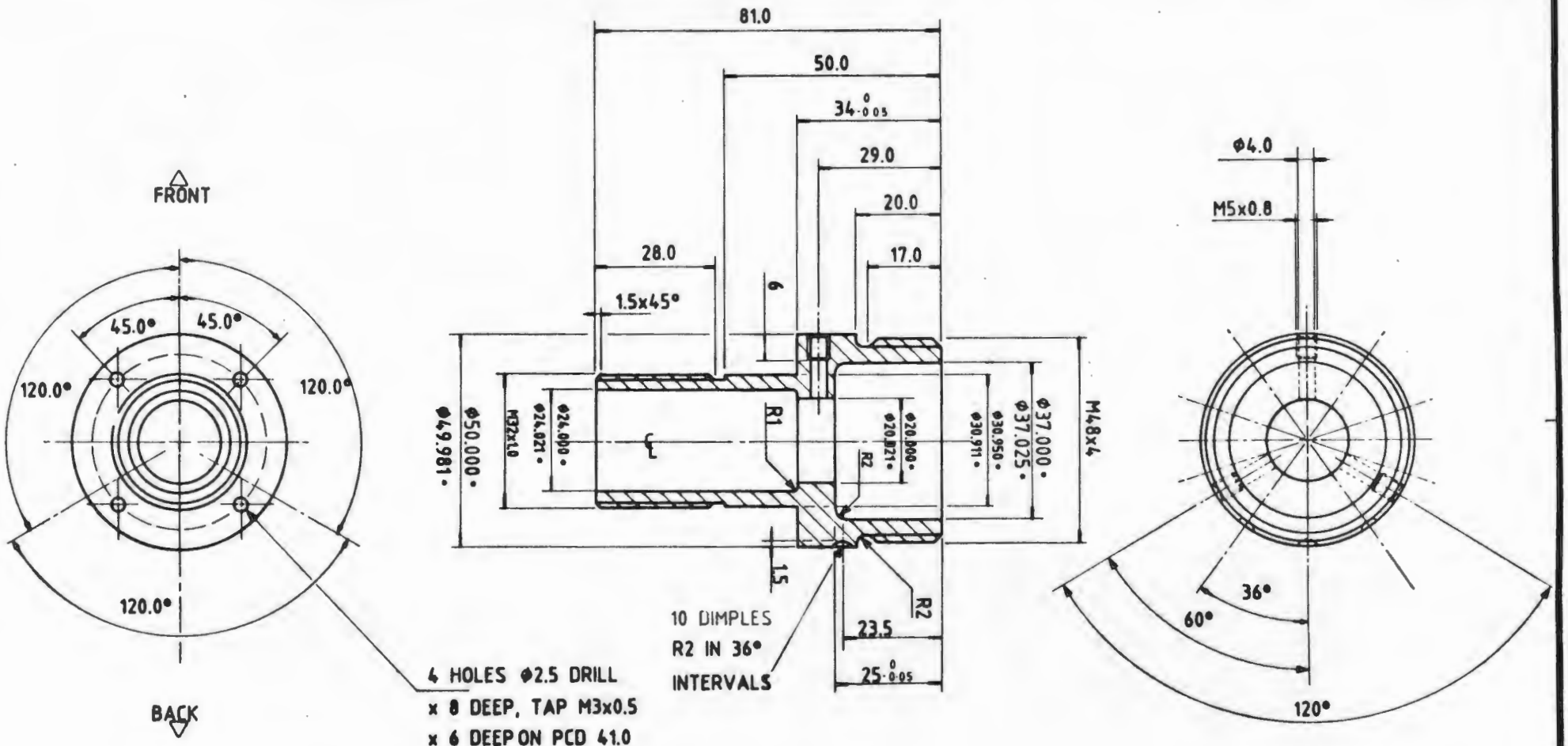

ITEM No. (15), LOAD ASSEMBLY HOUSING, 1 OFF, 316 S/S

NB

ALL ⌀ DENOTED BY ⌀ HAVE ∥ 0·01

DEPARTMENT OF MATERIALS ENGINEERING – WORKSHOP				UNIVERSITY OF CAPE TOWN	
TECHNICAL ASSISTANCE REQUESTED BY –	GENERAL ASSEMBLY	DETAIL		WORK CATEGORY M.Sc. THESIS	DATE ACCEPTED
STAFF MEMBER –	SHEET 8 OF 42	SCALE D.N.S.		WORK ASSIGNED TO	DATE REQUESTED
STUDENT ULRICH F.B. KIENLE	DRAWN BY ULRICH F.B. KIENLE			WORK SUPERVISED BY N. DREEZE	DATE PROMISED
SUPERVISOR PROF A. BALL	MATERIAL SCHEDULE SUPPLIED	YES	NO		DATE COMMENCED

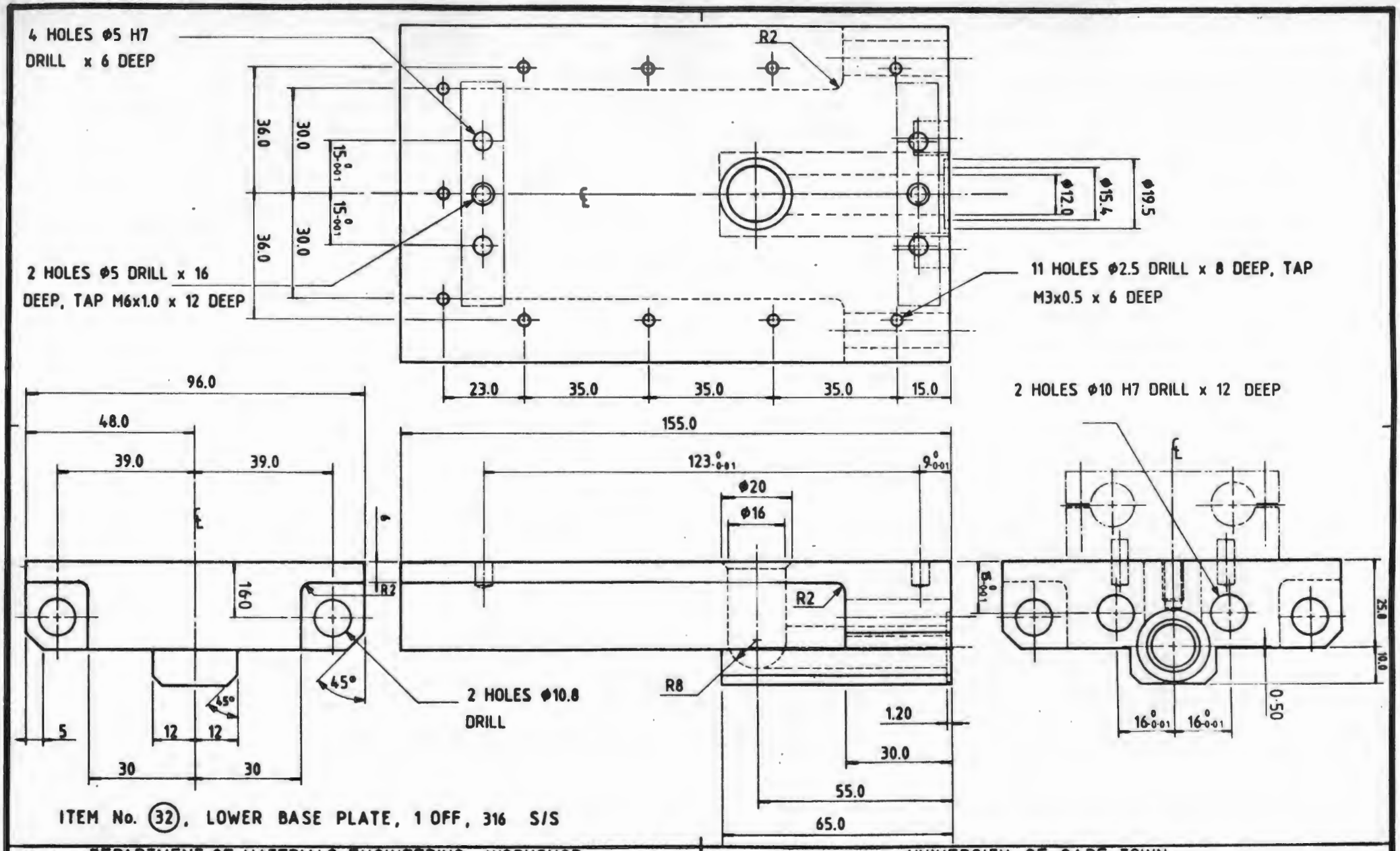

ITEM No. (32), LOWER BASE PLATE, 1 OFF, 316 S/S

DEPARTMENT OF MATERIALS ENGINEERING – WORKSHOP				UNIVERSITY OF CAPE TOWN	
TECHNICAL ASSISTANCE REQUESTED BY –	GENERAL ASSEMBLY	DETAIL		WORK CATEGORY M. Sc. THESIS	DATE ACCEPTED
STAFF MEMBER –	SHEET 9 OF 42	SCALE D.N.S.		WORK ASSIGNED TO	DATE REQUESTED
STUDENT ULRICH F.B. KIENLE	DRAWN BY ULRICH F.B KIENLE			WORK SUPERVISED BY N. DREEZE	DATE PROMISED
SUPERVISOR PROF A. BALL	MATERIAL SCHEDULE SUPPLIED	YES	NO		DATE COMMENCED

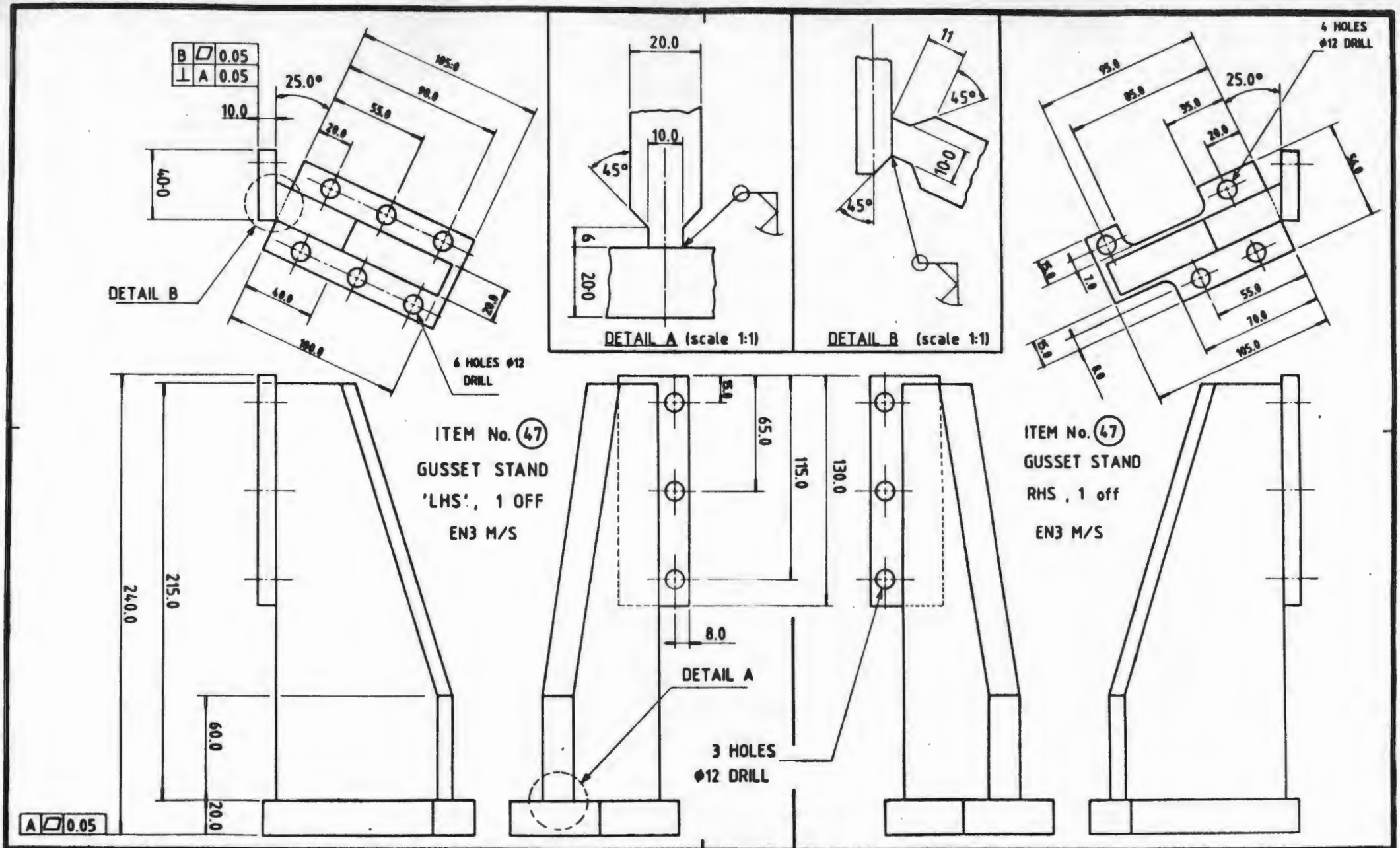

DEPARTMENT OF MATERIALS ENGINEERING – WORKSHOP				UNIVERSITY OF CAPE TOWN	
TECHNICAL ASSISTANCE REQUESTED BY –	GENERAL ASSEMBLY	DETAIL		WORK CATEGORY M.Sc. THESIS	DATE ACCEPTED
STAFF MEMBER –	SHEET 10 OF 42	SCALE D.N.S.		WORK ASSIGNED TO	DATE REQUESTED
STUDENT ULRICH F.B. KIENLE	DRAWN BY ULRICH F.B KIENLE			WORK SUPERVISED BY N. DREEZE	DATE PROMISED
SUPERVISOR PROF A. BALL	MATERIAL SCHEDULE SUPPLIED	YES	NO		DATE COMMENCED

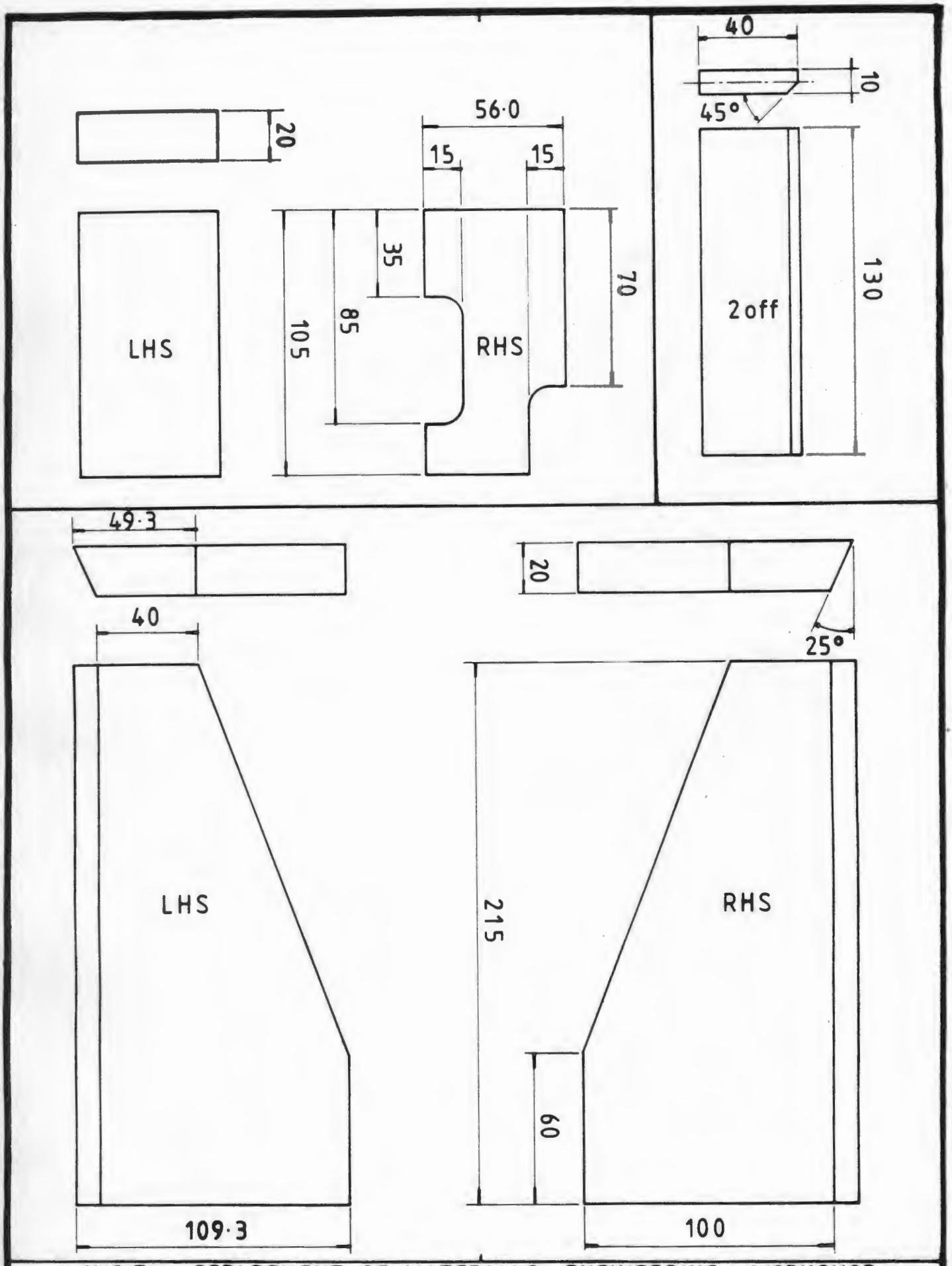

U.C.T. — DEPARTMENT OF MATERIALS ENGINEERING — WORKSHOP			
DRAWN BY U.F.B. KIENLE	WORK CATEGORY M. Sc. THESIS	MATERIAL En 3 M/S	
DATE ACCEPTED	WORK SUPERVISED BY N. DREEZE		
DATE PROMISED	MATERIAL SCHEDULE SUPPLIED	YES	NO
SUPERVISOR PROF A. BALL	SCALE 1 : 2	SHEET 10a OF 42	

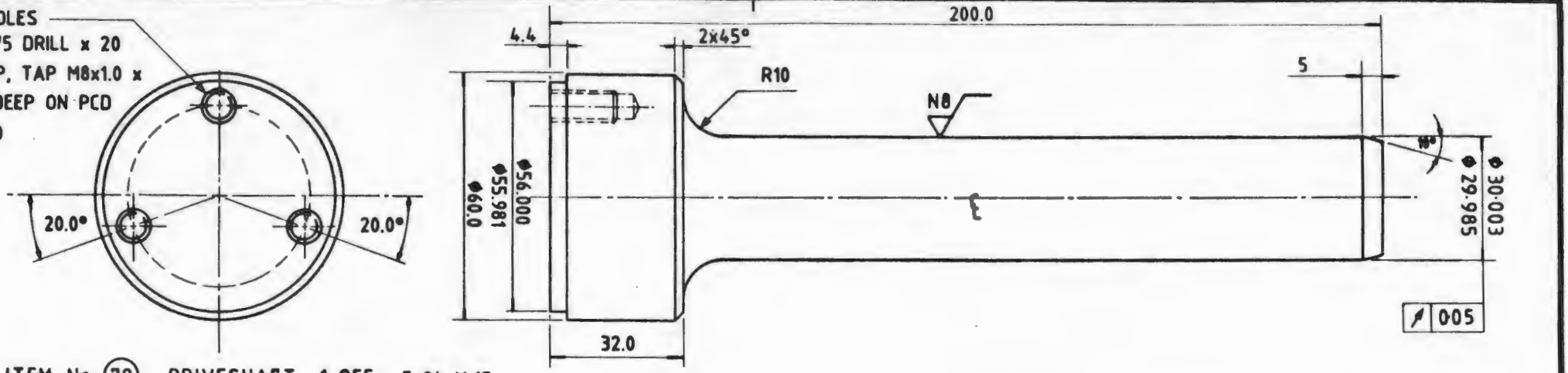

ITEM No. (79), DRIVESHAFT, 1 OFF, En24 M/S

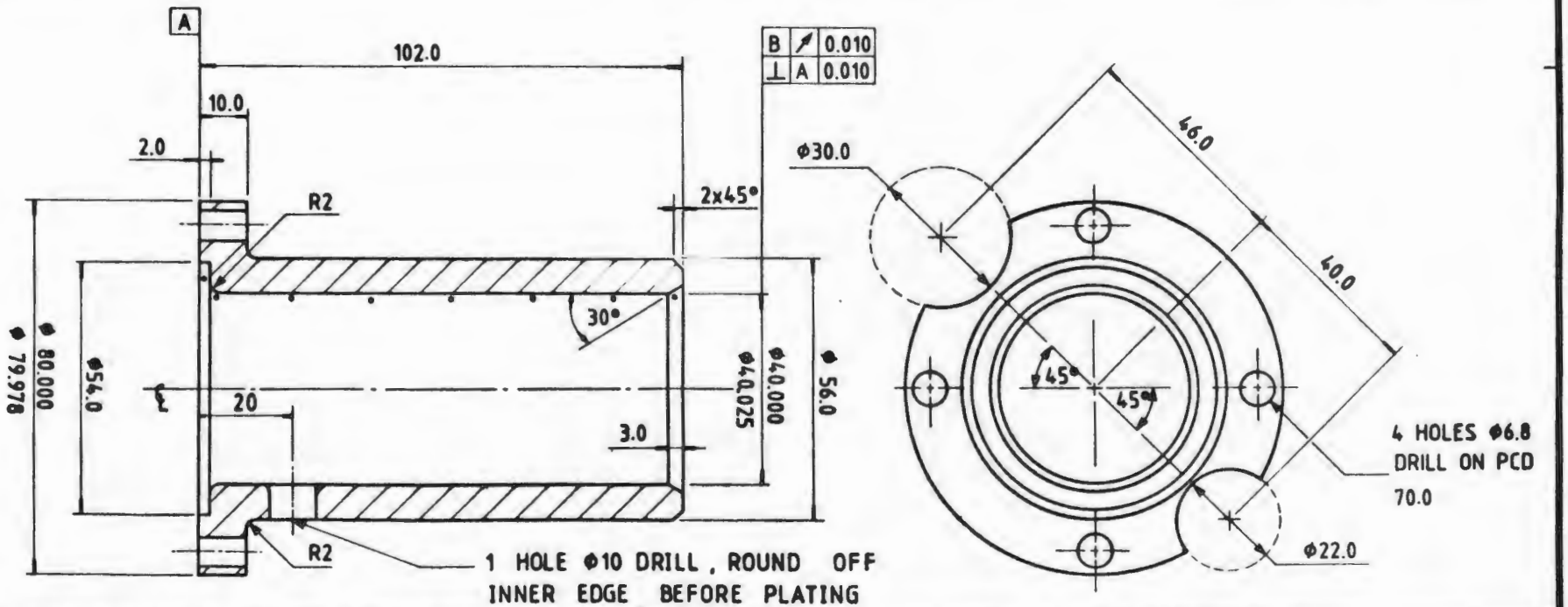

ITEM No. (69)
PISTON HOUSING
1 OFF
431 S/S

NB
- HARD CHROME BORE OF HOUSING AND GRIND TO FINAL ID SIZE SHOWN

DEPARTMENT OF MATERIALS ENGINEERING – WORKSHOP				UNIVERSITY OF CAPE TOWN	
TECHNICAL ASSISTANCE REQUESTED BY –	GENERAL ASSEMBLY	DETAIL		WORK CATEGORY M.Sc. THESIS	DATE ACCEPTED
STAFF MEMBER –	SHEET 11 OF 42	SCALE D.N.S.		WORK ASSIGNED TO	DATE REQUESTED
STUDENT ULRICH F.B. KIENLE	DRAWN BY ULRICH F.B KIENLE			WORK SUPERVISED BY N. DREEZE	DATE PROMISED
SUPERVISOR PROF A. BALL	MATERIAL SCHEDULE SUPPLIED	YES	NO		DATE COMMENCED

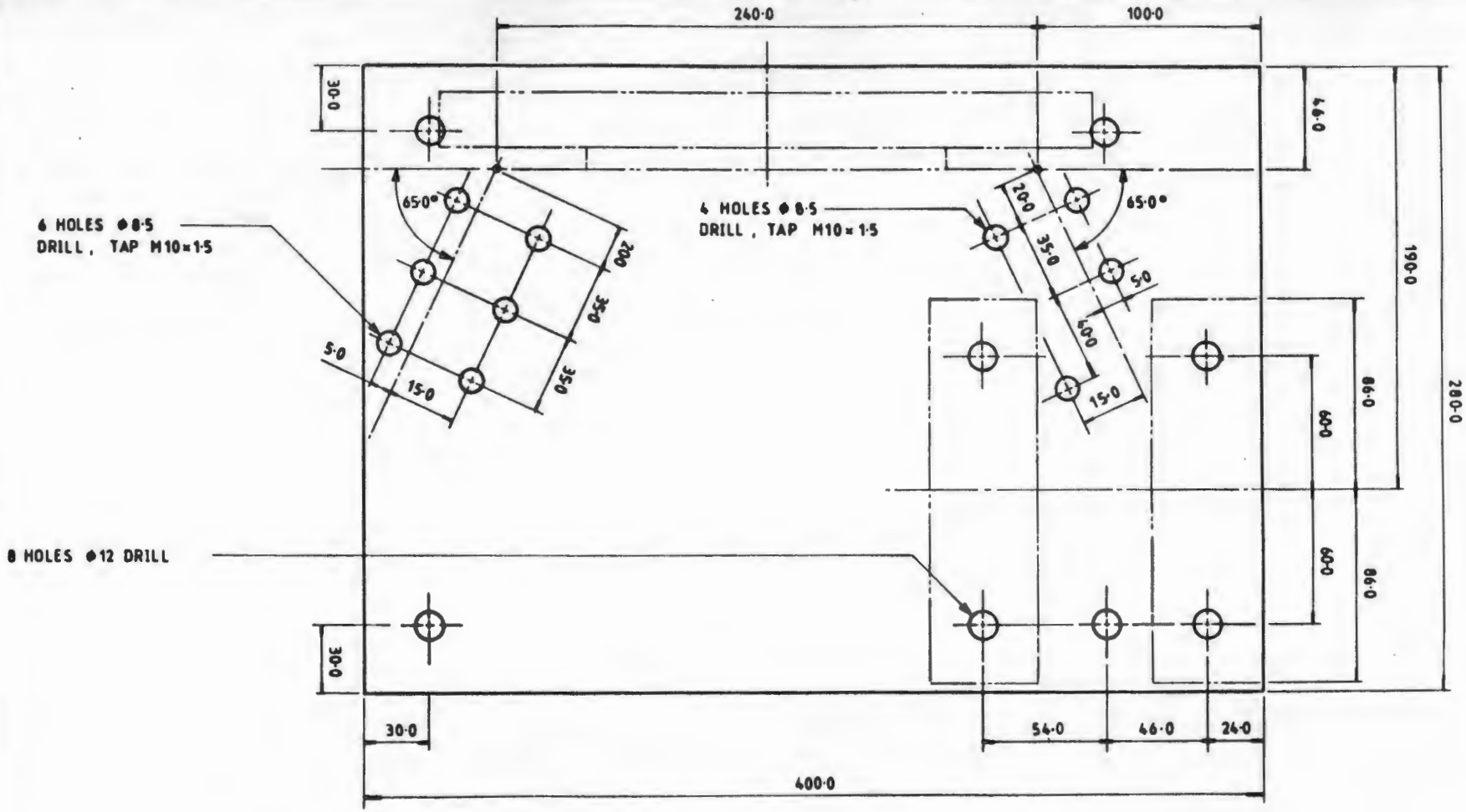

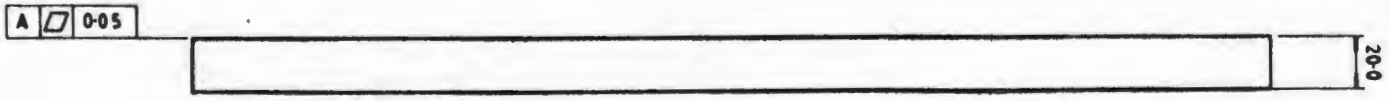

ITEM No. (82), PLATFORM, 1 OFF, En3

DEPARTMENT OF MATERIALS ENGINEERING – WORKSHOP					UNIVERSITY OF CAPE TOWN	
TECHNICAL ASSISTANCE REQUESTED BY –	GENERAL ASSEMBLY	DETAIL			WORK CATEGORY M.Sc. THESIS	DATE ACCEPTED
STAFF MEMBER –	SHEET 12 OF 42	SCALE D.N.S.			WORK ASSIGNED TO	DATE REQUESTED
STUDENT ULRICH F.B. KIENLE	DRAWN BY ULRICH F.B. KIENLE				WORK SUPERVISED BY N. DREEZE	DATE PROMISED
SUPERVISOR PROF A. BALL	MATERIAL SCHEDULE SUPPLIED	YES	NO			DATE COMMENCED

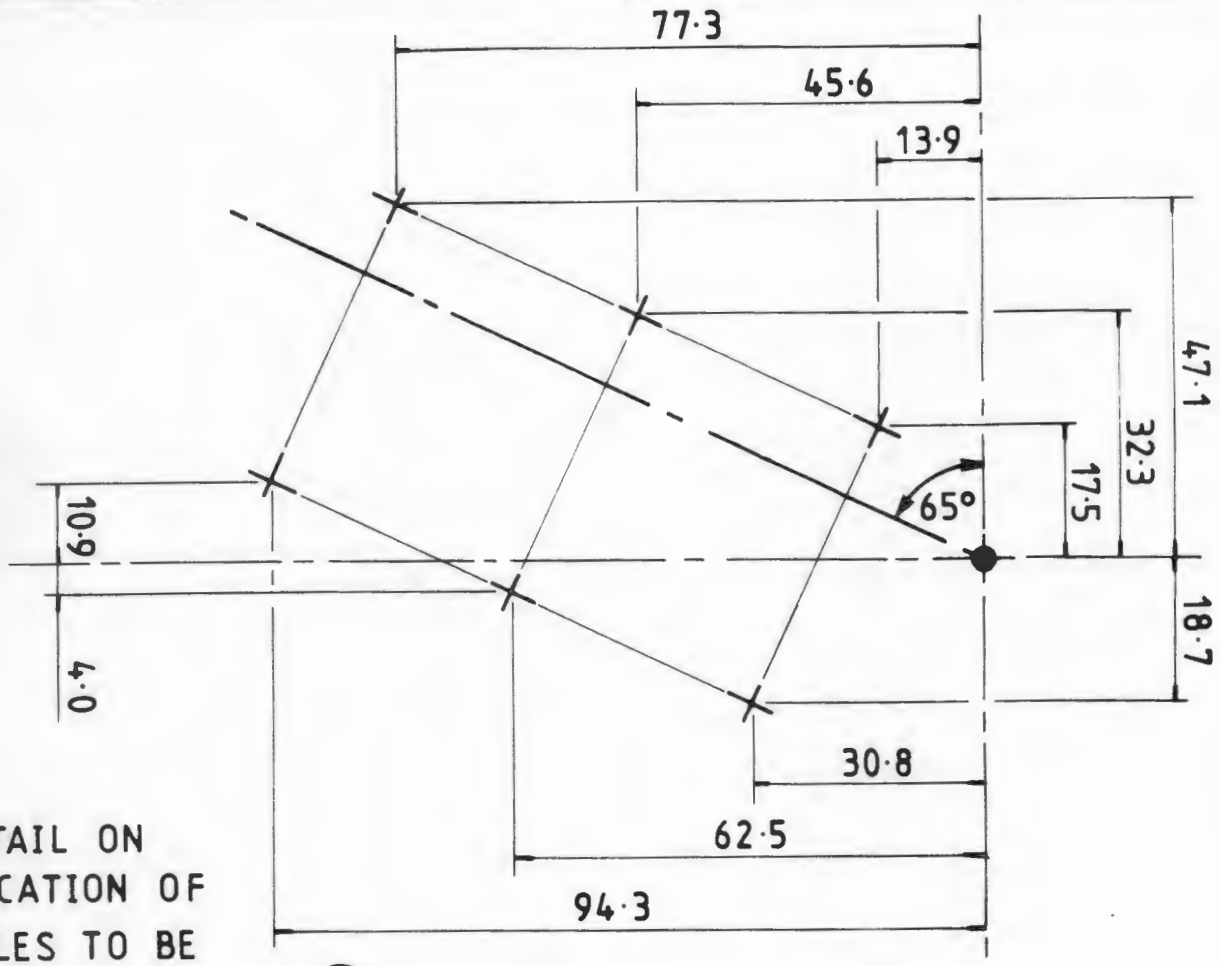

DETAIL ON LOCATION OF HOLES TO BE DRILLED IN ITEM (82)

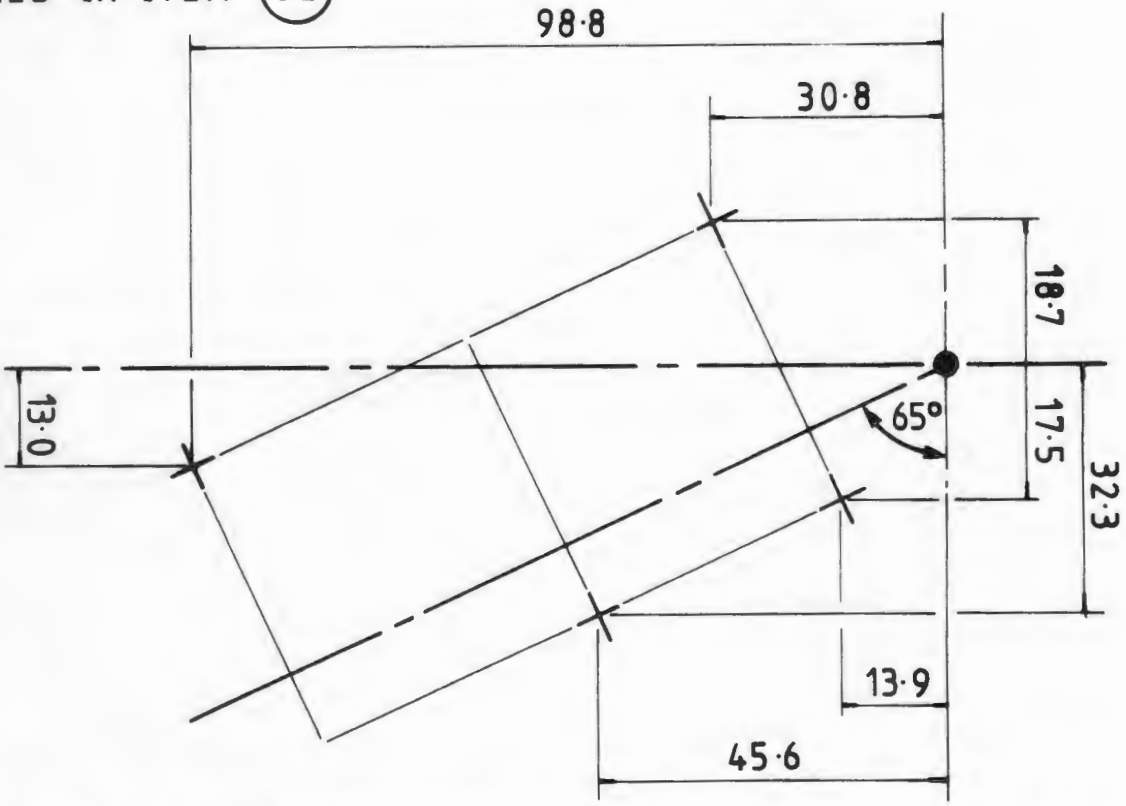

U.C.T. — DEPARTMENT OF MATERIALS ENGINEERING — WORKSHOP			
DRAWN BY U.F.B. KIENLE	WORK CATEGORY M. Sc. THESIS	MATERIAL	
DATE ACCEPTED	WORK SUPERVISED BY N. DREEZE		
DATE PROMISED	MATERIAL SCHEDULE SUPPLIED	YES	NO
SUPERVISOR PROF A. BALL	SCALE 1 : 1	SHEET 12 a OF 42	

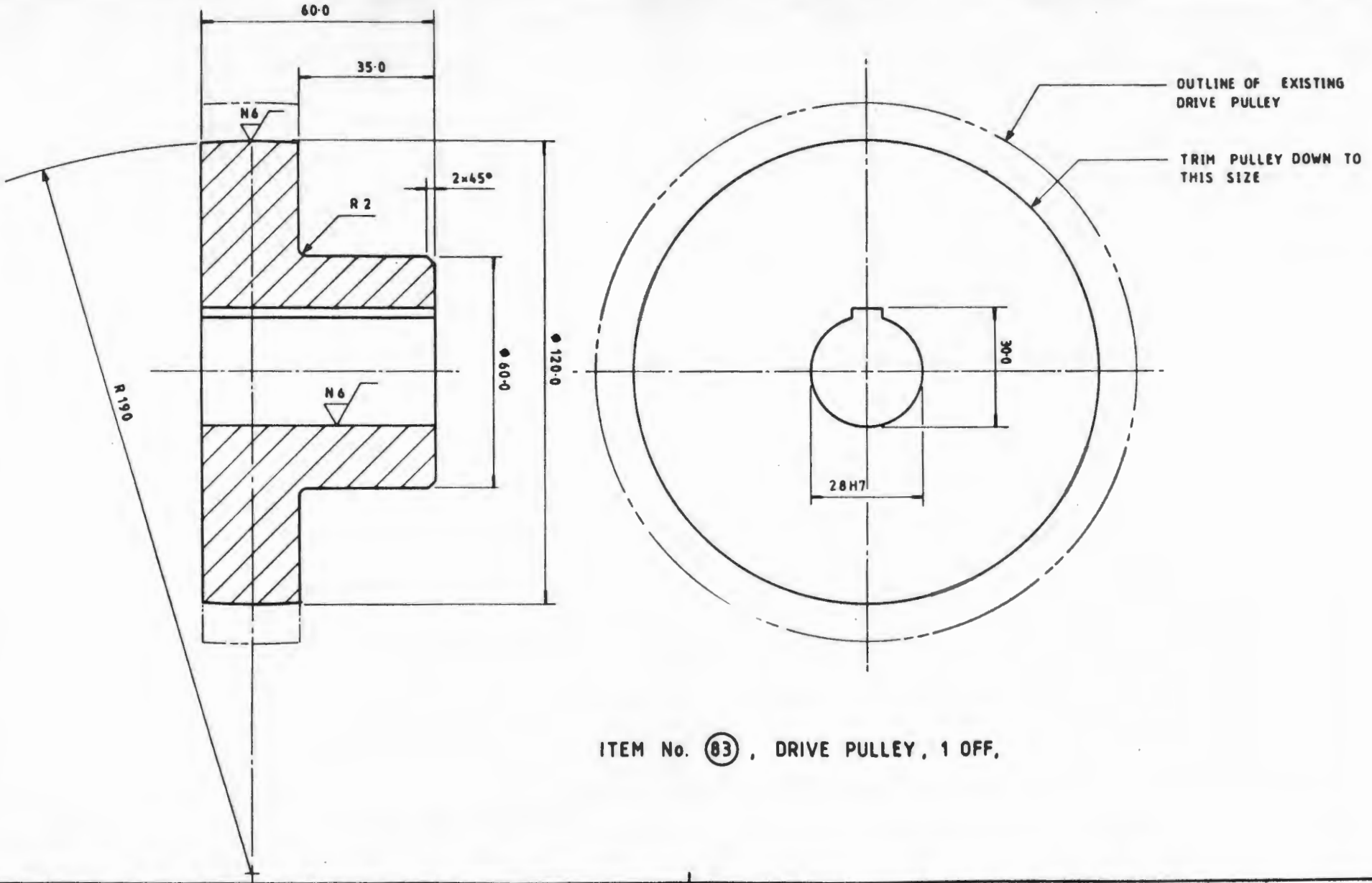

ITEM No. (83), DRIVE PULLEY, 1 OFF.

DEPARTMENT OF MATERIALS ENGINEERING – WORKSHOP					UNIVERSITY OF CAPE TOWN	
TECHNICAL ASSISTANCE REQUESTED BY –	GENERAL ASSEMBLY	DETAIL			WORK CATEGORY M.Sc. THESIS	DATE ACCEPTED
STAFF MEMBER –	SHEET 13 OF 42	SCALE D.N.S.			WORK ASSIGNED TO	DATE REQUESTED
STUDENT ULRICH F.B. KIENLE	DRAWN BY ULRICH F.B KIENLE				WORK SUPERVISED BY N. DREEZE	DATE PROMISED
SUPERVISOR PROF A. BALL	MATERIAL SCHEDULE SUPPLIED	YES	NO			DATE COMMENCED

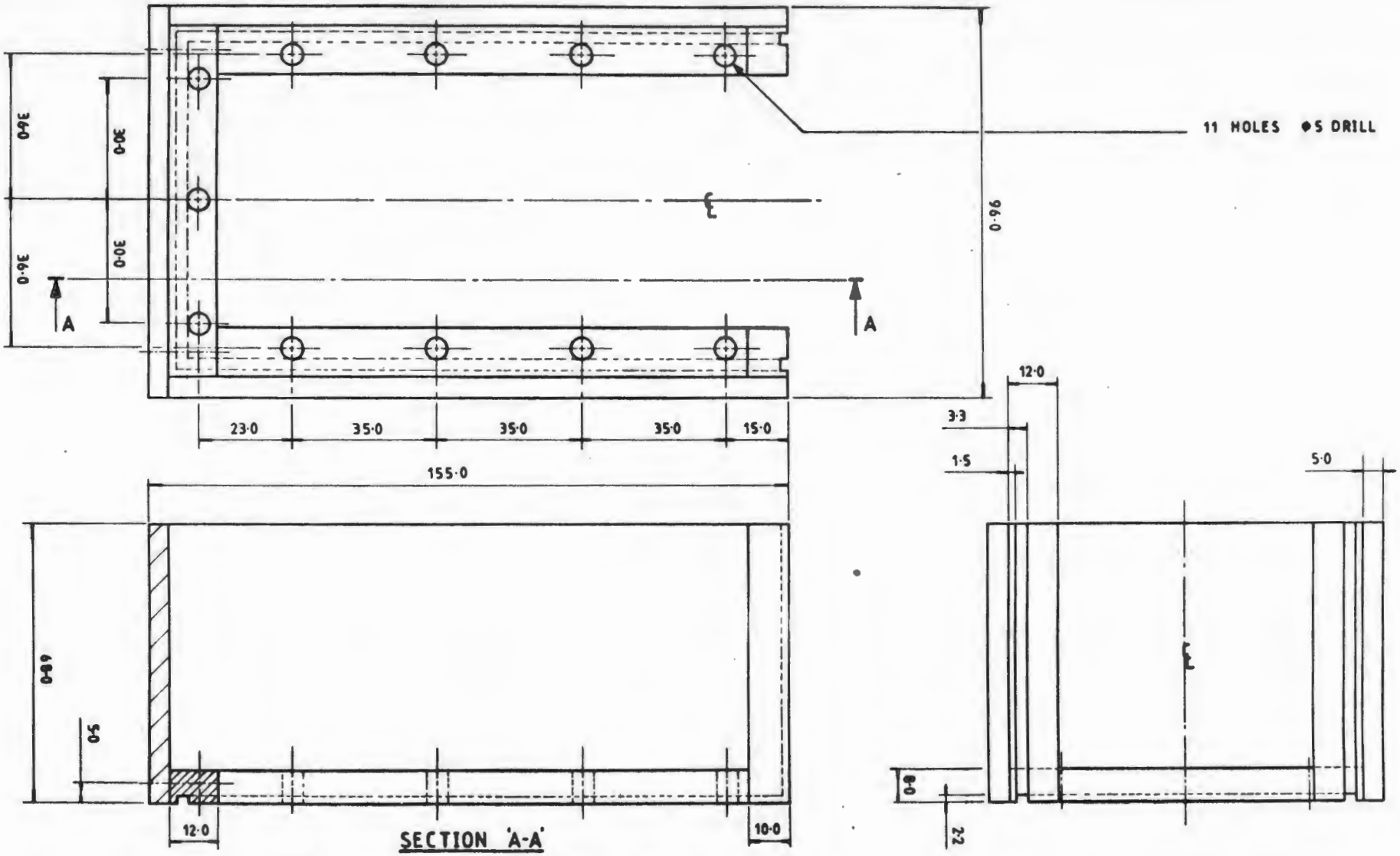

SECTION 'A-A'

ITEM No. (60), PERSPEX BATH, 1 OFF, PERSPEX

DEPARTMENT OF MATERIALS ENGINEERING – WORKSHOP				UNIVERSITY OF CAPE TOWN	
TECHNICAL ASSISTANCE REQUESTED BY –	GENERAL ASSEMBLY	DETAIL		WORK CATEGORY M.Sc. THESIS	DATE ACCEPTED
STAFF MEMBER –	SHEET 14 OF 42	SCALE D.N.S.		WORK ASSIGNED TO	DATE REQUESTED
STUDENT ULRICH F.B. KIENLE	DRAWN BY ULRICH F.B KIENLE			WORK SUPERVISED BY N. DREEZE	DATE PROMISED
SUPERVISOR PROF A. BALL	MATERIAL SCHEDULE SUPPLIED	YES	NO		DATE COMMENCED

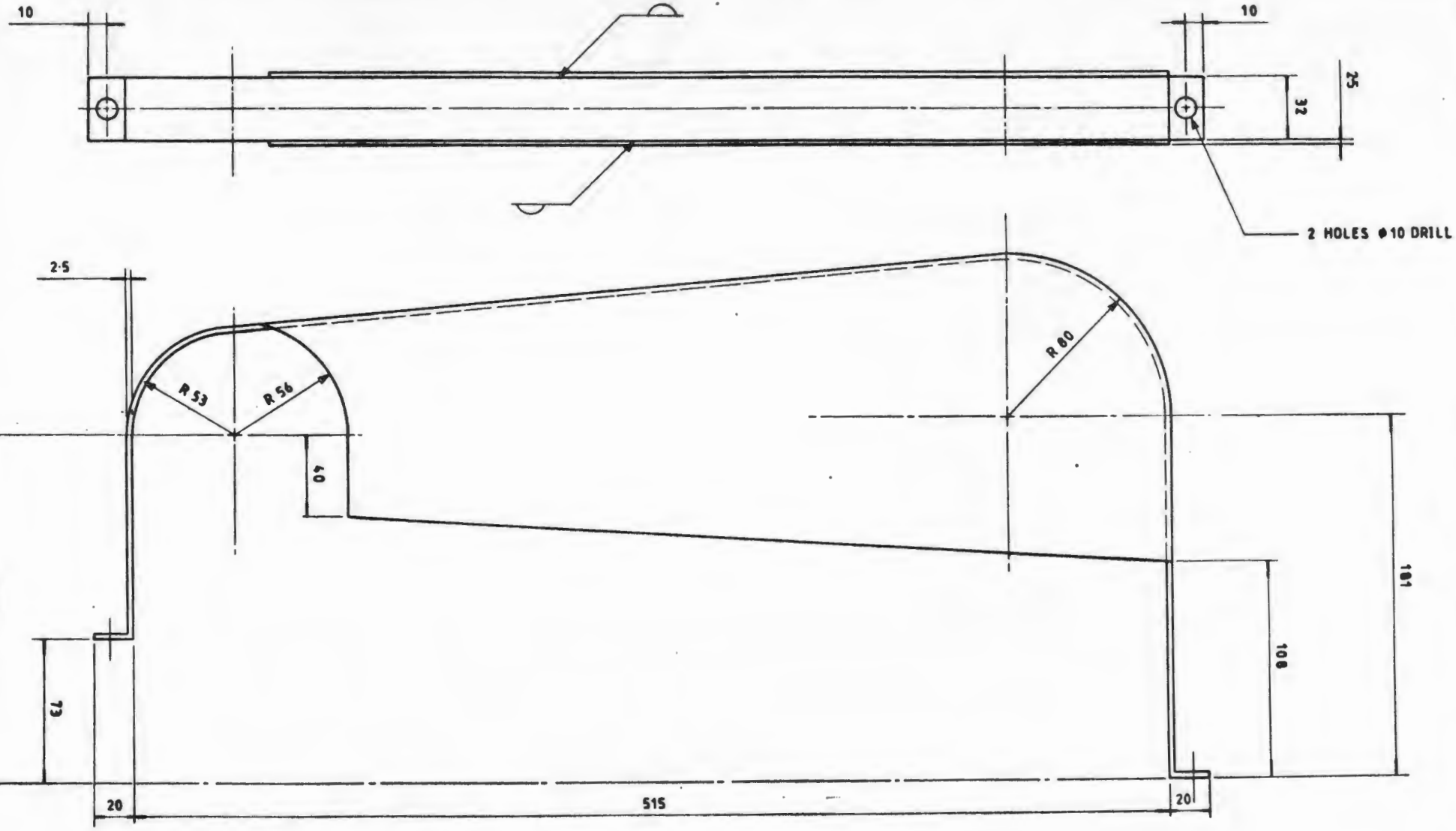

ITEM No. (92) , BELT DRIVE COVER , 1 OFF, En 3 M/S

DEPARTMENT OF MATERIALS ENGINEERING – WORKSHOP				UNIVERSITY OF CAPE TOWN	
TECHNICAL ASSISTANCE REQUESTED BY –	GENERAL ASSEMBLY	DETAIL		WORK CATEGORY M.Sc. THESIS	DATE ACCEPTED
STAFF MEMBER –	SHEET 15 OF 42	SCALE	D.N.S.	WORK ASSIGNED TO	DATE REQUESTED
STUDENT ULRICH F.B. KIENLE	DRAWN BY ULRICH F.B KIENLE			WORK SUPERVISED BY N. DREEZE	DATE PROMISED
SUPERVISOR PROF A. BALL	MATERIAL SCHEDULE SUPPLIED	YES	NO		DATE COMMENCED

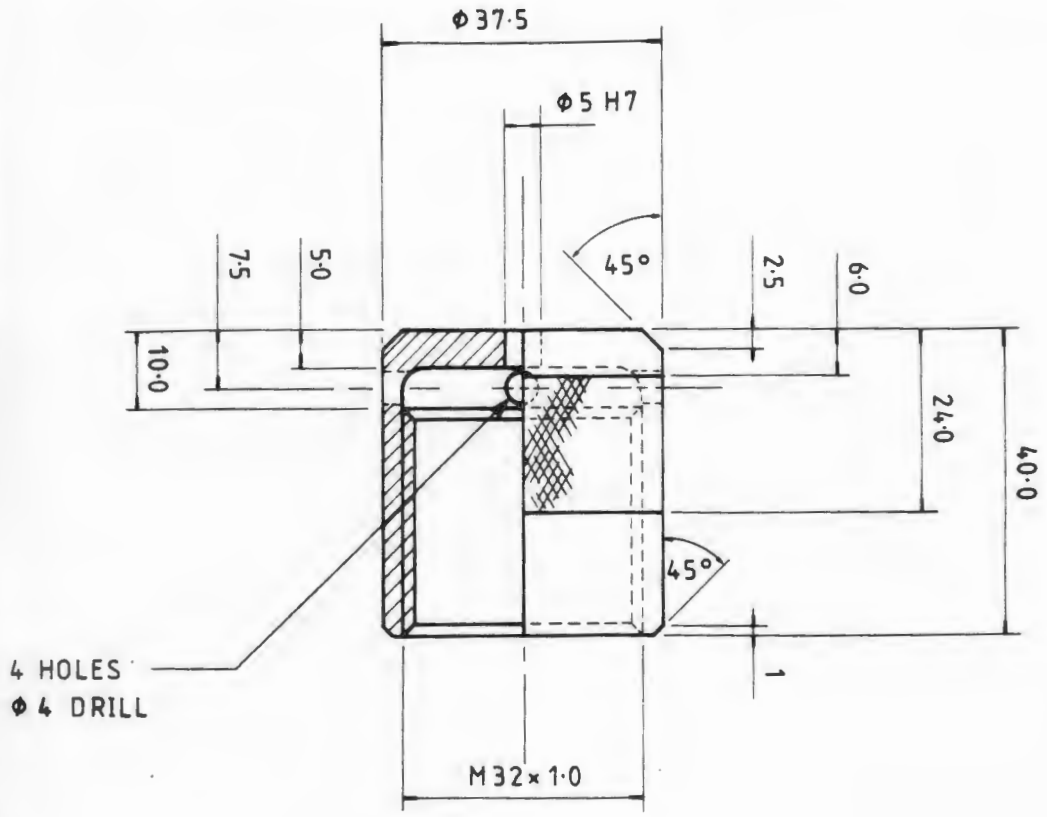

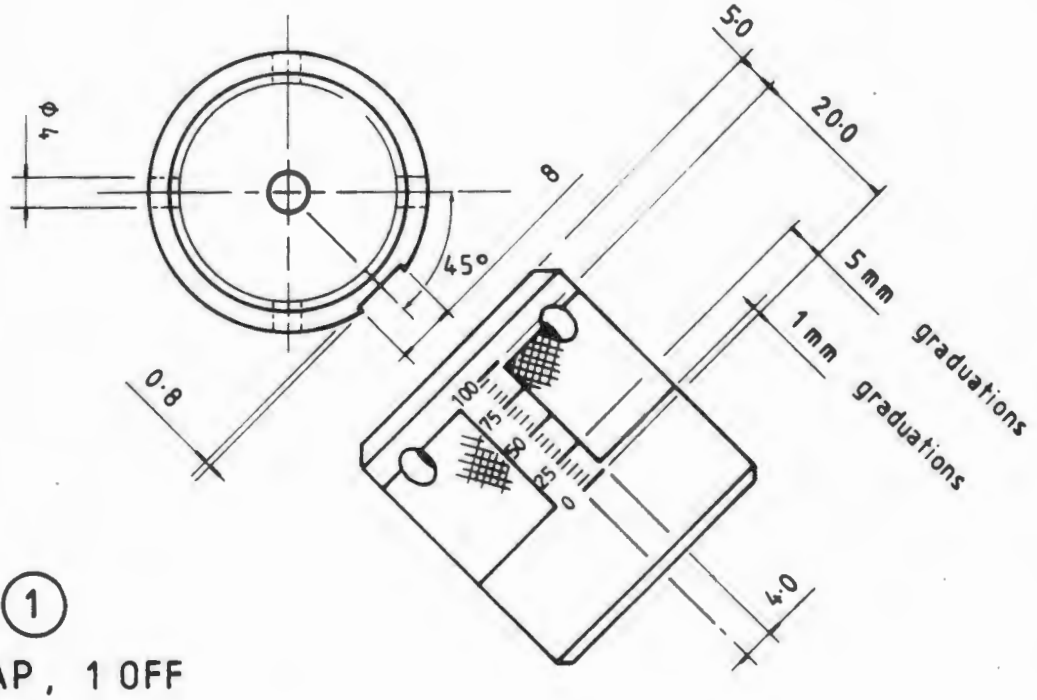

ITEM No. (1)

SCREW CAP, 1 OFF

U.C.T. — DEPARTMENT OF MATERIALS ENGINEERING — WORKSHOP				
DRAWN BY U.F.B. KIENLE	WORK CATEGORY M. Sc. THESIS		MATERIAL	
DATE ACCEPTED	WORK SUPERVISED BY N. DREEZE		P - BRONZE (034)	
DATE PROMISED	MATERIAL SCHEDULE SUPPLIED		YES	NO
SUPERVISOR PROF A. BALL	SCALE 1 : 1	SHEET 16 OF 42		

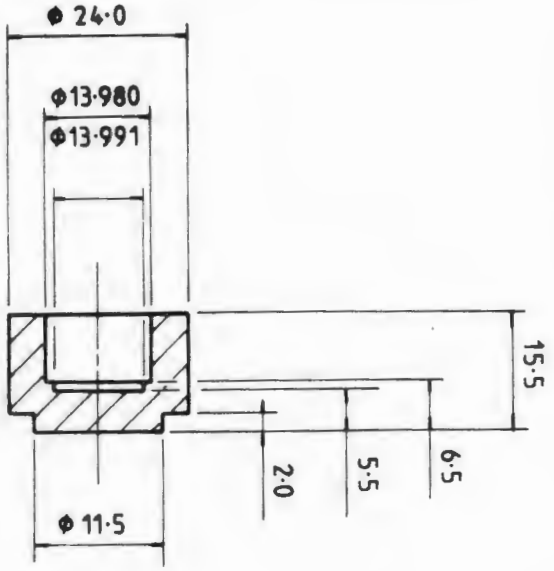

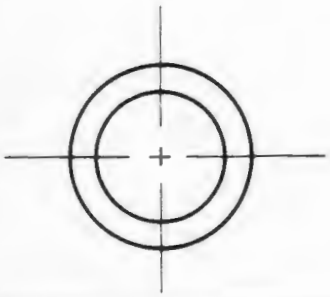

ITEM No. (3)

LOAD PLUNGER

1 OFF

316 S/S

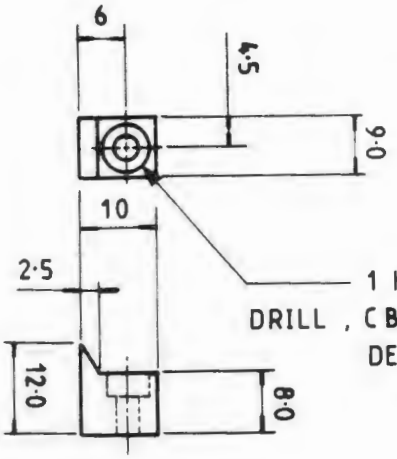

ITEM No. (6)

POINTER , 1 OFF

P - BRONZE (034)

ITEM No. (74)

COUNTERWEIGHT, 1 OFF

BRASS

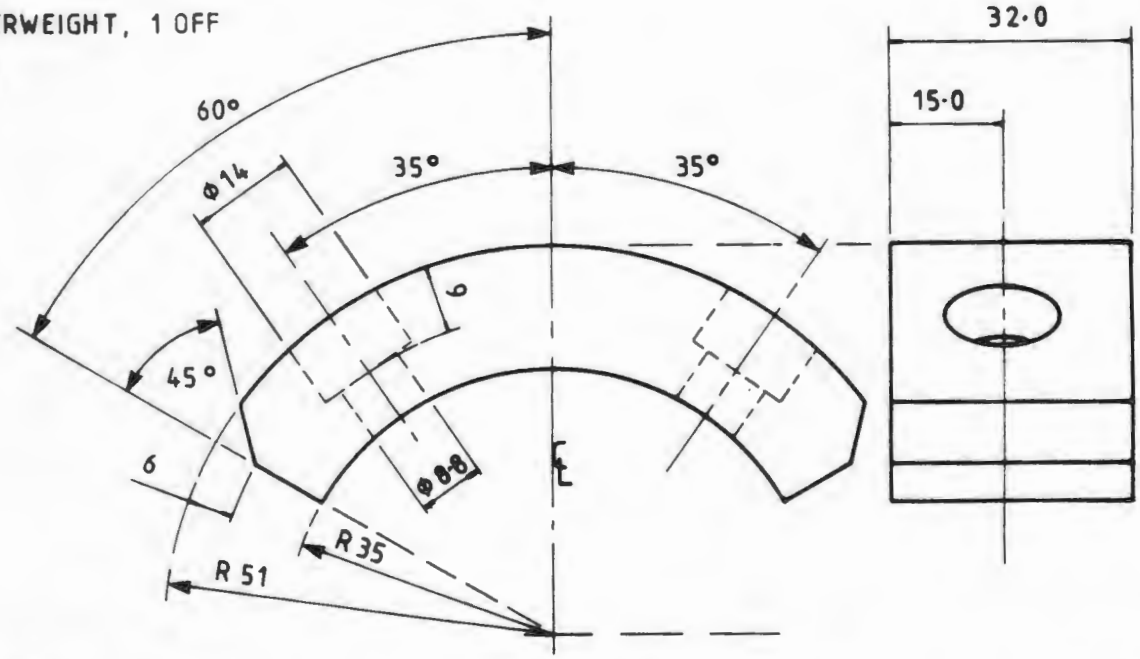

U.C.T. — DEPARTMENT OF MATERIALS ENGINEERING — WORKSHOP				
DRAWN BY U.F.B. KIENLE	WORK CATEGORY M. Sc. THESIS		MATERIAL	
DATE ACCEPTED	WORK SUPERVISED BY N. DREEZE		AS SHOWN	
DATE PROMISED	MATERIAL SCHEDULE SUPPLIED		YES	NO
SUPERVISOR PROF A. BALL	SCALE 1 : 1	SHEET 17	OF 42	

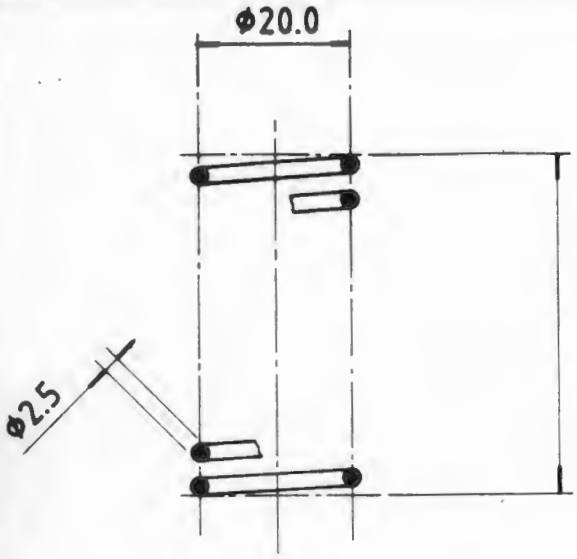

free length (L_f) = 45

solid length (L_s) = 25

deflection (Δ) = 20

spring index (C) = 8

no. of turns (N) = 10

ITEM No. (5)

LOAD SPRING

1 OFF

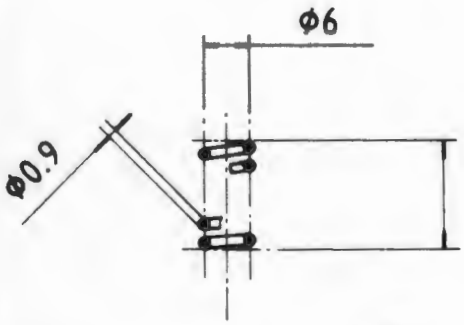

L_f = 14

L_s = 9

Δ = 5

C = $6\frac{2}{3}$

N = 10

ITEM No. (41), LATCH SPRING, 1 OFF

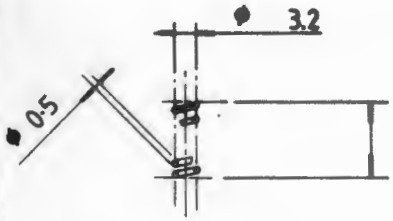

L_f = 10

C = 6·4

N = 12

ITEM No. (11)

BALL SPRING, 2 OFF

U.C.T. — DEPARTMENT OF MATERIALS ENGINEERING — WORKSHOP			
DRAWN BY U.F.B. KIENLE	WORK CATEGORY M. Sc. THESIS	MATERIAL	
DATE ACCEPTED	WORK SUPERVISED BY N. DREEZE	316 S/S	
DATE PROMISED	MATERIAL SCHEDULE SUPPLIED	YES	NO
SUPERVISOR PROF A. BALL	SCALE 1:1	SHEET 18	OF 42

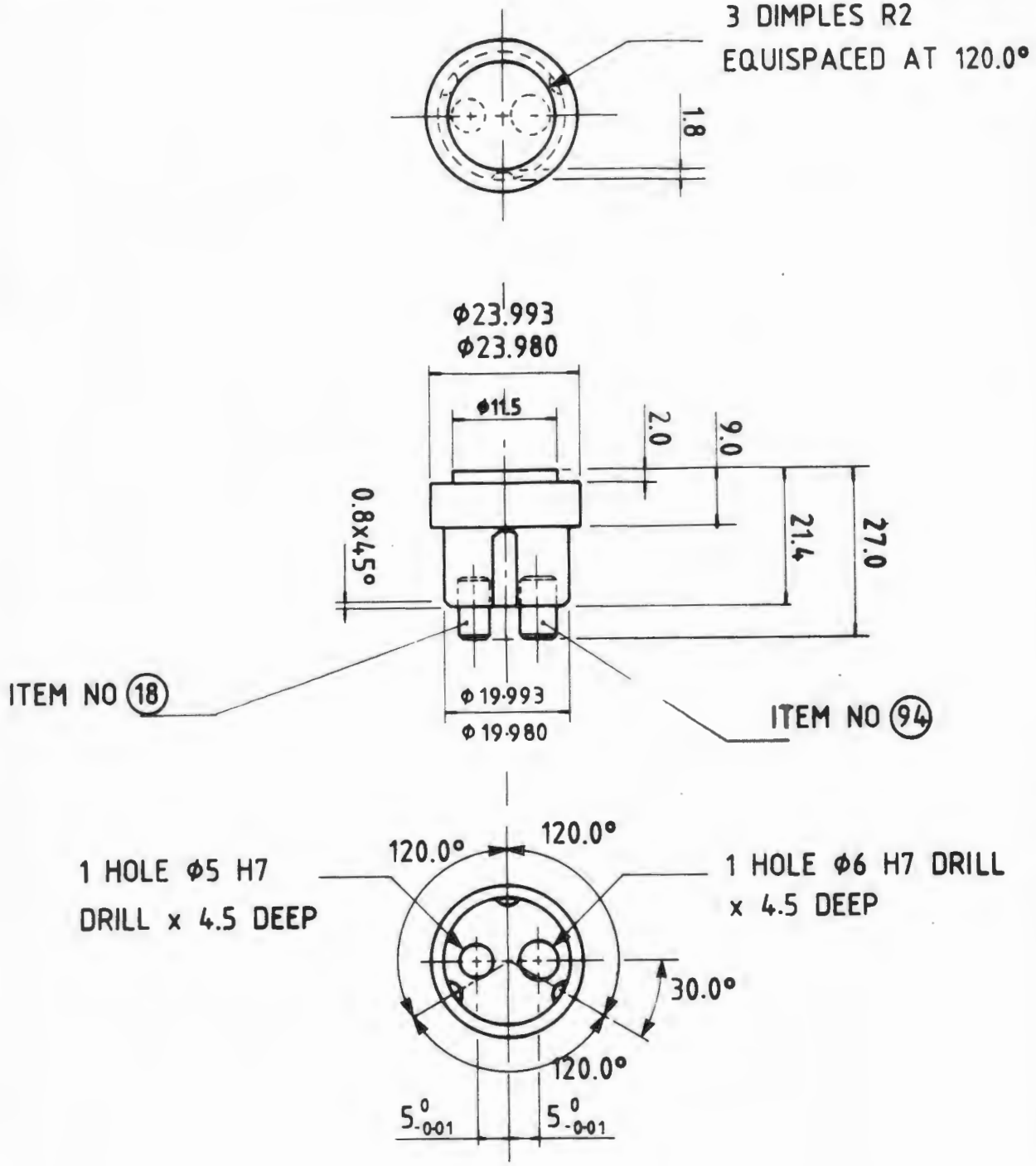

ITEM No. (10)

CONNECTING PLUNGER

1 OFF

U.C.T. — DEPARTMENT OF MATERIALS ENGINEERING — WORKSHOP				
DRAWN BY U.F.B. KIENLE	WORK CATEGORY M. Sc. THESIS		MATERIAL	
DATE ACCEPTED	WORK SUPERVISED BY N. DREEZE		316 S/S	
DATE PROMISED	MATERIAL SCHEDULE SUPPLIED		YES	NO
SUPERVISOR PROF A. BALL	SCALE 1:1	SHEET 19	OF 42	

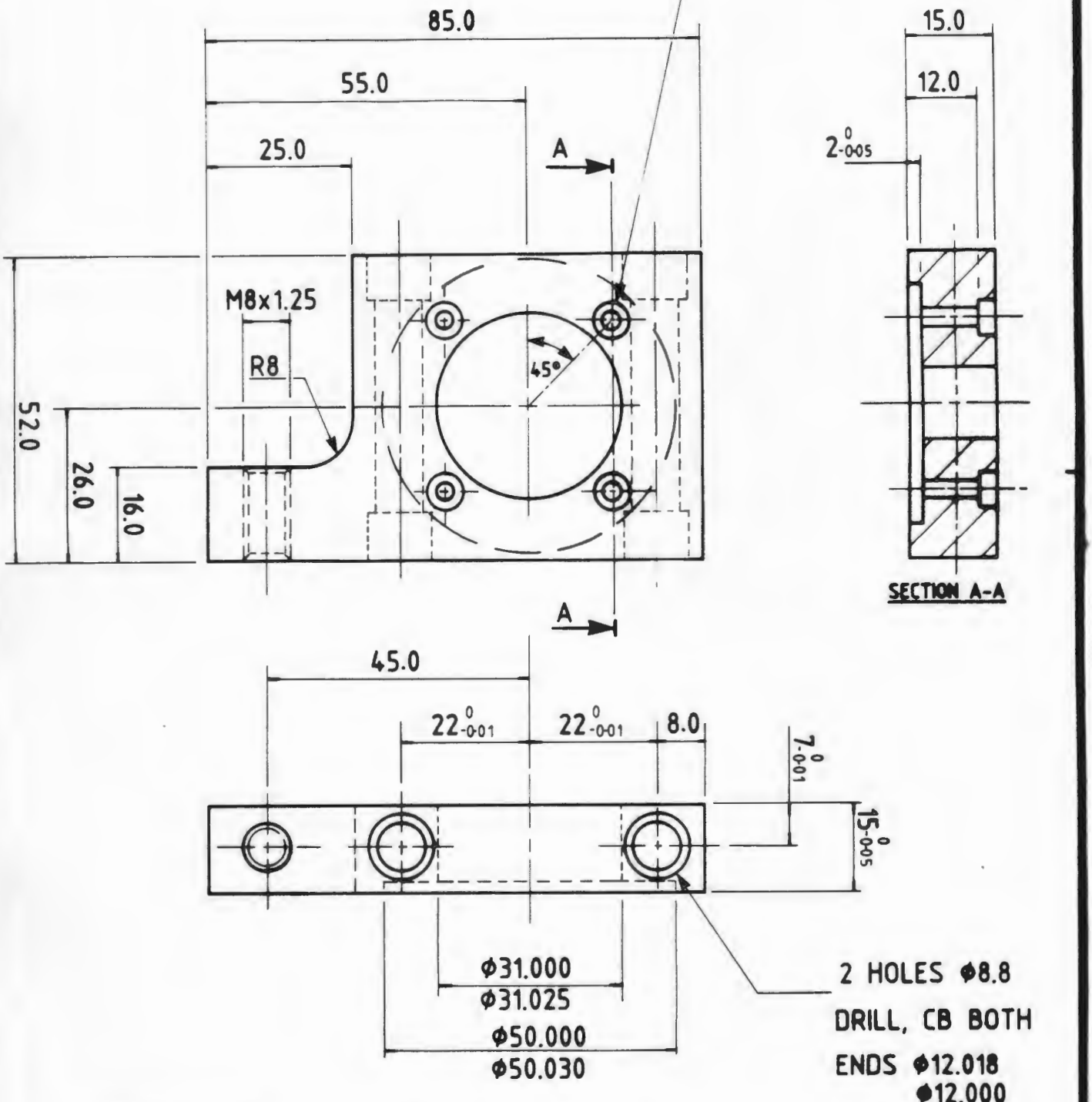

ITEM No. (12), FRICTION PLATE, 1 OFF

U.C.T. — DEPARTMENT OF MATERIALS ENGINEERING — WORKSHOP			
DRAWN BY U.F.B. KIENLE	WORK CATEGORY M. Sc. THESIS	MATERIAL	
DATE ACCEPTED	WORK SUPERVISED BY N. DREEZE	316 S/S	
DATE PROMISED	MATERIAL SCHEDULE SUPPLIED	YES	NO
SUPERVISOR PROF A. BALL	SCALE 1:1	SHEET 20	OF 42

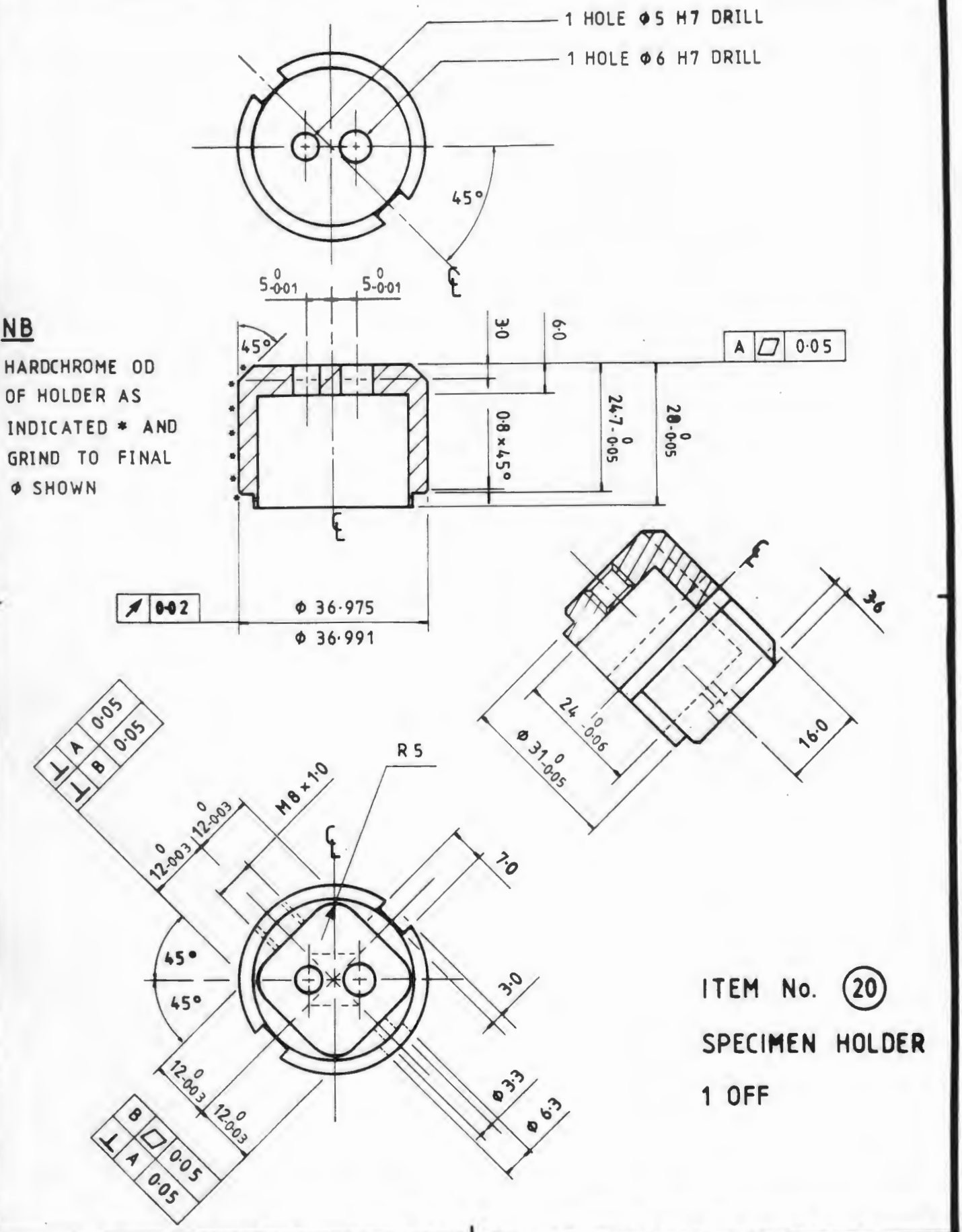

U.C.T. — DEPARTMENT OF MATERIALS ENGINEERING — WORKSHOP			
DRAWN BY U.F.B. KIENLE	WORK CATEGORY M. Sc. THESIS	MATERIAL	
DATE ACCEPTED	WORK SUPERVISED BY N. DREEZE	316 S/S	
DATE PROMISED	MATERIAL SCHEDULE SUPPLIED	YES	NO
SUPERVISOR PROF A. BALL	SCALE 1:1	SHEET 21	OF 42

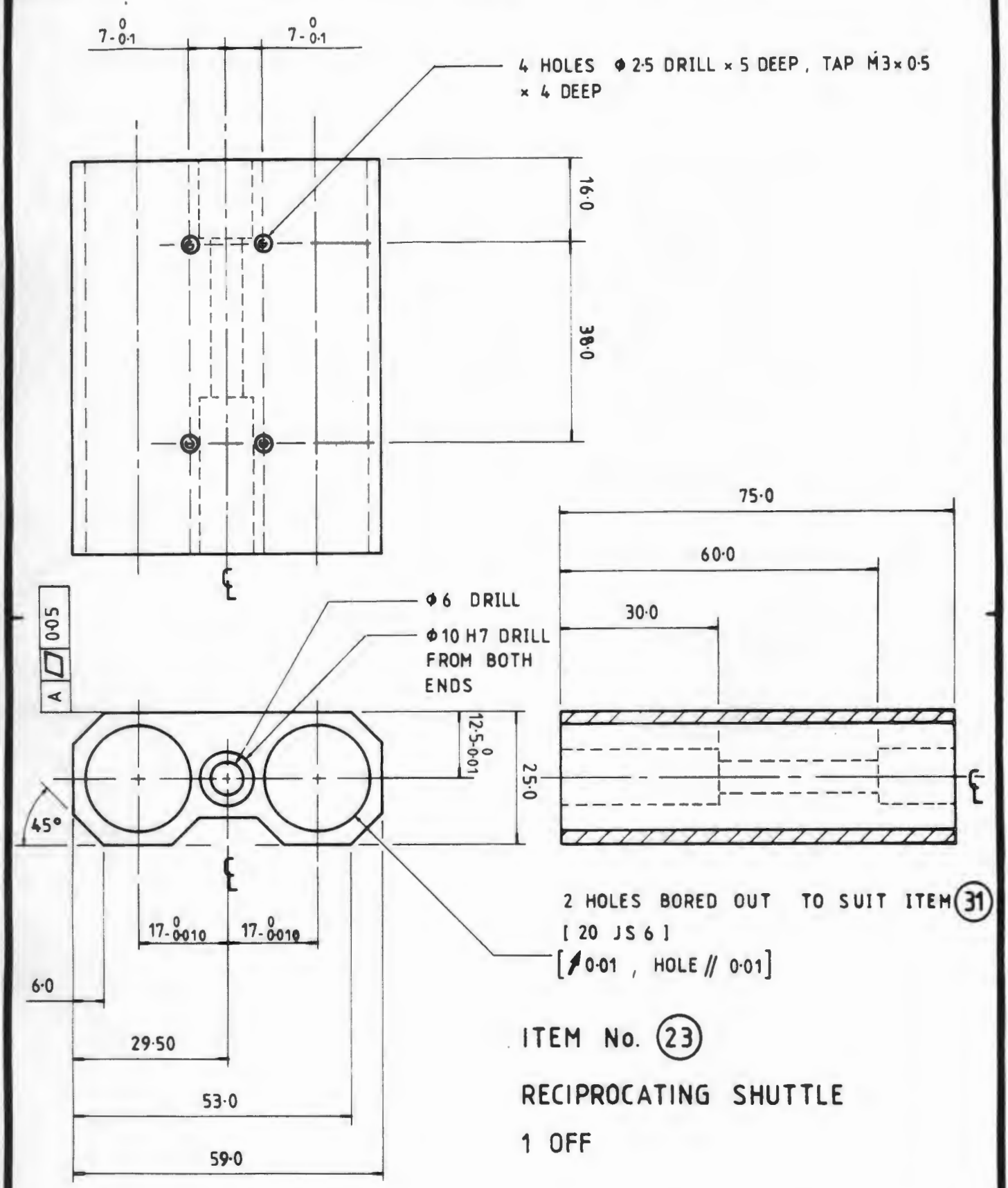

ITEM No. (23)

RECIPROCATING SHUTTLE

1 OFF

U.C.T. — DEPARTMENT OF MATERIALS ENGINEERING — WORKSHOP				
DRAWN BY U.F.B. KIENLE	WORK CATEGORY M. Sc. THESIS		MATERIAL	
DATE ACCEPTED	WORK SUPERVISED BY N. DREEZE		ALUMINIUM 7017	
DATE PROMISED	MATERIAL SCHEDULE SUPPLIED		YES	NO
SUPERVISOR PROF A. BALL	SCALE 1:1	SHEET 22	OF 42	

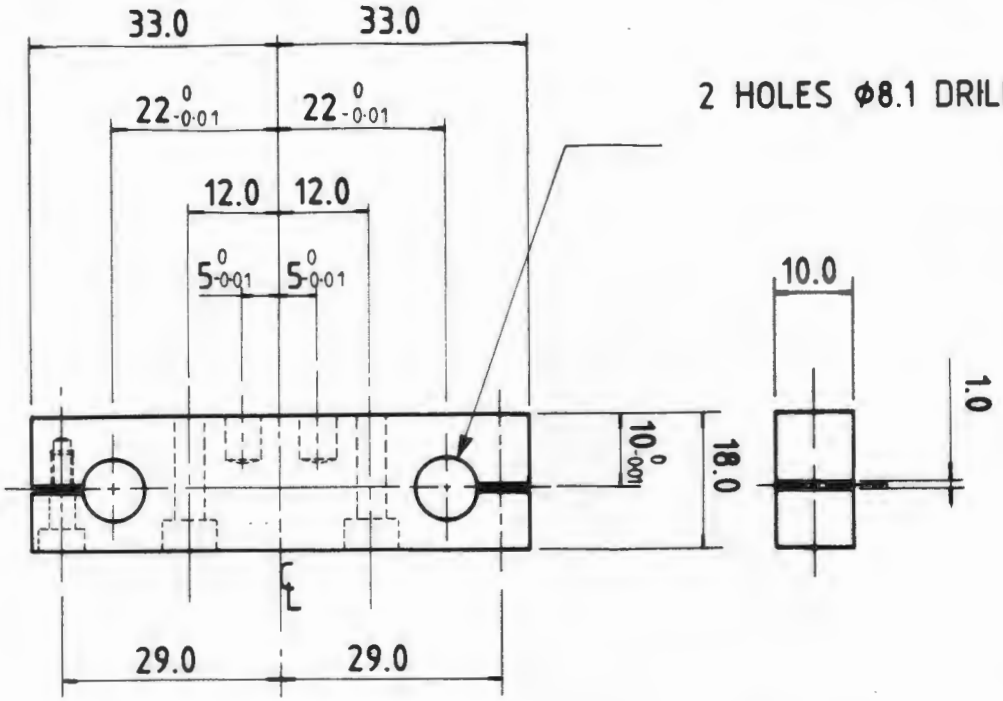

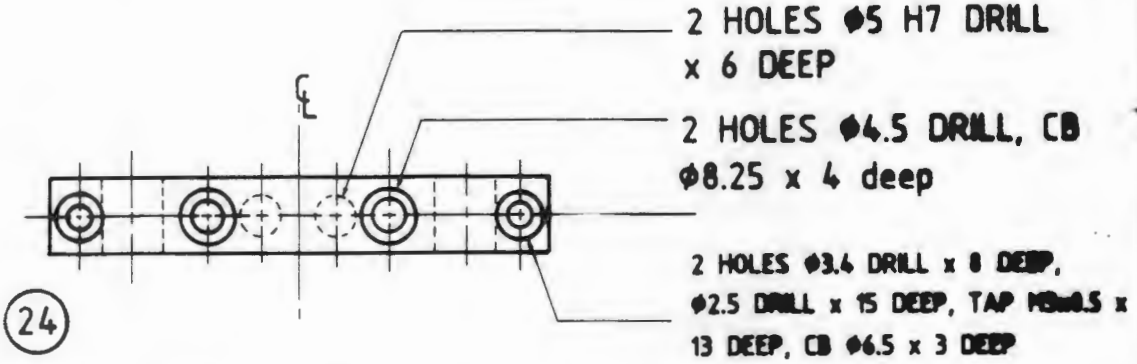

ITEM No. (24)

SUPPORT BRACKET - UPPER ASSEMBLY , 2 OFF, Al - 7017

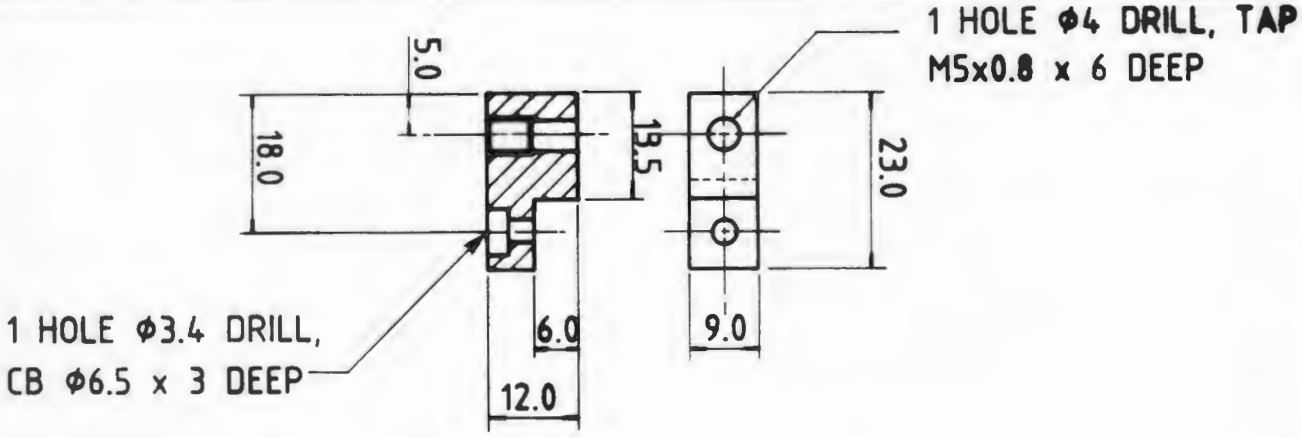

ITEM No. (25), RATCHET BRACKET, 1 OFF , P- BRONZE (034)

U.C.T. — DEPARTMENT OF MATERIALS ENGINEERING — WORKSHOP			
DRAWN BY U.F.B. KIENLE	WORK CATEGORY M. Sc. THESIS	MATERIAL	
DATE ACCEPTED	WORK SUPERVISED BY N. DREEZE	AS SHOWN	
DATE PROMISED	MATERIAL SCHEDULE SUPPLIED	YES	NO
SUPERVISOR PROF A. BALL	SCALE 1 : 1	SHEET 23	OF 42

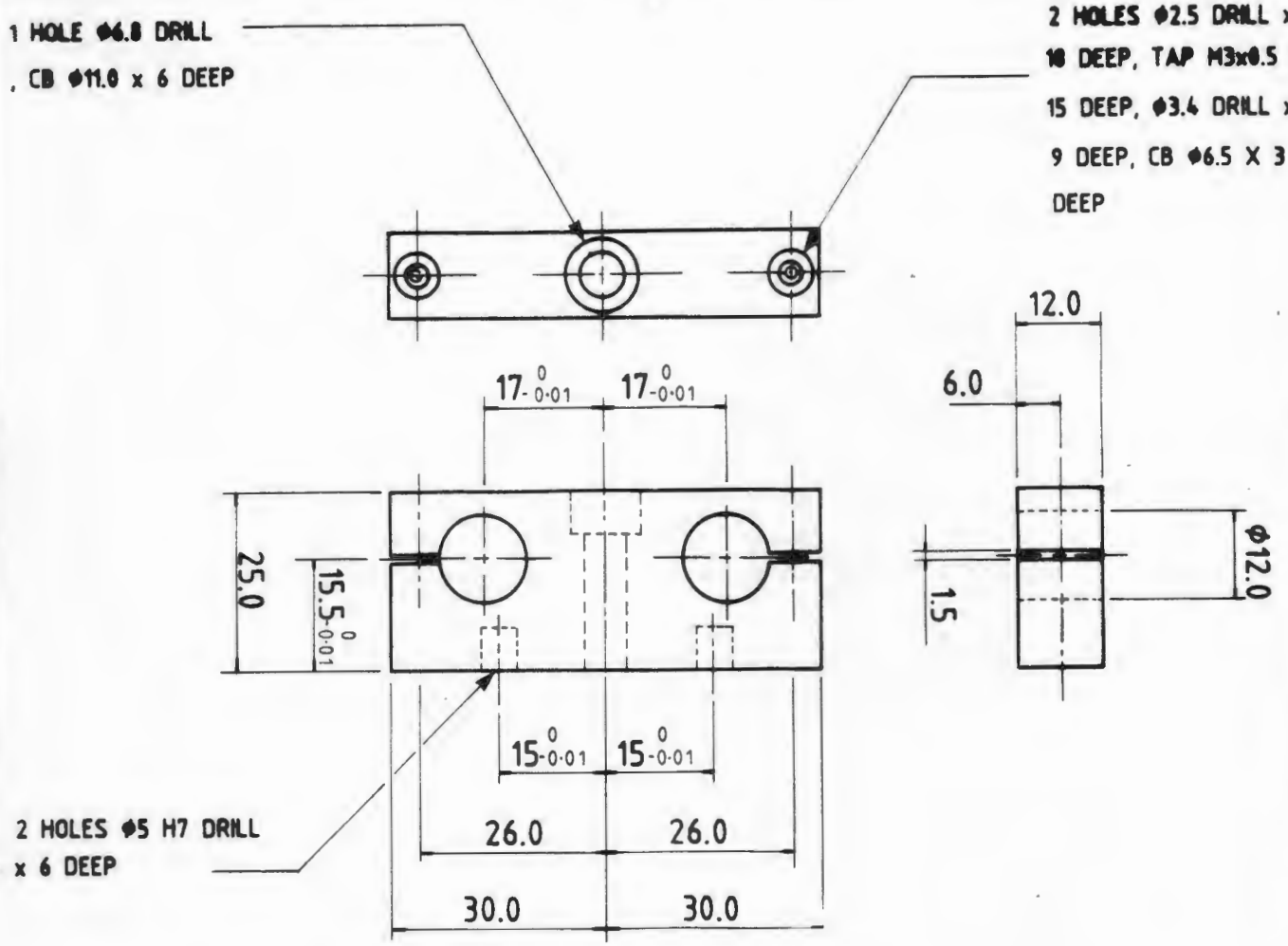

ITEM No. (30)

SUPPORT BRACKET - SHUTTLE ASSEMBLY, 2 OFF, Al - 7017

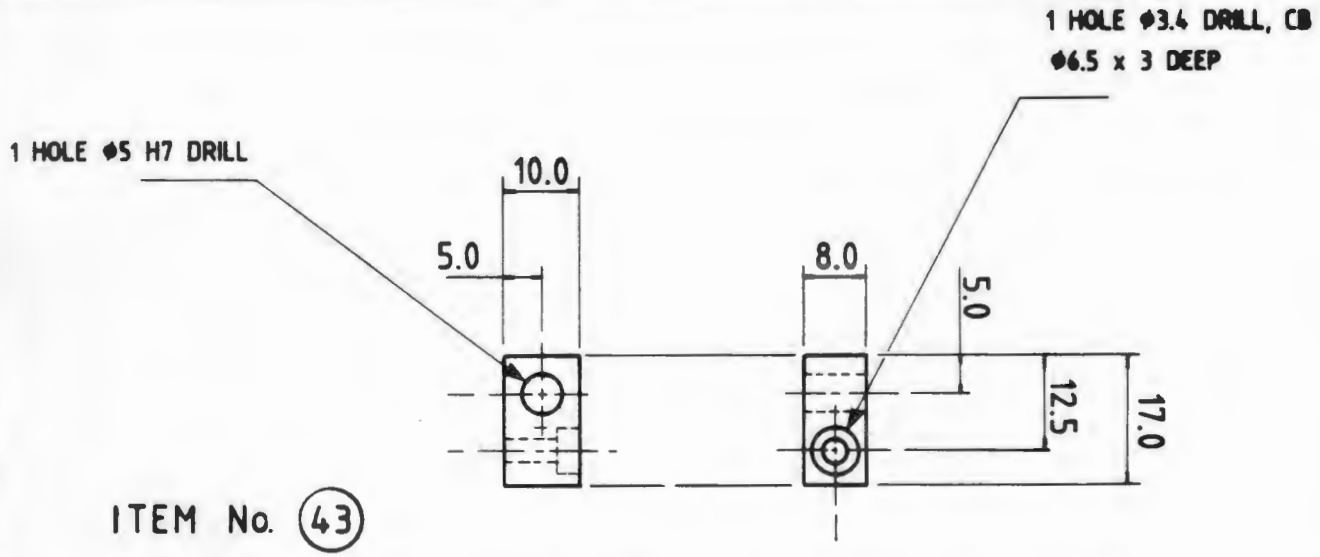

ITEM No. (43)

LATCHING LEVER HINGE MOUNTING, 2 OFF, 316 S/S

U.C.T. — DEPARTMENT OF MATERIALS ENGINEERING — WORKSHOP			
DRAWN BY U.F.B. KIENLE	WORK CATEGORY M. Sc. THESIS	MATERIAL	
DATE ACCEPTED	WORK SUPERVISED BY N. DREEZE	AS SHOWN	
DATE PROMISED	MATERIAL SCHEDULE SUPPLIED	YES	NO
SUPERVISOR PROF A. BALL	SCALE 1:1	SHEET 24	OF 42

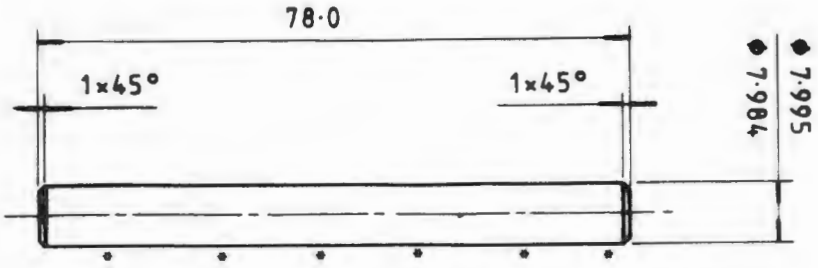

ITEM No. (14)

FRICTION PLATE GUIDE SHAFT

2 OFF, 431 S/S

NB

HARDCHROME SHAFT AS INDICATED * AND GRIND TO FINAL Φ SHOWN [/ 0·01]

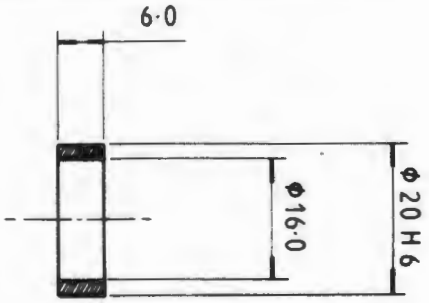

ITEM No. (33), SPACER RING, 1 OFF, P - BRONZE (034)

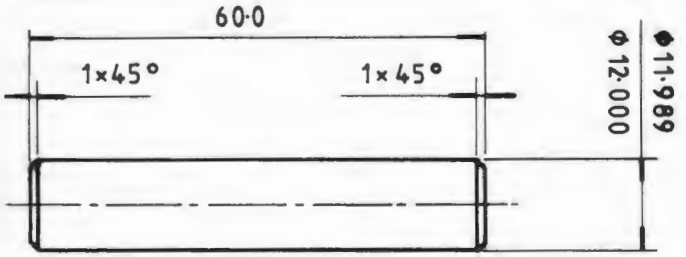

ITEM No. (36)

HINGE PIN, 1 OFF

316 S/S

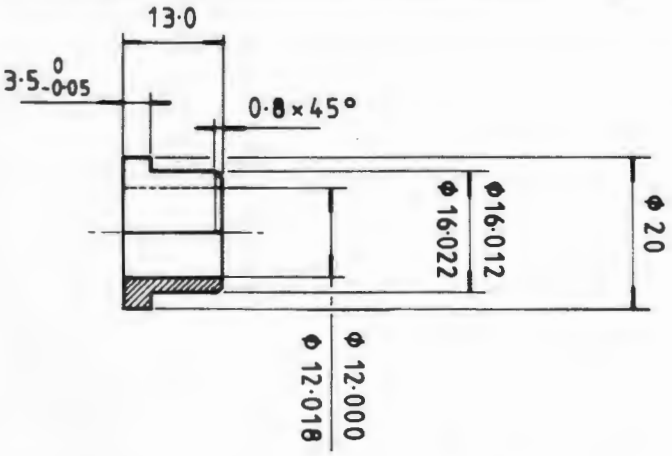

ITEM No. (39)

HINGE BUSHING

2 OFF

P - BRONZE (034)

U.C.T. — DEPARTMENT OF MATERIALS ENGINEERING — WORKSHOP			
DRAWN BY U.F.B. KIENLE	WORK CATEGORY M. Sc. THESIS	MATERIAL	
DATE ACCEPTED	WORK SUPERVISED BY N. DREEZE	AS SHOWN	
DATE PROMISED	MATERIAL SCHEDULE SUPPLIED	YES	NO
SUPERVISOR PROF A. BALL	SCALE 1:1	SHEET 25	OF 42

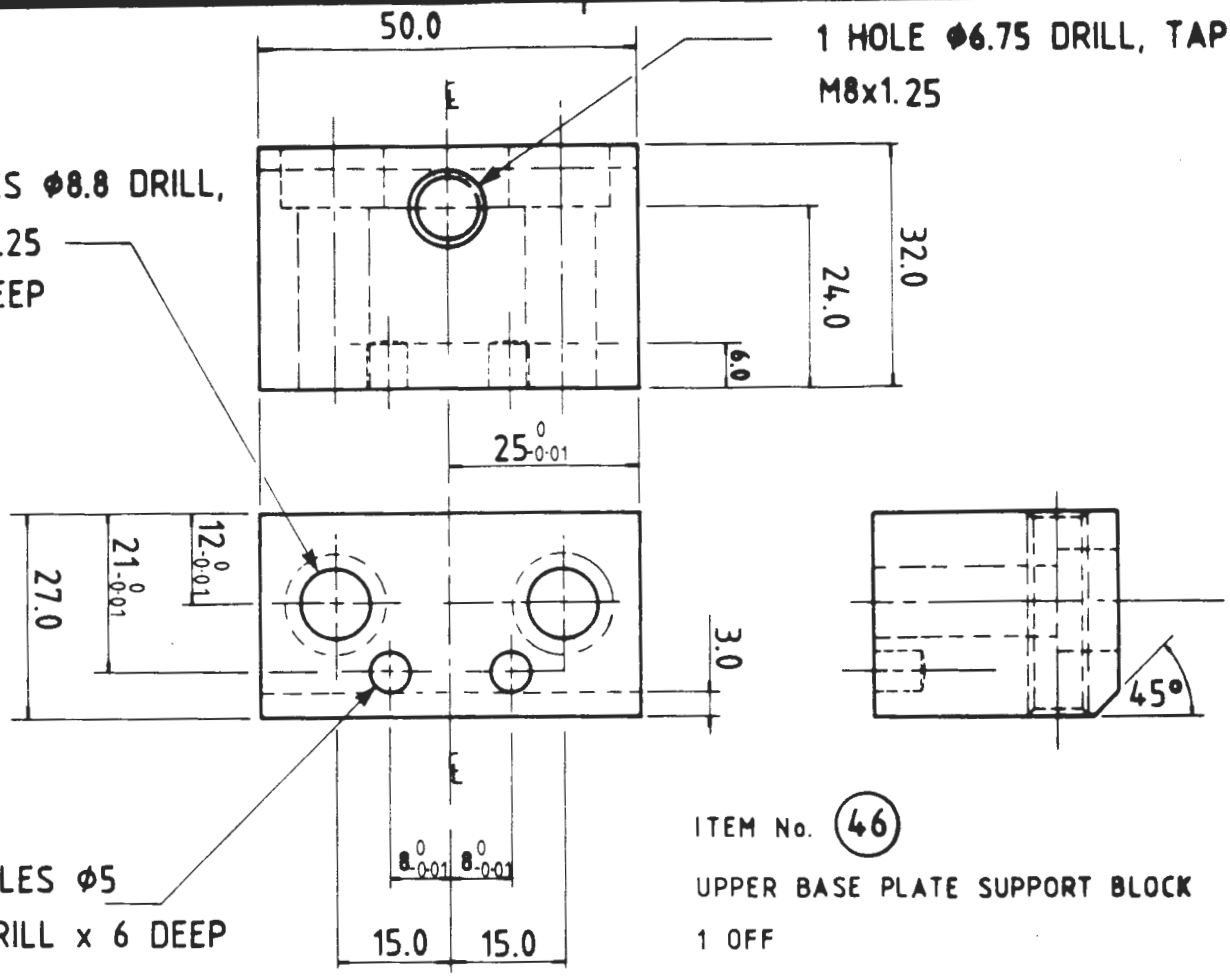

ITEM No. (46)

UPPER BASE PLATE SUPPORT BLOCK

1 OFF

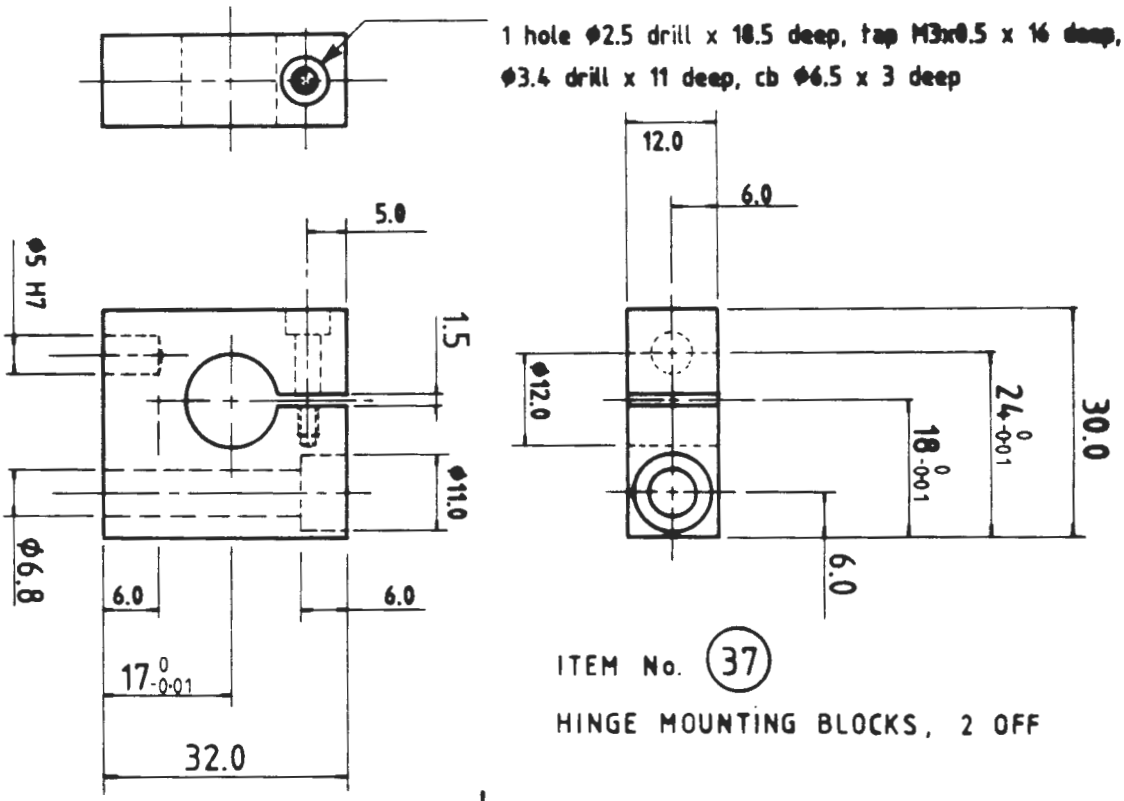

ITEM No. (37)

HINGE MOUNTING BLOCKS, 2 OFF

U.C.T. — DEPARTMENT OF MATERIALS ENGINEERING — WORKSHOP			
DRAWN BY U.F.B. KIENLE	WORK CATEGORY M. Sc. THESIS	MATERIAL	
DATE ACCEPTED	WORK SUPERVISED BY N. DREEZE	316 S/S	
DATE PROMISED	MATERIAL SCHEDULE SUPPLIED	YES	NO
SUPERVISOR PROF A. BALL	SCALE 1:1	SHEET 26	OF 42

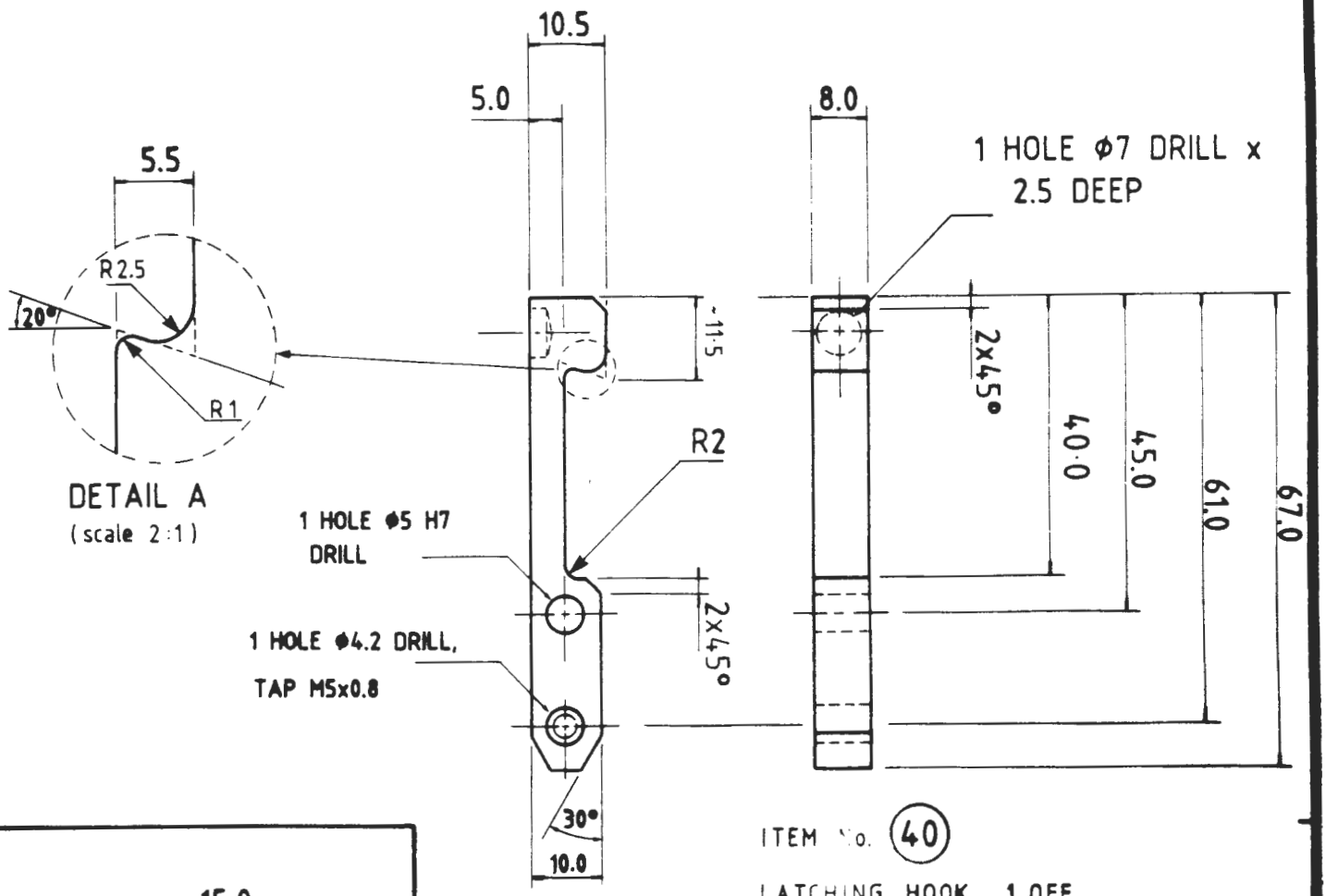

ITEM No. (40)

LATCHING HOOK, 1 OFF

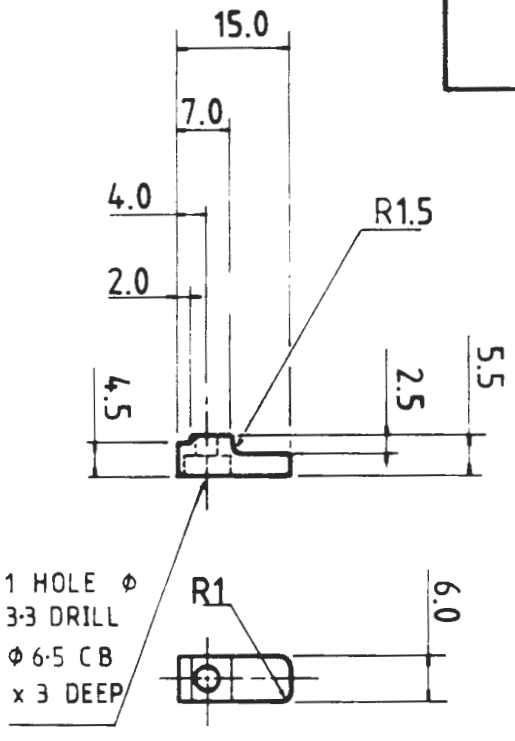

ITEM No. (17)

HOLD FINGERS, 2 OFF

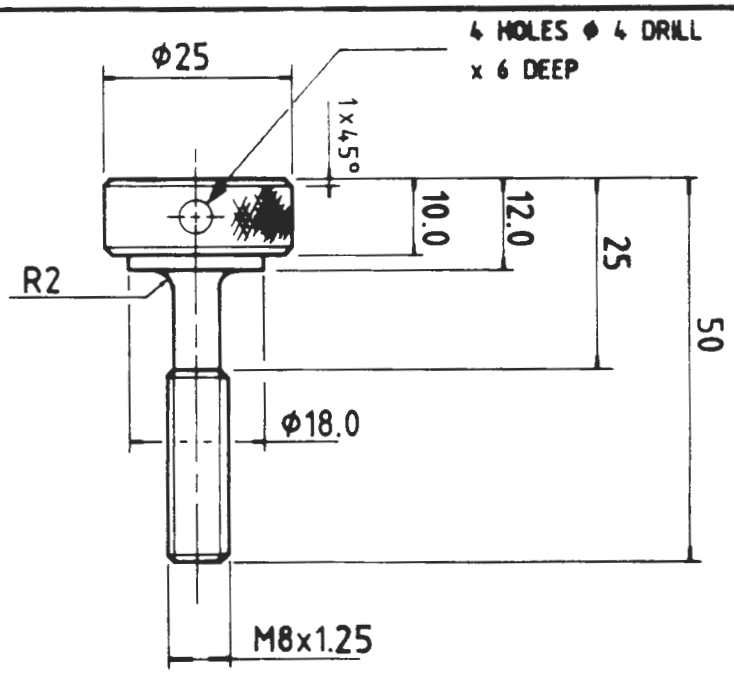

ITEM No. (44)

RETAINING THUMBSCREW, 1 OFF

U.C.T. — DEPARTMENT OF MATERIALS ENGINEERING — WORKSHOP			
DRAWN BY U.F.B. KIENLE	WORK CATEGORY M. Sc. THESIS	MATERIAL	
DATE ACCEPTED	WORK SUPERVISED BY N. DREEZE	316 S/S	
DATE PROMISED	MATERIAL SCHEDULE SUPPLIED	YES	NO
SUPERVISOR PROF A. BALL	SCALE 1:1	SHEET 27	OF 42

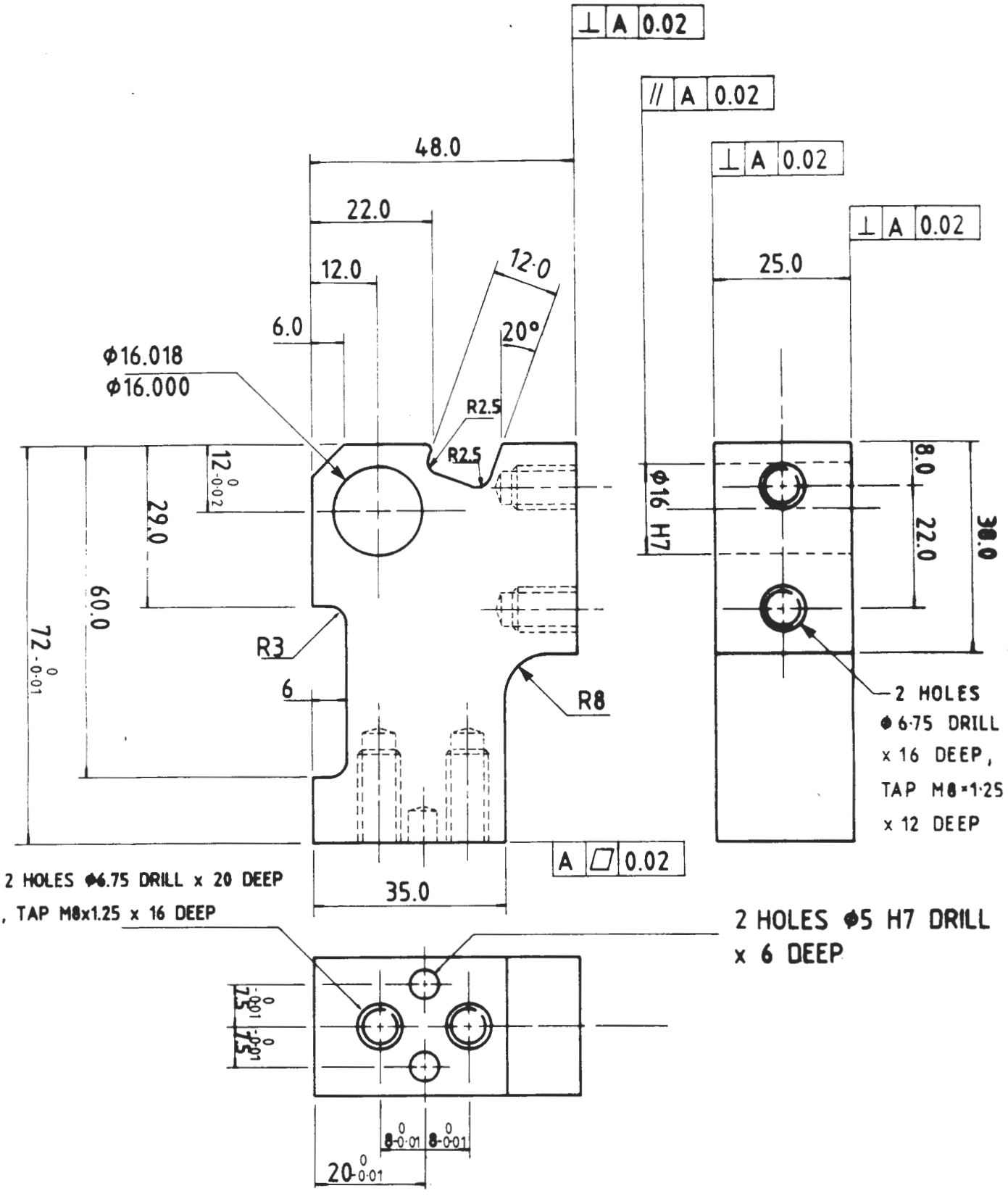

ITEM No. (45), HINGE PLATE, 1 OFF

U.C.T. — DEPARTMENT OF MATERIALS ENGINEERING — WORKSHOP			
DRAWN BY U.F.B. KIENLE	WORK CATEGORY M. Sc. THESIS	MATERIAL	
DATE ACCEPTED	WORK SUPERVISED BY N. DREEZE	316 S/S	
DATE PROMISED	MATERIAL SCHEDULE SUPPLIED	YES	NO
SUPERVISOR PROF A. BALL	SCALE 1:1	SHEET 28	OF 42

M/C ΦA TO SUIT ITEM (9)

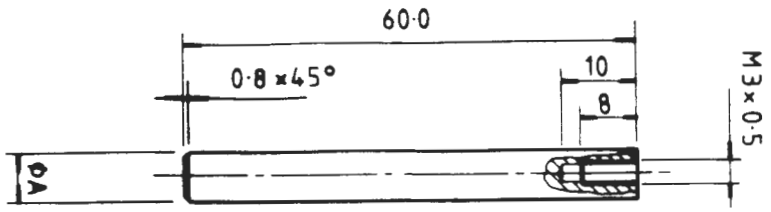

ITEM No. (34)

RESETTING RING LEVER, 1 OFF

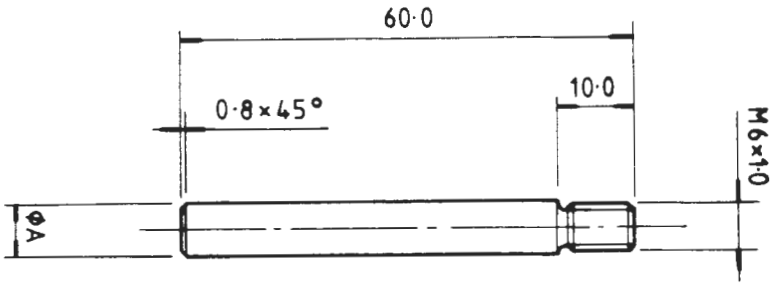

ITEM No. (8)

UPPER BASE PLATE LEVER, 1 OFF

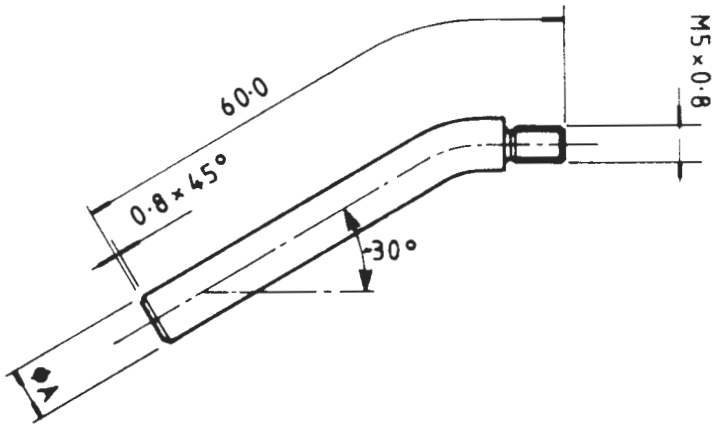

ITEM No. (35)

LATCH RELEASE LEVER

1 OFF

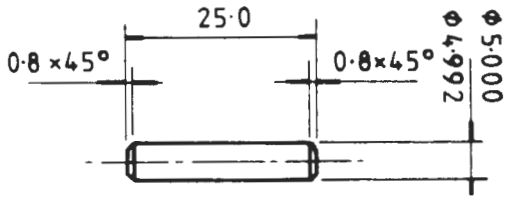

ITEM No. (58)

LATCH PIN, 1 OFF

U.C.T. — DEPARTMENT OF MATERIALS ENGINEERING — WORKSHOP				
DRAWN BY U.F.B. KIENLE	WORK CATEGORY M. Sc. THESIS		MATERIAL	
DATE ACCEPTED	WORK SUPERVISED BY N. DREEZE		316 S/S	
DATE PROMISED	MATERIAL SCHEDULE SUPPLIED		YES	NO
SUPERVISOR PROF A. BALL	SCALE 1:1	SHEET 29	OF 42	

ITEM No. (61)

PISTON SHAFT SEALING ASSEMBLY - OUTER RING

1 OFF, 431 S/S

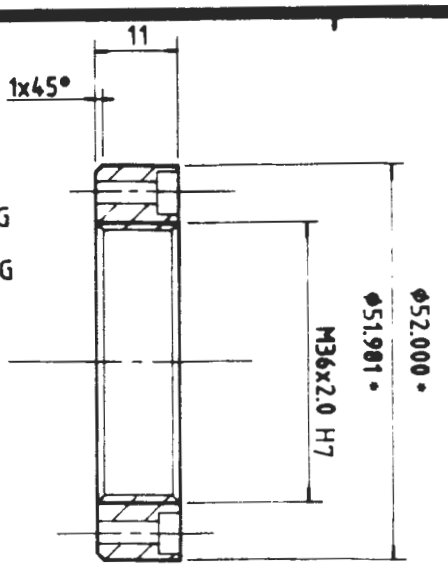

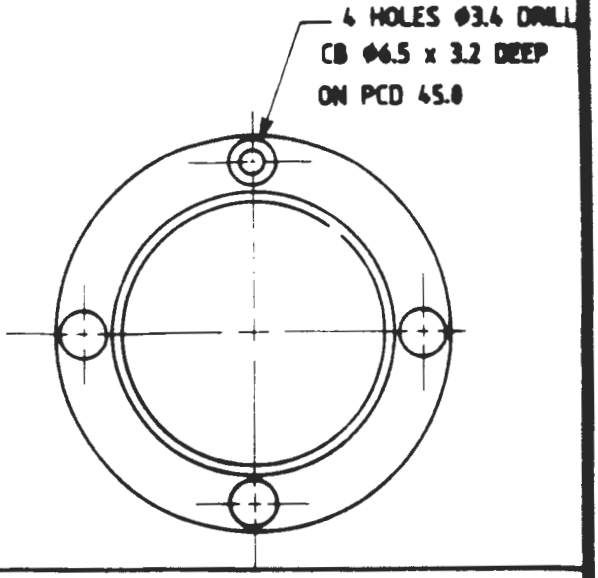

NB

ALL Φ DENOTED BY *

HAVE ↗ 0·01

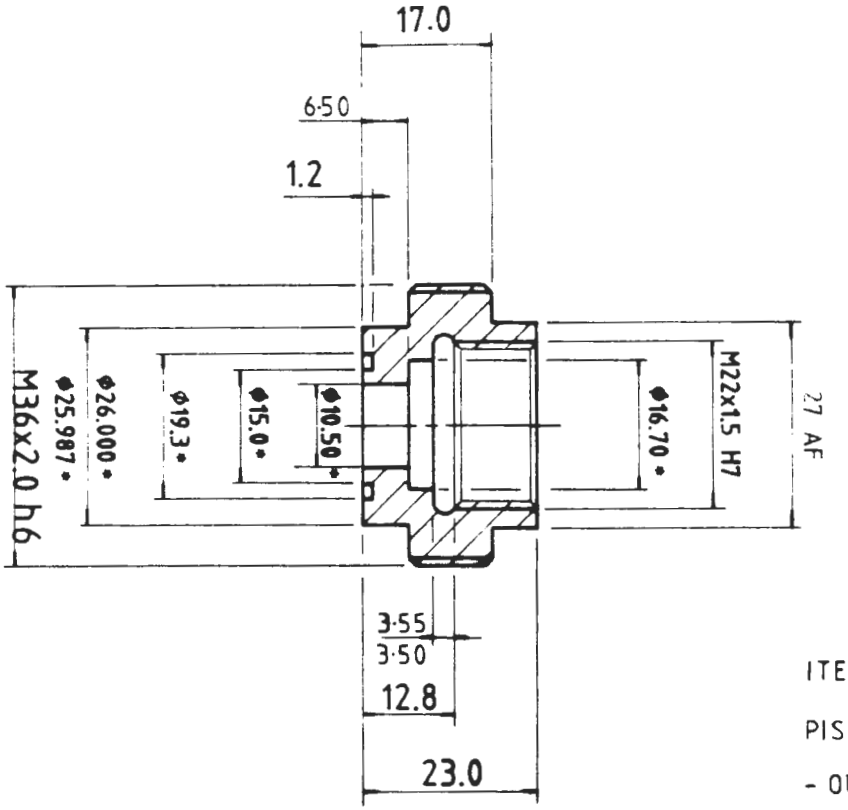

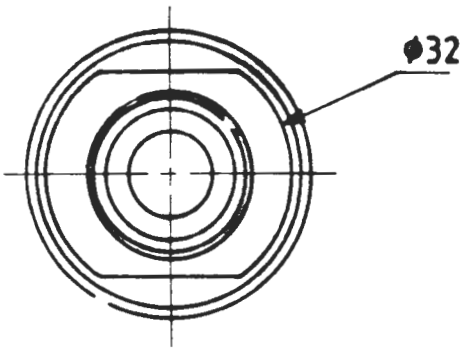

ITEM No. (62)

PISTON SHAFT SEALING ASSEMBLY - OUTER HOUSING, 1 OFF, P-BRONZE 034

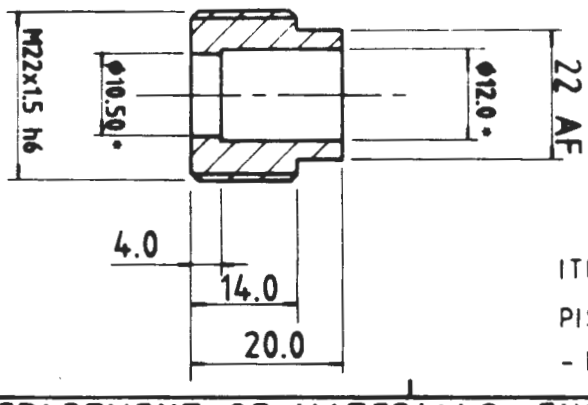

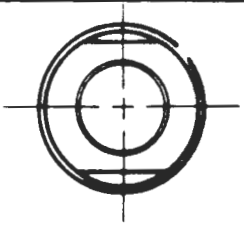

ITEM No. (63)

PISTON SHAFT SEALING ASSEMBLY - INNER HOUSING, 1 OFF, 431 S/S

U.C.T. — DEPARTMENT OF MATERIALS ENGINEERING — WORKSHOP			
DRAWN BY U.F.B. KIENLE	WORK CATEGORY M.Sc. THESIS	MATERIAL	
DATE ACCEPTED	WORK SUPERVISED BY N. DREEZE	AS SHOWN	
DATE PROMISED	MATERIAL SCHEDULE SUPPLIED	YES	NO
SUPERVISOR PROF A. BALL	SCALE 1:1	SHEET 30	OF 42

NB

HARD CHROM SHAFT AS INDICATED * AND GRIND TO FINAL SIZE SHOWN

ITEM No. (67)

RECIPROCATING PISTON SHAFT, 1 OFF

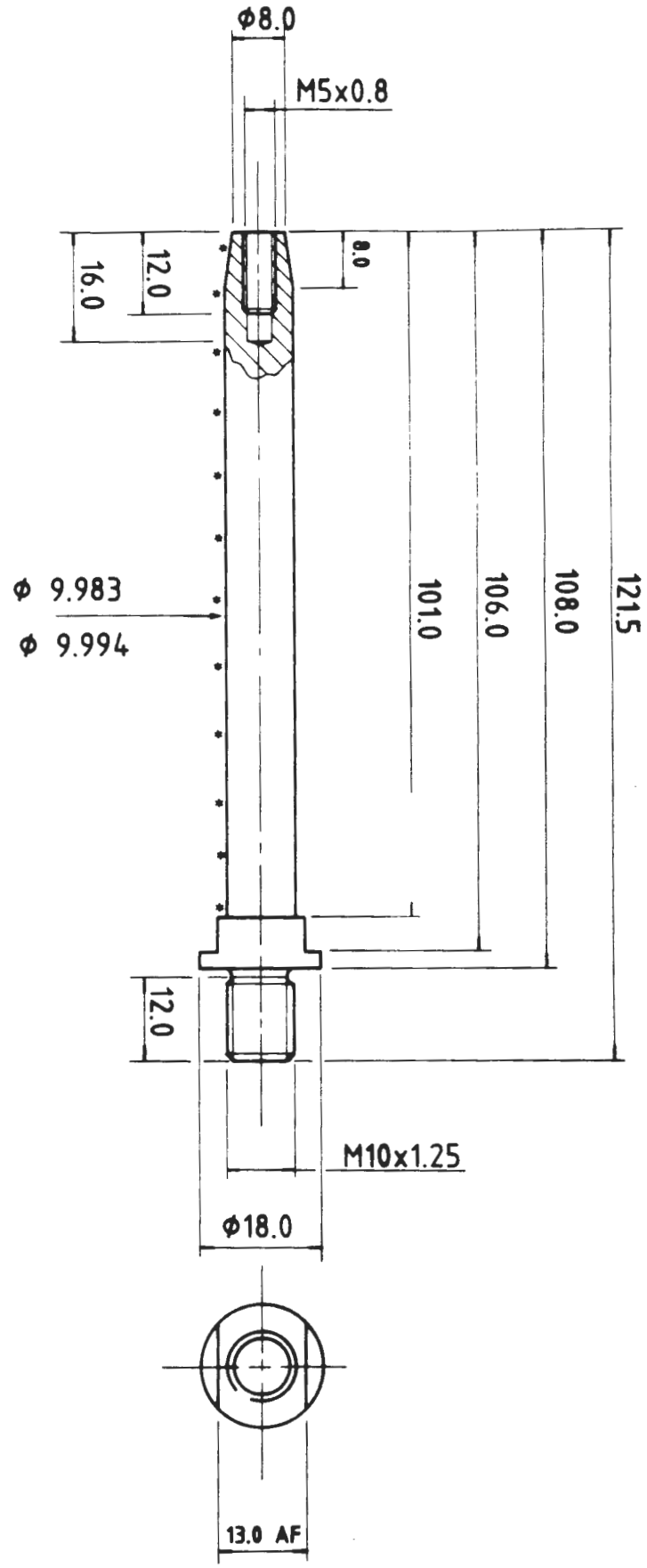

U.C.T. — DEPARTMENT OF MATERIALS ENGINEERING — WORKSHOP			
DRAWN BY U.F.B. KIENLE	WORK CATEGORY M. Sc. THESIS	MATERIAL	
DATE ACCEPTED	WORK SUPERVISED BY N. DREEZE	431 S/S	
DATE PROMISED	MATERIAL SCHEDULE SUPPLIED	YES	NO
SUPERVISOR PROF A. BALL	SCALE	SHEET 31	OF 42

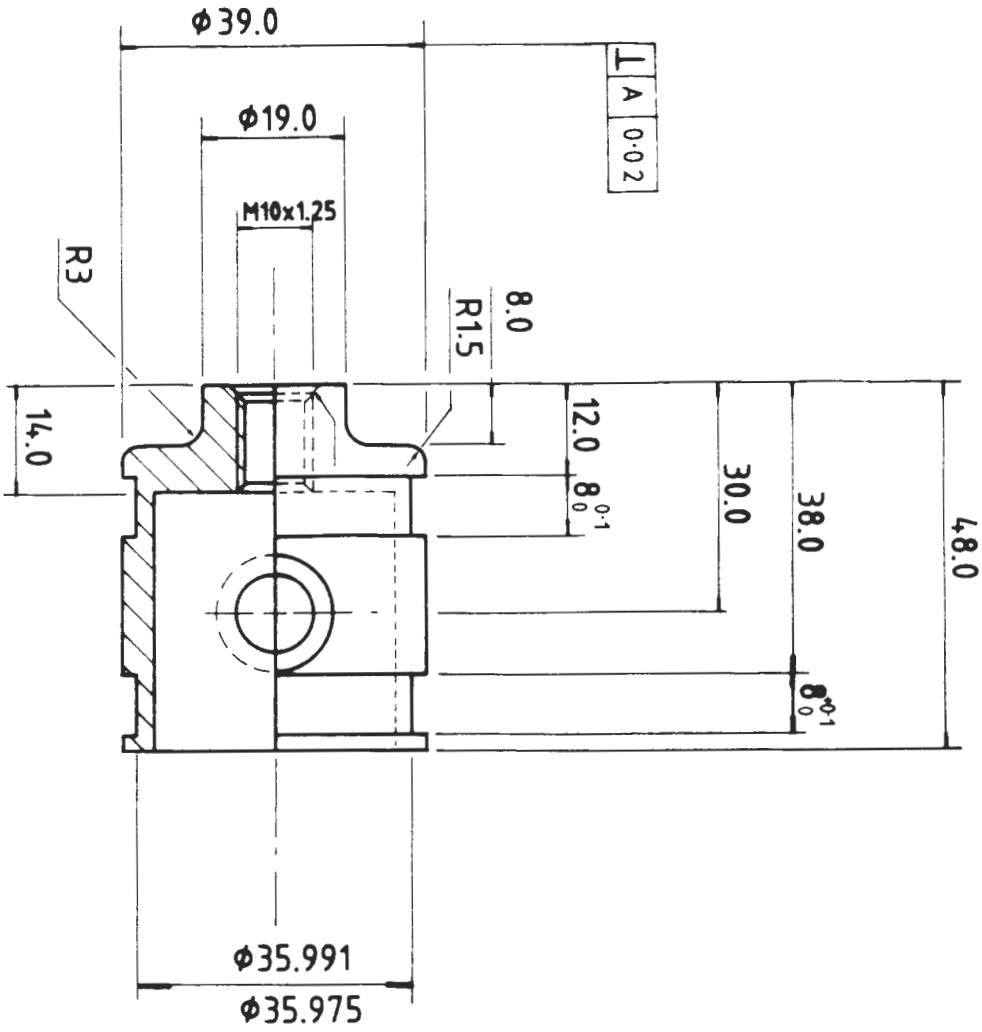

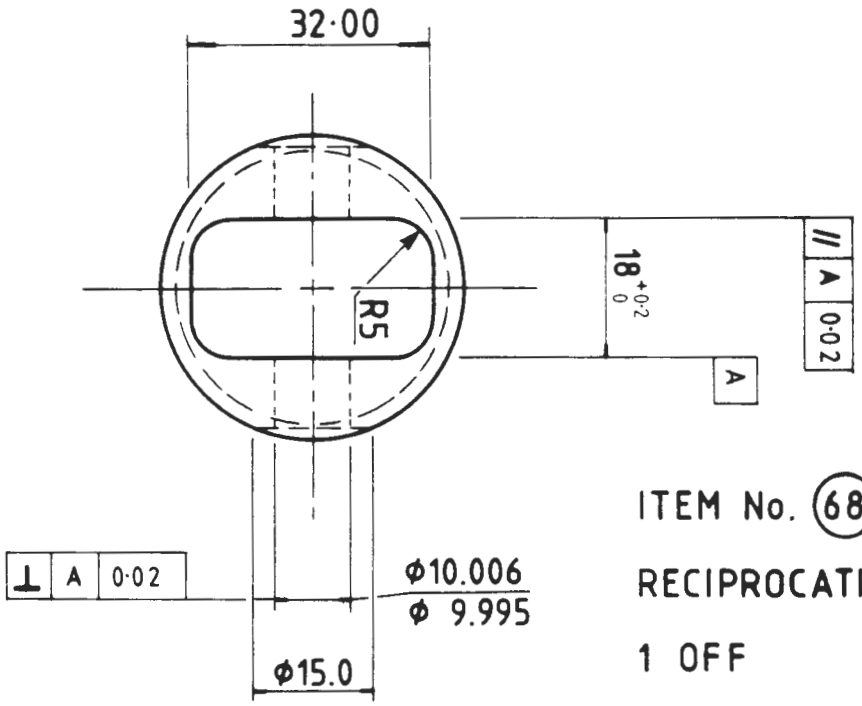

ITEM No. (68)

RECIPROCATING PISTON

1 OFF

U.C.T. — DEPARTMENT OF MATERIALS ENGINEERING — WORKSHOP			
DRAWN BY U.F.B. KIENLE	WORK CATEGORY M. Sc. THESIS	MATERIAL	
DATE ACCEPTED	WORK SUPERVISED BY N. DREEZE	ALUMINIUM - 7017	
DATE PROMISED	MATERIAL SCHEDULE SUPPLIED	YES	NO
SUPERVISOR PROF A. BALL	SCALE 1 : 1	SHEET 32	OF 42

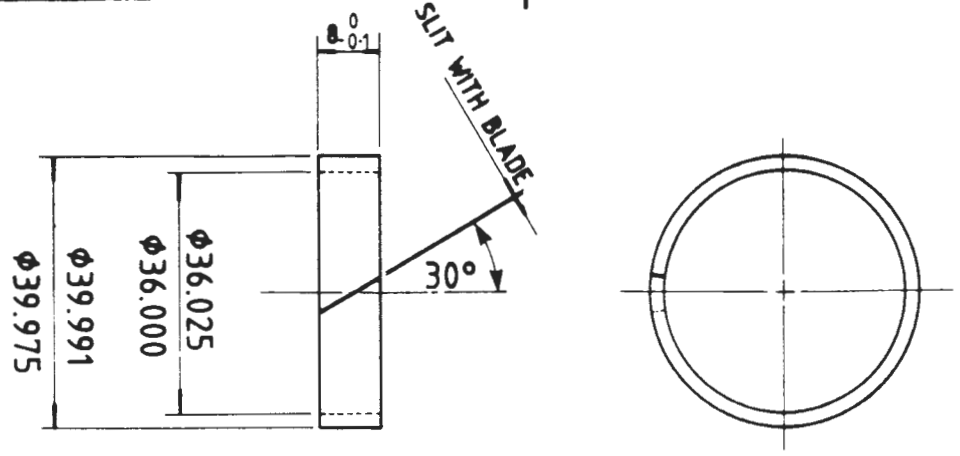

ITEM No. (70), PISTON SEAL, 2 OFF (SCALE 1:1)

ITEM No. (64) (PISTON SHAFT SEAL-BACKING 'O' RING)

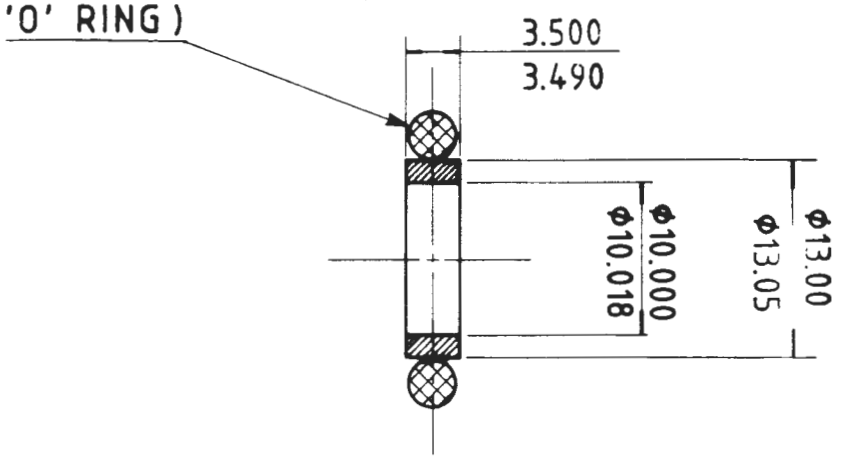

ITEM No (66), PISTON SHAFT SEAL, 1 OFF (SCALE 2:1)

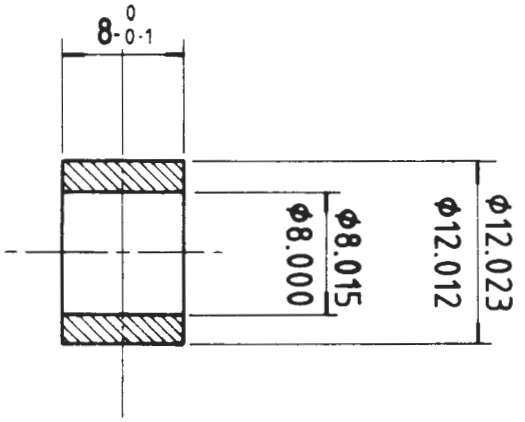

ITEM No. (13), FRICTION PLATE BEARING, 4 OFF (SCALE 2:1)

U.C.T. — DEPARTMENT OF MATERIALS ENGINEERING — WORKSHOP			
DRAWN BY U.F.B. KIENLE	WORK CATEGORY M.Sc. THESIS	MATERIAL	
DATE ACCEPTED	WORK SUPERVISED BY N. DREEZE	SOLIDUR DS	
DATE PROMISED	MATERIAL SCHEDULE SUPPLIED	YES	NO
SUPERVISOR PROF A. BALL	SCALE AS SHOWN	SHEET 33	OF 42

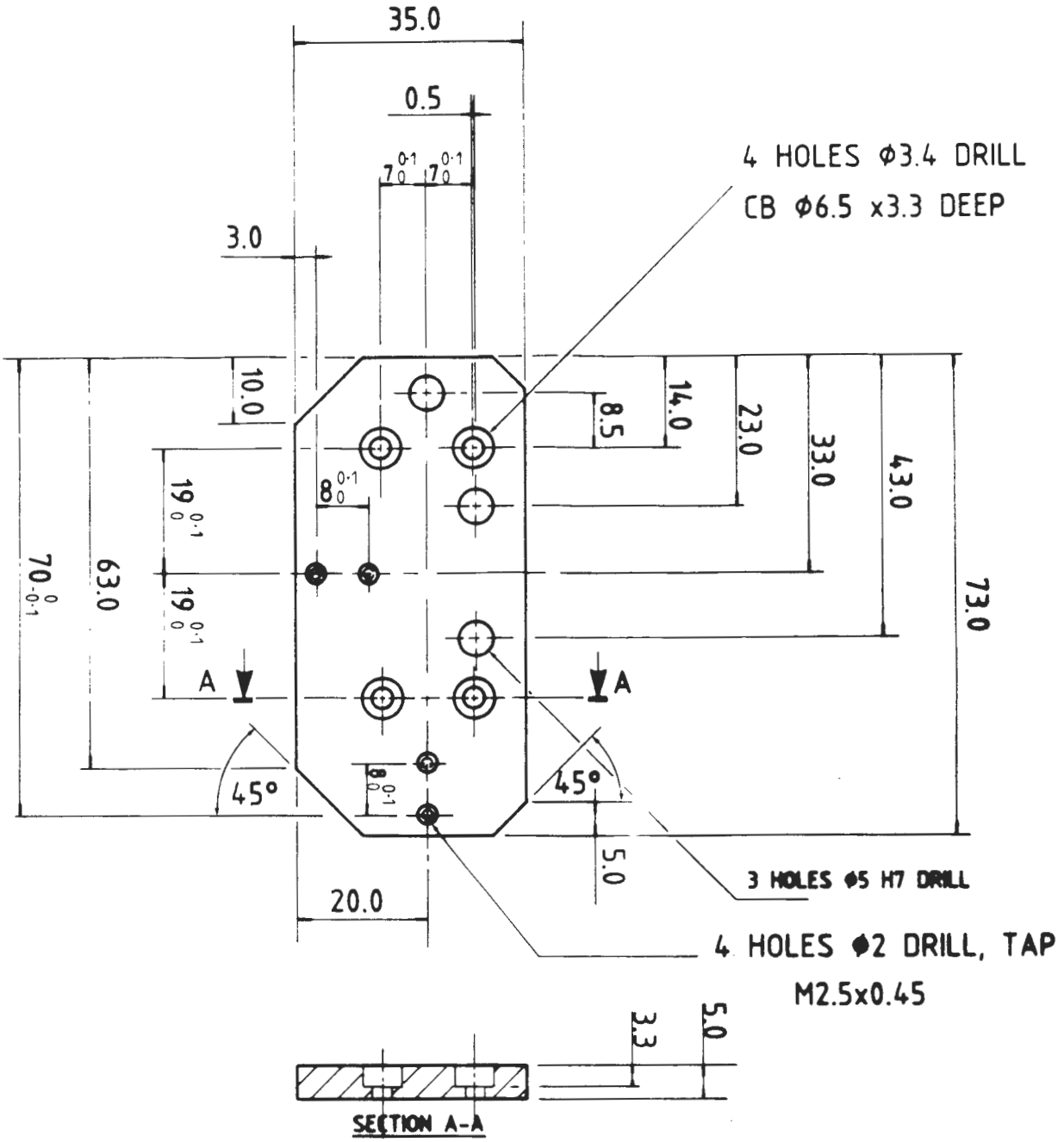

ITEM No. (28), SPECIMEN MOUNTING PLATE, 1 OFF

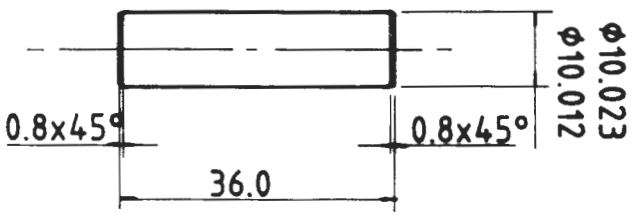

ITEM No. (72), WRISTPIN, 1 OFF

U.C.T. — DEPARTMENT OF MATERIALS ENGINEERING — WORKSHOP			
DRAWN BY U.F.B. KIENLE	WORK CATEGORY M. Sc. THESIS	MATERIAL	
DATE ACCEPTED	WORK SUPERVISED BY N. DREEZE	316 S/S	
DATE PROMISED	MATERIAL SCHEDULE SUPPLIED	YES	NO
SUPERVISOR PROF A. BALL	SCALE 1:1	SHEET 34	OF 42

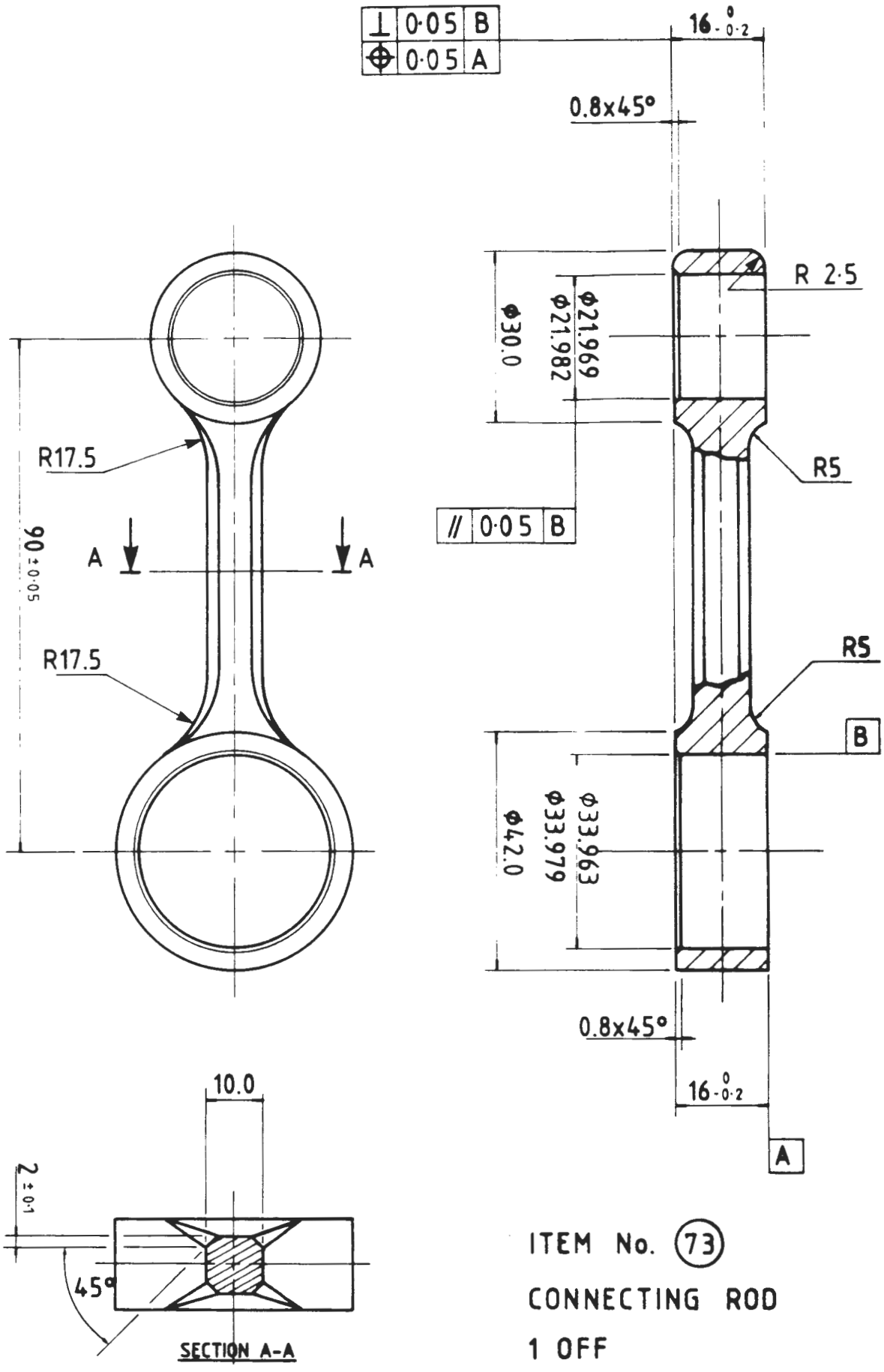

ITEM No. (73)

CONNECTING ROD

1 OFF

U.C.T. — DEPARTMENT OF MATERIALS ENGINEERING — WORKSHOP			
DRAWN BY U.F.B. KIENLE	WORK CATEGORY M. Sc. THESIS	MATERIAL	
DATE ACCEPTED	WORK SUPERVISED BY N. DREEZE	431 S/S	
DATE PROMISED	MATERIAL SCHEDULE SUPPLIED	YES	NO
SUPERVISOR PROF A. BALL	SCALE 1 : 1	SHEET 35	OF 42

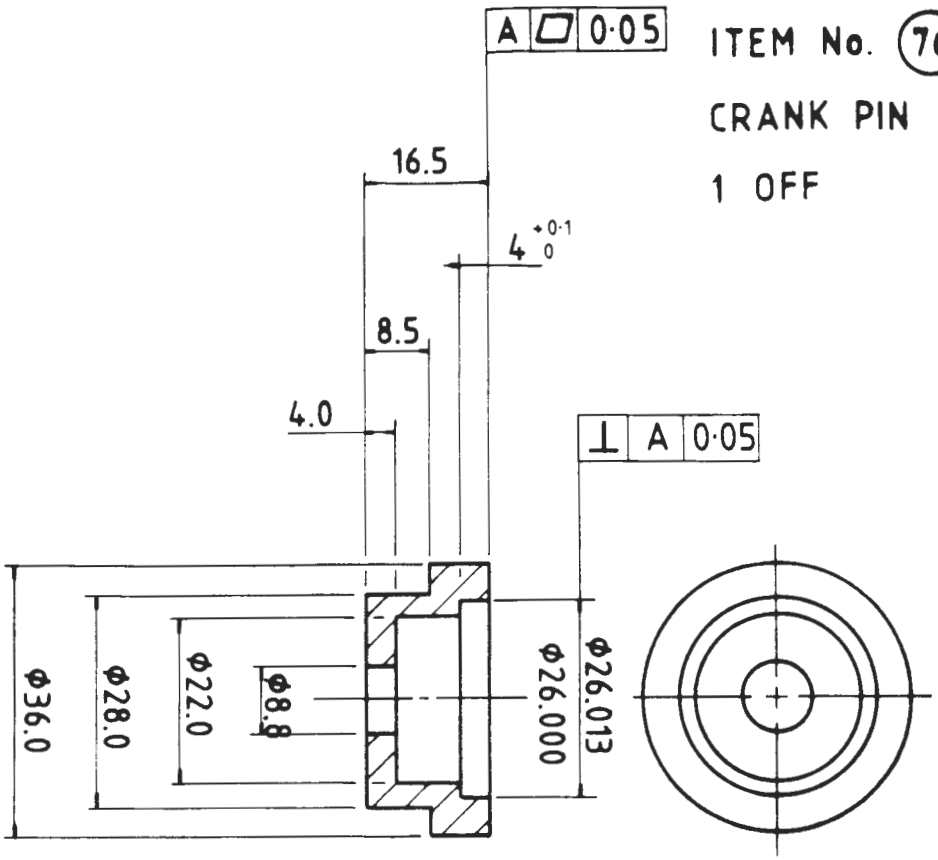

ITEM No. (76)

CRANK PIN END CAP

1 OFF

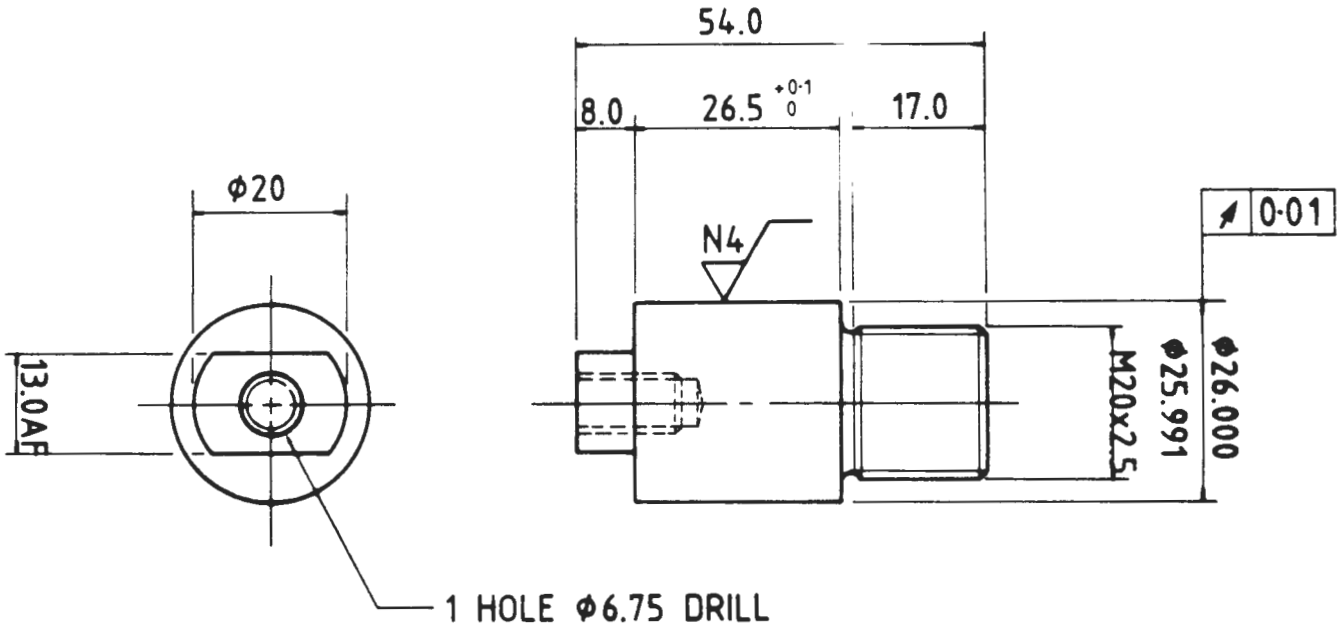

1 HOLE Φ6.75 DRILL

x 16 DEEP, TAP

M8x1.25 x 14 DEEP

ITEM No. (77)

CRANK PIN, 1 OFF

[CASE-HARDEN TO $R_C > 58$ TO 1 mm DEPTH]

U.C.T. — DEPARTMENT OF MATERIALS ENGINEERING — WORKSHOP			
DRAWN BY U.F.B. KIENLE	WORK CATEGORY M.Sc. THESIS	MATERIAL	
DATE ACCEPTED	WORK SUPERVISED BY N. DREEZE	431 S/S	
DATE PROMISED	MATERIAL SCHEDULE SUPPLIED	YES	NO
SUPERVISOR PROF A. BALL	SCALE 1:1	SHEET 36	OF 42

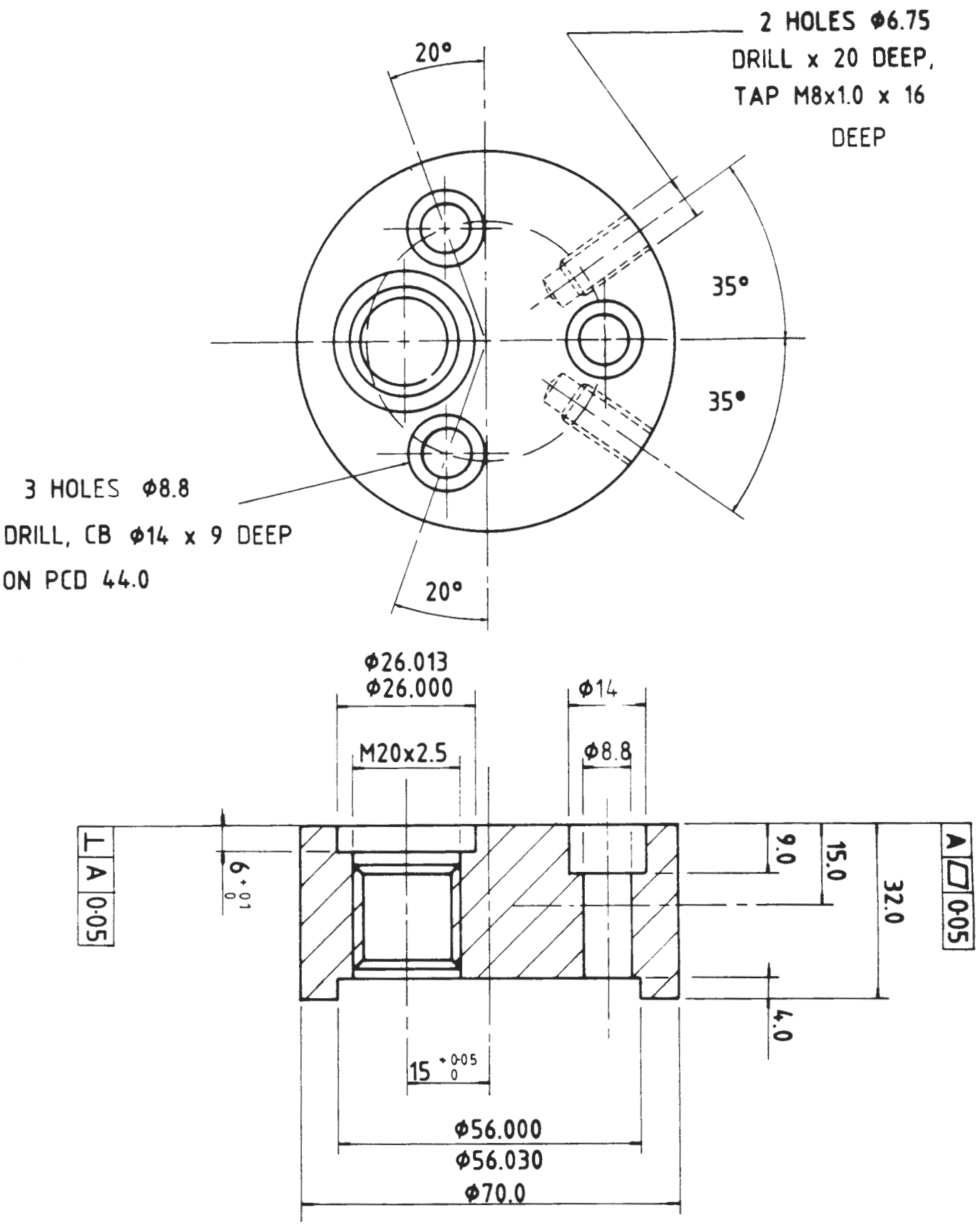

ITEM No. (78), CRANK PIN HOLDING PLATE, 1 OFF

U.C.T. — DEPARTMENT OF MATERIALS ENGINEERING — WORKSHOP			
DRAWN BY U.F.B. KIENLE	WORK CATEGORY M. Sc. THESIS	MATERIAL	
DATE ACCEPTED	WORK SUPERVISED BY N. DREEZE	431 S/S	
DATE PROMISED	MATERIAL SCHEDULE SUPPLIED	YES	NO
SUPERVISOR PROF A. BALL	SCALE 1:1	SHEET 37	OF 42

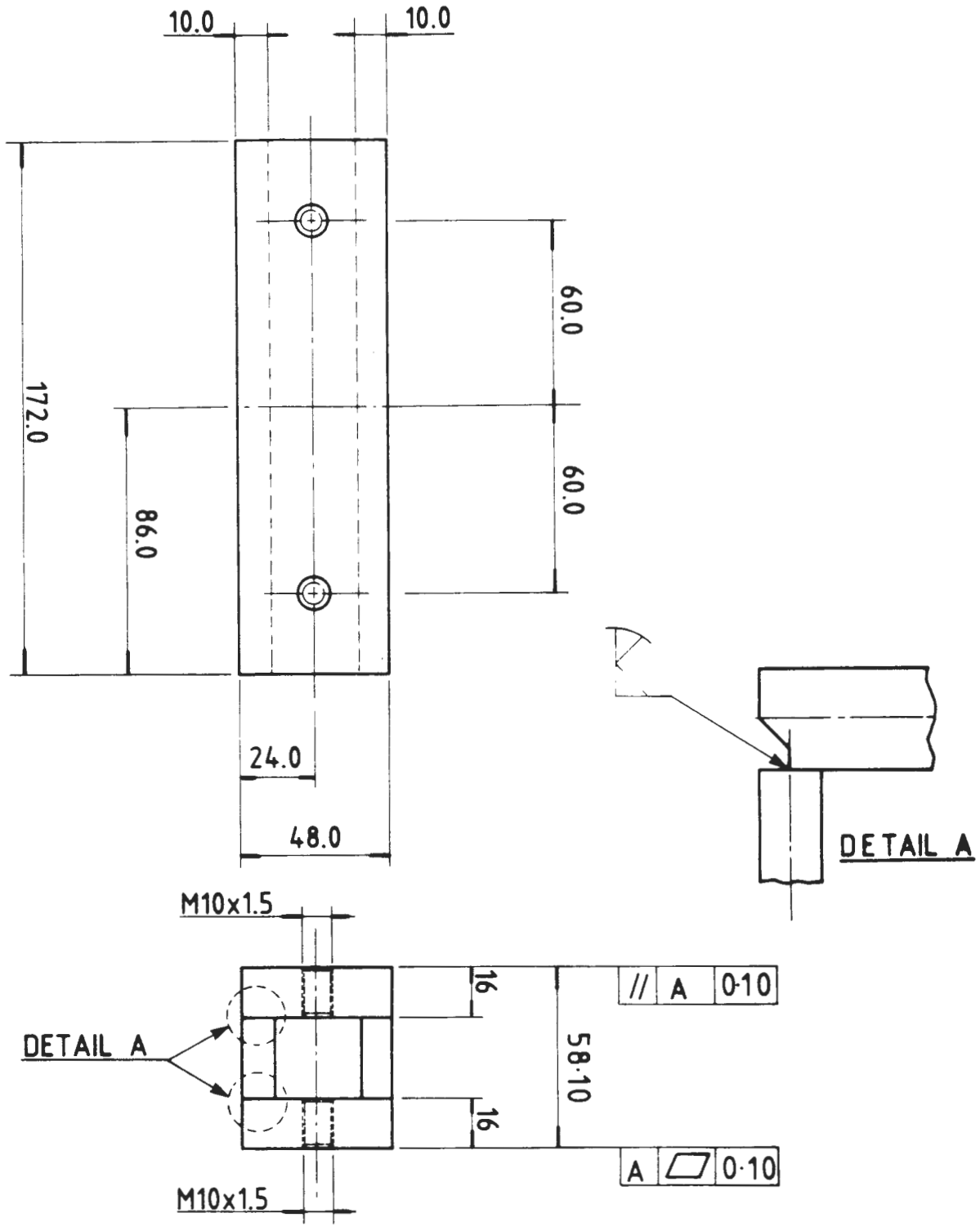

ITEM No. (88), BRACKET FOR PLUMMERBLOCKS, 2 OFF

U.C.T. — DEPARTMENT OF MATERIALS ENGINEERING — WORKSHOP			
DRAWN BY U.F.B. KIENLE	WORK CATEGORY M. Sc. THESIS		MATERIAL
DATE ACCEPTED	WORK SUPERVISED BY N. DREEZE		En3 M/S
DATE PROMISED	MATERIAL SCHEDULE SUPPLIED		YES / NO
SUPERVISOR PROF A. BALL	SCALE 1:2	SHEET 38	OF 42

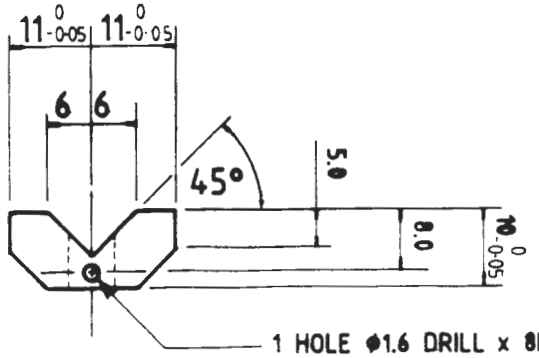

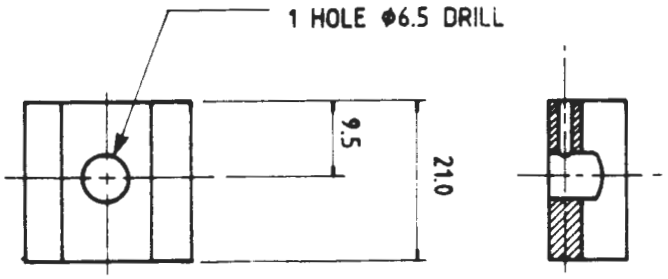

ITEM No. (90) SPECIMEN CHUCK - ADJUSTING JAW,
1 OFF, P - BRONZE (034), (SCALE 1:1)

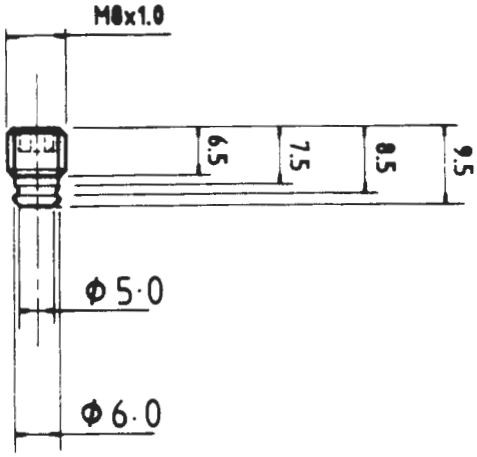

ITEM No. (89)
GRUB SCREW, 1 OFF
S/S, (SCALE 1:1)

ITEM No. (52)
STOP BLOCK, 2 OFF
316 S/S, (SCALE 2:1)

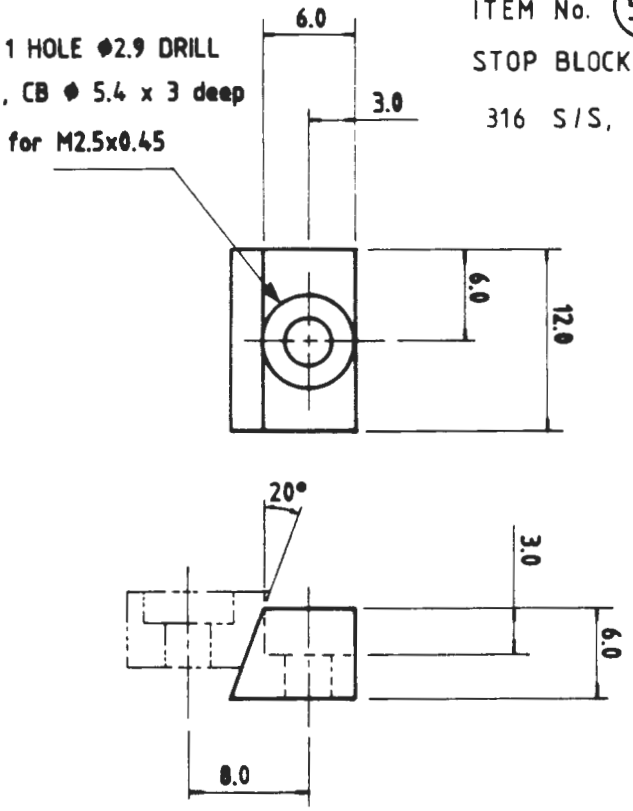

ITEM No. (22)
WEDGE BLOCK, 2 OFF
P - BRONZE (034), (SCALE 2:1)

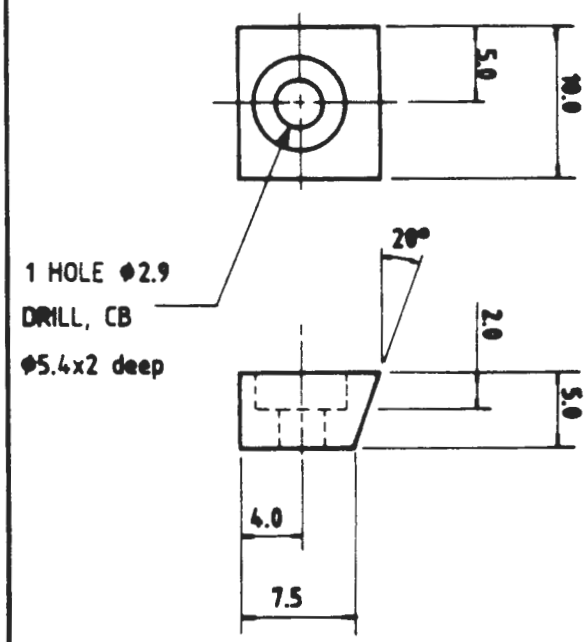

U.C.T. — DEPARTMENT OF MATERIALS ENGINEERING — WORKSHOP			
DRAWN BY U.F.B. KIENLE	WORK CATEGORY M. Sc. THESIS	MATERIAL AS SHOWN	
DATE ACCEPTED	WORK SUPERVISED BY N. DREEZE		
DATE PROMISED	MATERIAL SCHEDULE SUPPLIED	YES	NO
SUPERVISOR PROF A. BALL	SCALE AS SHOWN	SHEET 39	OF 42

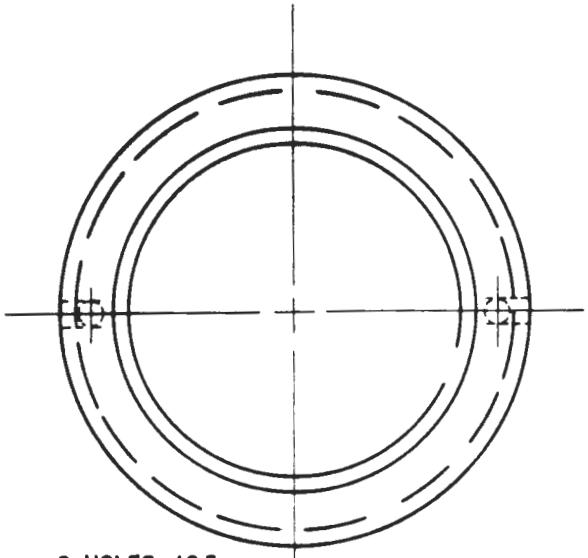

2 HOLES ϕ2.5
DRILL x 6.5 DEEP,
TAP M3x0.5 x 5 DEEP

2 HOLES ϕ2.5 DRILL
x 7.5 DEEP, TAP
M3x0.5 x 6 DEEP

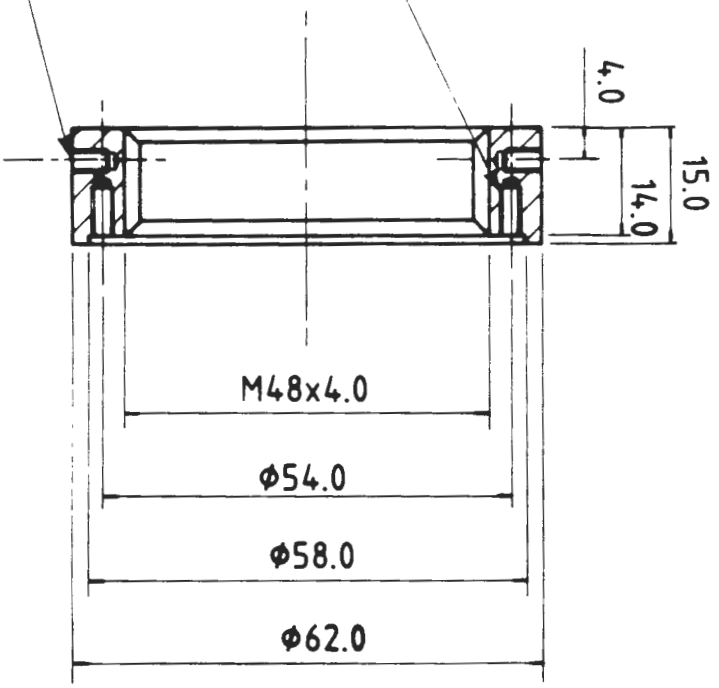

ITEM No. (26)
RESETTING RING, 1 OFF

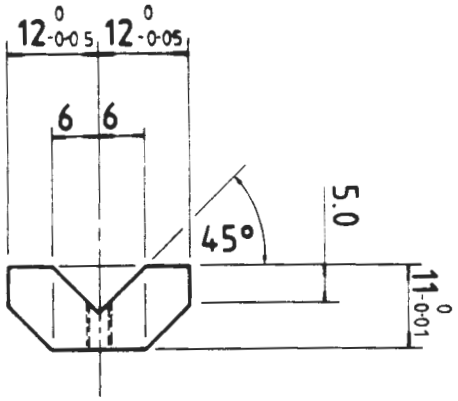

1 HOLE ϕ2.5 DRILL
TAP M3x0.5

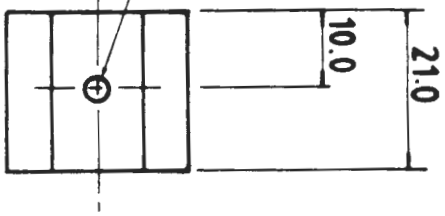

ITEM No. (91)
SPECIMEN CHUCK - FIXED JAW
1 OFF

ITEM No. (16)
LEVER BRACKET, 1 OFF

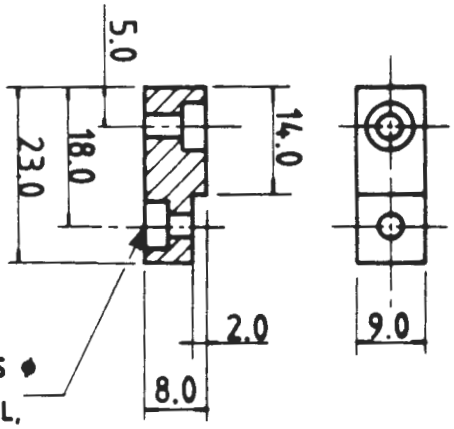

2 HOLES ϕ
3.4 DRILL,
CB ϕ6.5 x 3 DEEP

U.C.T. — DEPARTMENT OF MATERIALS ENGINEERING — WORKSHOP			
DRAWN BY U.F.B. KIENLE	WORK CATEGORY M. Sc. THESIS	MATERIAL	
DATE ACCEPTED	WORK SUPERVISED BY N. DREEZE	P - BRONZE (034)	
DATE PROMISED	MATERIAL SCHEDULE SUPPLIED	YES	NO
SUPERVISOR PROF A. BALL	SCALE 1:1	SHEET 40	OF 42

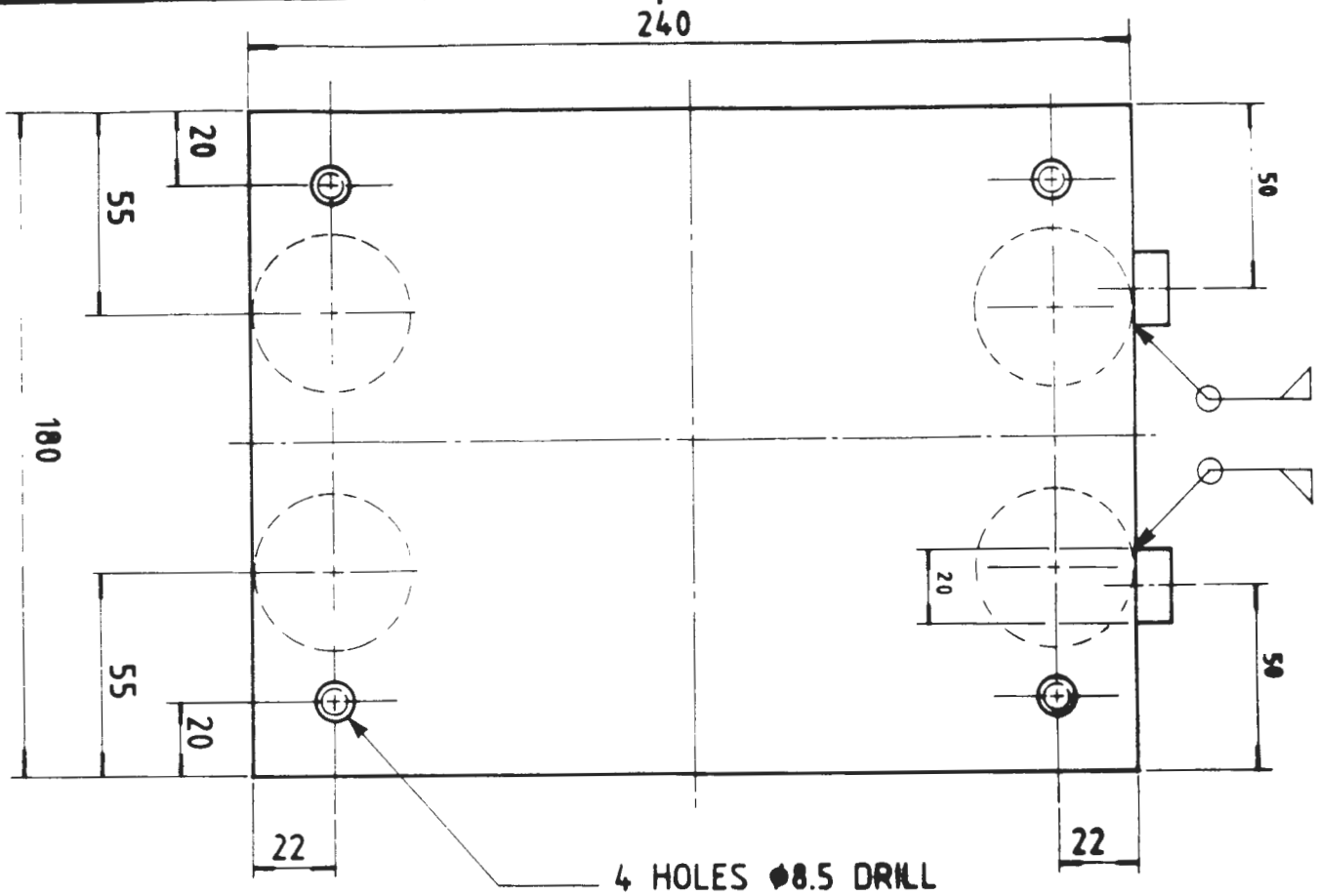

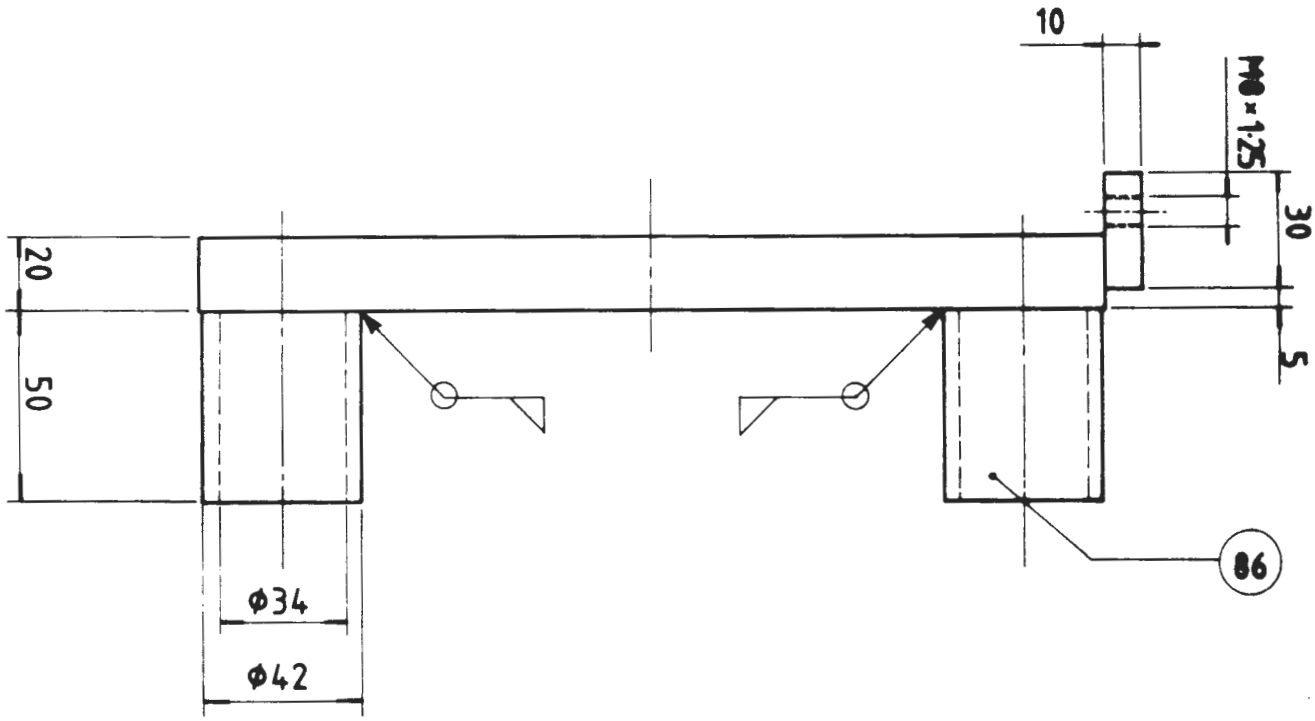

ITEM No. (84), MOTOR MOUNTING BASE, 1 OFF

U.C.T. — DEPARTMENT OF MATERIALS ENGINEERING — WORKSHOP			
DRAWN BY U.F.B. KIENLE	WORK CATEGORY M. Sc. THESIS	MATERIAL	
DATE ACCEPTED	WORK SUPERVISED BY N. DREEZE	En3 M/S	
DATE PROMISED	MATERIAL SCHEDULE SUPPLIED	YES	NO
SUPERVISOR PROF A. BALL	SCALE 1:2	SHEET 41	OF 42

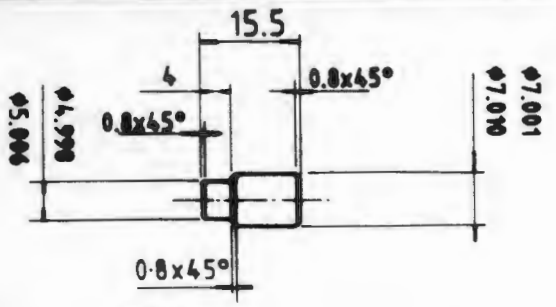

ITEM No. (4), PIN, 1 OFF

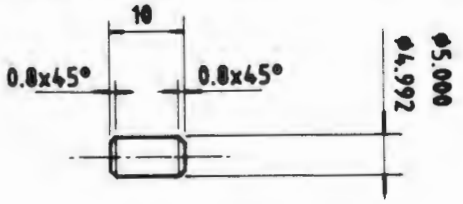

ITEM No. (18), LOCATING PIN, 18 OFF

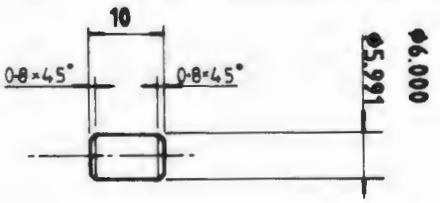

ITEM No. (94), LOCATING PIN, 2 OFF

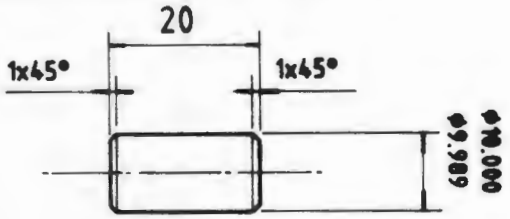

ITEM No. (95), LOCATING PIN, 2 OFF

U.C.T. — DEPARTMENT OF MATERIALS ENGINEERING — WORKSHOP			
DRAWN BY U.F.B. KIENLE	WORK CATEGORY M. Sc. THESIS	MATERIAL	
DATE ACCEPTED	WORK SUPERVISED BY N. DREEZE	316 S/S	
DATE PROMISED	MATERIAL SCHEDULE SUPPLIED	YES	NO
SUPERVISOR PROF A. BALL	SCALE 1:1	SHEET 42 OF 42	

APPENDIX G - SUBASSEMBLY DRAWINGS (FULL SIZE)

97	LOWER BASE PLATE O-RING SEAL		1	
96	BATH SEALING O-RING	nitrile rubber	1	GACO RM 1795-30
95	LOCATING PIN (ϕ10mm)	316 S/S	2	
82	PLATFORM	070M20 (En3)	1	
60	PERSPEX BATH	PERSPEX	1	
59	ENVIRONMENTAL CHAMBER	as required	1	OPTIONAL
58	LATCH PIN	316 S/S	1	

57	CHAMBER O-RING SEAL	nitrile rubber	1	GACO RM 2493-57
56	TUBING (9mm ϕ bore)	PLASTIC	-	cut to suit
55	HOSECLAMP	S/S	1	
54	FEMALE HOSE CONNECTOR	BRASS	1	
53	DOUBLE NIPPLE (type E) 1/4"	BRASS	1	
52	STOP BLOCK	316 S/S	2	
51	TUBING (13mm ϕ bore)	PLASTIC	-	cut to suit
50	HOSECLAMP	S/S	1	
49	FEMALE HOSE CONNECTOR	BRASS	1	
48	DOUBLE NIPPLE (type E) 1/2"	BRASS	1	
47	GUSSET STAND (LHS and RHS)	070M20 (En3)	@1	

46	UPPER BASE PLATE SUPPORT BLOCK	316 S/S	1	
45	HINGE PLATE	316 S/S	1	
44	RETAINING THUMBSCREW	316 S/S	1	
43	LATCHING LEVER HINGE MOUNTING	316 S/S	2	
42	BACKING DISC	316 S/S	1	
41	LATCH SPRING	316 S/S	1	
40	LATCHING HOOK	316 S/S	1	
39	HINGE BUSHING	P-BRONZE 034	2	
38	BEAM LOAD CELL TRANSDUCER	S/S	1	LCS HBL/G/20
37	HINGE MOUNTING BLOCKS	316 S/S	2	
36	HINGE PIN	316 S/S	1	

11	BALL SPRING	316 S/S	2	
10	CONNECTING PLUNGER	316 S/S	1	
9	BALL KNOB	PLASTIC	3	
8	UPPER BASE PLATE LEVER	316 S/S	1	
7	UPPER BASE PLATE	316 S/S	1	
6	POINTER	P-BRONZE 034	1	
5	LOAD SPRING	316 s/s	1	
4	PIN	316 S/S	1	
3	LOAD PLUNGER	316 S/S	1	
2	NEEDLE ROLLER BEARING - LOAD PLUNGER	-	1	FAG DNK7/10TN
1	SCREW CAP	P-BRONZE 034	1	
ITEM NO	DESCRIPTION	MATERIAL	NO OFF	REMARKS

23	RECIPROCATING SHUTTLE	aluminium 7017	1	
22	WEDGE BLOCK	P-BRONZE 034	2	
21	STATIONARY SPECIMEN	test material	1	
20	SPECIMEN HOLDER	316 S/S	1	HARD CHROME
19	BALLS (ϕ4 mm)	S/S	4	
18	LOCATING PINS (ϕ5 mm)	316 S/S	18	
17	HOLD FINGERS	316 S/S	2	
16	LEVER BRACKET	P-BRONZE 034	1	
15	LOAD ASSEMBLY HOUSING	316 S/S	1	
14	FRICTION PLATE GUIDE SHAFT	431 S/S	2	HARD CHROME
13	FRICTION PLATE SHAFT BEARINGS	filled UHMWPE	4	SOLIDUR DS
12	FRICTION PLATE	316 S/S	1	

35	LATCH RELEASE LEVER	316 S/S	1	
34	RESETTING RING LEVER	316 S/S	1	
33	SPACER RING	P-BRONZE 034	1	
32	LOWER BASE PLATE	316 S/S	1	
31	LINEAR BALL BUSHINGS (and SEALS)	-	4	0668-012-30 and 1331-512-30
30	SUPPORT BRACKET - SHUTTLE ASSEMBLY	aluminium 7017	2	
29	SHUTTLE GUIDE SHAFT	440C	2	hardened and ground
28	SPECIMEN MOUNTING PLATE	316 S/S	1	
27	RECIPROCATING SPECIMEN	test material	1	
26	RESETTING RING	P-BRONZE 034	1	
25	RATCHET BRACKET	P-BRONZE 034	1	
24	SUPPORT BRACKETT- UPPER ASSEMBLY	aluminium 7017	2	

outline of upper assembly in hold position

outline of optional environmental chamber

UNIVERSITY OF CAPE TOWN
DEPARTMENT OF MATERIALS ENGINEERING

SUBASSEMBLY DWG OF INTERNAL WORKINGS OF TEST CELL

SCALE : 1 : 1
DATE : 08/08/88
DRAWN BY : ULRICH F.B. KIENLE

SHEET 1 OF 42 SHEETS
DWG NO (1)

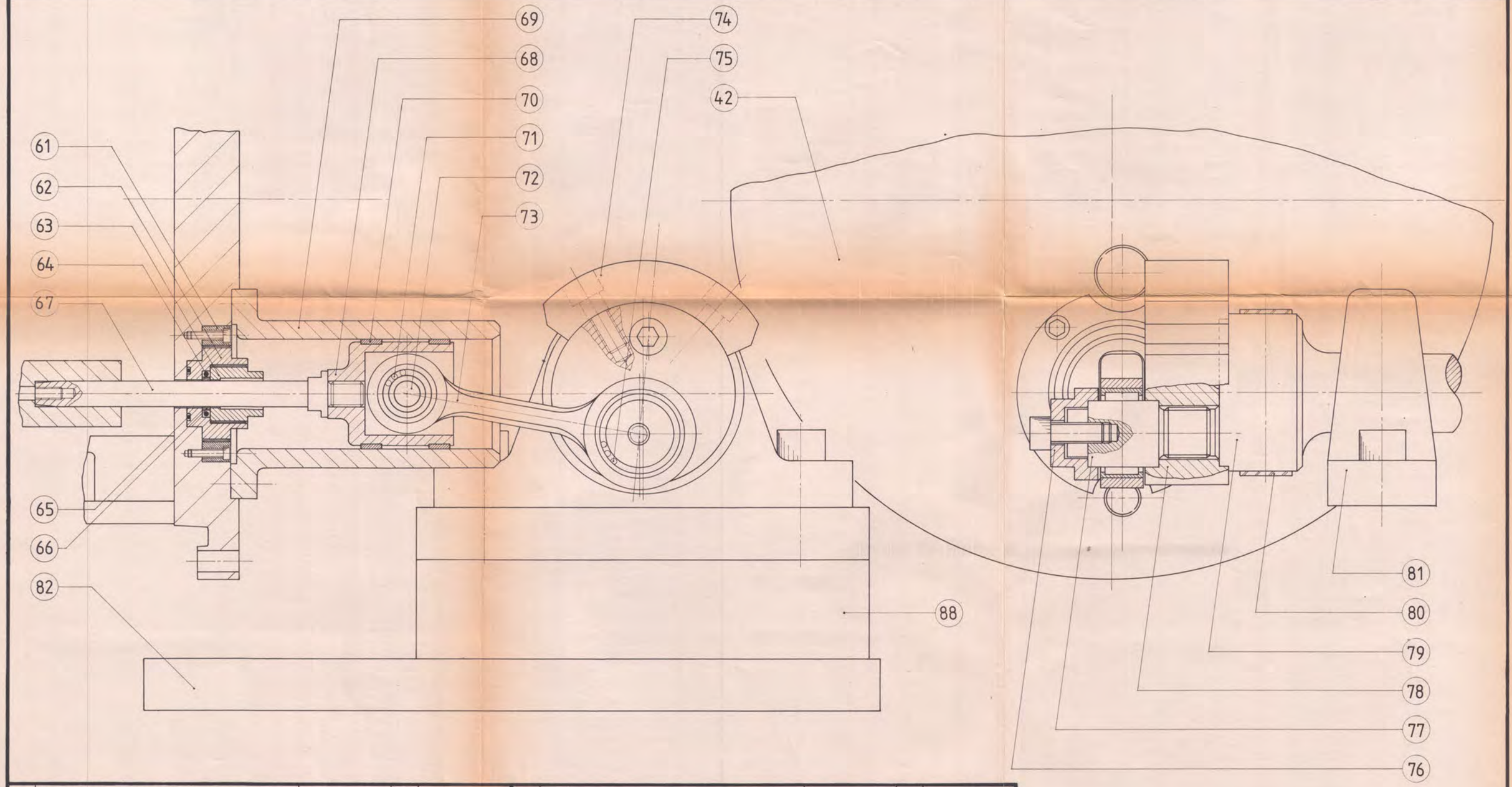

ITEM NO	DESCRIPTION	MATERIAL	NO OFF	REMARKS
71	NEEDLE ROLLER BEARING - WRIST END	-	1	FAG DNKJ10/16A
70	PISTON SEALS	filled UHMWPE	2	SOLIDUR DS
69	PISTON HOUSING	431 S/S	1	
68	RECIPROCATING PISTON	aluminium 7017	1	
67	RECIPROCATING PISTON SHAFT	431 S/S	1	
66	PISTON SHAFT SEAL	filled UHMWPE	1	
65	O-RING - PISTON SHAFT SEALING ASS.	nitrile rubber	1	GACO RM 0161-16
64	O-RING - PISTON SHAFT BACKING SEAL	nitrile rubber	1	GACO RM 0126-24
63	PISTON SHAFT SEAL. ASS. - INNER HOUSING	316 S/S	1	
62	PISTON SHAFT SEAL. ASS. - OUTER HOUSING	P-BRONZE	1	
61	PISTON SHAFT SEAL. ASS. - OUTER RING	431 S/S	1	
42	BACKING DISC	316 S/S	1	
88	BRACKET FOR PLUMMERBLOCKS	070M20 (En 3)	2	PAINTED
82	PLATFORM	070M20 (En 3)	1	PAINTED
81	PLUMMERBLOCK	-	2	RHP NP30
80	DRIVE BELT	FABRIC MIX	1	
79	DRIVESHAFT	817M40 (En 24)	1	
78	CRANK PIN HOLDING PLATE	431 S/S	1	
77	CRANK PIN	431 S/S	1	
76	CRANK PIN END CAP	431 S/S	1	
75	NEEDLE ROLLER BEARING - CRANK END	-	1	FAG DNK26/16A
74	COUNTERWEIGHT	BRASS	1	
73	CONNECTING ROD	431 S/S	1	
72	WRISTPIN	431 S/S	1	

UNIVERSITY OF CAPE TOWN
DEPARTMENT OF MATERIALS ENGINEERING

SUB ASSEMBLY DWG OF THE RECIPROCATING DRIVE

SCALE : 1 : 1
DATE : 08/08/88
DRAWN BY : ULRICH F.B. KIENLE

SHEET 2 OF 42 SHEETS

DWG NO (2)

UNIVERSITY OF CAPE TOWN
DEPARTMENT OF MATERIALS ENGINEERING

SUBASSEMBLY DWG OF PLATFORM LAYOUT

SCALE : 1 : 2	SHEET 3 OF 42 SHEETS
DATE : 08/08/88	DWG NO ③
DRAWN BY : ULRICH F.B. KIENLE	

ITEM NO	DESCRIPTION	MATERIAL	NO OFF	REMARKS
42	BACKING DISC	316 S/S	1	
59	ENVIRONMENTAL CHAMBER	as may be requd.	1	OPTIONAL
59a	QUICK RELEASE TOGGLE LATCH	Zn plated steel	4-8	OPTIONAL
59b	GUIDE ROLLERS	431 S/S	4	OPTIONAL
59c	GUIDE SHAFTS	431 S/S	2	OPTIONAL
47	GUSSET STAND (LHS and RHS)	070M20 (En 3)	1	
69	PISTON HOUSING	431 S/S	1	
73	CONNECTING ROD	431 S/S	1	
74	COUNTERWEIGHT	BRASS	1	
76	CRANK PIN END CAP	431 S/S	1	
79	DRIVESHAFT	817M40 (En 24)	1	
80	DRIVEBELT	FABRIC MIX	1	
81	PLUMMERBLOCKS	-	2	RHP NP30
82	PLATFORM	070M20 (En 3)	1	PAINTED
83	DRIVE PULLEY	070M20 (En 3)	1	trim down existing
84	MOTOR MOUNTING BASE	070M20 (En 3)	1	PAINTED
85	DC MOTOR (and CONTROLLER)	-	1	GEC (existing)
86	SPACERS	070M20 (En 3)	4	PAINTED
87	ANTI VIBRATION MOUNTINGS (type C)	RUBBER MIX	4	REMAG 5218-112
92	BELT DRIVE COVER	070M20 (En 3)	1	
93	TABLE	070M20 (En 3)	1